Effect of Variable Fluid Properties on the Flow of Viscous Fluid Past a Vertical and Rotating Cone

A thesis submitted to
NATIONAL INSTITUTE OF TECHNOLOGY WARANGAL, (T.S.)
for the award of the degree of
DOCTOR OF PHILOSOPHY
in
MATHEMATICS

by
BHANOTH RAJENDER
(Roll No. 719104)

UNDER THE SUPERVISION OF
Prof. D. SRINIVASACHARYA

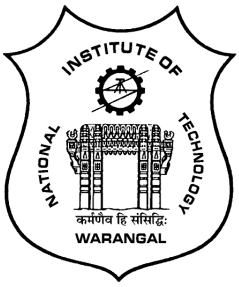

DEPARTMENT OF MATHEMATICS
NATIONAL INSTITUTE OF TECHNOLOGY
WARANGAL - 506 004, INDIA

OCTOBER 2022

C E R T I F I C A T E

This is to certify that the thesis entitled " **Effect of Variable Fluid Properties on the flow of Viscous fluid Past a Vertical and Rotating Cone** " submitted to National Institute of Technology Warangal, for the award of the degree of ***Doctor of Philosophy***, is the bonafide research work done by **Mr. BHANOTH RAJENDER** under my supervision.The contents of this thesis have not been submitted elsewhere for the award of any degree.

Dr. D. Srinivasacharya
Professor
Department of Mathematics
National Institute of Technology,
Warangal, T.S., INDIA

.

DECLARATION

This is to certify that the work presented in the thesis entitled **"Effect of Variable Fluid Properties on the Flow of Viscous Fluid Past a Vertical and Rotating Cone"**, is a bonafide work done by me under the supervision of **Prof. D. SRINIVASACHARYA** and has not been submitted elsewhere for the award of any degree.

I declare that this written submission represents my ideas in my own words and where others' ideas or words have been included, I have adequately cited and referenced the original sources. I also declare that I have adhered to all principles of academic honesty and integrity and have not misrepresented or fabricated or falsified any idea / data / fact /source in my submission. I understand that any violation of the above will be a cause for disciplinary action by the Institute and can also evoke penal action from the sources which have thus not been properly cited or from whom proper permission has not been taken when needed.

Bhanoth Rajender

Roll No. 719104

Date:_____

Dedicated to

My Parents

&

Smt. Jyothi, Sai Sayesha and Abhinav Sai

ACKNOWLEDGEMENTS

It is a rare privilege and boon that I could associate myself with Dr. D. Srinivasacharya, Professor of Mathematics, National Institute of Technology Warangal, India, for pursuing my research work. I sincerely record my gratitude for his invaluable guidance and constant encouragement throughout the preparation of this thesis and his involvement and meticulous supervision while my work was in progress. With his inimitable qualities as a good teacher, he chiseled my path towards perfection. He has been a perpetual source of inspiration, spiritual guidance, encouragement, and enlightenment since I first met him. He is the one who ensured that the duration of my research work was both educational and fun. He has been a great source of motivation and inspiration. The thesis would not have seen the light of the day without his unrelenting support and cooperation. I deem it a privilege to have worked under his amiable guidance. My vocabulary is inadequate to express my gratitude. I also thank madam Smt. D. Jaya Srinivasacharya for her hospitality and patience during our elongated discussions with my supervisor.

I am grateful to Prof. H.P. Rani, Head, and Prof. D. Srinivasacharya, Dr. P. Muthu, former Heads, Department of Mathematics for providing necessary help and support throughout my research period.

I take this opportunity to thank Prof. Y. N. Reddy, Prof. K. N. S. Kasi Viswanadham, Prof. Debashis Dutta, Dr.K.Kaladhar and Department of Mathematics for their valuable suggestions, moral support and encouragement during my stay.

I thank the members of the Doctoral Scrutiny Committee, Prof. J. V. Ramana Murthy, Dr. Ch. Ramreddy and Dr. E. Sathyanarayana, Department of Mathematics, and Dr. S. Ravichandra, Department of CSE for their valuable suggestions, moral support, and encouragement while my work was in progress.

I place on record my gratitude to all the faculty members of the Department of Mathematics, for their constant encouragement. I express my sincere thanks to the Director, National Institute of Technology, Warangal for providing me QIP Fellowship (AICTE, GoI) to carry

out my research work.

I thank Dr.I.Sreenath, Dr.Dipak Barman,Dr. K. Sita Ramana, Mr.R.Shravan Kumar, Ms. Nidhi Humnekar, Mr.Pankaj Barman, Mrs. G. Saritha, Mr.Sarthak Sharma ,Dr.J.Sharath kumar Reddy, Dr. Abhinav Srivasthav and all other research colleagues in the Department of mathematics and my friends, who helped me during my Ph.D.for being cooperative and also for making my stay in the NITW campus fruitful and enjoyable every moment.

I owe my special thanks to Dr. N. Vijender and Mr. B. Raman, my classmates, for all their continuous encouragement while doing my research work.

My heartfelt gratitude goes to my parents, Sree Sajya and Smt. Parengan, whose encouragement and blessings inspired me to finish my job ahead of schedule.I am overjoyed to thank my family members for their contributions to the completion of this job. All of their prayers, support, love, and affection have been the driving force behind what has happened.

Also, most importantly, I would like to thank my better half, Smt. Jyothi and my children Sai Sayesha, Abhinav Sai for their support,prayers,patience and understanding that were vital to complete this thesis. Without their help and encouragement, I would not have been finished this thesis.

I thank to my extended Family consisting of My Brother Sree B.Devendar, Sister in law Smt.Vinoda, father in law Sree G.Balaji Naik, mother in law Smt. Kavitha and family for their continuous support and constant encouragement over the years. All of their love and affection have been motivating force behind what I am today.

Bhanoth Rajender

A B S T R A C T

A free convective flow of an incompressible viscous fluid past an isothermal vertical cone is investigated with variable viscosity and variable thermal conductivity. As thermal boundary conditions at the surface of the cone, the constant wall temperature (CWT) and constant wall heat flux (CHF) cases are considered.The successive linearization approach is applied to linearize a system of nonlinear differential equations that describes the flow under investigation.The numerical solution for the resulting linear equations is attainedby means of Chebyshev spectral collocation method. Theimpact of significant parameters on the velocity and temperature, in addition to heat and mass transfer rates, is evaluated and presented graphically for the CWT and CHF situations. This thesis consists of Ten chapters.
Chapter- 1 This chapter is introductory in nature and gives motivation to the investigations carried out in the thesis.A survey of pertinent literature is presented to show the significance of the problems considered. The basic equations governing the flow of viscous and incompressible fluid are given. Chapter-2 Influence of variable properties on free convection flow past a vertical cone. Chapter- 3 the influence of the variable properties on boundary layer flow past a vertical cone is examined. Similarity transformations are utilized to reduce the equations describing the flow into ordinary differential equations. The non-dimensional equations are linearized using successive linearization procedure and then the solution of the consequent system is found using Chebyshev spectral method. Chapter- 4 deals with the free convection flow across a vertical cone is investigated by presuming the viscosity and thermal conductivity varies with temperature in the manifestation of Soret and Dufour effects. Chapter- 5 The effects of Soret and Dufour on the boundary layer flow across a vertical cone is investigated by assuming the viscosity and thermal conductivity varies with temperature is presented in this chapter. Chapter- 6 In this chapter, the laminar free convection flow across a rotating cone is investigated by taking the temperature dependent viscosity and thermal conductivity. Similarity transformed are utilized to reduce the equations governing the flow into ordinary differential equations. The non-dimensional equations linearized using successive linearization procedure and then the solution of the consequent system is found using Chebyshev spectral method. Chapter- 7 This chapter deals with the influence of the variable properties on boundary layer flow past a rotating cone is examined. Chapter- 8 The cross diffusion effects on the free convection flow across a rotating cone is investigated with temperture dependent viscosity and thermal condictivity is considered in this chapter. Chapter - 9 Influence of variable properties on boundary layer flow past a rotating cone with Radiation effect and chemical reaction. In all the above chapters, A coordinate transformation is applied to convert the ordinary differential equations into partial differential

equations.The successive linearization approach is applied to linearize a system of nonlinear differential equations that describes the flow under investigation.The numerical solution for the resulting linear equations is attainedby means of Chebyshev spectral collocation method. The last chapter, Chapter - 10, gives a summary and overall conclusions and scope for future work.

N O M E N C L A T U R E

A	Viscosity parameter.
k	Thermal conductivity of the fluid.
Gr	Grashof Number.
Re	Reynolds number.
Pr	Prandtl number.
T	Fluid Temperature.
C	Concentration.
E	electric field.
L	characteristic length.
T_w	Temperature at the surface.
T_∞	Temperature of the ambient fluid.
Nu	Nusselt number.
f	Dimensionless stream function.
Sr	Soret number.
D_f	Dufour number.
Sc	Shmidth number.
D_{TC}	Dufour type diffusivity.
D_{CT}	Soret type diffusivity.
D_s	Solutal diffusivity.
g	Acceleration due to gravity.
B	buoyancy ratio.
λ	buoyancy parametr.
Rd	radiation parameter.
γ	chemical reaction parameter.
q_r	Heat flux of the thermal radiation.
L	the cone slant height.
T_L	the cone surface temperature.
q_w	Surface heat flux.
H', G, H	the dimensionless velocity components along the tangential,azimuthal and normal directions.
u	Velocity component in the x- direction.
v	Velocity component in the y-direction.
w	Velocity component in the z-direction.
x, y, z	curvilinear coordinates system.

Greek Symbols

η	Non-dimensional variable.
ρ	Density of the fluid.
θ	Dimensionless temperature.
$\mu(T)$	Temperature dependent Viscosity of the fluid.
α	Amplitude associated with the wavy surface
ξ	Non-dimensional variable / dimensionless distance.
ψ	Stream function.
Ω	angular velocity of the cone.
τ	Dimensionlesstime.
ϕ	Semivertical cone angle.
ϵ	The pressure work parameter.
β	pressure gradient parameter.
ν	Magnetic diffusivity.

Contents

[1] Accepted for publication in "**Journal of Applied Mathematics and Computational Mechanics**"

[2]Communicated to "**Applications and Applied Mathematics: An International Journal**"
[3]Accepted for publication in "**Heat Transfer**",
[4]Published to "**Journal of Xidian University**"

[5] Communicated to "**International Journal of Applied and Computational Mathematics**"
[6] Communicated to "**Computational Thermal Science**"
[7] Communicated to "**Journal of Applied Nonlinear Dynamics**"
[8] Communicated to "**Heat Transfer**"

Chapter 1

Preliminaries and Review

1.1 Introduction

Fluid dynamics is proven to be a passionate, provocative and demanding subject of modern sciences due to its connectivity to nature with real-life problems and a wide range of applications. The pursuit for profound understanding of the subject has not only stimulated it's own development of subject but also made the progress in allied areas of mathematical sciences such as applied mathematics, numerical computing, physical and mechanical sciences. The listing of fluid dynamics applications in technology would be almost impossible due to its ubiquitous nature of a fluid in the technological devices. The axioms/principles of fluid dynamics can be applied in pure science like Atmospheric sciences(global circulation, global warming, mesoscale weather patterns), Oceanography (pollution effect on living organisms, ocean circulation patterns), Geophysics (study of plate tectonics, earthquakes, volcanoes, magnetic field), Astrophysics (galactic structure, clustering, stellar evolution, supernovae) and Biological sciences (circulatory, cellular processes and respiratory systems in animals).

In the ever increasing literature on fluid dynamics, studies on convective heat and mass transfer across various geometries with different corss sections have made significant contributions. The patterns of fluid flow around surfaces of different cross-sections, such as spheres, cylinders, and cones are realistic to examine. These flows gained strong interest in view of their wide range of applications in a broad variety of engineering processes, fiber

technology, high-speed thermal aerodynamics, nuclear cooling systems, surface treatment, spray deposition process, polymer engineering, etc. In the past, the behaviour of fluid flows has been analytically examined for simplified formulations. With the advancement of fast computing machines in recent years, emphasis has shifted to numerical methods for solving real-world problems involving a wide variety of geometric and fluid flow characteristics.

The problem of convective heat and mass transfer around rotating bodies is of paramount significance due to its application in several areas of geophysics, engineering, and technology. The study of such investigations is critical in the design of turbines and turbo-machines, estimating the flight path of rotating wheels, satellites, space vehicles, nuclear reactors, modelling of several geophysical vortices and spin stabilized missiles etc.

1.2 Viscous fluid

The majority of most common fluids such as water, gasoline, honey, organic solvents, oils, air, steam, nitrogen or rare gases are characterized as Newtonian fluids. These fluids resist movement or the movement of an object through the fluid. The magnitude of resistance to this deformation is represented by the viscosity of fluid. The study of a Newtonian fluid flow gained much attention in last few decades because of their industrial and engineering applications. A Newtonian fluid is one that obeys Newton's viscosity law or has a linear relationship between viscosity and shear stress i.e. the shear stress induced by flow is proportional to the rate of strain and the constant of proportionality in this relation denotes the viscosity of the fluid.

The basic governing equations of a viscous fluid are

$$\frac{\partial \rho}{\partial t} + (\nabla \cdot \rho \overline{q}) = 0 \tag{1.1}$$

$$\rho \left(\frac{\partial \overline{q}}{\partial t} + (\overline{q} \cdot \nabla)\overline{q} \right) = \rho \overline{f} + \frac{4}{3}\mu \nabla(\nabla \cdot \overline{q}) - \mu \nabla \times (\bigtriangledown \times \overline{q}) \tag{1.2}$$

where $\overline{q}$ is the velocity vector, ρ is the density, $\overline{f}$ is the body force per unit mass, and t is the time variable

1.3 Basic Terminology

Heat Transfer

The heat transfer takes place when internal energy is exchanged between regions or elements within a medium. It usually happens from a higher to a lower temperature region. The heat transfer occurs in three different modes. They are conduction, convection and radiation. Conduction is the molecular transport of heat inside or between bodies in a thermodynamical system. Convection is concerned with the fluid medium and/or the fluid in the medium. The heat transfer due to the movement of fluid from one region to the other region in the medium is called convection. Radiation heat transfer is a mechanism in which the internal energy of a substance is converted into radiant energy. The transport of heat by convection together with conduction is known as convective heat transfer.Furthermore, there are three types of convection: forced, free, and mixed convection. To compute the heat transfer rate in the medium, the temperature distribution is to be determined from the heat or energy (conservation of energy) equation.

$$\rho C_p \left(\frac{\partial T}{\partial t} + (\overline{q}.\nabla)T \right) = \nabla.(k\nabla T) \tag{1.3}$$

where T is the local equilibrium temperature, C_p is the specific heat and k is the thermal conductivity of the medium.

Mass Transfer

The tendency of a component in a mixture to travel from a region of high to low concentration is called mass transfer. Mass transfer occurs by two mechanisms namely, Diffusion mass transfer and Convective mass transfer. Diffusion mass transfer can take place as a consequence of a concentration gradient, a temperature gradient, or a pressure gradient. Convective mass transfer is a phenomenon that transfers mass between a fluid and a solid surface as a result of matter moving from the fluid to the solid surface or fluid. The species mass flux can be determined from the statement of conservation of mass species, which is given by The conservation of mass is given by

$$\left(\frac{\partial C}{\partial t} + (\overline{q} \cdot \nabla)C \right) = \nabla \cdot (D_s \nabla C) \tag{1.4}$$

where C is the concentration, and D_s is the solutal diffusivity.

Boundary Layer Theory

Ludwig Prandtl proposed the boundary layer theory in 1904. Prandtl reasoned that in the analysis of a flow field, it may be sufficient to examine the effect of viscosity inside the boundary layers, while the flow outside the boundary layers may be regarded inviscid. He then simplified the conservation equation by determining the order of magnitude of the individual terms in the conservation equations, resulting in the so-called boundary layer equations. It can be demonstrated that "the effects of wall boundaries on flows are limited to a small region (thin layer) near the walls in flows where the acceleration forces are large when compared to the viscous forces, or the diffusion times are large in contrast to the convection times, or the convection velocities are large in comparison to the diffusion velocities". This thin layer is called the boundary layer. Boundary layer approximations provide sufficient simplifications to tackle the problems mathematically and then to understand the convective mechanism in the continuum fluid flows. Using boundary layer assumptions, the two dimensional form of the equations (1.1) - (1.4), in terms of cartesian coordinates are given by

$$\frac{\partial U}{\partial X} + \frac{\partial V}{\partial Y} = 0, \tag{1.5}$$

$$\rho\left(\frac{\partial U}{\partial t} + U\frac{\partial U}{\partial X} + v\frac{\partial U}{\partial Y}\right) = -\frac{1}{\rho}\frac{\partial p}{\partial X} + \frac{\partial}{\partial Y}\left(\mu\frac{\partial U}{\partial Y}\right), \tag{1.6}$$

$$-\frac{1}{\rho}\frac{\partial p}{\partial Y} = 0, \tag{1.7}$$

$$\rho c_p\left(\frac{\partial T}{\partial t} + U\frac{\partial T}{\partial X} + V\frac{\partial T}{\partial Y}\right) = \frac{\partial}{\partial Y}\left(k\frac{\partial T}{\partial Y}\right), \tag{1.8}$$

$$\frac{\partial C}{\partial t} + U\frac{\partial C}{\partial X} + V\frac{\partial C}{\partial Y} = \frac{\partial}{\partial Y}(D_s\frac{\partial C}{\partial Y}), \tag{1.9}$$

where U and V are the velocity components in X and Y directions.

Soret and Dufour Effects

The flow in simultaneous heat and mass transfer mechanisms is driven by density variations induced by a temperature or concentration gradient, and material composition all at the same time. The development of species interaction in an initial homogeneous fluid applied

to a temperature gradient is known as thermal diffusion, also identified as thermo-diffusion or the Soret effect [80]. The Dufour effect, also characterized as the diffusion-thermo effect, is the heat flux caused by a concentration gradient.

Variable fluid properties

In most of the studies, the thermophysical properties of fluid were assumed to be constant. However, it is known that these properties may change with the temperature, especially for a fluid viscosity and thermal conductivity. For example the absolute viscosity of water decreases by 240% when the temperature increases from 10^oC to 500^oC. The enhancement in the temperature in lubricating fluids generate internal friction, which modifies the viscosity of the fluid, which will no longer remain constant. The intensification in temperature speed up the transport phenomena by decreasing viscosity all over the temperature boundary layer, which influences the heat transfer rate. Therefore, to predict the heat transfer rate accurately, it is necessary to take into account this variation of viscosity and thermal conductivity. Kays and Crawford [37] provided a variety of relationships between fluid physical properties and temperature. Herwig and Gersten [27] were the first to examine the consequence of changeable fluid properties on laminar boundary layer flow. Applications include drawing of plastic films, glass fibre, the study of spilling pollutant crude oil over the surface of seawater, cooling of nuclear reactors, petroleum reservoir operations, food processing, welding and casting in manufacturing processes, wire drawing, paper production, glass fibre production, glueing of labels on hot bodies, etc. Despite its importance in many applications, this effect has received little attention. In recent years, fewer researchers have analyzed the influence of variable properties on convective flows over-stretching surfaces.

Thermal Radiation

The radiative effect has important applications in physics and engineering fields, the space technology and high temperature processes, liquid metal fluids, power generation, cooling of nuclear reactors, etc. But very little is known about the effect of radiation on the boundary layer flows. Thermal radiation has a considerable impact on heat transfer and temperature distribution in the boundary layer flow when temperatures are high. Thermal radiation influence may play a significant role in managing heat transfer in industries where the quality of the final product is partially dependent on heat controlling factors. In most of the studies available in the literature, the linearization process for the radiation term is used.

1.4 Successive Linearization Method

The Successive Linearisation Method (SLM) is one of the linearization methods and it is proposed and developed by Makukula *et al.* [46] and Motsa and Sibanda [56]. This procedure has been used effectively to linearize several boundary value problems in heat and mass transfer investigations ([44, 45], [77], [4] erc.).

To solve the nonlinear boundary value problem in an unknown function $z(x)$ using SLM, we assume that $z(x)$ is approximated by

$$z(x) = z_r(x) + \sum_{m=0}^{r-1} z_m(x) \tag{1.10}$$

where $z_r(x)$ is an unknown function and $z_0(x)$, $z_1(x) \cdots z_{r-1}(x)$ are known approximate solutions. The unknown function $z_r(x)$ can be determined by solving the linearized differential equation in $z_r(x)$ obtained by substituting (1.10) in the given nonlinear differential equation and linearizing the resulting differential equation using Taylor's series expansion. Hence, the subsequent solutions $z_r(x), r \geq 1$, are obtained by successively solving the linear equations for $z_r(x), r \geq 1$ given that the previous guess $z_{r-1}(x)$ is known. The initial guess $z_0(x)$ is taken such that it satisfy the given conditions on the boundary.

Any numerical scheme can used to solve the above iterative sequence of linearized differential equations. The SLM method has been successfully applied to a wide variety of scientific models over finite and semi-infinite intervals. The SLM approximation was applied to boundary value problems which possess smooth solutions.

1.5 Chebyshev Collocation Method

The Chebyshev collocation method ([9, 10, 15, 85]) is based on the Chebyshev polynomials defined on the interval $[-1, 1]$. To solve a differential equation, in an unknown function $z(x)$, on $[-1, 1]$, the interval $[-1, 1]$ is to be descritized at $N+1$ Gauss-Lobatto collocation points, which are given by

$$\xi_j = \cos \frac{\pi j}{N}, \quad j = 0, 1, 2, ..., N \tag{1.11}$$

Next, the unknown function $z(x)$ and its derivatives are guestimated at the collocation

points as follows

$$z(\xi) = \sum_{k=0}^{N} z(\xi_k) T_k(\xi_j) \quad \frac{d^{\boldsymbol{r}} z}{dx^{\boldsymbol{r}}} = \sum_{k=0}^{N} \left[\frac{2}{(b-a)} \mathbf{D}_{kj} \right]^{\boldsymbol{r}} z(\xi_k), \tag{1.12}$$

where $T_k(\xi) = \cos(k\cos^{-1}\xi)$ is the k^{th} Chebyshev polynomial and $\mathbf{D}$ being the Chebyshev spectral differentiation matrix whose entries are defined as ([9, 15, 85]) "

$$\left.\begin{array}{l} \mathbf{D}_{00} = \frac{2N^2+1}{6} \\ \mathbf{D}_{jk} = \frac{c_j}{c_k} \frac{(-1)^{j+k}}{\xi_j - \xi_k}, \;\; j \neq k; \;\; j,k = 0,1,2\cdots,N, \\ \mathbf{D}_{kk} = -\frac{\xi_k}{2(1-{\xi_k}^2)}, \;\; k = 1,2\cdots,N-1, \\ \mathbf{D}_{NN} = -\frac{2N^2+1}{6} \end{array}\right\} \tag{1.13}$$

" Substituting equations (1.11)-(1.12) into the given differential equation, we obtain the system of the algebraic equation gven by

$$\mathbf{A}_{r-1}\mathbf{X}_r = \mathbf{R}_{r-1}, \tag{1.14}$$

in which A_{r-1} is a square matrix of order $(N+1)\times(N+1)$ while X_r and R_{r-1} are $(N+1)^{th}$ order coloumn vectors. Writing the boundary conditions in terms of Chebyshev polynomials, incorporating them in the above system of equations and solving the reduced system of algebraic equations, we obtain the solution of the given differential equation. If the domain is $[a,b]$, then it will be transformed to the domain $[-1,1]$ by using the using suitable transformation.

1.6 Literature Review

The study of convective heat and mass transfer from various geometries, such as plate, wedge, cylinder, sphere, cone, etc. In particular, the convective heat and mass transfer from a vertical cone has fascinated much attention due to its vast application in the industrial and engineering processes. The most recent technological advancements have challenging applications in fluid flows past a cone. The cone geometry is useful for measuring the flow and rheological properties of soils and soft materials found in food and personal care product testing, where the cone penetration test is a typical quality control technique. It has demanding applications in a wide range of real-world situations, including health care and hospitality management systems, geosciences, energy storage systems, aeronautical engineer-

ing, development of electronic chips, astro-physics, space technology, hydrology, automotive engine oil controlling systems, environment controlling factors, nuclear safety and cleaning management systems, solar collectors, preparation of transmission missile gun operations, lubricating grease for seals, valves, and threaded connections, homeo-therapy treatment, radiology treatment, endoscopy scanning, dental applications paper production industries, etc,.

Laminar boundary-layer flows with similarity have long been used to investigate the effects of physical, dynamical, and thermal characteristics. When the similarity conditions are fulfilled, the complex system of partial differential equations regulating the flow is simplified into a system of ordinary differential equations, resulting in a significant mathematical simplification of the problem. Studies on existence of similarity solutions for isothermal, axi-symmetric and vertical cone problems have been attracted by several researchers over non-similarity solutions. Merk and Prins [51, 52] were the pioneers in the development of similarity solutions for the natural convection flow past a vertical cone considering an axisymmetric form. Braun *et al.* [8] discussed the natural convection similarity flows about two dimensional axisymmetric bodies with closed lower ends. Hering and Grosh [26] obtained the similarity solution for a non-isothermal right circular cone. Later, extensive studies on analytical and experimental studies are conducted for convective heat and mass transfer under varied conditions along a vertical cone. Kafoussias [32] scrutinized the consequence of mass transfer on a viscous fluid flow past a vertical cone due to buoyancy. Hossain and Paul[30] considered the laminar natural convection from a permeable vertical cone with non-uniform surface heat flux. Yih *et al.* [91] analyzed numerically the thermal radiation impact on mixed convection around an isothermal cone embedded in a porous medium.

Using similarity analysis, Ece [17] explored the impact of magnetic field on a laminar natural convection flow past a vertical cone subject to the mixed thermal boundary condition. Pop *et al.* [66] studied the steady mixed convection flow over an isothermal vertical cone using a boundary-layer assumption. Singh *et al.* [78] investigated the unstable mixed convection flow of viscous fluid over a vertical cone when the fluid in the external stream is set to be an impulsive motion. Ravindran *et al.* [69] investigated the mixed convective heat and mass transfer from a vertical cone. Patil *et al.* [64] analyzed numerically the effect of thermal and mass diffusion and linear chemical reaction on unstable mixed convection flow over a vertical cone. Ganapathirao *et al.* [20] considered a transient mixed convection laminar boundary layer flow on vertical cone with non-uniform surface mass transfer through slot while the cone's axis is in line of the flow. Palani and Ragavan [62] investigated the simultaneous influence of the transverse magnetic field, buoyancy, and chemical reaction

on the flow of natural convection heat and mass transfer past an isothermal vertical cone. Rosali *et al.* [71] studied the steady mixed convection boundary layer flow past a vertical cone embedded in a porous medium using convective boundary condition. Pullepu *et al.* [67] considered the simultaneous effects of heat absorption/generation and chemical reaction on unsteady laminar natural convective heat and mass transfer past a permeable vertical cone with uniform wall temperature and concentration in an incompressible viscous fluid. Kannan *et al.* [35] developed group transformation approach to study the effect of viscous dissipation on an unsteady free convection flow over a vertical cone with wall surface wall temperature varying as a power function of the distance from the apex. Meena *et al.* [50] investigated the effects of double dispersion and injection/suction on mixed convection flow over a vertical cone in a viscous fluid-saturated porous medium. Kannan *et al.* [34] discussed the outcome of heat sink/source and magnetic field on natural convection from a vertical cone with variable surface heat flux.

The properties of fluids, for instance, the viscosity and thermal conductivity, are well known to change with the temperature. Kays and Crawford [37] provided a variety of relationships between fluid physical properties and temperature. The enhancement of temperature in lubricating fluids generates internal friction, which modifies the viscosity of working fluid, which will no longer remain constant. A number of researchers have since been examining the impact of variable thermal conductivity and variable viscosity on the flow, heat transfer, and mass transfer in various physical configurations. Chen and Ren [42] studied the natural convection heat transfer and fluid flow past a vertical cone by expressing the viscosity as an inverse linear function of temperature. Hossain and Munir [29] considered the convection flow along a truncated cone with the viscosity depending on the temperature. Molla *et al.* [53, 54] provided the consequences of variable properties on the fluid flow past a sphere and horizontal circular cylinder. Rahman *et al.* [68] presented the effect of heat conduction and magnetic field on the free convection flow past a vertical flat plate by considering the thermal conductivity as a function of temperature. Shateyi and Motsa [77] numerically analyzed the viscous fluid flow and heat transfer past a semi-infinite unsteady stretching sheet in the presence of variable viscosity, variable thermal diffusivity, magnetic field, and Hall currents.

The influence of variable fluid properties on the non-linear stretching sheet has been explored by Khan *et al.* [40]. Umavathi *et al.* [89] undertaken the problem of free convection viscous fluid flow in a vertical channel with the effect of variable viscosity and thermal conductivity. Srinivasacharya and Jagadeeshwar [81] investigated viscous fluid flow over a sheet, which is stretching exponentially, presuming viscosity and thermal conductivity to be

dependent linearly on the temperature. Ahmed *et al.* [2] explained the impact of exothermic catalytic chemical reaction on the free convection flow of a viscous fluid past a curved surface where the viscosity and thermal conductivity are dependent on the temperature. The consequences of temperature-dependent viscosity on the free convective flow from a vertical cone, which is permable, with uniform heat flux has been analyzed by Hasan *et al.* [23]. Khan *et al.* [38] presented the irreversibility analysis of a boundary layer flow over a heated flat-plate with viscosity, which depends on temperature, and viscous dissipation.

The relationships amongst driving potentials and the fluxes are intricate as soon as heat and mass transfer exist concurrently in a flowing liquid. Energy fluxes have been discovered to be induced by both concentration and temperature gradients. These factors are mainly overlooked in heat and mass transfer studies because they are of a less significant with respect to order of magnitude than that of phenomena defined by Fourier's and Fick's principles. These influences, on the other hand, are categorized as 2^{nd} order manifestations and they could be important in fields such as petrology, geosciences, and hydrology. Eckert and Drake [18] discussed various illustrations of the diffusion-thermo effect. The Soret effect is utilized to separate isotopes and mixtures of gases with medium (N_2, air) molecular weights and very light (H_2, He) molecular weights. A considerable amount of research on Newtonian and non-Newtonian fluid flows in various geometries has been published in the literature, with a focus on the Soret and Dufour effects.

The impact of Dufour and Soret on the free convection heat and mass transfer past a vertical cone placed in a porous medium filled with Newtonian fluids has been analysed by Cheng *et al.* [12] . Cheng *et al.* [13] explored the cross-diffusion effects in double diffusion across a truncated vertical cone in a fluid-saturated porous medium with changeable wall temperature and concentration. Mahdy [43] obtained numerical solutions for the non-Newtonian fluid flow about a cylinder, which is permeable and stretching, with suction or blowing, as well as the Soret and Dufour effects. Sharma *et al.* [75] researched the significance of changeable viscosity, variable thermal conductivity, Soret, and Dufour on free convective flow past a vertical cone. Zuoco *et al.* [93] numerically analyzed the magnetic field, thermal diffusion, dissipative heat and Soret effects on an unsteady natural convective over a moving semi-infinite vertical permeable plate. Sivaraj *et al.* [79] analyzed the unsteady free convective flow over a moving flat plate and vertical cone with varying fluid properties and chemical reactions.

The influnce of cross-diffusion on the Blasius and Sakiadis flows has been examined by Oyem *et al.* [61]. Kaushik [36] studied an unsteady flow of a viscous incompressible fluid past a vertical cone with variable viscosity and thermal conductivity. Naseem *et al.*

[59] investigated the Dufour and Soret impacts on the magnetic nanofluid flow across a sheet stretching exponentially using variable thermal conductivity and diffusion coefficient. Patil *et al.* [63] investigated the unsteady double-diffusive mixed convection flow over an exponentially permeable vertical stretching surface in the presence of Darcy-Forchheimer, Dufour, and Soret effects. Ghoneim *et al.* [21] explored the Soret and Dufour effects along with interaction of thermal radiation and variable diffusivity through vertical cone. Das *et al.* [14] investigated the radiation, heat generation, Chemical reaction, magnetic field, Soret and Dufour effects on nonlinear convective flow of tangent hyperbolic nanofluid over a permeable stretching surface. Hazarika *et al.* [25] theoretically investigated the consequence of suction/injection, internal heat generation, chemical reaction and diffusion-thermo on a the flow of Cu–water nanofluid over a semi-infinite vertical surface.

There has recently been great interest in the mechanics governing the flow around a rotating cone. The broad rotating cone considered in this paper can be used to model the behavior of air flowing over the central nose cone of an aero-engine fan. The large half angles used in these nose cones are chosen to deflect the ensuing turbulent flow from entering the turbofan core, whilst also ensuring that sufficient amount of airflow is flowing into the fan blades. It is important due to environmental and noise concerns to understand the system that governs the intake of this airflow, with the aim to improve the efficiency of the system. Moreover, applications of heat and mass transfer from a rotating cone are used to design of canisters for nuclear reactor cooling system, nuclear waste disposal, and geothermal reservoirs. Hartnett and Deland [22] considered the impact of Prandtl number on the heat transfer by rotating bodies. Tien and Tsuji [84] theoretical analyzed the heat transfer effects on the laminar forced flow about a rotating cone. Krieth [31] presented the study of the flow and heat transfer in rotating systems. Himasekhar *et al.* [28] discussed analytically the flow past a vertical rotating cone for different values of Prandtl numbers. An effective solution method to solve the conjugate problems of forced convection in a boundary layer flow along a wedge and rotating cone was proposed by Yu *et al.* [92]. Takhar *et al.* [83] analysed the effect of magnetic field and time dependent angular velocity on the transient mixed convection flow over a rotating cone in an ambient fluid

An unsteady mixed convection flow over a rotating cone in a rotating viscous fluid with the free stream with time dependent angular velocities has been undertaken by Roy and Anilkumar [72]. The same authors dealt with the combined effects of thermal and mass diffusion on an unsteady mixed convection flow over a rotating cone in a rotating fluid [3]. Osalusi *et al.* [60]analysed the effect of viscous dissipation, Joule heating, Hall and ion-slip current on unsteady mixed convention magnetohydrodynamics flow on a rotating cone.

Turkyilmazoglu [86] obtained an analytical solution forthe steady flow of a viscous Newtonian fluid over a rotating cone Chamkha *et al.* [11] focused on the effects of magnetic field, chemical reaction, Soret and Dufour on unsteady mixed convection flow over a vertical cone rotating with a time-dependent angular velocity. Saleem and Nadeem [74] analysed the mutual effects of viscous dissipation and slip effects on a rotating vertical cone in a viscous fluid Malik*et al.* [47] examined the effects of temperature-dependent viscosity and thermal conductivity on the flow of a viscous fluid over a rotating vertical cone. Mallikarjuna *et al.* [48] analysed the importance of chemical reaction and magnetic field on the mixed convective flow past a rotating cone placed in a porous medium. Reddy and Sandeep [70] explored the effects of bioconvection, non linear thermal radiation, and cross diffusion effects on the heat and mass transfer behaviour of natural convective flow past a permeable rotating cone. Adachi *et al.* [1] studied experimentally the effect of viscosity on flow of pumping-up of liquid generated by a rotating cone at the liquid surface with various concentrations of glycerol aqueous solution. Sulochana *et al.* [82] investigated the effects of thermal radiation, chemical , magnetic field and Soret effects on the flow over a vertical rotating cone through porous medium. Sharma and Hemanta [76] considered the importance of chemical reaction, thermal radiation and heat absorption/ generation on the flow, heat and mass transfer about a rotating vertical cone.

The influences of traveling modes on the boundary layer flow over a rotating cone in a still fluid system has been analysed by Fildes *et al.* [19] . Hayat *et al.* [24] investigated the unsteady mixed convective magnetohydrodynamics chemically reactive flow of a viscous liquid over a rotating cone. Khan *et al.* [39] examined the thermo-diffusion, diffusion-thermo and viscous dissipation behaviors in mixed convection radiative flow by a rotating cone. Li *et al.* [41] explored the influence of heat source/sink, dissipation and binary chemical reaction on the entropy optimization in convective viscous fluid flows due to a rotating cone. Ullah *et al.* [88] presented instability analyses for cones rotating within magnetic field. Verma *et al.* [90] investigated the thermal radiation, Soret and Dufour effect on MHD flow about a rotating vertical cone. Mustafa *et al.* [57] considered the radiation, dissipation and nanofluid features on unsteady magnetohydrodynamics flow by a rotary cone.

1.7 The Aim of the Thesis

Several studies have introduced the temperature dependent properties and reported its significant influences over the flow characteristics. Further, it is clear that adequate literature

is not available to study the effect of temperature dependent viscosity and thermal conductivity on the convective flow of a viscous incompressible fluid along an isothermal vertical cone and rotating cone.

The aim of present thesis is to understand the usefulness of variable fluid properties, namely, variable viscosity and variable thermal conductivity on the viscous incompressible boundary layer flow over a vertical and rotating cone. The characteristics such as thermal radiation, corss-duffusion, thermal radiation and chemical reaction are included in our study. The problems considered deal with vertical and rotating cone geometries for the two cases: the surface is (i) maintained at uniform wall temperature and concentration conditions (ii) subjected to uniform heat and mass fluxes.

1.8 Overview of the Thesis

This thesis consists of FOUR parts and TEN chapters

Chapter 1 is an introductory chapter that gives insight for the study undertaken in the thesis. A review of relevant literature is outlined, emphasising the significance of the problems addressed in the thesis.

Part-II deals with the influence of variable properties on convective flow past a vertical cone. This consists of four chapters i.e. Chapter 2 to Chapter 5 . In these chapters, the governing equations, which are non-linear in nature, and their corresponding boundary conditions are first transformed into non - dimensional forms using similarity variables. The resulting nonlinear system of equations is linearized by using the successive linearisation and then the linearized system is solved by using Chebyshev spectral collocation. The computed numerical findings are compared and found to be in good agreement with earlier findings as special cases.

In Chapter - 2, the laminar free convection flow across a vertical cone is investigated by presuming the temperature dependent viscosity and thermal conductivity. Similarity transformations are utilized to reduce the flow governing equations into ordinary differential equations. The effects of variable viscosity and thermal conductivity parameters, Prandtl number on the coefficient of skin friction and local Nusselt number are analysed.

Chapter - 3 deals with influence of the variable properties on the boundary layer flow past a vertical cone. Similarity transformations are utilized to reduce the equations describing

the flow into ordinary differential equations. The non-dimensional equations are linearized using successive linearization procedure and then the solution of the consequent system is found using Chebyshev spectral method.

Chapter - 4 considers the free convection flow across a vertical cone by presuming the viscosity and thermal conductivity varies with temperature in the manifestation of Soret and Dufour effects.

The effects of Soret and Dufour on the boundary layer flow across a vertical cone is investigated by assuming the viscosity and thermal conductivity varies with temperature is presented in Chapter - 5.

Part-III deals with the influence of variable properties on convective flow past a rotating cone. This consists of four Chapters i.e. chapter 6 to chapter 9 . In these chapters, the nonlinear governing nonlinear system of equations is linearized using successive linearisation and then solved by using Chebyshev spectral collocation.

In chapter - 6, the laminar free convection flow across a rotating cone is investigated by taking the temperature dependent viscosity and thermal conductivity. Similarity transformations are utilized to reduce the equations governing the flow into ordinary differential equations. The non-dimensional equations are linearized using successive linearization procedure and then the solution of the consequent system is found using Chebyshev spectral method.

Chapter - 7 deals with the influence of the variable properties on boundary layer flow past a rotating cone.

The cross diffusion effects on the free convection flow across a rotating cone with temperture dependent viscosity and thermal conductivity is considered in Chapter - 8.

Chapter - 9 explores the influence of chemical and thermal radiation on the boundary layer flow across a rotating cone by taking the viscosity and thermal conductivity as a function of temperature.

Part - IV consists of single chapter i.e. Chapter - 10. The key conclusions of the previous chapters are summarised in this chapter, along with possible future research directions.

In all the above chapters (Chapter 2 to Chapter 9), the similarity transformations are employed to convert the governing system of partial differential equations to nonlinear ordinary differential equations. Initially, the resulting equations are linearized using the successive linearization method. Finally, the obtained linear equations are solved using the Chebyshev

collocation method.

A list of references is provided at the end of the thesis and is organised alphabetically.

A significant portion of the work in the thesis has been published or accepted for publication in reputable international journals. The remaining is communicated for potential publication. The details are presented below.

List of papers Published

1. "Influence of Variable fluid properties on the boundary layer flow past a vertical cone with Soret and Dufour effects", ***Journal of the Xidian University***, Vol.16(8) : 222-233, : 2022, doi.org/10.37896/jxu16.8/023.

2. "Combined influence of cross-diffusion and variable fluid properties on free convective flow past avertical cone ", ***Heat Transfer***, 2022;1-22. doi:10.1002/htj.22738

List of papers Accepted

3. "The impact of variable fluid properties on natural convective flow past a vertical cone", ***Journal of Applied Mathematics and Computational Mechanics***

List of papers communicated

4. "The boundary layer flow past a vertical cone with variable fluid properties", ***Applications and Applied Mathematics: An International Journal***

5. "The effect of temperature dependent viscosity and thermal conductivity on the free convective flow past a rotating cone", ***International Journal of Applied and Computational Mathematics***

6. "The cross-diffusion effects on the free convection flow across a rotating cone with variable fluid properties", ***Computational Thermal Science***

7. "The influence of chemical and thermal radiation on the boundary layer flow across a rotating cone with variable fluid properties", ***Heat Transfer***

Chapter 2

The impact of variable fluid properties on natural convection flow past a vertical cone [1]

2.1 Introduction

Free convection flows have received the most attention because they appear in nature in addition to in scientific and engineering applications. Temperature differences produce buoyancy forces, which cause free convection when a heated surface comes into contact with a fluid. The atmospheric circulation, which includes hurricanes, blizzards, and monsoons, is driven by free convection. Mainly these type of heat transfer problems are encountered in the design of nuclear reactors, solar power collectors, power transformers, steam generators, etc. Moreover, free convection flow past a vertical cone has attracted much attention due to its vast application in industrial and engineering processes. Several researchers considered the free convection flow over a vertical cone in Newtonian and non-Newtonian fluid

The majority of researchers have only examined the influence of constant viscosity and thermal conductivity on the boundary layer formed by a vertical cone. However, it is well understood that fluid viscosity varies with temperature. Variable thermal conductivity is used in a variety of engineering applications, including heat transmission in furnaces, boilers, porous burners, volumetric solar receivers, and fibrous and foam insulations. A number of researchers have been examining the effect of variable thermal conductivity and viscosity on

[1] Accepted for publication in "**Journal of Applied Mathematics and Computational Mechanics**"

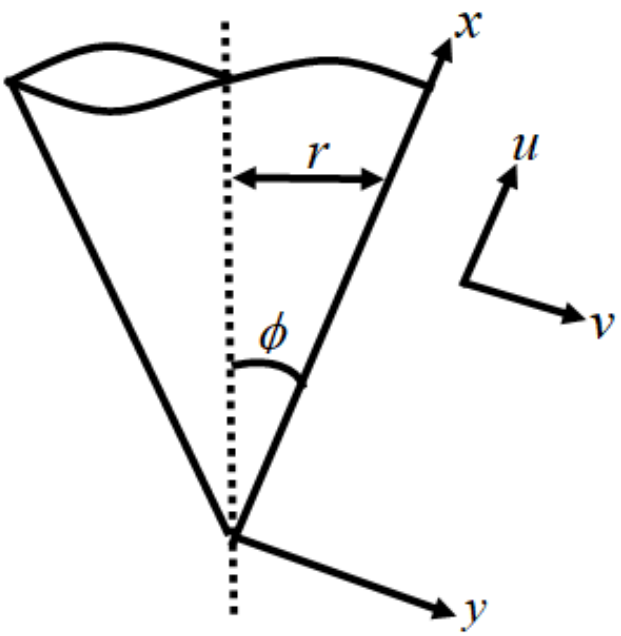

Figure 2.1: "Schematic of the problem".

flow, heat transfer, and mass transfer in a variety of physical configurations. Sivaraj *et al.* [79] analyzed the unsteady free convective flow over a moving flat plate and vertical cone with varying fluid properties and chemical reactions. Recently, Hasan *et al.* [23] investigated the effects of temperature-dependent viscosity on the natural convection flow from a vertical permeable circular cone with uniform heat flux.

In this chapter, a free convective flow of an incompressible viscous fluid past an isothermal vertical cone is investigated with variable viscosity and variable thermal conductivity. The constant wall temperature (CWT) and constant wall heat flux (CHF) conditions are used as temperature boundary conditions at the surface of the cone. The successive linearization method is applied to linearize the governing nonlinear differential equations of the flow. The numerical solution for the resulting linear equations is obtained through the Chebyshev spectral collocation method. The impact of significant parameters on the velocity and temperature, in addition to heat and mass transfer rates, is evaluated and represented graphically for the CWT and CHF conditions.

2.2 Mathematical Formulation

Consider an incompressible, steady-state and laminar flow of Newtonian fluid along a vertical down-pointing cone with local radius r and half-angle ϕ. Choose a coordinate system in which the origin is taken as the apex of the cone, the x-axis runs along the cone's surface, and the y-axis is upright to it, as depicted schematically in Fig. (2.1). The local radius at a point located and the radius of a cone can be guesstimated by $r = (xsin\phi)$. The ambient temperature is assumed as T_∞.

Applying Boussinesq approximation and utilizing the boundary layer assumptions, the equations describing the flow are.

$$\frac{\partial}{\partial x}(ur) + \frac{\partial}{\partial y}(vr) = 0 \tag{2.1}$$

$$\rho\left(u\frac{\partial u}{\partial x} + v\frac{\partial u}{\partial y}\right) = \frac{\partial}{\partial y}\left(\mu\frac{\partial u}{\partial y}\right) + \rho g\beta\cos\phi(T - T_\infty) \tag{2.2}$$

$$u\frac{\partial T}{\partial x} + v\frac{\partial T}{\partial y} = \frac{1}{\rho c_p}\frac{\partial}{\partial y}\left(k\frac{\partial T}{\partial y}\right) \tag{2.3}$$

where $(u, v, 0)$ signify the velocity vector, T denotes the temperature of the fluid, g denotes the gravitational acceleration, μ represents the variable viscosity, ρ represents the fluid density, β denotes the coefficient of thermal expansion, C_p represents the specific heat and, k represents the variable thermal conductivity of the fluid.

The viscosity and thermal conductivity are considered to be a linear function of the temperature [5] and are given by

$$\mu = \mu_\infty[1 + \lambda(T_\infty - T) \quad \text{and} \quad k = k_0[1 + \gamma(T - T_\infty)], \tag{2.4}$$

where μ_∞ and, k_0 represent the absolute viscosity and the thermal conductivity of the fluid, respectively, λ and γ are constants.

No-slip at the surface of the cone and no stream condition in the ambient medium are the associated conditions on the boundary for the flow configuration. These are expressed as follows.

$$u = 0, \quad v = 0 \quad \text{at} \quad y = 0 \quad \text{and} \quad u \to 0 \quad \text{as} \quad y \to \infty \tag{2.5}$$

In addition, for the temperature on the surface of the cone, one can either have constant temperature T_w (CWT) or a constant heat flux q_w (CHF). Thus, the conditions for the tem-

perature on the boundary conditions are written as

$$\textbf{Type - I} : T = T_w \quad \text{at} \quad y = 0 \tag{2.6}$$

$$\textbf{Type - II} : k\frac{\partial T}{\partial y} = q_w \quad \text{at} \quad y = 0 \tag{2.7}$$

and far away from the cone, the temperature of the free stream is constant i.e. $T \to T_\infty$, as $y \to \infty$

The stream function is defined in context of Eq. (2.1) as $u = \frac{1}{r}\frac{\partial \psi}{\partial y}$, $v = -\frac{1}{r}\frac{\partial \psi}{\partial x}$

For type – I boundary conditions, we define the following similarity transformations

$$\xi = \frac{x}{L}, \quad \eta = \frac{y}{L}\left(\frac{Gr}{\xi}\right)^{\frac{1}{4}}, \quad \psi = r\nu Gr^{\frac{1}{4}}\xi^{\frac{3}{4}} f(\eta), \quad T = T_\infty + (T_w - T_\infty)\theta(\eta), \tag{2.8}$$

where $G_r = \frac{L^3 g\beta \cos\phi (T_w - T_\infty)}{\upsilon^2}$ is the Grashof number

For type – II boundary conditions, the similarity transformations are given by

$$\xi = \frac{x}{L}, \quad \eta = \frac{y}{L}\left(\frac{Gr}{\xi}\right)^{\frac{1}{5}}, \quad \psi = r\nu Gr^{\frac{1}{5}}\xi^{\frac{4}{5}} f(\eta), \quad T = T_\infty + \frac{q_w L}{k} Gr^{-\frac{1}{5}}\xi^{\frac{1}{5}}\theta, \tag{2.9}$$

where $G_r = \frac{L^2 g\beta \cos\phi q_w}{\nu^2}$ is the Grashof number and L is the characterstic length.

Applying the similarity transformations Eqs. (2.9) and (2.8) in the Eqs. (2.2) and (2.3), we get the non-dimensional equations are shown below

For type - I boundary conditions:

$$(1+A)f''' - A\theta f''' - A\theta' f'' + \frac{7}{4}ff'' - \frac{1}{2}f'^2 + \theta = 0 \tag{2.10}$$

$$\frac{1}{\mathrm{Pr}}\theta'' + \frac{\in}{\mathrm{Pr}}(\theta\theta'') + \frac{\in}{\mathrm{Pr}}(\theta')^2 + \frac{7}{4}f\theta' = 0 \tag{2.11}$$

For type - II boundary conditions

$$(1+A)\, f''' + \frac{9}{5}ff'' - \frac{3}{5}f'^2 - A\theta' f'' - A\theta f''' + \theta = 0 \tag{2.12}$$

$$\frac{1}{\Pr}\theta'' + \frac{\in}{\Pr}\theta\theta'' + \frac{1}{\Pr} \in \theta'^2 - \frac{1}{5}f'\theta + \frac{9}{5}f\theta' = 0 \tag{2.13}$$

where $\Pr = \dfrac{\upsilon}{\alpha_0}$ denotes the Prandtl number, A denotes the viscosity parameter and ϵ denotes the thermal conductivity parameter.

The dimensionless form of conditions on the boundary are

$$f(0) = f'(0) = 0, \quad \theta(0) = 1, \quad f'(\infty) = \theta(\infty) = 0 \quad \text{for CWT case.} \tag{2.14}$$

$$f(0) = f'(0) = 0, \quad \theta'(0) = -1, \quad f'(\infty) = \theta(\infty) = 0 \quad \text{for CHF case.} \tag{2.15}$$

The most important results of practical interests are the local skin-friction coefficient and local rate of heat-transfer in terms of Nusselt number. The non-dimensional form of skin-friction coefficient C_f and Nusselt number (Nu) for CWT boundary conditions are

$$C_f^I = Gr^{\frac{3}{4}}\xi^{-\frac{1}{4}}f''(0), \quad \text{and} \quad Nu^I = -Gr^{\frac{1}{4}}\xi^{-\frac{1}{4}}\theta'(0), \tag{2.16}$$

and for CHF boundary conditions are

$$C_f^{II} = Gr^{\frac{3}{5}}\xi^{-\frac{2}{5}}f''(0), \quad \text{and} \quad Nu^{II} = Gr^{\frac{1}{5}}\xi^{\frac{4}{5}}\frac{1}{\theta(0)}. \tag{2.17}$$

2.3 Methodology

The set of differential equations (2.10) – (2.11) and (2.12) – (2.13) are linearized by means of a successive linearization method (SLM) [55].The solutions of the ensuing linearized equations are attained by employing the Chebyshev spectral method [7].

Using SLM, unknown functions $f(\eta)$ and $\theta(\eta)$ are taken as

$$f(\eta) = f_i(\eta) + \sum_{m=0}^{i-1} f_m(\eta), \quad \theta(\eta) = \theta_i(\eta) + \sum_{m=0}^{i-1} \theta_m(\eta) \tag{2.18}$$

where $f_i(\eta)$ and $\theta_i(\eta)$ (i = 1, 2, . . .) are unknown function and $f_m(\eta)$ and $\theta_m(\eta)$ $(m \geq 1)$ are guesstimates which can be determined by repeatedly solving the linear terms of the system of equations obtained by substituting Eq. (2.18) in the Eqs.(2.10)-(2.11) and Eqs. (2.12)-(2.13). The underlying idea of the SLM is that f_i and θ_i are quite small even as i turns out to be large, so nonlinear terms in f_i and θ_i and their derivatives are reasoned to

be infinitesimal and thus ignored.

The initial guesses $f_0(\eta)$ and $\theta_0(\eta)$ are selected to match the conditions on the boundary (2.14) and (2.15). The iterative solutions f_i and θ_i are attained by recursively solving the following linearized equations for CWT boundary conditions.

$$a_1 f_i^{'''} + a_2 f_i^{''} + a_3 f_i^{'} + a_4 f_i + a_5 \theta_i^{'} + a_6 \theta_i = a_7 \tag{2.19}$$

$$b_1 f_i + b_2 \theta_i^{''} + b_3 \theta_i^{'} + b_4 \theta_i = b_5 \tag{2.20}$$

The linearized equations for CHF boundary conditions are

$$c_1 f_i^{'''} + c_2 f_i^{''} + c_3 f_i^{'} + c_4 f_i + c_5 \theta_i^{'} + c_6 \theta_i = c_7, \tag{2.21}$$

$$d_1 f_i^{'} + d_2 f_i + d_3 \theta_i^{''} + d_4 \theta_i^{'} + d_5 \theta_i = d_6 \tag{2.22}$$

where

$$a_1 = c_1 = (1+A) - A(\sum_{m=0}^{i-1} \theta_m),\ a_2 = \frac{7}{4}\sum_{m=0}^{i-1} f_m - A\sum_{m=}^{i-1} \theta_m{}^{'},\ a_3 = -\sum_{m=0}^{i-1} f_m{}^{'},$$

$$a_4 = 7/4 \sum f_m^{''}, a_5 = c_5 = -A\sum_{m=0}^{i-1} f_m{}^{''}, a_6 = c_6 = 1 - A(\sum_{m=0}^{i-1} f_m{}^{''}),$$

$$a_7 = \left(-(1+A) + A\sum_{m=0}^{i-1}\theta_m\right) f_m^{'''} + \left(A\sum_{m=0}^{i-1}\theta_m^{'} - \frac{7}{4}\sum_{m=0}^{i-1} f_m\right) f_m^{''} + \frac{1}{2}\left(\sum_{m=0}^{i-1} f_m^{'}\right)^2 - \theta_m$$

$$b_1 = \frac{7}{4}\sum_{m=0}^{i-1}\theta_m^{'}, b_2 = d_3 = \frac{1}{\mathrm{Pr}} + \frac{\in}{\mathrm{Pr}}\sum_{m=0}^{i-1}\theta_m,$$

$$b_3 = \frac{2\in}{\mathrm{Pr}}\sum_{m=0}^{i-1}\theta_m^{'} + \frac{7}{4}\sum_{m=0}^{i-1} f_m, \quad b_4 = \frac{\in}{\mathrm{Pr}}\sum_{m=0}^{i-1}\theta_m^{'}$$

$$b_5 = \left(-\frac{1}{\mathrm{Pr}} - \frac{\in}{\mathrm{Pr}}(\sum_{m=0}^{i-1}\theta_m)\right)\sum_{m=0}^{i-1}\theta_m{}^{''} - \frac{\in}{\mathrm{Pr}}\left(\sum_{m=0}^{i-1}\theta_m^{'}\right)^2 - \frac{7}{4}\left(\sum_{m=0}^{i-1} f_m\right)\left(\sum_{m=0}^{i-1}\theta_m^{'}\right)$$

$$c_2 = \frac{9}{5}\sum f_m - A\sum \theta_m^{'},\ c_3 = -\frac{6}{5}\sum f_m^{'}, c_4 = \frac{9}{5}\sum f_m^{''}$$

$$c_7 = -(1+A)\sum f_m^{'''} - \frac{9}{5}\sum f_m \sum f_m^{''} + \frac{3}{5}\sum \left(f_m^{'}\right)^2 + A\theta_m^{'}\sum f_m^{''} + A\sum \theta_m \sum f_m^{''} - \sum \theta_m$$

$$d_1 = -\frac{1}{5}\theta_m,\ d_2 = \frac{9}{5}\theta_m^{'}, d_4 = \frac{2\in}{\mathrm{Pr}}\sum \theta_m^{'} + \frac{9}{5}\sum f_m, \quad d_5 = \frac{\in}{\mathrm{Pr}}\sum \theta_m^{''} - \frac{1}{5}\sum f_m^{'}$$

$$d_6 = -\frac{1}{\mathrm{Pr}}\sum \theta_m^{''} - \frac{\in}{\mathrm{Pr}}\sum \theta_m \sum \theta_m^{''} - \frac{\in}{\mathrm{Pr}}\left(\sum \theta_m^{'}\right)^2 + \frac{1}{5}\sum \theta_m \sum f_m^{'} - \frac{9}{5}\sum f_m \sum \theta_m^{'}$$

The equivalent conditions to (2.14) and (2.15)

$$f_i(0) = f_i^{'}(0) = f_i^{'}(\infty) = \theta_i(\infty) = 0,\ \theta(0) = 1 \tag{2.23}$$

The solution to the linearized Equations (2.19) - (2.22) are achieved by means of the Chebyshev collocation method which is constructed on the Chebyshev polynomials. In this problem, the domain of the solution $[0, \infty]$ is transformed to $[0, L]$, where L is a constant utilized to acquire the ambient boundary conditions. To apply this method, $[0, L]$ is again changed to [-1, 1] by using the mapping

$$\frac{\eta}{L} = \frac{\xi + 1}{2}, \quad -1 \leq \xi \leq 1 \tag{2.24}$$

The functions f_i and θ_i are approximated at the following collocation points due to Gauss-Lobatto

$$\xi_j = \cos\frac{\pi j}{N}, \quad j = 0, 1, 2, 3.....N \tag{2.25}$$

as

$$f_i(\xi) = \sum_{k=0}^{N} f_i(\xi_K)T_k(\xi_j), \quad \theta_i(\xi) = \sum_{k=0}^{N} \theta_i(\xi_k)T_k(\xi_j), \quad j = 0, 1, 2...N \tag{2.26}$$

where $T_k(\xi) = \cos\left[k\cos^{-1}(\xi)\right]$ is the k^{th} degree Chebyshev polynomial.

r^{th} derivative of f_i and θ_i are approximated from

$$\frac{d^r f_i}{d\eta^r} = \sum_{k=0}^{N} D^r_{kj} f_i(\xi_k), \quad \frac{d^r \theta_i}{d\eta^r} = \sum_{k=0}^{N} D^r_{kj} \theta_i(\xi_k), \quad j = 0, 1, 2...N \tag{2.27}$$

where $D = \frac{2}{L} D$ with D is the Chebyshev spectral differentiation matrix.

Substitution of Eqs. (2.26)-(2.27) into Eqs. (2.19)- (2.20) and (2.21) - (2.22) gives the equation in matrix form as

$$A_{i-1} X_i = R_{i-1} \tag{2.28}$$

where A_{i-1} is a square matrix of order $(2N + 2)$ and X_i and R_{i-1} are column matrices of order $(2N + 2)$ given by

$$A_{i-1} = \begin{pmatrix} A^{(i)}_{11} & A^{(i)}_{12} \\ A^{(i)}_{21} & A^{(i)}_{22} \end{pmatrix}, X_i = \begin{pmatrix} F_i \\ \Theta_i \end{pmatrix}, R_{i-1} = \begin{pmatrix} r^{(i)}_1 \\ r^{(i)}_2 \end{pmatrix} \tag{2.29}$$

where

$$F_i = [f_i(\xi_0), f_i(\xi_1), ..., f_i(\xi_{N-1}), f_i(\xi_N)]^T,$$

$$\Theta_i = [\theta_i(\xi_0), \theta_i(\xi_1), .., \theta_i(\xi_{N-1}), \theta_i(\xi_N)]^T,$$

$$A^{(1)}_{11} = a_1 D^3 + a_2 D^2 + a_3 I, A^{(1)}_{12} = a_4 D + a_5 I,$$

A

$$^{(1)}_{21} = b_1 I, A^{(1)}_{22} = b_2 D^2 + b_3 D + b_4 I$$

$$r^{(1)}_1 = [a_6(\xi_0), a_6(\xi_1), ..., a_6(\xi_{N-1}), a_6(\xi_N)]^T,$$

$$r^{(1)}_2 = [b_5(\xi_0), b_5(\xi_1), ..., b_5(\xi_{N-1}), b_5(\xi_N)]^T,$$

$$A^{(2)}_{11} = c_1 D^3 + c_2 D^2 + c_3 I, A^{(2)}_{12} = c_4 D + c_5 I,$$

$$A^{(2)}_{21} = d_1 D + d_2 I, A^{(2)}_{22} = d_3 D^2 + d_4 D + d_5 I$$

$$r^{(1)}_2 = [c_6(\xi_0), c_6(\xi_1), ..., c_6(\xi_{N-1}), c_6(\xi_N)]^T,$$

$$r^{(2)}_2 = [d_6(\xi_0), d_6(\xi_1), ..., d_6(\xi_{N-1}), d_6(\xi_N)]^T$$

where the superscript T stands for transpose, I is the identity, and O is the zero matrix. Finally, the solution is given by

$$X_i = A^{-1}_{i-1} R_{i-1} \tag{2.30}$$

2.4 Results and Discussion

The present study computes the velocity component $f^{'}$, the temperature θ, local Nusselt Number N_u, the coefficient of local skin friction C_f for diverse values of viscosity parameter A, thermal conductivity parameter $\in$ for constant wall temperature and heat flux cases are depicted graphically.

The impact of viscosity parameter A on the velocity component, temperature, coefficient of skin friction, and heat transfer rate is depicted in Fig.2.2 for type – I boundary conditions. It is detected from Fig.2.2(a) that the velocity rises near the cone, reaches its extreme value and then declines gradually to zero as $\eta \to \infty$. Furthermore, it is perceived that for enhancing values of A, the velocity reduces near the cone and enhances away from the cone. The temperature decreases slightly for an increase in A as portrayed in Fig. 2.2(b). As shown in Fig.2.2(c), increasing A increases the skin friction coefficient. The rate of heat transfer decreases as A increases as presented in the Fig.2.2(d).

The variation of f', θ, C_f and Nu with the thermal conductivity parameter $\in$ is given in Fig. 2.3 for type – I boundary conditions. Figures. 2.3(a) and 2.3(b) exhibit that as the value of $\in$ grows, so do the velocity f' and the temperature θ. The coefficient of skin friction is increasing, whereas the rate of heat transfer is decreasing for rising values of $\in$ as shown in Figs. 2.3(c) ad 2.3(d).

Figure 2.4 presents the influence of viscosity parameter A on the velocity component, temperature, coefficient of skin friction, and heat transfer rate for type – II boundary conditions. The impact of the viscosity parameter is less significant in comparison to the type – I boundary conditions, as seen in Fig. 2.4. For increasing values of A, the velocity enhances adjacent to the cone and decays away from the cone. The temperature is also decreasing for increasing values of A as revealed in Fig. 2.4(b). As seen in Fig. 2.4(c), increasing A slightly enhances the skin friction coefficient. As A increases, so does the heat transfer rate as presented in Fig. 2.4(d)

The variation of the velocity component, temperature, coefficient of skin friction, and Nusselt number with the thermal conductivity parameter $\in$, is shown in Fig. 2.5 for type – II boundary conditions. According to Figure 2.5(a), velocity declines with enhancing the thermal conductivity parameter. Fig. 2.5(b) reveals that the effect of $\in$ on the temperature is not very significant. The skin friction coefficient is decreasing, whereas the Nusselt number is escalating for increasing values of $\in$ as shown in Figs.2.5(c) ad 2.5(d).

2.5 Conclusion

The free convection flow across a vertical cone is investigated under the supposition that viscosity and thermal conductivity change with temperature. Similarity transformation is utilized to convert the equations administering the flow into ordinary differential equations. The non-dimensional equations are linearized by employing a successive linearization procedure, and then the solution of the consequent system is found using the Chebyshev spectral method.

- If the viscosity parameter is enhanced, the velocity adjacent to the cone surface increases, while the reverse tendency is detected sufficiently away from the cone surface.
- The local heat transfer rate decreases with increasing the viscosity and thermal conductivity parameters for CWT conditions but the reverse tend is noticed for CHF conditions.
- For CWT state, an improvement in viscosity and thermal conductivity infers to a rise in the coefficient of the skin friction, whereas for CWF conditions, the opposite is the case.

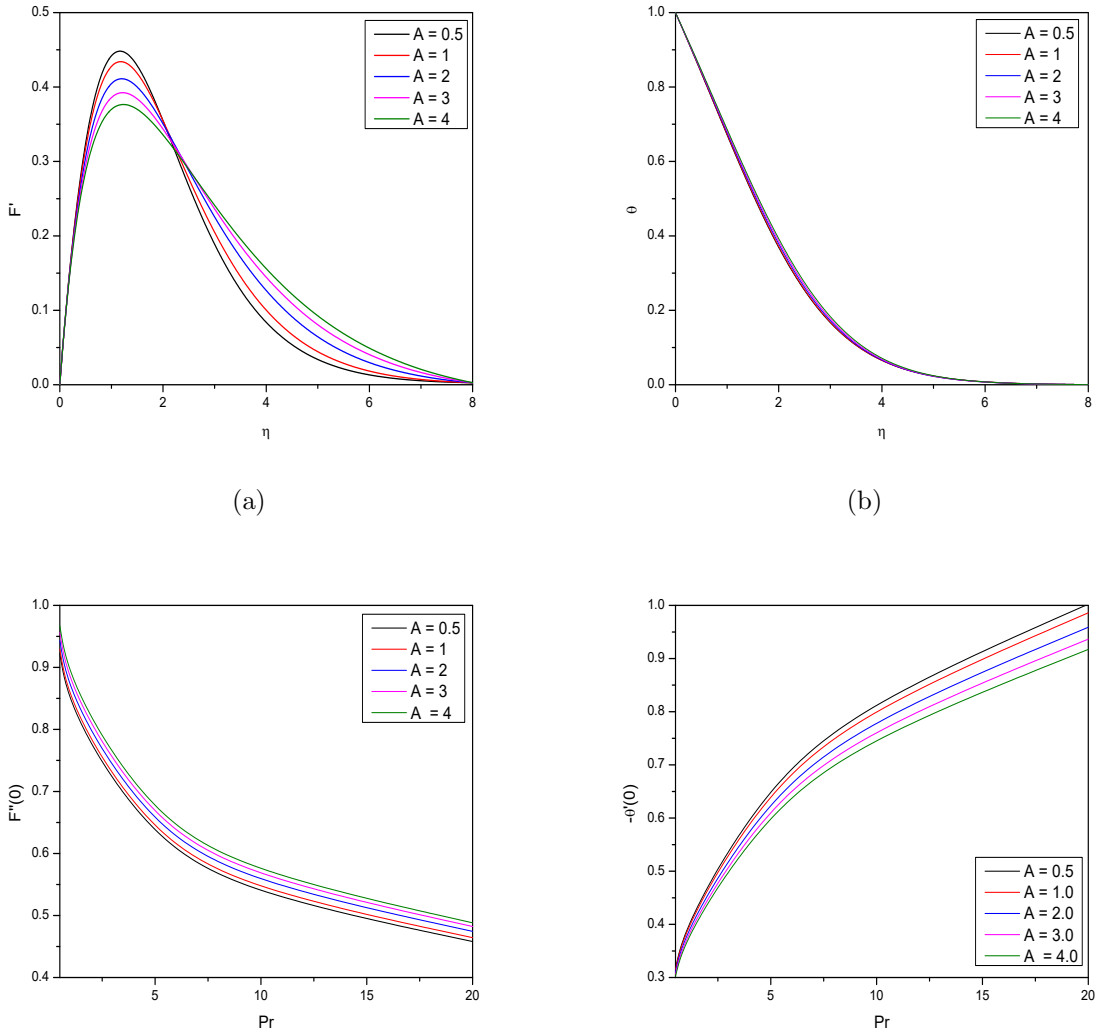

(a) (b)

(c) (d)

Figure 2.2: "Effect of A on the Velocity, Temperature, skin friction coefficient and Nusselt number for CWT boundary conditions".

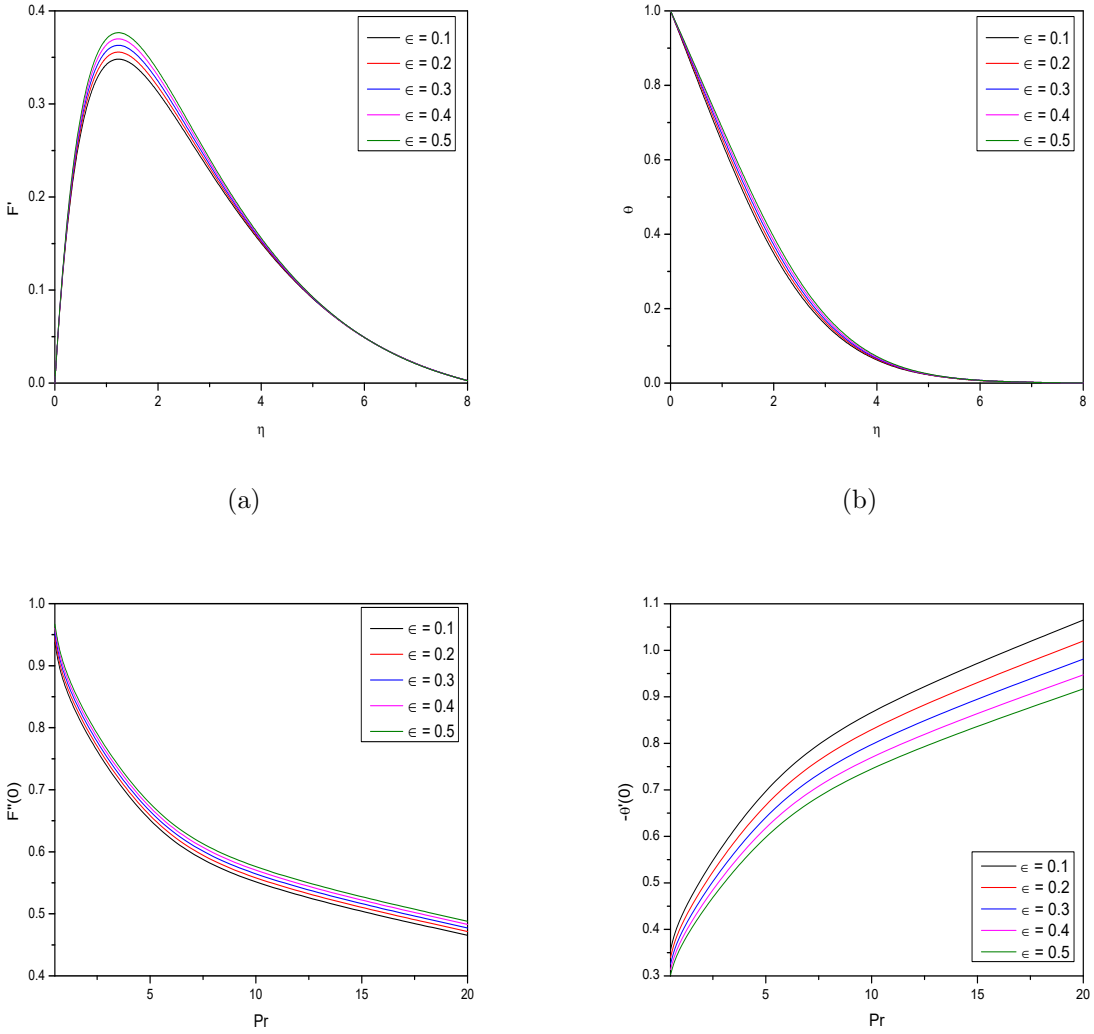

(a) (b)

(c) (d)

Figure 2.3: "Effect of $\in$ on the Velocity, Temperature, skin friction coefficient and Nusselt number for CWT boundary conditions".

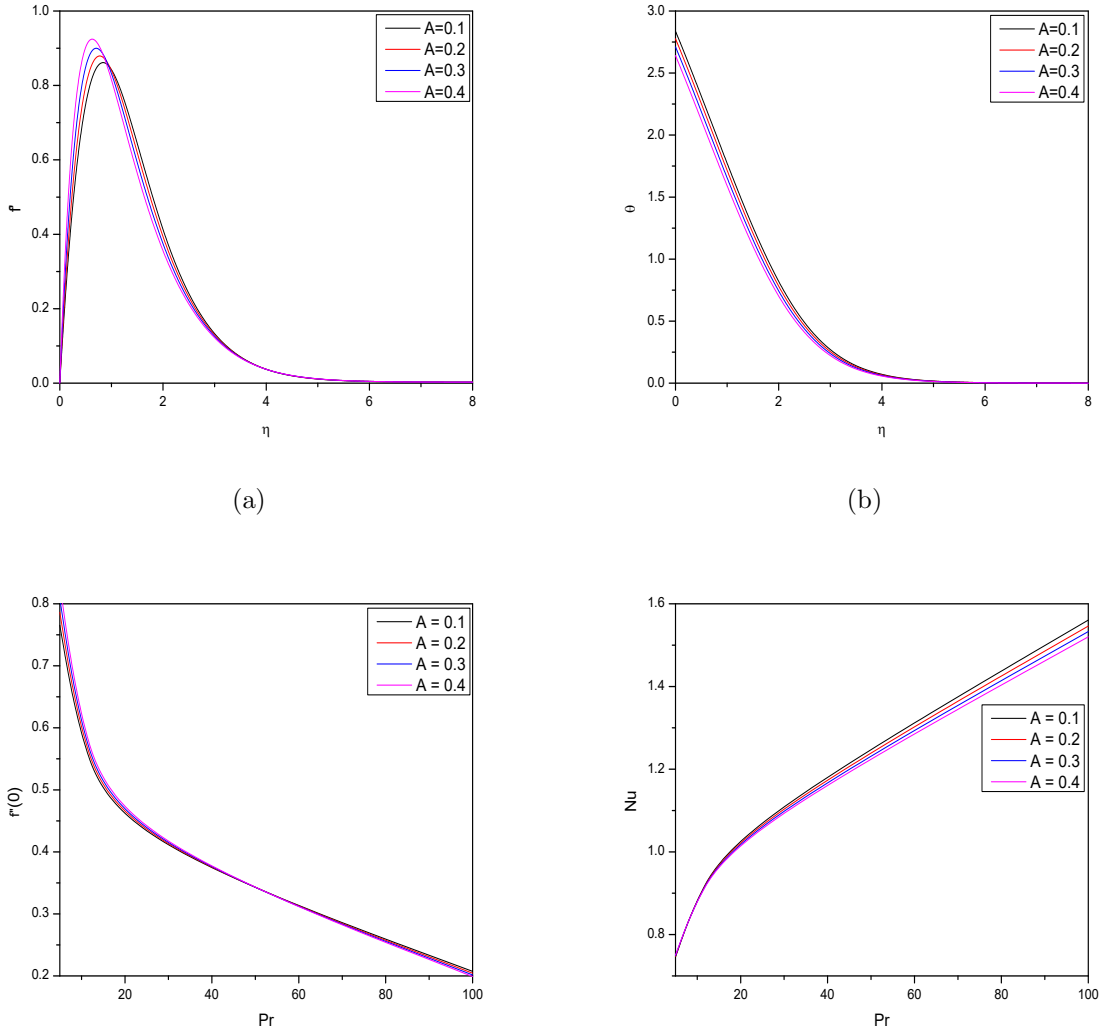

(a) (b)

(c) (d)

Figure 2.4: "Effect of A on the Velocity, Temperature, skin friction coefficient and Nusselt number for CHF boundary conditions".

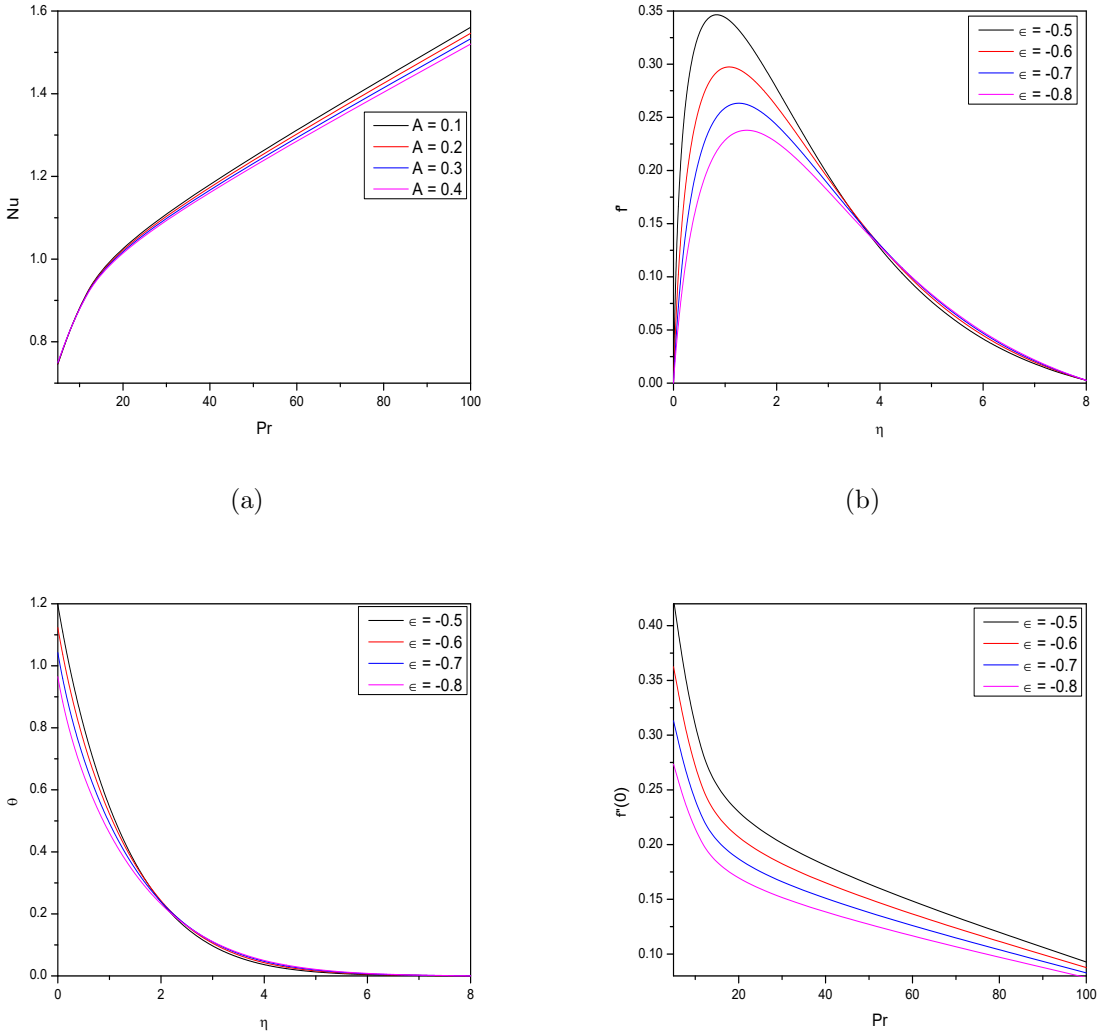

(a) (b)

(c) (d)

Figure 2.5: "Effect of $\in$ on the Velocity, Temperature, skin friction coefficient and Nusselt number for CHF boundary conditions".

Chapter 3

The Boundary Layer Flow Past a Vertical Cone with Variable Fluid Properties. [1]

3.1 Introduction

The theory of boundary layer has recently gained prominence due to its multiple uses in engineering breakthroughs and industrial operations. The determination of friction drag on bodies in a flow is an essential application of boundary layer theory. Prandtl developed the boundary layer theory in order to investigate the flow structure of viscous fluids near solid boundaries. Blasius [6] made an early contribution to fluid dynamics by solving the renowned boundary layer equation for a flat moving plate problem and discovering a power series solution to the model. Analysis of laminar boundary layer flow about a vertical cone in a uniform stream of fluid continue to gain significant attention due to its usefulness in many practical applications in a wide range of engineering systems. Patrulescu *et al.* [65] examined the persistent mixed convection boundary layer movement from such a cone's vertical frustum. Ganapathirao *et al.* [20] produced an unsteady mixed convection laminar boundary layer flow over a vertical cone with non-uniform surface mass transfer through slot while the cone's axis is in line with the flow. Rosali *et al.* [71] initiated a convective boundary layer flow past a vertical cone embedded in a porous medium. Khan *et al.* [38] presented the entropy generation of an incompressible boundary layer flow over a heated flat-plate with

[1] Communicated to "**Applications and Applied Mathematics: An International Journal**"

temperature dependent viscosity and viscous dissipation.

In this chapter, the effect of variable viscosity and variable thermal conductivity on the boundary layer flow of an incompressible viscous fluid past an vertical cone is considered. The constant wall temperature (CWT) and constant wall heat flux (CHF) conditions are used as temperature boundary conditions at the surface of the cone. The successive linearization method is applied to linearize the governing nonlinear differential equations of the flow. The numerical solution for the resulting linear equations is obtained through the Chebyshev spectral collocation method. The impact of significant parameters on the velocity and temperature, in addition to heat and mass transfer rates, is evaluated and represented graphically for the CWT and CHF conditions.

3.2 Mathematical Formulation

Consider an incompressible boundary layer flow of viscous fluid along a vertical down-pointing cone with local radius r and half-angle ϕ under steady state and laminar flow conditions. The coordinate system and physical model are as depicted in Fig. (2.1). Apart from the assumptions made in Chapter - 2, here we assume that the ambient velocity of the fluid is U_∞ without Boussinesq approximation.

Using the boundary layer assumptions, the equations describing the flow are:

$$\frac{\partial}{\partial x}(ur) + \frac{\partial}{\partial y}(vr) = 0 \tag{3.1}$$

$$\rho\left(u\frac{\partial u}{\partial x} + v\frac{\partial u}{\partial y}\right) = \frac{\partial}{\partial y}\left(\mu\frac{\partial u}{\partial y}\right) \tag{3.2}$$

$$u\frac{\partial T}{\partial x} + v\frac{\partial T}{\partial y} = \frac{1}{\rho c_p}\frac{\partial}{\partial y}\left(k\frac{\partial T}{\partial y}\right) \tag{3.3}$$

The quantities appearing in the above equations are already defined in Chapter - 2.

The viscosity and thermal conductivity are considered to be a linear function of the temperature [5] and are given by

$$\mu = \mu_\infty[1 + \lambda(T_\infty - T) \quad \text{and} \quad k = k_0[1 + \gamma(T - T_\infty)], \tag{3.4}$$

where μ_∞ and, k_0 represent the absolute viscosity and the thermal conductivity of the fluid, respectively, λ and γ are constants.

The boundary conditions for the velocity are no slip condition and uniform velocity in the ambient medium i.e.

$$u = 0, \quad v = 0, \quad \text{at} \quad y = 0 \quad u \to U_\infty \quad as \quad y \to \infty \tag{3.5}$$

As in the chapter- 2, here also we consider two types of boundary conditions for the temperature.

$$\textbf{Type - I} : T = T_w \quad \text{at} \quad y = 0 \tag{3.6}$$

$$\textbf{Type - II} : k\frac{\partial T}{\partial y} = q_w \quad \text{at} \quad y = 0 \tag{3.7}$$

and far away from the cone, the temperature of the free stream is constant i.e. $T \to T_\infty$, as $y \to \infty$

The stream function is defined in context of Eq. (2.1) as $u = \frac{1}{r}\frac{\partial \psi}{\partial y}$, $v = -\frac{1}{r}\frac{\partial \psi}{\partial x}$

For type - I boundary conditions, we define the following similarity transformations

$$\xi = \frac{x}{L}, \quad \eta = \frac{y}{L}\left(\frac{\mathrm{Re}}{\xi}\right)^{\frac{1}{2}}, \quad \psi = rLU_\infty \mathrm{Re}^{-\frac{1}{2}}\xi^{\frac{1}{2}} f(\eta) \quad T = T_\infty + (T_w - T_\infty)\theta \tag{3.8}$$

For type - II boundary conditions, the similarity transformations are given by

$$\xi = \frac{x}{L}, \quad \eta = \frac{y}{L}\left(\frac{\mathrm{Re}}{\xi}\right)^{\frac{1}{2}}, \quad \psi = rLU_\infty \mathrm{Re}^{-\frac{1}{2}}\xi^{\frac{1}{2}} f(\eta) \quad T = T_\infty + \frac{q_w L}{k}\mathrm{Re}^{-\frac{1}{2}}\xi^{\frac{1}{2}} \tag{3.9}$$

where $Re = \dfrac{\rho U_\infty L}{\mu_\infty}$ is the Reynolds number and L is the characteristic length

Applying the similarity transformations Eqs. (3.8) and (3.9) in the Eqs. (3.2) and (3.3), we get the following non-dimensional equations.

For type - I boundary conditions:

$$(1 + A)f''' - A\theta f''' - A\theta' f'' + \frac{3}{2} f f'' = 0 \tag{3.10}$$

$$\frac{1}{\mathrm{Pr}}\theta'' + \frac{1}{\mathrm{Pr}} \in \theta\theta'' + \frac{1}{\mathrm{Pr}} \in (\theta')^2 + \frac{3}{2} f\theta' = 0 \tag{3.11}$$

For type - II boundary conditions

$$(1+A)f''' - A\theta f''' - A\theta' f'' + \frac{3}{2}ff'' = 0 \tag{3.12}$$

$$\frac{2}{\mathrm{Pr}}\theta'' + \frac{2\in}{\mathrm{Pr}}\theta\theta'' + \frac{2\in}{\mathrm{Pr}}\theta'^2 + 3f\theta' - f'\theta = 0 \tag{3.13}$$

where $\mathrm{Pr} = \dfrac{\nu}{\alpha_0}$ is the Prandtl number, A is the viscosity parameter and $\in$ is the thermal conductivity parameter.

The dimensionless form of conditions on the boundary are

$$f(0) = 0, \quad f'(0) = 0, \quad \theta(0) = 1, \quad f'(\infty) = 1, \quad \theta(\infty) = 0, \quad \text{for CWT case.} \tag{3.14}$$

$$f(0) = 0, \quad f'(0) = 0, \quad \theta'(0) = -1, \quad f'(\infty) = 1, \quad \theta(\infty) = 0, \quad \text{for CHF case.} \tag{3.15}$$

The local rate of heat transmission in terms of Nusselt number and the local skin-friction coefficient are the two key findings with the most practical importance. The non-dimensional form of skin-friction coefficient C_f and Nusselt number (Nu) for CWT boundary conditions are

$$C_f^I = Re^{\frac{1}{2}}\xi^{-\frac{1}{2}}f''(0) \quad and \quad Nu^I = -Re^{\frac{1}{2}}\xi^{-\frac{1}{2}}\theta'(0) \tag{3.16}$$

and for CHF boundary conditions are

$$C_f^{II} = Re^{\frac{1}{2}}\xi^{-\frac{1}{2}}f''(0) \quad and \quad Nu^{II} = -Re^{\frac{1}{2}}\xi^{-\frac{1}{2}}\theta'(0) \tag{3.17}$$

3.3 Methodology

The system of differential equations (3.10) – (3.11) and (3.12) – (3.13) are linearized by means of a successive linearization method (SLM) [55]. The solutions of the resulting linearized equations are obtained by employing the Chebyshev spectral method [7].

On applying the procedure explained in Chapter 2 to the equations (3.10) – (3.11) and (3.12) – (3.13), we get the following linearized equations for CWT boundary conditions.

$$a_1 f_i''' + a_2 f_i'' + a_3 f_i + a_4 \theta_i' + a_5 \theta_i = a_6 \tag{3.18}$$

$$b_1 f_i + b_2 \theta_i'' + b_3 \theta_i' + b_4 \theta_i = b_5 \tag{3.19}$$

For the CHF boundary conditions, the linearized equations are

$$c_1 f_i^{'''} + c_2 f_i^{''} + c_3 f_i + c_4 \theta_i^{'} + c_5 \theta_i = c_6 \tag{3.20}$$

$$d_1 f_i^{'} + d_2 f_i + d_3 \theta_i^{''} + d_4 \theta_i^{'} + d_5 \theta_i = d_6 \tag{3.21}$$

$$a_1 = c_1 = (1+A) - A\sum \theta_m,\ a_2 = \frac{3}{2}\sum f_m - A\sum \theta_m^{'},\ a_3 = c_3 = \frac{3}{2}\sum f_m^{''}$$

$$a_4 = c_4 = -A\sum f_m^{''},\ a_5 = c_5 = -A\sum f_m^{'''}$$

$$a_6 = \left(-(1+A) + A\sum \theta_m\right)\sum f_m^{'''} + A\sum \theta_m^{'}\sum f_m^{''} - \frac{3}{2}\sum f_m \sum f_m^{''}$$

$$b_1 = \frac{3}{2}\theta_m^{'},\ b_2 = \frac{1}{\mathrm{Pr}} + \frac{\in}{\mathrm{Pr}}\sum \theta_m$$

$$b_3 = \frac{2\in}{\mathrm{Pr}}\sum \theta_m^{'} + \frac{3}{2}\sum f_m,\ b_4 = \frac{\in}{\mathrm{Pr}}\sum \theta_m^{''}$$

$$b_5 = -\frac{1}{\mathrm{Pr}}\sum \theta_m^{''} - \frac{\in}{\mathrm{Pr}}\sum \theta_m \sum \theta_m^{''} - \frac{\in}{\mathrm{Pr}}\sum \theta_m^{'^2} - \frac{3}{2}\sum f_m \sum \theta_m^{'}$$

$$c_2 = \frac{3}{2}\sum f_m - A\sum \theta_m^{'}$$

$$c_6 = \left(-(1+A) + A\sum \theta_m\right)\sum f_m^{'''} + A\sum \theta_m^{'}\sum f_m^{''} - \frac{3}{2}\sum f_m \sum f_m^{''}$$

$$d_1 = -\theta_m, d_2 = 3\left(\sum \theta_m^{'}\right), d_3 = \frac{2}{\mathrm{Pr}} + \frac{2\in}{\mathrm{Pr}}\left(\sum \theta_m\right)$$

$$d_4 = \frac{4\in}{\mathrm{Pr}}\left(\sum \theta_m^{'}\right) + 3\left(\sum f_m\right), d_5 = -\left(\sum f_m^{'}\right)$$

$$d_6 = \frac{-2}{\mathrm{Pr}}\sum \theta_m^{''} - \frac{2\in}{\mathrm{Pr}}\left(\sum \theta_m\right)\left(\sum \theta_m^{''}\right) - \frac{2\in}{\mathrm{Pr}}\left(\sum \theta_m^{'}\right)^2 - 3\left(\sum f_m\right)\left(\sum \theta_m^{'}\right) + \left(\sum f_m^{'}\right)\left(\sum \theta_m\right)$$

As explained in Chapter 2, applying Chebyshev pseudo spectral method on the system of linearized equations (3.16) - (3.17) and (3.18) - (3.19), we get the following equation in the matrix form

$$A_{i-1}X_i = R_{i-1} \tag{3.22}$$

whereA_{i-1} is a square matrix of order $2N+2$ and X_i and R_{i-1} are column matrices of order

$2N+2$ given by

$$A_{i-1} = \begin{pmatrix} A_{11}^{(i)} & A_{12}^{(i)} \\ A_{21}^{(i)} & A_{22}^{(i)} \end{pmatrix}, X_i = \begin{pmatrix} F_i \\ \Theta_i \end{pmatrix}, R_{i-1} = \begin{pmatrix} r_1^{(i)} \\ r_2^{(i)} \end{pmatrix} \tag{3.23}$$

where

$$A_{11}^{(1)} = a_1 D^3 + a_2 D^2 + a_3 I, A_{12}^{(1)} = a_4 D + a_5 I$$

$$A_{21}^{(1)} = b_1 I, A_{22}^{(1)} = b_2 D^2 + b_3 D + b_4 I$$

$$r_1^{(1)} = [a_6(\xi_0), a_6(\xi_1), ..., a_6(\xi_{N-1}), a_6(\xi_N)]^T$$

$$r_2^{(1)} = [b_5(\xi_0), b_5(\xi_1), ..., b_5(\xi_{N-1}), b_5(\xi_N)]^T,$$

$$A_{11}^{(2)} = c_1 D^3 + c_2 D^2 + c_3 I, A_{12}^{(2)} = c_4 D + c_5 I$$

$$A_{21}^{(2)} = d_1 D + d_2 I, A_{22}^{(2)} = d_3 D^2 + d_4 D + d_5 I$$

$$r_2^{(1)} = [c_6(\xi_0), c_6(\xi_1), ..., c_6(\xi_{N-1}), c_6(\xi_N)]^T$$

$$r_2^{(2)} = [d_6(\xi_0), d_6(\xi_1), ..., d_6(\xi_{N-1}), d_6(\xi_N)]^T$$

where the superscript T stands for transpose, I is the identity O is the zero matrix. Finally, the solution is given by

$$X_i = A_{i-1}^{-1} R_{i-1}$$

3.4 Results and Discussion

The variation of the velocity component, temperature, coefficient of skin friction, and heat transfer rate with the viscosity parameter A is presented in Fig. 3.1 for type – I boundary conditions. It is noticed from Fig. 3.1(a) that the velocity increases near the cone, reaches its maximum value and then decreases gradually to zero as $\eta \to \infty$. Further, it is apparent that for inreasing values of A, the velocity diminishes near the cone and enhances away from the cone. There is a slight decrease in the temperature with an increase in A as shown in Fig. 3.1(b). As revealed in Fig. 3.1(c), increasing A increases the skin friction coefficient. The rate of heat transfer decreases as A increases as depicted in the Fig. 3.1(d).

The impact of viscosity parameter $\in$ on the velocity component, temperature, coefficient of skin friction, and heat transfer rate is depicted in Fig. 3.2 for type – I boundary conditions. The effect of $\in$ on the velocity is almost negligible as shown in Fig. 3.2(a). The temperature

increases slightly for an increase in $\in$ as displayed in Fig. 3.2(b). It is shown in Fig. 3.2(c) that increasing $\in$ decreases the skin friction coefficient. The rate of heat transfer decreases as $\in$ increases as presented in the Fig. 3.2(d).

Figure 3.3 depicts the influence of viscosity parameter A on f', θ, C_f and Nu for type – II boundary conditions. From Fig. 3.3(a) it is observed that for increasing values of A, the velocity increases slightly adjacent to the cone and decreases away from the cone. The influence of $\in$ on the temperature is almost negligible as shown in Fig. 3.2(b). It is noticed from Fig. 3.3(c) that increasing A increases the skin friction coefficient. The rate of heat transfer increases a little as A increases as presented in the Fig. 3.3(d).

The consequence of viscosity parameter $\in$ on f', θ, C_f and Nu is portrayed in Fig. 3.4 for type – II boundary conditions. It is detected from Fig. 3.4(a) that increasing values of $\in$, the velocity increases slightly. The temperature increases for an increase in $\in$ as portrayed in Fig. 3.4(b). It is known from Fig. 3.4(c) that increasing $\in$ decreases the skin friction coefficient. The rate of heat transfer decreases as $\in$ increases as presented in Fig.3.4(d).

3.5 Conclusion

The boundary layer flow across a vertical cone is investigated by presuming the temperature dependent viscosity and thermal conductivity. Similarity transformed are utilized to reduce the equations governing the flow into ordinary differential equations. The non-dimensional equations are linearized using successive linearization procedure and then the resulting system is solved using Chebyshev spectral method.

- There is a slight decrease in the temperature, increase in the skin friction coefficient and decrease in the rate of heat transfer as A increase for CWT boundary conditions.
- The effect of $\in$ on the velocity is almost negligible but increases the temperature, and decreases the skin friction coefficient and the rate of heat transfer for CWT boundary conditions
- For increasing values of A, the velocity increases slightly, increases the skin friction coefficient rate of heat transfer for CHF case.
- An increase in the values of $\in$, increases the velocity, temperature and decreases the skin friction coefficient and the rate of heat transfer for CHF case.

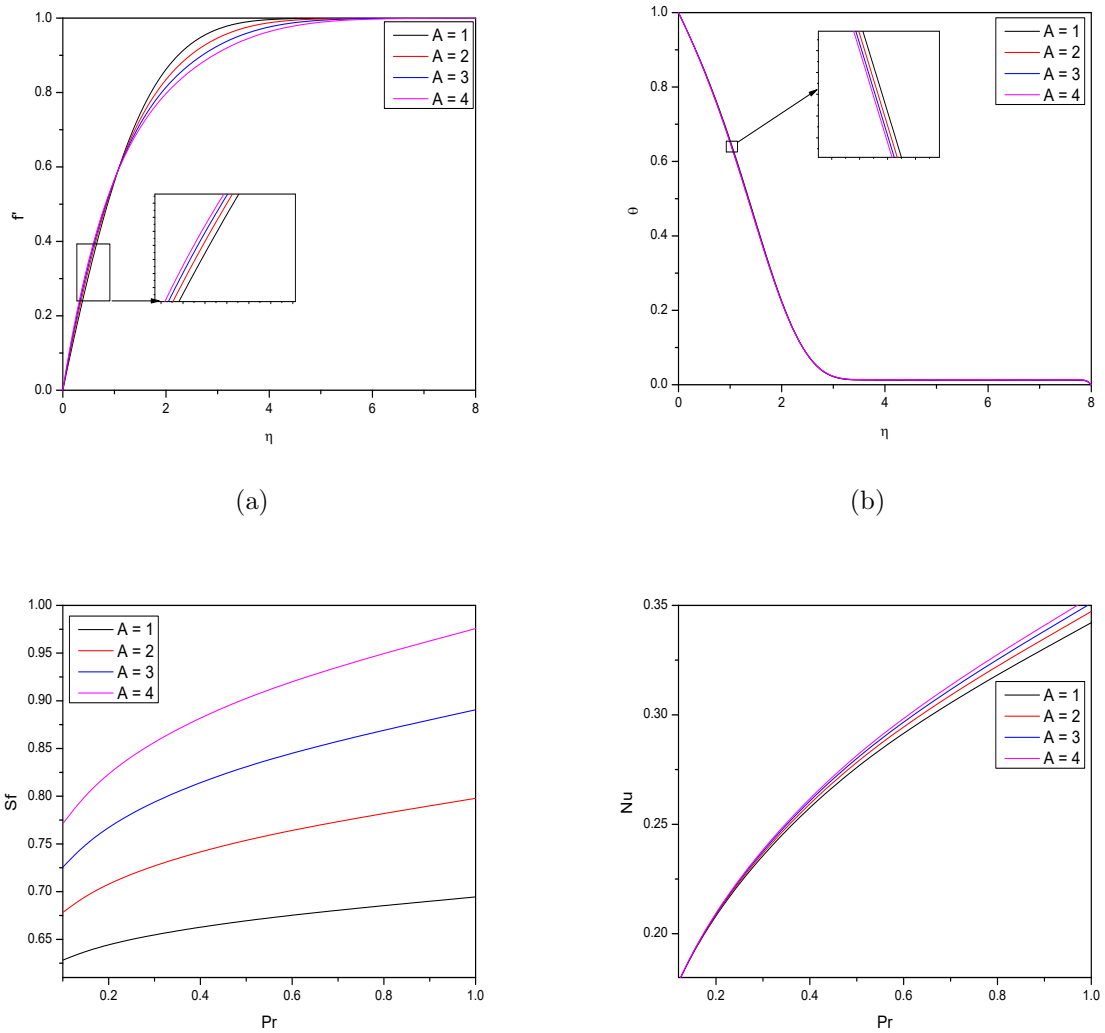

(a) (b)

(c) (d)

Figure 3.1: "Effect of A on the Velocity, Temperature, skin friction coefficient and Nusselt number for CHF boundary conditions".

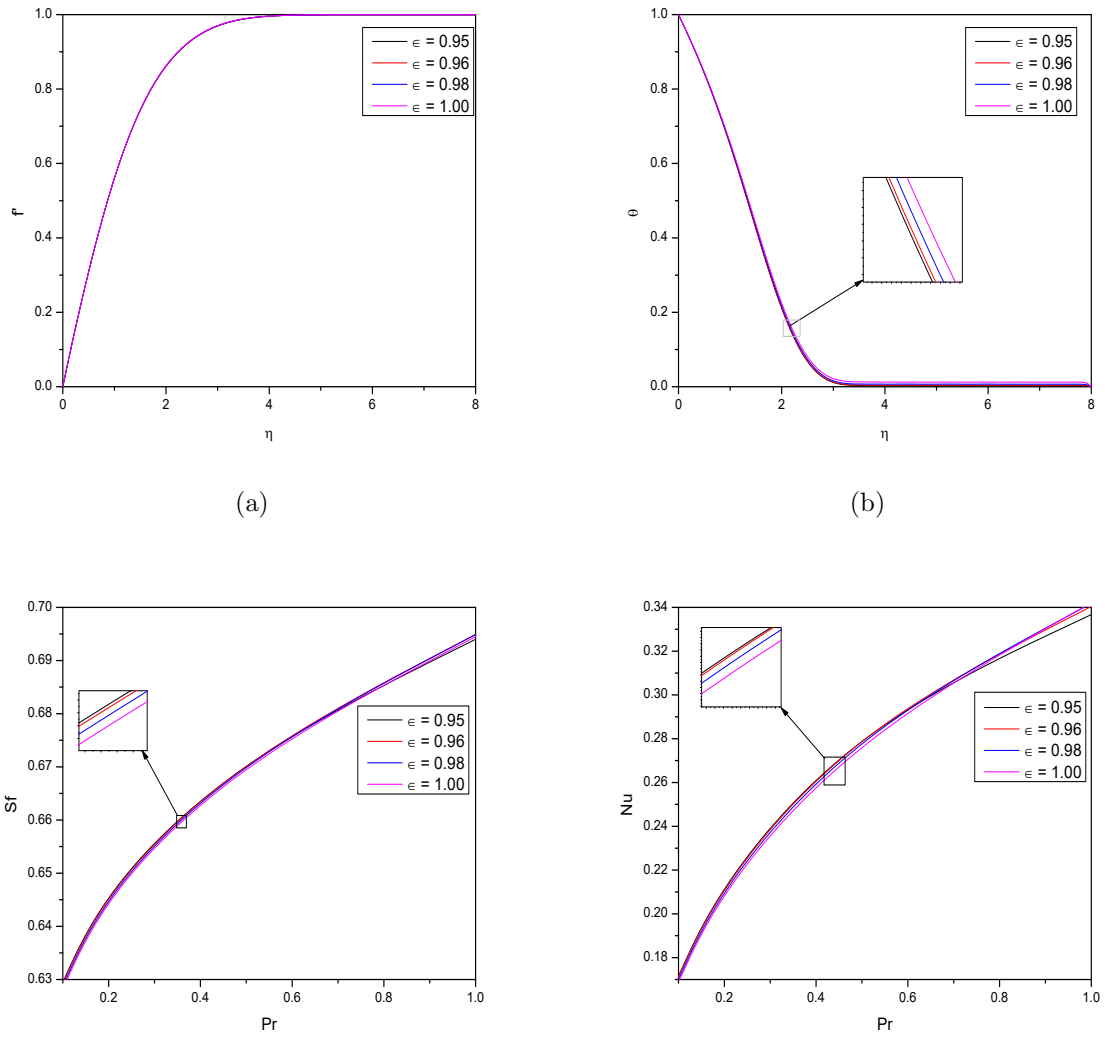

(a) (b)

(c) (d)

Figure 3.2: "Effect of $\in$ on the Velocity, Temperature, skin friction coefficient and Nusselt number for CHF boundary conditions".

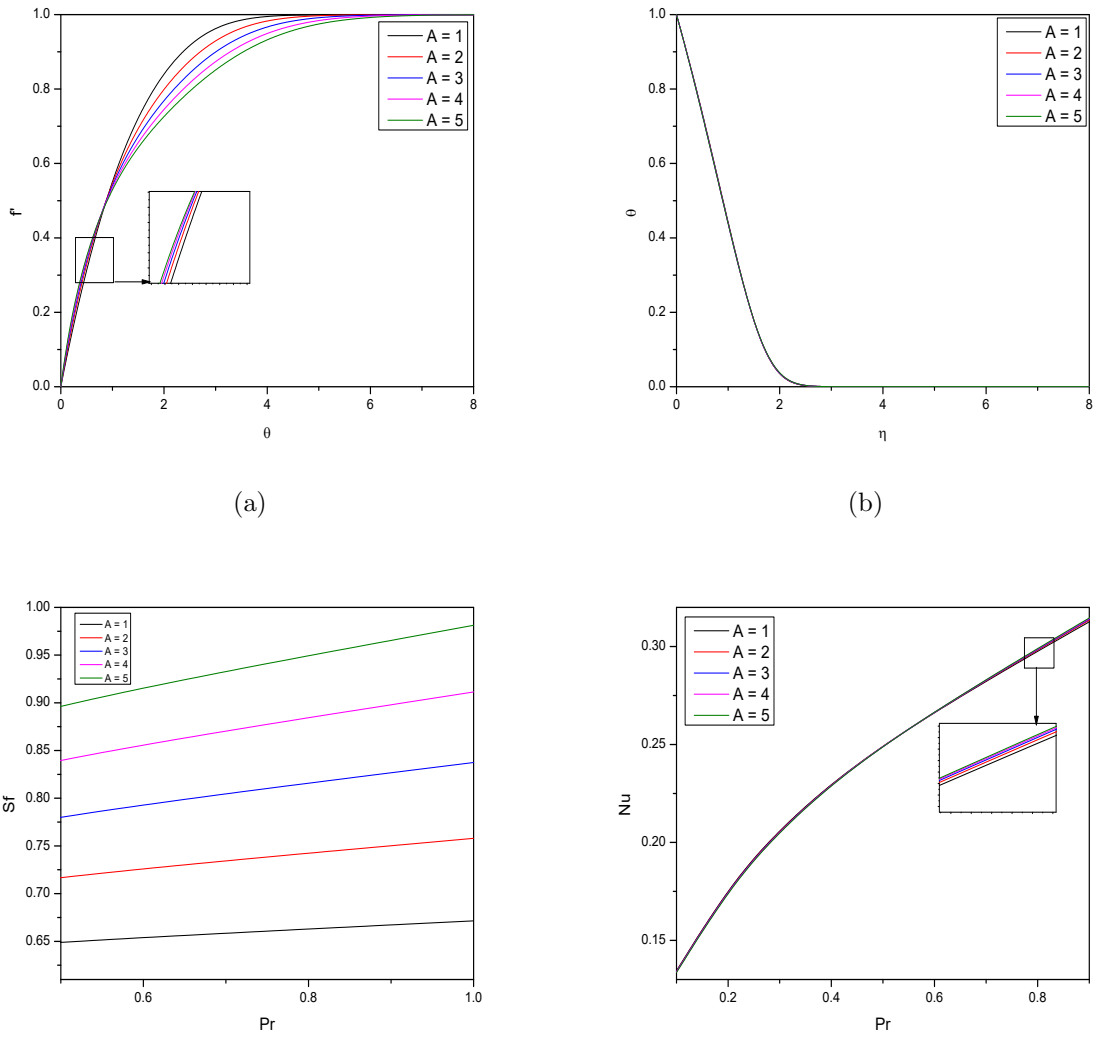

(a) (b)

(c) (d)

Figure 3.3: "Effect of A on the Velocity, Temperature, skin friction coefficient and Nusselt number for CWT boundary conditions".

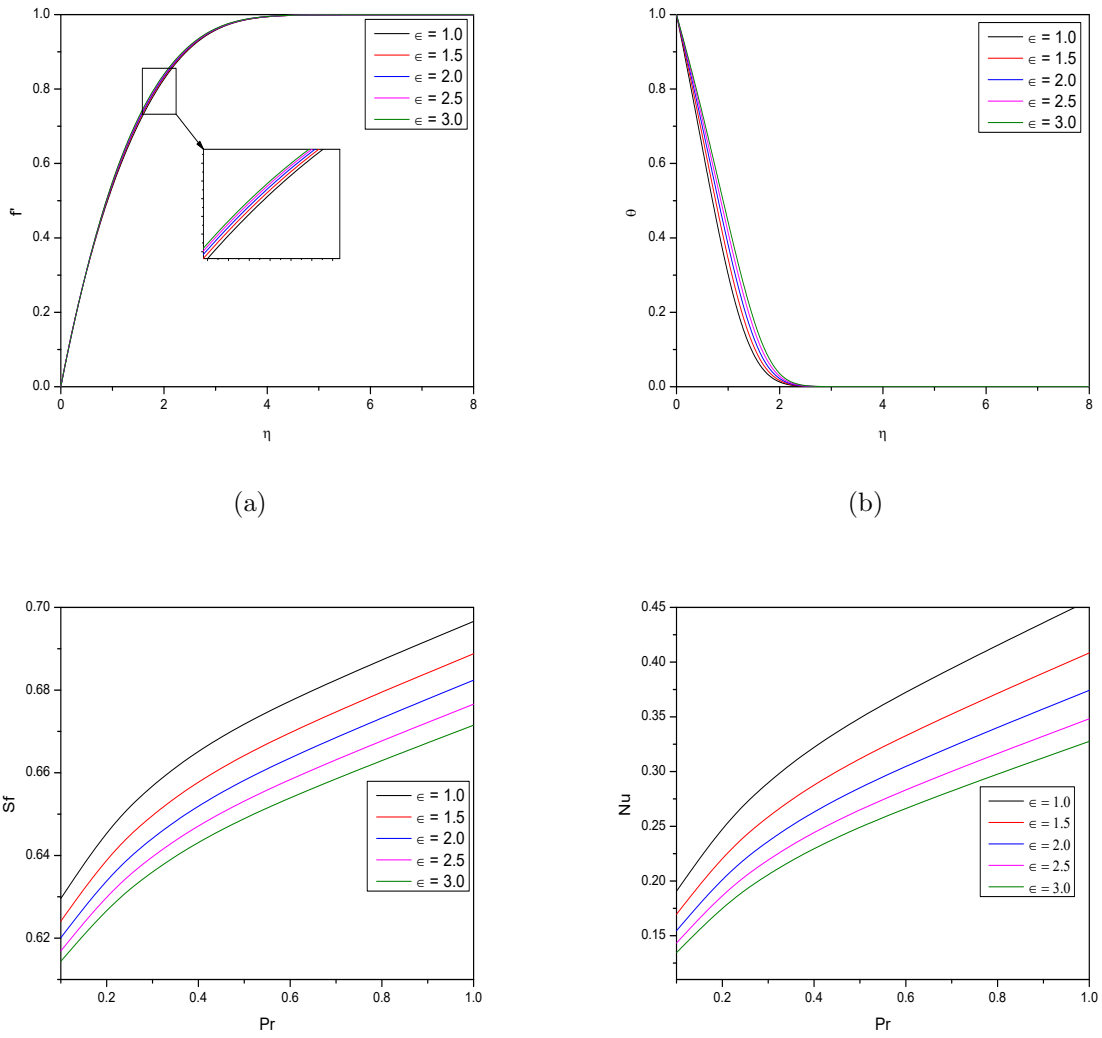

(a) (b)

(c) (d)

Figure 3.4: "Effect of $\in$ on the Velocity, Temperature, skin friction coefficient and Nusselt number for CWT boundary conditions".

Chapter 4

Combined influence of Cross Diffusion and Variable Fluid Properties on The Free Convective Flow Past a Vertical Cone [1]

4.1 Introduction

The Dufour effect refers to the energy flux caused by a concentration gradient. Temperature gradients, on the other hand, can generate mass fluxes, which embodies the Soret effect. A considerable amount of research on Newtonian and non-Newtonian fluid flows in various geometries has been published in the literature, with a focus on the Soret and Dufour effects. Oyem *et al.* [61] examined the consequences of the impact of cross-diffusion on the Blasius and Sakiadis flows. Ghoneim *et al.* [21] explored the Soret and Dufour effects along with interaction of thermal radiation and variable diffusivity through vertical cone. Meena *et al.* [49] examined the influence of Soret and Dufour effects on mixed convection flow across a vertical cone with injection/suction.

In this chapter, the free convective flow of an incompressible viscous fluid over an isothermal vertical cone with variable viscosity and variable thermal conductivity is examined in the presence of the Soret and Dufour effects. As thermal and solutal boundary conditions at the surface of the cone, the constant temperature and concentration (WTC) and constant

[1] Accepted for publication in "**Heat Transfer**",

heat and mass flux (HMF) cases are taken into account. The successive linearization method is applied to linearize a system of nonlinear differential equations that describes the flow under investigation. The numerical solution for the resulting linear equations is attained by means of the Chebyshev spectral method. The obtained numerical results are compared and found to be in good agreement with previously published results. The impact of significant parameters on the heat and mass transfer rates is evaluated and presented graphically for the WTC and HMF situations

4.2 Mathematical Formulation

Consider an an incompressible, laminar and steady flow of viscous fluid along a vertical down-pointing cone with local radius r and half-angle ϕ under steady state and laminar flow conditions. The coordinate system and physical model are as depicted in Fig. (2.1). In addition to the assumptions made in the previous chapters, thermo diffusion and diffusion thermo effects are incorporated in the flow. The ambient temperature and concentration are T_∞ and C_∞, respectively.

Applying Boussinesq approximation and utilizing the boundary layer concepts, the equations describing the flow are [33].

$$\frac{\partial}{\partial x}(ur) + \frac{\partial}{\partial y}(vr) = 0 \tag{4.1}$$

$$\rho\left(u\frac{\partial u}{\partial x} + v\frac{\partial u}{\partial y}\right) = \frac{\partial}{\partial y}\left(\mu\frac{\partial u}{\partial y}\right) + \rho g\beta\cos\phi\left((T-T_\infty) + (C-C_\infty)\right) \tag{4.2}$$

$$u\frac{\partial T}{\partial x} + v\frac{\partial T}{\partial y} = \frac{\partial}{\partial y}\left(\alpha\frac{\partial T}{\partial y}\right) + \frac{D_s K_T}{C_S C_P}\frac{\partial^2 c}{\partial y^2} \tag{4.3}$$

$$u\frac{\partial C}{\partial x} + v\frac{\partial C}{\partial y} = \frac{\partial}{\partial y}(D_s\frac{\partial C}{\partial y}) + \frac{D_s K_T}{T_m}\frac{\partial^2 T}{\partial y^2} \tag{4.4}$$

where β_T and β_C denote the coefficient of thermal and solutal expansions, C_p denotes the specific heat D_s is the diffusivity of the solute, C_s denotes the concentration susceptibility, K_T thermal diffusion ratio and T_m is the mean fluid temperature. The remaining quantities are already defined in the previous chapters.

The viscosity and thermal conductivity are considered to be a linear function of the

temperature [5] and are given by

$$\mu = \mu_\infty[1 + \lambda(T_\infty - T) \quad \text{and} \quad k = k_0[1 + \gamma(T - T_\infty)], \tag{4.5}$$

where μ_∞ and, k_0 represents the absolute viscosity and the thermal conductivity of the fluid, respectively, and λ, γ are constants.

The velocity boundary conditions are no slip condition and zero velocity in the ambient medium i.e.

$$\text{“}u = 0, \quad v = 0, \quad \text{at} \quad y = 0 \quad u \to 0 \quad as \quad y \to \infty'' \tag{4.6}$$

In addition, for the temperature and concentration on the cone surface, one can either have constant temperature T_w and constant wall concentration C_w (WTC) or a constant heat flux q_w and constant mass flux q_m (HMF). Thus, the temperature and concentration conditions at the boundary are written as

$$\begin{aligned} &\textbf{Case-I (WTC)} : T = T_w, \quad C = C_w \quad \text{at} \quad y = 0. \\ &\textbf{Case-II (HMF)} : -k\frac{\partial T}{\partial y} = q_w, \quad -D_s\frac{\partial C}{\partial y} = q_m \quad \text{at} \quad y = 0. \end{aligned} \tag{4.7}$$

Far-off from the cone, the following conditions are considered.

$$T \to T_\infty, \quad C \to C_\infty \quad \text{as} \quad y \to \infty \tag{4.8}$$

The similarity transformations for WTC case are given by

$$\xi = \frac{x}{L}, \quad \eta = \frac{y}{L}\left(\frac{Gr}{\xi}\right)^{\frac{1}{4}}, \quad \psi = r\nu Gr^{\frac{1}{4}}\xi^{\frac{3}{4}}f(\eta), \quad \theta(\eta) = \frac{T - T_\infty}{T_w - T_\infty}, \quad \phi(\eta) = \frac{C - C_\infty}{C_w - C_\infty}. \tag{4.9}$$

where $G_r = \dfrac{L^3 g\beta\cos\phi(T_w - T_\infty)}{\nu^2}$ represents the thermal Grashof number and L is the characteristic length.

Utilizing equation (4.9) in the equations (4.2) to (4.4), we get the non-dimensional equations as

$$(1 + A)f''' - A\theta f''' - A\theta' f'' + \frac{7}{4}ff'' - \frac{1}{2}f'^2 + \theta + B\phi = 0 \tag{4.10}$$

$$\frac{1}{\mathrm{Pr}}\theta'' + \frac{\in}{\mathrm{Pr}}(\theta\theta'') + \frac{\in}{\mathrm{Pr}}(\theta')^2 + D_f\phi'' + \frac{7}{4}f\theta' = 0 \tag{4.11}$$

$$\frac{1}{Sc}\phi'' + Sr\theta'' + \frac{7}{4}f\phi' = 0 \tag{4.12}$$

where $\Pr = \dfrac{\nu}{\alpha_0}$ denotes the Prandtl number, $B = \dfrac{\beta_c(C_w - C_\infty)}{\beta_T(T_w - T_\infty)}$ denotes the Buoyancy ratio, $D_f = \dfrac{D_S K_T(C_w - C_\infty)}{C_s C_p \nu(T_w - T_\infty)}$ denotes the Dufour number, $Sr = \dfrac{D_S K_T(T_w - T_\infty)}{T_m \nu(C_w - C_\infty)}$ denotes the Soret number, and $Sc = \dfrac{\nu}{D_s}$ denotes the Schmidt number.

The similarity transformations for HMF case are given by

$$\xi = \frac{x}{L}, \quad \eta = \frac{y}{L}\left(\frac{Gr}{\xi}\right)^{\frac{1}{5}}, \quad \psi = r\nu Gr^{\frac{1}{5}}\xi^{\frac{4}{5}} f(\eta), \tag{4.13}$$
$$T = T_\infty + \frac{q_w L}{k} Gr^{-\frac{1}{5}}\xi^{\frac{1}{5}}\theta, \quad C = C_\infty + \frac{q_w k}{L} Gr^{-\frac{1}{5}}\xi^{\frac{1}{5}}\phi$$

where $G_r = \dfrac{L^3 g\beta\cos\phi(T_w - T_\infty)}{\upsilon^2}$ is the thermal Grashof number. Utilizing the (4.13) in the equations (4.2) to (4.4), we obtain

$$(1+A)f''' - A\theta f''' - A\theta' f'' + \frac{9}{5}ff'' - \frac{3}{5}f'^2 + \theta + \phi = 0 \tag{4.14}$$

$$\frac{1}{\Pr}\theta'' + \frac{\in}{\Pr}\theta\theta'' + \frac{\in}{\Pr}\theta'^2 - \frac{1}{5}f'\theta + \frac{9}{5}f\theta' + Df\phi'' = 0 \tag{4.15}$$

$$\frac{1}{Sc}\phi'' + Sr\theta'' - \frac{1}{5}f'\theta + \frac{9}{5}f\phi' = 0 \tag{4.16}$$

$B = \dfrac{\beta_c k_0 q_m}{\beta_T D_s q_w}$ denotes the Buoyancy ratio, $Df = \dfrac{D_S K_T q_m k_0}{C_s C_p \nu q_w}$ denotes the Dufour number, $Sr = \dfrac{D_S K_T q_w D_s}{T_m \nu q_m k_0}$ denotes the Soret number,

The dimensionless form of Equation (4.7) and (4.8) are

$$\text{“}f(0) = f'(0) = 0,\ \theta(0) = \phi(0) = 1,\ f'(\infty) = \theta(\infty) = \phi(\infty) = 0'' \text{ for WTC case.} \tag{4.17}$$

$$\text{“}f(0) = f'(0) = 0,\ \theta'(0) = \phi'(0) = -1,\ f'(\infty) = \theta(\infty) = \phi(\infty) = 0'' \text{ for HMF case.} \tag{4.18}$$

The most fundamental technical findings are the local skin-friction coefficient and rate of heat and transfers. The dimensionless representation of skin-friction coefficient C_f, Nusselt number (Nu), and Sherwood number (Sh) for WTC case are

$$G_r^{-\frac{3}{4}}\xi^{-\frac{3}{4}}C_f^I = f''(0), \quad G_r^{-\frac{1}{4}}\xi^{\frac{1}{4}}Nu^I = -\theta'(0) \quad \text{and} \quad G_r^{-\frac{1}{4}}\xi^{\frac{1}{4}}Sh^I = -\phi'(0) \tag{4.19}$$

and for CHF boundary conditions are

$$G_r^{-\frac{3}{5}}\xi^{-\frac{2}{5}}C_f^{II} = f''(0), \quad G_r^{-\frac{1}{5}}\xi^{-\frac{4}{5}}Nu^{II} = \frac{1}{\theta(0)} \quad \text{and} \quad G_r^{-\frac{1}{5}}\xi^{-\frac{4}{5}}Sh^{II} = \frac{1}{\phi(0)} \tag{4.20}$$

4.3 Methodology

The set of differential equations (4.10) - (4.12) and (4.14) - (4.16) are linearized by means of a successive linearization method (SLM) [55]. The solutions of the resulting linearized equations are attained by employing the Chebyshev spectral method [7].

On applying the procedure explained in Chapter 2 to the Eqs. (4.10) - (4.12) and Eqs. (4.14) - (4.16) , we get the following linearized equations.

$$a_1{}^{(n)} f_i''' + a_2{}^{(n)} f_i'' + a_3{}^{(n)} f_i' + a_4{}^{(n)} f_i + a_5{}^{(n)}\theta_i' + a_6{}^{(n)}\theta_i + a_7{}^{(n)}\phi_i = a_8{}^{(n)} \tag{4.21}$$

$$b_1{}^{(n)} f_i{}' + b_2{}^{(n)} f_i + b_3{}^{(n)}\theta_i{}'' + b_4{}^{(n)}\theta_i{}' + b_5{}^{(n)}\theta_i + b_6{}^{(n)}\phi_i'' = b_7{}^{(n)} \tag{4.22}$$

$$C_1{}^{(n)} f_i{}' + C_2{}^{(n)} f_i + C_3{}^{(n)}\theta_i'' + C_4{}^{(n)}\phi_i'' + C_5{}^{(n)}\phi_i' + C_6{}^{(n)}\phi_i = c_7{}^{(n)} \tag{4.23}$$

where n=1 corresponds to WTC boundary conditions and n=2 corresponds to HMF boundary conditions. The coefficients in the above equations are given by

$$a_1{}^{(1)} = a_1{}^{(2)} = (1+A) - A(\sum \theta_m), \quad a_2{}^{(1)} = \frac{7}{4}\sum f_m - A\sum_{m=}^{i-1}\theta_m{}',$$

$$a_2^{(2)} = \frac{9}{5}\sum f_m - A\sum \theta_m' \quad a_3{}^{(1)} = -\sum f_m{}', \quad a_3{}^{(2)} = \frac{-6}{5}\sum f_m',$$

$$a_4{}^{(1)} = 7/4\sum f_m'', \quad a_4{}^{(2)} = 7/4\sum f_m''. \quad a_5{}^{(1)} = a_5{}^{(2)} = -A\sum f_m{}'',$$

$$a_6{}^{(1)} = a_6{}^{(2)} = 1 - A(\sum f_m{}''), a_7{}^{(1)} = a_7{}^{(2)} = B$$

$$a_8{}^{(1)} = \left(-(1+A) + A\sum\theta_m\right) f_m''' + \left(A\sum\theta_m' - \frac{7}{4}\sum f_m\right) f_m''$$
$$+\frac{1}{2}\left(\sum f_m'\right)^2 - \sum\theta_m - B\sum\phi_m,$$

$$a_8{}^{(2)} = \left(-(1+A) + A\sum\theta_m\right) f_m''' + \left(A\sum\theta_m' - \frac{9}{5}\sum f_m\right) f_m''$$
$$+\frac{3}{5}\left(\sum f_m'\right)^2 - \sum\theta_m - B\sum\phi_m$$

$$b_1{}^{(1)} = \frac{7}{4}\sum \theta_m', \quad b_1{}^{(2)} = -\frac{1}{5}\sum \theta_m, \quad b_2{}^{(1)} = \frac{1}{\mathrm{Pr}} + \frac{\in}{\mathrm{Pr}}\sum \theta_m, \quad b_2{}^{(2)} = \frac{9}{5}\sum \theta_m',$$

$$b_3{}^{(1)} = \frac{2\in}{\mathrm{Pr}}\sum \theta_m' + \frac{7}{4}\sum f_m, \quad b_3{}^{(2)} = \frac{1}{\mathrm{Pr}} + \frac{\in}{\mathrm{Pr}}\sum \theta_m, \quad b_4{}^{(1)} = \frac{\in}{\mathrm{Pr}}\sum \theta_m', \quad b_5{}^{(1)} = D_f,$$

$$b_4{}^{(2)} = \frac{9}{5}\sum f_m + \frac{2\in}{\mathrm{Pr}}\sum \theta_m', \quad b_5{}^{(2)} = \frac{\in}{\mathrm{Pr}}\sum \theta_m'' - \frac{1}{5}\sum f_m' \quad b_6{}^{(1)} = 0, \quad b_6{}^{(2)} = D_f$$

$$b_7{}^{(1)} = \left(-\frac{1}{\mathrm{Pr}} - \frac{\in}{\mathrm{Pr}}(\sum \theta_m)\right)\sum \theta_m{}'' - \frac{\in}{\mathrm{Pr}}\left(\sum \theta_m'\right)^2 - \frac{7}{4}\left(\sum f_m\right)\left(\sum \theta_m'\right) - D_f\sum \phi_m'',$$

$$b_7{}^{(2)} = -\left(\frac{1}{\mathrm{Pr}} + \frac{\in}{\mathrm{Pr}}\sum \theta_m\right)\sum \theta_m'' - \frac{\in}{\mathrm{Pr}}\sum \theta_m'^2 + \frac{1}{5}\sum f_m'\sum \theta_m - \frac{9}{5}\sum f_m\sum \theta_m' - D_f\sum \phi_m''$$

$$c_1{}^{(1)} = \frac{7}{4}\sum \phi_m', c_1{}^{(2)} = -\frac{1}{5}\sum \phi_m, c_2{}^{(1)} = Sr, c_2{}^{(2)} = \frac{9}{5}\sum \phi_m', c_3{}^{(1)} = \frac{1}{Sc}, c_3{}^{(2)} = Sr,$$

$$c_4{}^{(1)} = \frac{7}{4}\sum f_m c_4{}^{(2)} = \frac{1}{Sc}, \quad , c_5{}^{(1)} = 0, c_5{}^{(2)} = \frac{9}{5}\sum f_m, \quad c_6{}^{(1)} = 0,$$

$$c_6{}^{(2)} = -\frac{1}{5}\sum f_m', \quad c_7{}^{(1)} = -\frac{1}{Sc}\sum \phi_m'' - Sr\sum \theta_m'' - \frac{7}{4}\sum f_m\sum \phi_m'$$

$$c_7{}^{(2)} = -\frac{1}{Sc}\sum \phi_m'' - Sr\sum \theta_m'' + \frac{1}{5}\sum f_m'\sum \phi_m - \frac{9}{5}\sum f_m\sum \phi_m'$$

The conditions (4.17) and (4.18) changes to

$$f_i(0) = f_i{}'(0) = f_i{}'(\infty) = \theta_i(\infty) = \phi_i(\infty) = 0,\ \theta_i(0) = \phi_i(0) = 1 \tag{4.24}$$

$$f_i(0) = f_i{}'(0) = f_i{}'(\infty) = \theta_i(\infty) = \phi_i(\infty) = 0,\ \theta'{}_i(0) = \phi'{}_i(0) = -1 \tag{4.25}$$

As explained in Chapter 2, applying Chebyshev pseudo spectral method on the system of linearized equations (4.21) to (4.23), we get the following equation in the matrix form

$$A_{i-1}X_i = R_{i-1} \tag{4.26}$$

where A_{i-1} is a square matrix of order $3N+3$ and X_i and R_{i-1} are column matrices of order $3N+3$ given by

$$A_{i-1} = \begin{pmatrix} A_{11}^{(i)} & A_{12}^{(i)} & A_{13}^{(i)} \\ A_{21}^{(i)} & A_{22}^{(i)} & A_{23}^{(i)} \\ A_{31}^{(i)} & A_{32}^{(i)} & A_{33}^{(i)} \end{pmatrix}, X_i = \begin{pmatrix} F_i \\ \Theta_i \\ \Phi_i \end{pmatrix}, R_i = \begin{pmatrix} r_1^{(i)} \\ r_2^{(i)} \\ r_3^{(i)} \end{pmatrix} \tag{4.27}$$

where

$$F_i = [f_i(\zeta_0), f_i(\zeta_1), ..., f_i(\zeta_{N-1}), f_i(\zeta_N)]^T,$$

$$\Theta_i = [\theta_i(\zeta_0), \theta_i(\zeta_1), .., \theta_i(\zeta_{N-1}), \theta_i(\zeta_N)]^T,$$

$$\Phi_i = [\phi_i(\zeta_0), \phi_i(\zeta_1), ...\phi_i(\zeta_{N-1}), \phi_i(\zeta_N)]^T,$$

$$A_{11}^{(1)} = a_1{}^{(1)}D^3 + a_2{}^{(1)}D^2 + a_3{}^{(1)}D + a_4{}^{(1)}I, A_{12}^{(1)} = a_5{}^{(1)}D + a_6{}^{(1)}I, A_{13}^{(1)} = a_7{}^{(1)}I$$

$$A_{21}^{(1)} = b_1{}^{(1)}I, A_{22}^{(1)} = b_2{}^{(1)}D^2 + b_3{}^{(1)}D + b_4{}^{(1)}I, A_{23}^{(1)} = b_5{}^{(1)}D^2$$

$$A_{31}^{(1)} = c_1{}^{(1)}I, A_{32}^{(1)} = c_2{}^{(1)}D^2, A_{33}^{(1)} = c_3{}^{(1)}D^2 + c_4{}^{(1)}D$$

$$A_{11}^{(2)} = a_1{}^{(2)}D^3 + a_2{}^{(2)}D^2 + a_3{}^{(2)}D + a_4{}^{(2)}I, A_{12}^{(2)} = a_5{}^{(2)}D + a_6{}^{(2)}I, A_{13}^{(2)} = a_7{}^{(2)}I$$

$$A_{21}^{(2)} = b_1{}^{(2)}D + b_2{}^{(2)}I, A_{22}^{(2)} = b_3{}^{(2)}D^2 + b_4{}^{(2)}D + b_5{}^{(2)}I, A_{23}^{(2)} = b_6{}^{(2)}D^2$$

$$A_{31}^{(2)} = c_1{}^{(2)}D + c_2{}^{(2)}I, A_{32}^{(2)} = c_3{}^{(2)}D^2, A_{33}^{(2)} = c_4{}^{(2)}D^2 + c_5{}^{(2)}D + c_6{}^{(2)}I$$

$$r_1^{(n)} = \left[a_8{}^{(n)}(\zeta_0), a_8{}^{(n)}(\zeta_1), ..., a_8{}^{(n)}(\zeta_{N-1}), a_8{}^{(n)}(\zeta_N)\right]^T$$

$$r_n^{(2)} = [b_7(\zeta_0), b_7(\zeta_1), ..., b_7(\zeta_{N-1}), b_7(\zeta_N)]^T$$

$$r_3^{(n)} = [c_7(\zeta_0), c_7(\zeta_1), ..., c_7(\zeta_{N-1}), c_7(\zeta_N)]^T$$

Where the superscript T stands for transpose, I is the identity O is the zero matrix.

Finally, the solution is given by

$$X_i = A_{i-1}^{-1} R_{i-1}$$

4.4 Results and Discussion

The current model is basically focused on determining the impact of the four dimensionless parameters: viscosity parameter A, thermal conductivity parameter ϵ, Soret parameter Sr, Dufour parameter Df on the local Nusselt Number N_u, the coefficient of local skin friction C_f, and Sherwood number Sh for WTC and HMF cases. To ensure a better understanding of the scientific problem, a thorough numerical parametric evaluation is carried out, and the findings are exhibited graphically (Figs. (2) – (9)). Numerical computations have been performed for diverse values of A, ϵ, Df, and Sr. In all the calculations, the values of Pr, B, and Scwere fixed as 2.0, 4.0 and 1.0, respectively, unless otherwise specified.

To confirm the correctness of the method, the code developed is verified by comparing our computational results of $-\theta(0)$ for WTC case and $\theta(0)$ for HMF case with the published results of Na and Chiou [58] for diverse values of Prandtl number Pr by ignoring the parameters A, $\in$, D_f, Sr and B. The computed results are presented in Table 4.1 and the comparisons are found to be in very good agreement.

Table 4.1: Comparative analysis for the values of $-\theta(0)$ for WTC case and $\theta(0)$ for HMF case by the present method for $A = 0$, $\in= 0$, $D_f = 0$, $Sr = 0$ and $B = 0$ with the results of Na and Chiou [58]

	$-\theta(0)$ for WTC case		$\theta(0)$ for HMF case	
Pr	Na and Chiou [58]	Present	Na and Chiou [58]	Present
0.01	0.07493	0.7492765	-	-
0.1	-	-	3.2781	3.2780756
0.70	0.45101	0.4510092	-	-
1.0	0.51039	0.5103894	1.6329	1.6327658
10.0	1.03397	1.0339685	0.9336	0.9335867
100.0	1.92197	1.9219665	0.5738	0.5738012

The impact of viscosity parameter A on the coefficient of skin friction, heat transfer rate, and the mass transfer rate is portrayed in Fig. 4.1 for WTC boundary conditions. As shown in Fig.4.1(a), increase in A enhances the skin friction coefficient. As A rises, the rate of heat and mass transfer decreases, as seen in Figs.4.1(b) and 4.1(c). This is due to due to the fact that increasing viscosity parameter increases the velocity and its gradient which, in turn, increases the viscous dissipation and then increases the temperature, which reduces the temperature difference.

The variation of coefficient of skin friction, Nusselt number, and Sherwood number with the thermal conductivity parameter $\in$ is given in the Fig. 4.2 for WTC boundary conditions. It is understood from Fig. 4.2(a) that the coefficient of skin friction improves as the variable thermal conductivity parameter rises. The rate of heat transfer is reducing with an enhancement in $\in$ as depicted in Fig. 4.2(b) From Fig. 4.2(c) it is perceived that the Sherwood number is rising for increasing values of $\in$.

The influence of Soret number Sr on the coefficient of skin friction, Nusselt number, and Sherwood number is given in the Fig. 4.3 for WTC boundary conditions. According to Fig. 4.3(a) enhancing the value of the Soret number enhances the coefficient of skin friction. As the value of Sr rises, so does the amount of heat transfer as displayed in Fig. 4.3(b). Fig. 4.3(c) reveals that the Sherwood number is lessening an Sr increases. Soret number is the

ratio of a temperature difference to the concentration. Hence, the increase in Soret number stands for an increase in the temperature difference and precipitous gradient.

The variation of skin friction coefficient, heat and mass transfer rate against the Dufour parameter Df is shown in the Fig. 4.4 for WTC boundary conditions. The coefficient of skin friction rises as the Dufour parameter value is increased, as shown in Fig. 4.4(a) The heat transfer rate is reducing with a rise in Df as portrayed in Fig. 4.4(b). According to Fig. 4.4(c), the Sherwood numbers appear to be increasing for growing Df values. The Dufour number signifies the influence of the solutal gradients to the thermal energy flux in the flow. Hence, an enhance in the Dufour number results in an increase in the temperature and a drop in the concentrations

The consequence of viscosity parameter A on the coefficient of skin friction, Nusselt number and Sherwood number is depicted in Fig.4.5for HMF boundary conditions. As presented in Fig. 4.5(a), intensifying A increases the skin friction coefficient. The heat transfer rate and Sherwood numbers are increasing initially and then decreasing with an escalation in the variable viscosity parameter A as given in the Figs. 4.5(b) and 4.5(c).

The influence of $\in$ on the skin friction coefficient, Nusselt number and Sherwood number is depicted in Fig.4.6 for HMF boundary conditions. According to Fig. 4.6(a), the coefficient of skin friction intensifies as the value of the thermal conductivity parameter rises. The heat transfer rate is decreasing with a rise $\in$ as indicated in Fig. 4.6(b). Fig. 4.6(c) discloses that the Sherwood number is enhancing for enhancing values of ϵ.

The variation of skin friction coefficient, Nusselt number and Sherwood number with the Soret number Sr is displayed in the Fig. 4.7 for HMF boundary conditions. Fig. 4.7(a) shows that the coefficient of skin friction is rising with a rise in the value of the Soret parameter. As Sr is enhancing, the heat transfer is also enhancing as displayed in the Fig. 4.7(b). Fig. 4.7(c) explains that the Sherwood number is diminishing as the values of Sr increase.

The deviation of coefficient of skin friction with the Dufour number parameter Df is presented in Fig. 4.8 for HMF boundary conditions. Fig. 4.8(a) exhibits that the coefficient of skin friction is increasing with an increase in the value of the Dufour parameter. The rate of heat transfer is diminishing with a rise in Df as portrayed in Fig. 4.8(b). From Fig. 4.8(c), it is detected that the Sherwood number is increasing for enhancing values of Df.

4.5 Conclusion

The free convection flow across a vertical cone is investigated by presuming the viscosity and thermal conductivity varies with temperature in the manifestation of Soret and Dufour effects. Similarity conversions are utilized to reduce the equations describing the flow into ordinary differential equations. The non-dimensional equations linearized using successive linearization procedure and then the solution of the consequent system is found using Chebyshev spectral method.

- The skin friction coefficient increases for both WTC and HMF conditions. The rate of heat and mass transfer decrease with increasing the viscosity parameter for WTC conditions. The heat and mass transfer rate increase initially and then decrease with an increase in the variable viscosity parameter.
- For both the conditions, the coefficient of skin friction and mass transfer improves and rate of heat transfer reduce with the variable thermal conductivity parameter increases.
- An enhancement in Soret number enhances the coefficient of skin friction and rate of heat transfer but reduces the Sherwood number for both WTC and HMF cases.
- The coefficient of skin friction and Sherwood numbers rise whereas the heat transfer rate is reducing as the Dufour parameter increase.

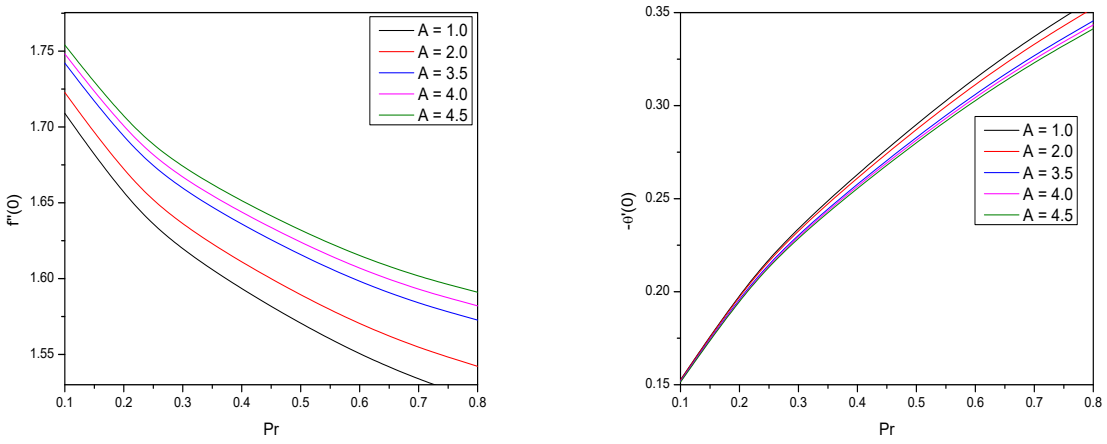

(a) (b)

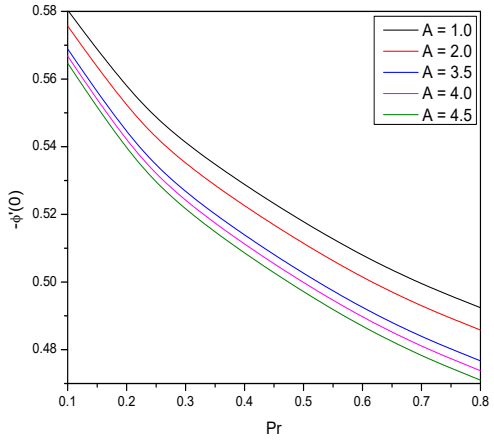

(c)

Figure 4.1: "Effect of A on the skin friction coefficient, Nusselt number and Sherwood number for WTC boundary conditions".

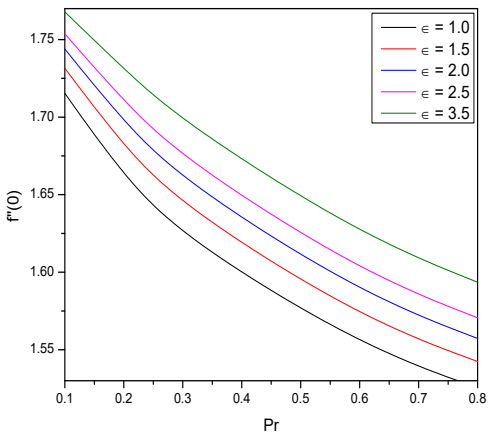

(a)

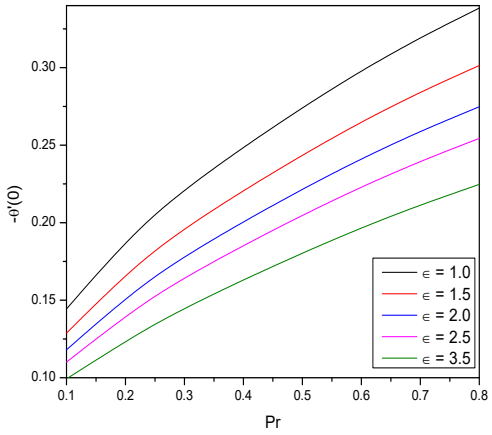

(b)

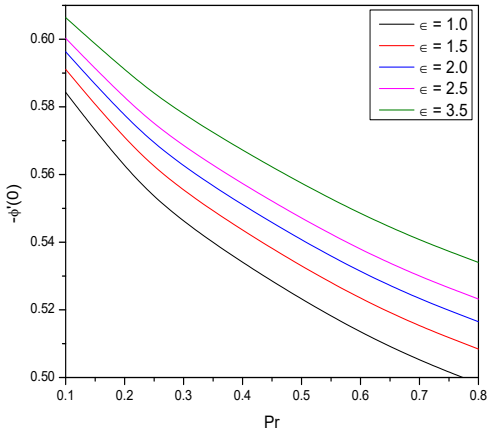

(c)

Figure 4.2: "Effect of $\in$ on the skin friction coefficient, Nusselt number and Sherwood number for WTC boundary conditions".

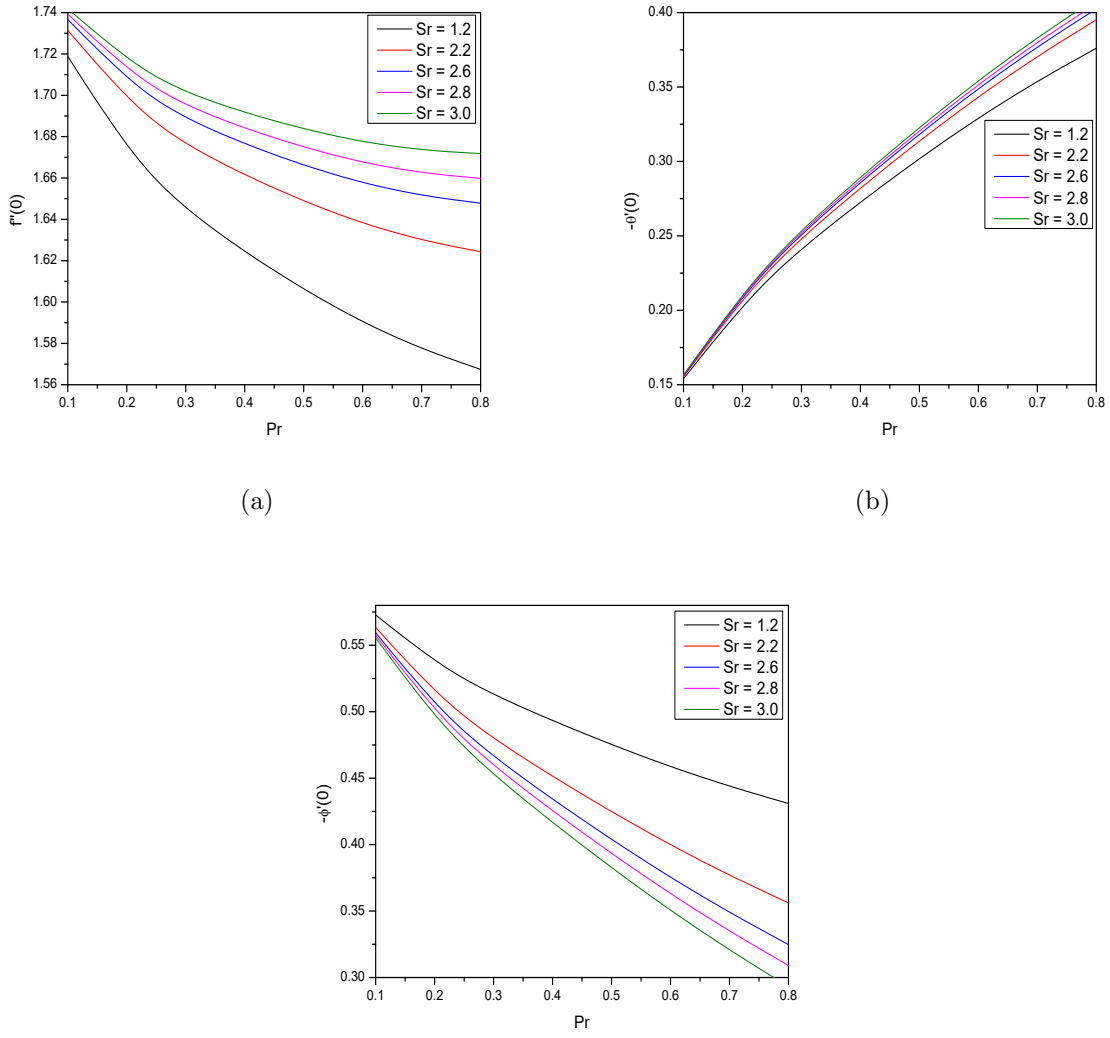

(a) (b)

(c)

Figure 4.3: "Effect of Sr on the skin friction coefficient, Nusselt number and Sherwood number for WTC boundary conditions".

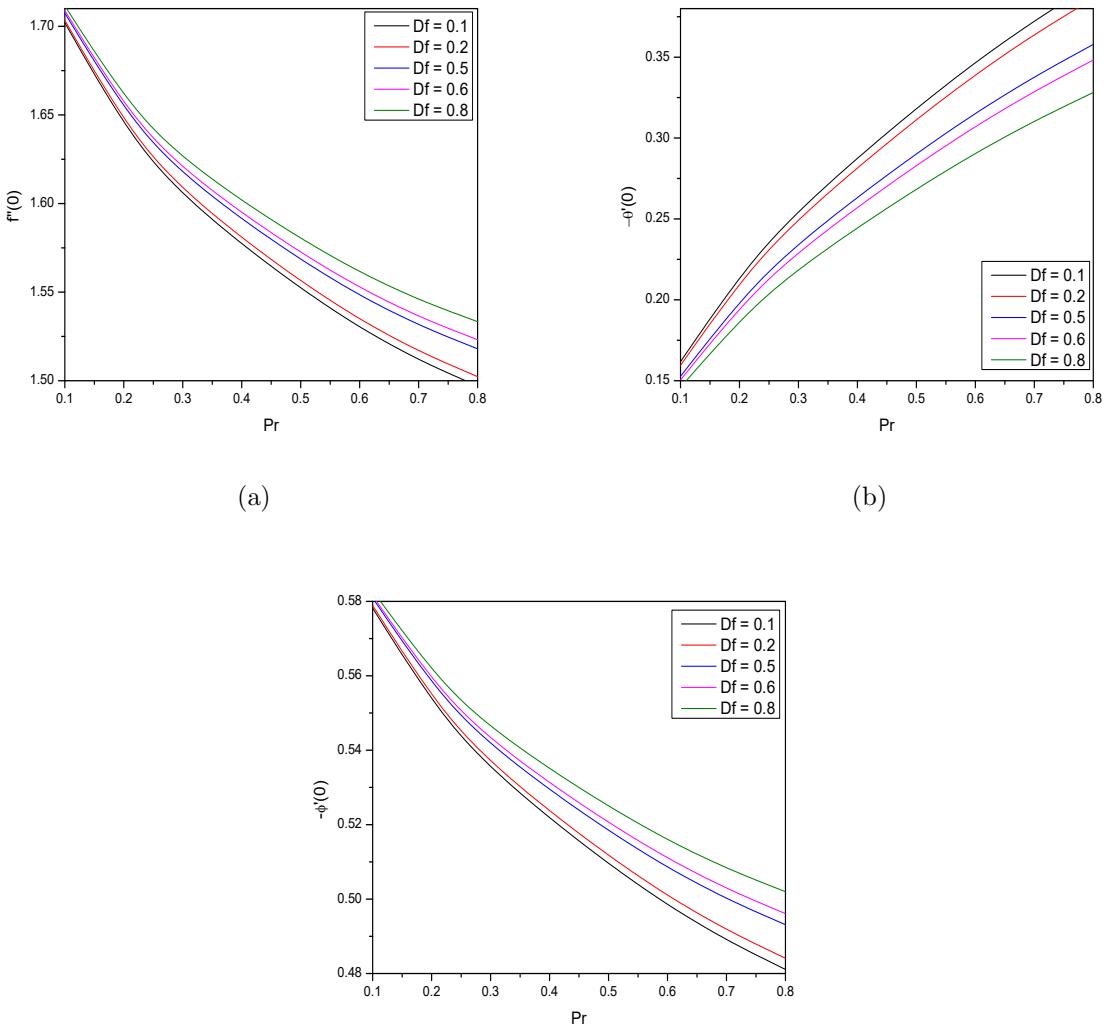

(a)

(b)

(c)

Figure 4.4: "Effect of Df on the skin friction coefficient, Nusselt number and Sherwood number for WTC boundary conditions".

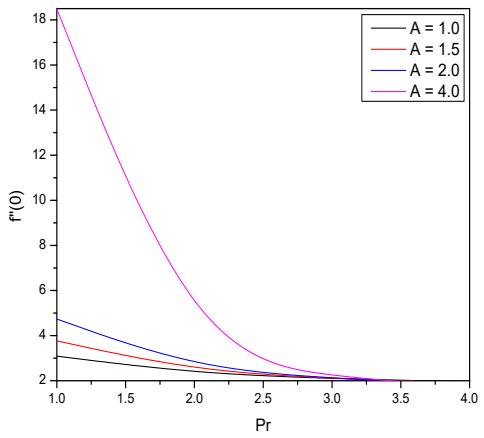

(a)

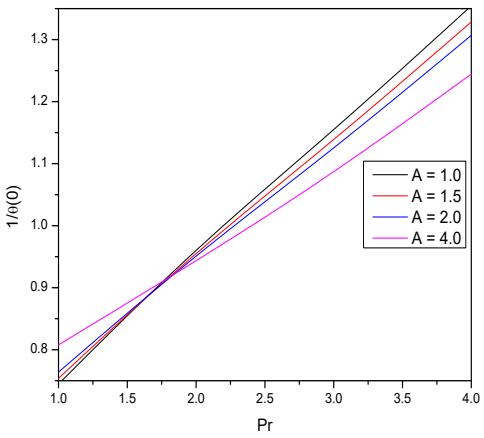

(b)

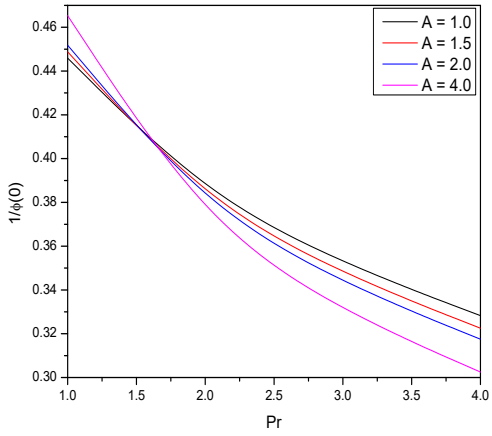

(c)

Figure 4.5: "Effect of A on the skin friction coefficient, Nusselt number and Sherwood number for WTC boundary conditions".

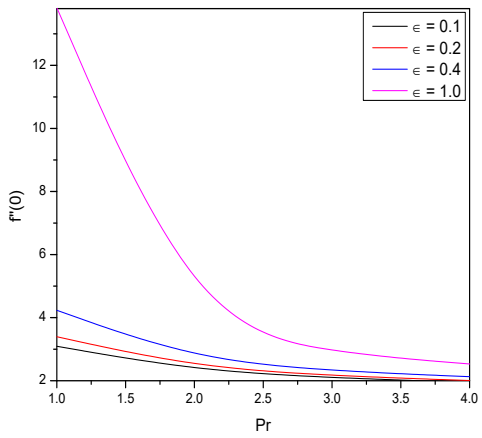

(a)

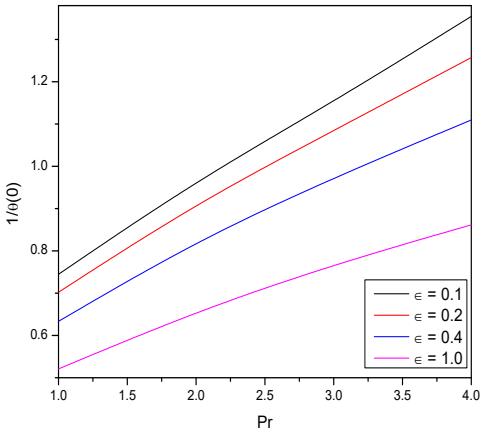

(b)

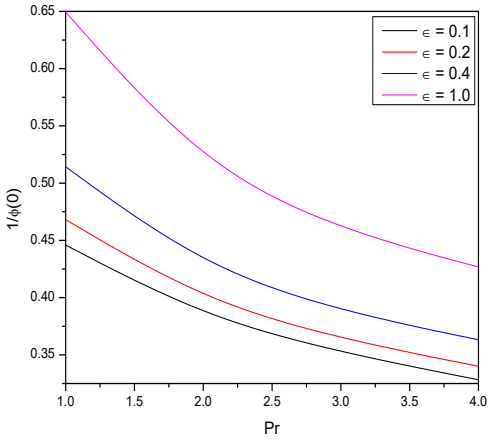

(c)

Figure 4.6: "Effect of $\in$ on the skin friction coefficient, Nusselt number and Sherwood number for WTC boundary conditions".

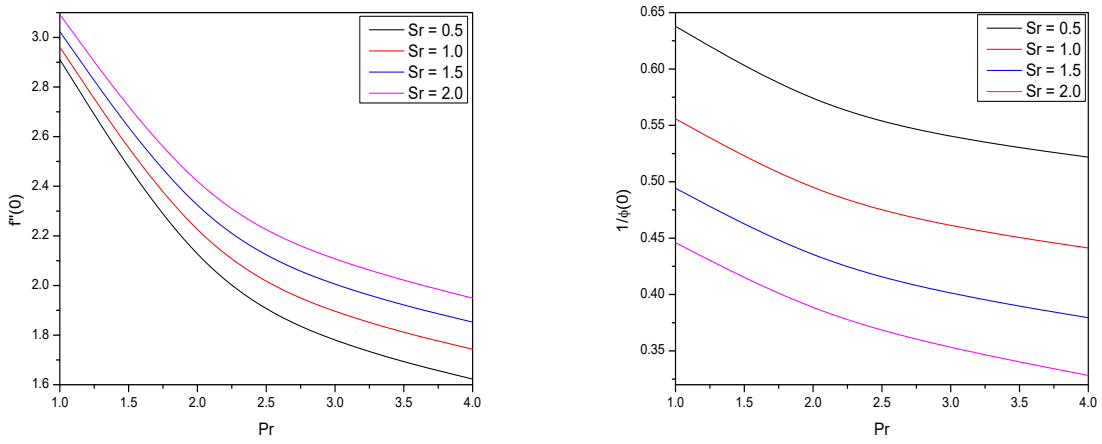

(a) (b)

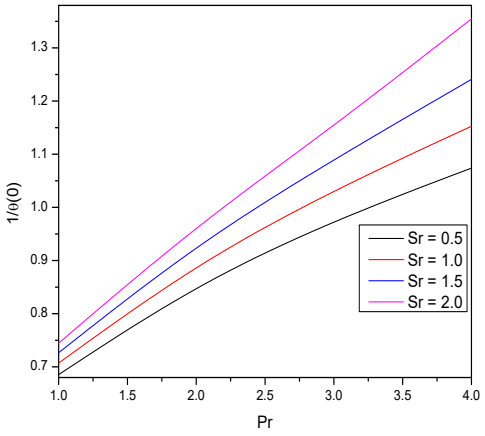

(c)

Figure 4.7: "Effect of Sr on the skin friction coefficient, Nusselt number and Sherwood number for WTC boundary conditions".

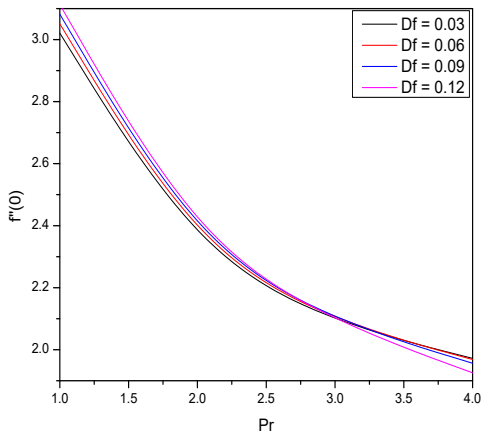

(a)

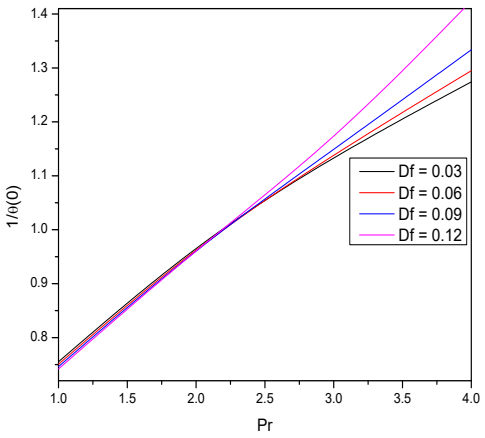

(b)

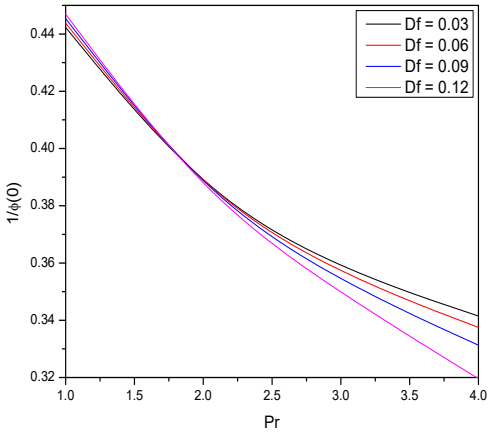

(c)

Figure 4.8: "Effect of Df on the skin friction coefficient, Nusselt number and Sherwood number for WTC boundary conditions".

Chapter 5

Influence of Variable Fluid Properties on The Boundary Layer Flow Past a Vertical Cone With Soret and Dufour Effects [1]

5.1 Introduction

The flow over a vertical cone has fascinated much importance on account of its vast application in engineering and industrial processes. For example, the cone penetration test is a standard quality control procedure for measuring the rheological properties of soils, soft solids found in food, and personal care products. Several authors developed similarity solutions for the steady flow across a vertical cone. Dufour effect is the energy flux caused by a concentration gradient. The Soret effect is the mass fluxe created by temperature gradient. Due to the importance of Dufour and Soret effects for the fluids with very light molecular weight as well as medium molecular weight, many investigators [93], [79], *et al.* [63], Ghoneim *et al.* [21], Meena *et al.* [49] have studied and reported results for these flows.

The current chapter emphasizes the study of a viscous incompressible boundary layer flow along a vertical cone with changeable viscosity and thermal conductivity in the existence of Dufour and Soret effects. The pseudo-spectral approach is implemented to solve the governing equations after they have been linearized by employing the successive linearization

[1] Published to "**Journal of Xidian University**"

method. The impacts of various flow and geometry factors on the skin friction coefficient as well as the rate of heat and mass transfer, are thoroughly examined.

5.2 Mathematical Formulation

Consider an incompressible boundary layer flow of viscous fluid along a vertical down-pointing cone with local radius r and half-angle ϕ under steady state and laminar flow conditions. The coordinate system and physical model are as depicted in Fig. (2.1). Apart from the assumptions made in Chapter - 4, here we assume that the ambient velocity of the fluid is U_∞ and no Boussinesq approximation is used. The ambient temperature and concentration are T_∞ and C_∞, respectively. Applying Boussinesq approximation and utilizing the boundary layer assumptions, the equations describing the flow are.

$$\frac{\partial}{\partial x}(ur) + \frac{\partial}{\partial y}(vr) = 0 \tag{5.1}$$

$$\rho\left(u\frac{\partial u}{\partial x} + v\frac{\partial u}{\partial y}\right) = \frac{\partial}{\partial y}\left(\mu\frac{\partial u}{\partial y}\right) \tag{5.2}$$

$$u\frac{\partial T}{\partial x} + v\frac{\partial T}{\partial y} = \frac{\partial}{\partial y}\left(\alpha\frac{\partial T}{\partial y}\right) + \frac{D_s K_T}{C_S C_P}\frac{\partial^2 c}{\partial y^2} \tag{5.3}$$

$$u\frac{\partial C}{\partial x} + v\frac{\partial C}{\partial y} = \frac{\partial}{\partial y}(D_s\frac{\partial C}{\partial y}) + \frac{D_s K_T}{T_m}\frac{\partial^2 T}{\partial y^2} \tag{5.4}$$

The viscosity and thermal conductivity are considered to be a linear function of the temperature [5] and are given by

$$\mu = \mu_\infty[1 + \lambda(T_\infty - T) \quad \text{and} \quad k = k_0[1 + \gamma(T - T_\infty)], \tag{5.5}$$

where μ_∞ and,k_0 represent the absolute viscosity and the thermal conductivity of the fluid, respectively, λ and γ are constants.

The boundary conditions for the velocity are no slip condition and uniform velocity in the ambient medium i.e.

$$u = 0, \quad v = 0, \quad \text{at} \quad y = 0 \quad u \to U_\infty \quad as \quad y \to \infty \tag{5.6}$$

As in the chapter- 4, here also we consider two types of boundary conditions for the

temperature.

$$\begin{aligned} &\textbf{Case-I (WTC)} : T = T_w, \quad C = C_w \quad \text{at} \quad y = 0. \\ &\textbf{Case-II (HMF)} : -k\frac{\partial T}{\partial y} = q_w, \quad -D_s\frac{\partial C}{\partial y} = q_m \quad \text{at} \quad y = 0. \end{aligned} \tag{5.7}$$

Far away from the cone, the following conditions are considered.

$$T \to T_\infty, \quad C \to C_\infty \quad \text{as} \quad y \to \infty \tag{5.8}$$

In the context of equation (5.1), the stream function is introduced as $u = \frac{1}{r}\frac{\partial \psi}{\partial y}$, $v = -\frac{1}{r}\frac{\partial \psi}{\partial x}$

The similarity transformations for WTC case are given by

$$\left.\begin{aligned} &\xi = \frac{x}{L}, \quad \eta = \frac{y}{L}\left(\frac{\mathrm{Re}}{\xi}\right)^{\frac{1}{2}}, \quad \psi = rLU_\infty \mathrm{Re}^{-\frac{1}{2}}\xi^{\frac{1}{2}} f(\eta), \\ &T = T_\infty + (T_w - T_\infty)\theta, \quad C = C_\infty + (C_w - C_\infty)\phi, \end{aligned}\right\} \tag{5.9}$$

where $Re = \dfrac{\rho U_\infty L}{\mu_\infty}$ represents the Reynolds number and L is the characteristic length.

Utilizing Equation (5.9) in the Equation (5.2),(5.3) and (5.4) we get the non-dimensional equations as

$$(1+A)f''' - A\theta f''' - A\theta' f'' + \frac{3}{2}ff'' = 0 \tag{5.10}$$

$$\frac{1}{\mathrm{Pr}}\theta'' + \frac{1}{\mathrm{Pr}} \in \theta\theta'' + \frac{1}{\mathrm{Pr}} \in (\theta')^2 + \frac{3}{2}f\theta' + Df\phi'' = 0 \tag{5.11}$$

$$Sr\theta'' + \frac{1}{Sc}\phi'' + \frac{3}{2}f\phi' = 0 \tag{5.12}$$

The similarity transformations for HMF case are given by

$$\left.\begin{aligned} &\xi = \frac{x}{L}, \quad \eta = \frac{y}{L}\left(\frac{\mathrm{Re}}{\xi}\right)^{\frac{1}{2}}, \quad \psi = rLU_\infty \mathrm{Re}^{-\frac{1}{2}}\xi^{\frac{1}{2}} f(\eta), \\ &T = T_\infty + \frac{q_w L}{k}\mathrm{Re}^{-\frac{1}{2}}\xi^{\frac{1}{2}} \quad C = C_\infty + \frac{q_w L}{k}Re^{-\frac{1}{2}}\xi^{\frac{1}{2}}\phi \end{aligned}\right\} \tag{5.13}$$

Utilizing the (5.13) in the Equations (5.2) to (5.4),we obtain

$$(1+A)f''' - A\theta f''' - A\theta' f'' + \frac{3}{2}ff'' = 0 \tag{5.14}$$

$$\frac{2}{\mathrm{Pr}}\theta'' + \frac{2\in}{\mathrm{Pr}}\theta\theta'' + \frac{2\in}{\mathrm{Pr}}\theta'^2 + 3f\theta' - f'\theta + Df\phi'' = 0 \tag{5.15}$$

$$Sr\theta'' + \frac{1}{Sc}\phi'' - \frac{1}{2}f'\phi + \frac{3}{2}f\phi' \tag{5.16}$$

The dimensionless form of boundary conditions (5.7) and (5.8) are

$$\text{“}f(0) = f'(0) = 0,\ \theta(0) = \phi(0) = 1,\ f'(\infty) = 1,\ \theta(\infty) = \phi(\infty) = 0'' \text{ for WTC case.} \tag{5.17}$$

$$\text{“}f(0) = f'(0) = 0,\ \theta'(0) = \phi'(0) = -1,\ f'(\infty) = 1,\ \theta(\infty) = \phi(\infty) = 0'' \text{ for HMF case.} \tag{5.18}$$

The most fundamental technical findings are the local skin-friction coefficient and rate of heat and transfers. The dimensionless representation of skin-friction coefficient C_f, Nusselt number (Nu), and Sherwood number(Sh) for WTC case are

$$Re^{-\frac{1}{2}}\xi^{\frac{1}{2}}C_f^I = f''(0), \quad Re^{-\frac{1}{2}}\xi^{\frac{1}{2}}Nu^I = -\theta'(0) \quad \text{and} \quad Re^{-\frac{1}{2}}\xi^{\frac{1}{2}}Sh^I = -\phi'(0) \tag{5.19}$$

and for CHF boundary conditions are

$$Re^{-\frac{1}{2}}\xi^{-\frac{1}{2}}C_f^{II} = f''(0), \quad Re^{-\frac{1}{2}}\xi^{-\frac{1}{2}}Nu^{II} = \frac{1}{\theta(0)} \quad \text{and} \quad Re^{-\frac{1}{2}}\xi^{-\frac{1}{2}}Sh^{II} = \frac{1}{\phi(0)} \tag{5.20}$$

5.3 Methodology

The set of differential equations (5.10) - (5.12) and (5.14) - (5.16) are linearized by means of a successive linearization method (SLM). The solutions of the ensuing linearized equations are attained by employing the Chebyshev spectral method.

On applying the procedure explained in Chapter 2 to the Eqs. (5.10) - (5.12) and Eqs. (5.14) - (5.16) , we get the following linearized equations.

$$a_1{}^{(n)}f_i''' + a_2{}^{(n)}f_i'' + a_3{}^{(n)}f_i + a_4{}^{(n)}\theta_i' + a_5{}^{(n)}\theta_i = a_6{}^{(n)} \tag{5.21}$$

$$b_1{}^{(n)}f_i' + b_2{}^{(n)}f_i + b_3{}^{(n)}\theta_i'' + b_4{}^{(n)}\theta_i' + b_5{}^{(n)}\theta_i + b_6{}^{(n)}\phi_i'' = b_7{}^{(n)} \tag{5.22}$$

$$C_1{}^{(n)} f_i{}' + C_2{}^{(n)} f_i + C_3{}^{(n)} \theta_i'' + C_4{}^{(n)} \phi_i'' + C_5{}^{(n)} \phi_i' + C_6{}^{(n)} \phi_i = c_7{}^{(n)} \tag{5.23}$$

where n=1 corresponds to WTC boundary conditions and n=2 corresponds to HMF boundary conditions.The coefficients in the above equations are given by

$$a_1{}^{(1)} = a_1{}^{(2)} = (1+A) - A\sum \theta_m,\ a_2{}^{(1)} = a_2{}^{(2)} = \frac{3}{2}\sum f_m - A\sum \theta_m{}'$$

$$a_3{}^{(1)} = a_3{}^{(2)} = \frac{3}{2}\sum f_m{}'', \quad a_4{}^{(1)} = a_4{}^{(2)} = -A\sum f_m'', \quad a_5{}^{(1)} = a_5{}^{(2)} = -A\sum f_m'',$$

$$a_6{}^{(1)} = a_6{}^{(2)} = \Big(-(1+A) + A\sum \theta_m\Big)\sum f_m''' + A\sum \theta_m' \sum f_m'' - \frac{3}{2}\sum f_m \sum f_m''$$

$$b_1{}^{(1)} = \frac{3}{2}\sum \theta_m', \quad b_1{}^{(2)} = -\sum \theta_m, \quad b_2{}^{(1)} = \frac{1}{\mathrm{Pr}} + \frac{\in}{\mathrm{Pr}}\sum \theta_m, \quad b_2{}^{(2)} = 3\sum \theta_m'$$

$$b_3{}^{(1)} = \frac{2\in}{\mathrm{Pr}}\sum \theta_m' + \frac{3}{2}\sum f_m, \quad b_3{}^{(2)} = \frac{2}{\mathrm{Pr}} + \frac{2\in}{\mathrm{Pr}}\sum \theta_m, b_4{}^{(1)} = \frac{\in}{\mathrm{Pr}}\sum \theta_m',$$

$$b_4{}^{(2)} = 3\sum f_m + \frac{4\in}{\mathrm{Pr}}\sum \theta_m', \quad b_5{}^{(1)} = b_6{}^{(2)} = D_f, \quad b_5{}^{(2)} = -\sum f_m',\ b_6{}^{(1)} = 0$$

$$b_7{}^{(n)} = -\frac{1}{\mathrm{Pr}}\sum \theta_m'' - \frac{\in}{\mathrm{Pr}}\sum \theta_m \sum \theta_m'' - \frac{\in}{\mathrm{Pr}}\sum \theta_m'^2 - \frac{3}{2}\sum f_m \sum \theta_m' - Df\sum \phi_m''$$

$$c_1{}^{(1)} = \frac{3}{2}\sum \phi_m', c_1{}^{(2)} = \frac{1}{2}\sum \phi_m, c_2{}^{(1)} = Sr, \quad c_2{}^{(2)} = -\frac{3}{2}\sum \phi_m',$$

$$c_3{}^{(1)} = \frac{1}{Sc}, \quad c_3{}^{(2)} = -Sr, \quad c_4{}^{(1)} = \frac{3}{2}\sum f_m, \quad c_4{}^{(2)} = -\frac{1}{Sc},$$

$$c_5{}^{(1)} = -\frac{3}{2}\sum f_m \sum \phi_m' - \frac{1}{Sc}\sum \phi_m'' - Sr\sum \theta_m'', \quad c_5{}^{(2)} = -\frac{3}{2}\sum f_m, \quad c_6{}^{(1)} = 0,$$

$$c_6{}^{(2)} = \frac{1}{2}\sum f_m', \quad c_7{}^{(1)} = -\frac{1}{Sc}\sum \phi_m'' - Sr\sum \theta_m'' - \frac{7}{4}\sum f_m \sum \phi_m'$$

$$c_7{}^{(1)} = 0, c_7{}^{(2)} = -\frac{1}{2}\sum f_m' \sum \phi_m + \frac{3}{2}\sum f_m \sum \phi_m' + \frac{1}{Sc}\sum \phi_m'' + Sr\sum \theta_m''$$

The equivalent conditions (5.17) and (5.18) changes to

$$f_i(0) = f_i{}'(0) = f_i{}'(\infty) = 1, \theta_i(\infty) = \phi_i(\infty) = 0,\ \theta_i(0) = \phi_i(0) = 1 \tag{5.24}$$

$$f_i(0) = f_i{}'(0) = 0, f_i{}'(\infty) = 1, \theta_i(\infty) = \phi_i(\infty) = 0,\ \theta_i(0) = \phi_i(0) = 1 \tag{5.25}$$

As explained in Chapter 2, applying Chebyshev pseudo spectral method on the system of linearized equations (5.21),(5.22) and (5.23), we get the following equation in the matrix form

$$A_{i-1}X_i = R_{i-1} \tag{5.26}$$

whereA_{i-1} is a square matrix of order $3N+3$ and X_i and R_{i-1} are column matrices of order $3N+3$ given by

$$A_{i-1} = \begin{pmatrix} A_{11}^{(i)} & A_{12}^{(i)} & A_{13}^{(i)} \\ A_{21}^{(i)} & A_{22}^{(i)} & A_{23}^{(i)} \\ A_{31}^{(i)} & A_{32}^{(i)} & A_{33}^{(i)} \end{pmatrix}, X_i = \begin{pmatrix} F_i \\ \Theta_i \\ \Phi_i \end{pmatrix}, R_i = \begin{pmatrix} r_1^{(i)} \\ r_2^{(i)} \\ r_3^{(i)} \end{pmatrix} \tag{5.27}$$

where

$$F_i = [f_i(\zeta_0), f_i(\zeta_1), ..., f_i(\zeta_{N-1}), f_i(\zeta_N)]^T,$$

$$\Theta_i = [\theta_i(\zeta_0), \theta_i(\zeta_1), .., \theta_i(\zeta_{N-1}), \theta_i(\zeta_N)]^T,$$

$$\Phi_i = [\phi_i(\zeta_0), \phi_i(\zeta_1), ...\phi_i(\zeta_{N-1}), \phi_i(\zeta_N)]^T,$$

$$A_{11}^{(1)} = a_1{}^{(1)}D^3 + a_2{}^{(1)}D^2 + a_3{}^{(1)}D + a_4{}^{(1)}I, A_{12}^{(1)} = a_5{}^{(1)}D + a_6{}^{(1)}I, A_{13}^{(1)} = a_7{}^{(1)}I$$

$$A_{21}^{(1)} = b_1{}^{(1)}I, A_{22}^{(1)} = b_2{}^{(1)}D^2 + b_3{}^{(1)}D + b_4{}^{(1)}I, A_{23}^{(1)} = b_5{}^{(1)}D^2$$

$$A_{31}^{(1)} = c_1{}^{(1)}I, A_{32}^{(1)} = c_2{}^{(1)}D^2, A_{33}^{(1)} = c_3{}^{(1)}D^2 + c_4{}^{(1)}D$$

$$A_{11}^{(2)} = a_1{}^{(2)}D^3 + a_2{}^{(2)}D^2 + a_3{}^{(2)}D + a_4{}^{(2)}I, A_{12}^{(2)} = a_5{}^{(2)}D + a_6{}^{(2)}I, A_{13}^{(2)} = a_7{}^{(2)}I$$

$$A_{21}^{(2)} = b_1{}^{(2)}D + b_2{}^{(2)}I, A_{22}^{(2)} = b_3{}^{(2)}D^2 + b_4{}^{(2)}D + b_5{}^{(2)}I, A_{23}^{(2)} = b_6{}^{(2)}D^2$$

$$A_{31}^{(2)} = c_1{}^{(2)}D + c_2{}^{(2)}I, A_{32}^{(2)} = c_3{}^{(2)}D^2, A_{33}^{(2)} = c_4{}^{(2)}D^2 + c_5{}^{(2)}D + c_6{}^{(2)}I$$

$$r_1^{(n)} = \left[a_8{}^{(n)}(\zeta_0), a_8{}^{(n)}(\zeta_1), ..., a_8{}^{(n)}(\zeta_{N-1}), a_8{}^{(n)}(\zeta_N)\right]^T$$

$$r_n^{(2)} = [b_7(\zeta_0), b_7(\zeta_1), ..., b_7(\zeta_{N-1}), b_7(\zeta_N)]^T$$

$$r_3^{(n)} = [c_7(\zeta_0), c_7(\zeta_1), ..., c_7(\zeta_{N-1}), c_7(\zeta_N)]^T$$

Where the superscript T stands for transpose, I is the identity O is the zero matrix.

Finally, the solution is given by

$$X_i = A_{i-1}^{-1} R_{i-1}$$

5.4 Results and Discussion

The impact of the four dimensionless parameters, viscosity parameter A, thermal conductivity parameter ϵ, Soret parameter Sr, Dufour parameter Df on the local Nusselt Number

N_u, the coefficient of local skin friction C_f, and Sherwood number Sh for WTC and HMF cases is presented graphically. In all the calculations, the values of Pr,B, and Scwere fixed as 2.0, 4.0and 1.0, respectively, unless otherwise specified.

The variation of the coefficient of skin friction, heat transfer rate, and the mass transfer rate with the impact of viscosity parameter A is portrayed in Fig.5.1 for WTC boundary conditions. It is observed from the Fig.5.1(a) that an increasing A increases the skin friction coefficient. As A rises, the rate of heat and mass transfer decreases, as presented in Figs.5.1(b) and 5.1(c).

The influence of thermal conductivity parameter $\in$ on the coefficient of skin friction, Nusselt number, and Sherwood number is given in the Fig.5.2 for WTC boundary conditions. It is revealed from Fig.5.2(a) that the coefficient of skin friction enhances as the variable thermal conductivity parameter rises. An enhancement in $\in$ leads to increase in the rate of heat transfer as depicted in 5.2(b). From Fig.5.2(c) it is noted that the Sherwood number is increasing for increasing values of $\in$.

The consequence of Soret number Sr on N_u, C_f, and Sh is portrayed in Fig.5.3 for WTC boundary conditions. From Fig.5.3(a) it is seen that decreasing the value of the Soret number enhances the sherewood number. The rate of heat transfer increases with an increase in the value of Sr as displayed in 5.3(b). Fig.5.3(c) reveals that the Sherwood number is increasing as Sr increases.

The variation of skin friction coefficient, heat and mass transfer rate against the Dufour parameter Df is shown in the Fig.5.4 for WTC boundary conditions. As shown in Fig. 5.4(a), the coefficient of skin friction decreases as the Dufour parameter increase. The heat transfer rate is reducing with a rise in Df as portrayed in Fig.5.4(b). From Fig. 5.4(c), it is noticed that the Sherwood numbers appear to be increasing for increasing Df values.

The influence of viscosity parameter A on N_u, C_f, and Sh is depicted in Fig.5.5 for HMF boundary conditions. As shown in Fig. 5.5(a),5.5(c) intensifying A increases the skin friction coefficient and sherewood number. The heat transfer rate is increasing initially and then decreasing with an increase in the variable viscosity parameter A as given in the Figs.5.5(b).

The effect of $\in$ on the skin friction coefficient, Nusselt number and Sherwood number is depicted in Fig.5.6 for HMF boundary conditions. According to Fig. 5.6(a), the coefficient of skin friction increases as the value of the thermal conductivity parameter decreases. The heat transfer rate is decreasing with a rise $\in$ as indicated in 5.6(b). Fig.5.6(c) discloses that

the Sherwood number is enhancing for enhancing values of $\in$.

The variation of N_u, C_f, and Sh with the Soret number Sr is displayed in the Fig.5.7 for HMF boundary conditions. Fig.5.7(a) shows that the coefficient of skin friction and heat transfer rate are decreasing with a rise in the value of the Soret parameter. As Sr is enhancing, the heat transfer is also enhancing as displayed in the Fig.5.7(b). Fig.5.7(c) explains that the Sherwood number is increases as the values of Sr increase.

The consequence of N_u, C_f, and Sh with the Dufour number parameter Df is presented in Fig.5.8 for HMF boundary conditions. Fig.5.8(a) exhibits that the coefficient of skin friction is decreasing with an increase in the value of the Dufour parameter. The rate of heat transfer is diminishing with a rise in Df as portrayed in Fig.5.8(b) From Fig. 5.8(c) it is detected that the Sherwood number is increasing for enhancing values of Df.

5.5 Conclusion

The boundary layer flow across a vertical cone is considered by assuming the variable viscosity and variable thermal conductivity in the presence of Soret and Dufour effects. Similarity conversions are utilized to reduce the equations describing the flow into ordinary differential equations. The non-dimensional equations linearized using successive linearization procedure and then the solution of the resulting system is found using Chebyshev spectral method.

- The heat transfer rate decrements with intensifying the viscosity and thermal conductivity parameters for WTC conditions but the reverse tend is noticed for HMF conditions.
- For WTC state, an improvement in viscosity and thermal conductivity infers to a rise in the coefficient of the skin friction, whereas for HMF conditions, the opposite is the case
- An enhancement in Soret number enhances the coefficient of skin friction and rate of heat transfer but reduces the Sherwood number for both WTC and HMF cases.
- The coefficient of skin friction and Sherwood numbers rise whereas the heat transfer rate is reducing as the Dufour parameter increase.

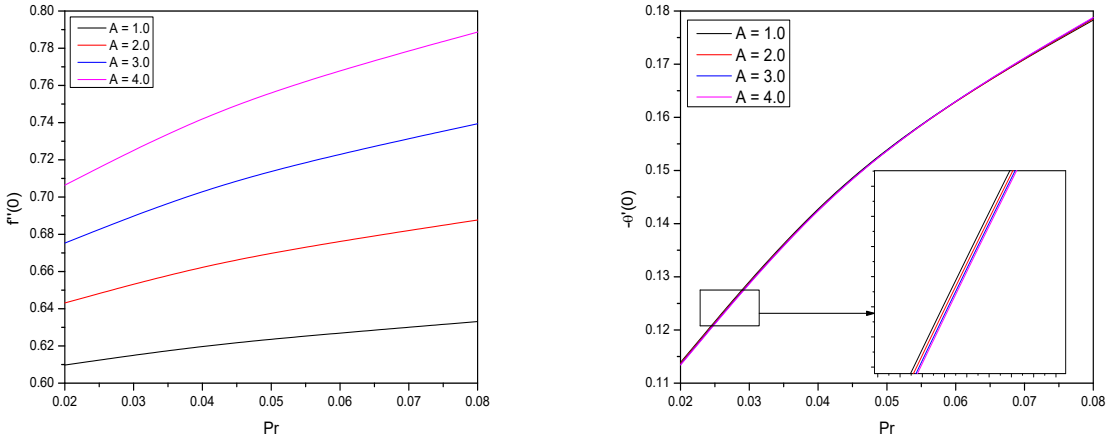

(a)

(b)

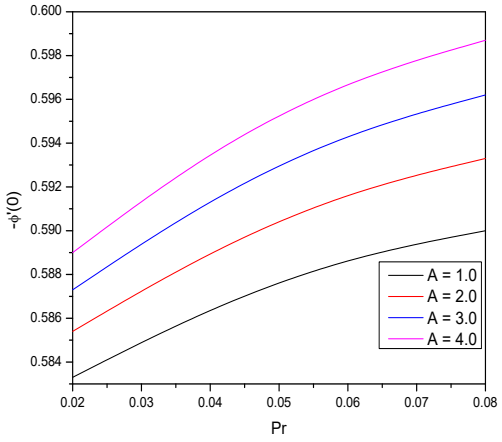

(c)

Figure 5.1: "Effect of A on the skin friction coefficient, Nusselt number and Sherwood number for WTC boundary conditions".

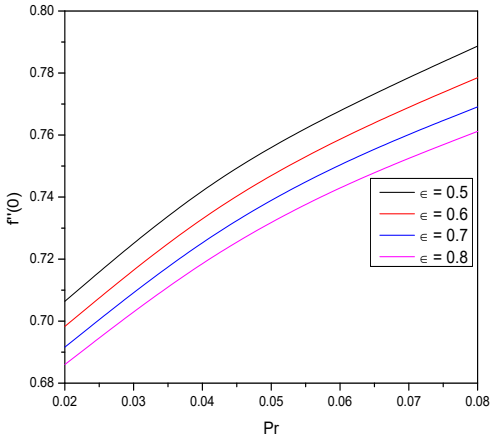

(a)

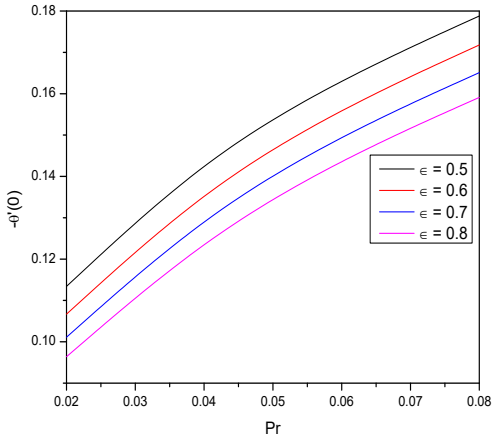

(b)

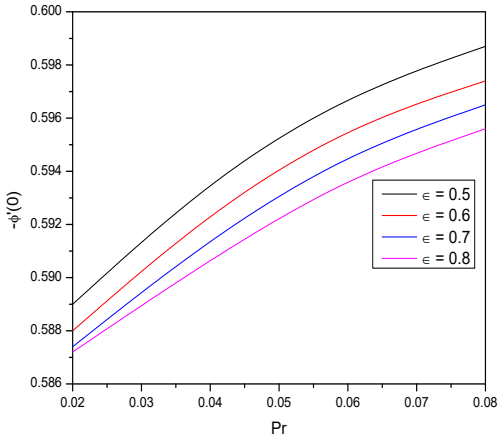

(c)

Figure 5.2: "Effect of $\in$ on the skin friction coefficient, Nusselt number and Sherwood number for WTC boundary conditions".

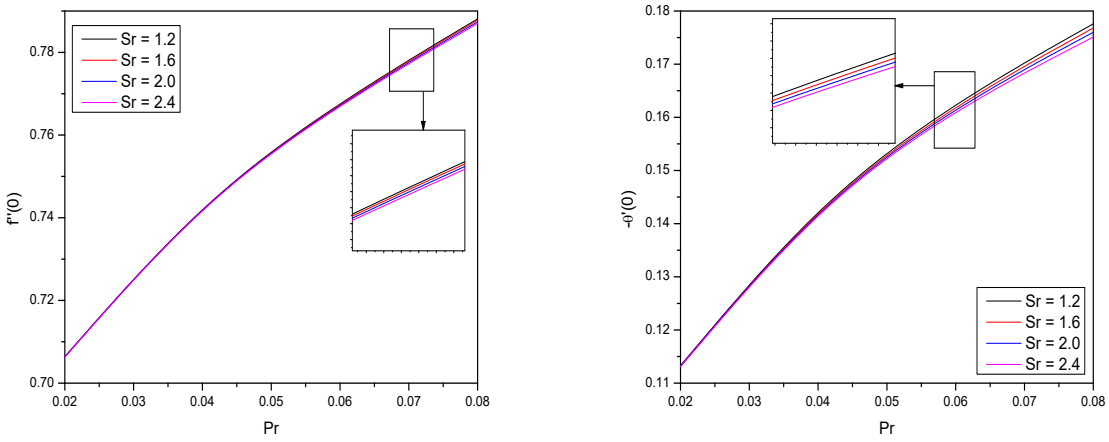

(a)

(b)

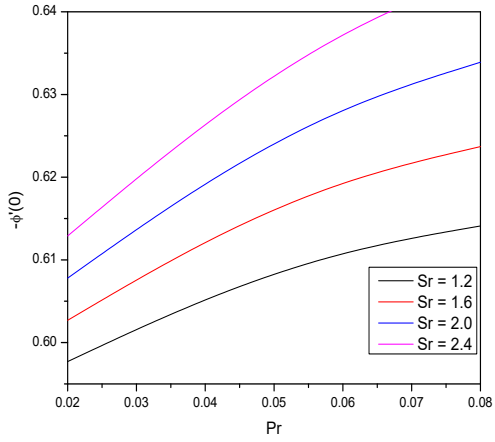

(c)

Figure 5.3: "Effect of Sr on the skin friction coefficient, Nusselt number and Sherwood number for WTC boundary conditions".

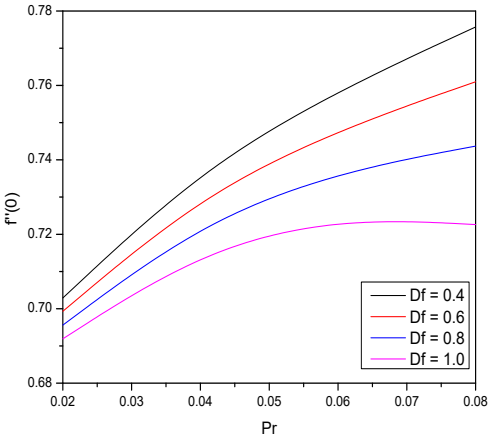

(a)

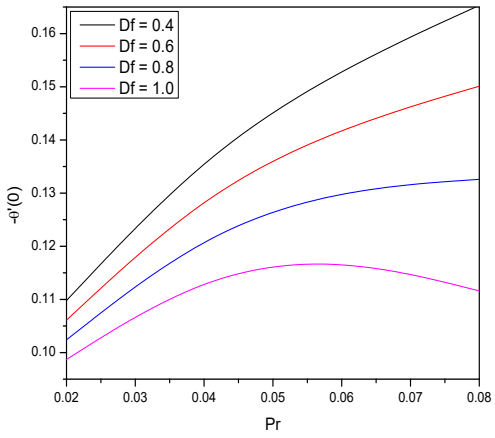

(b)

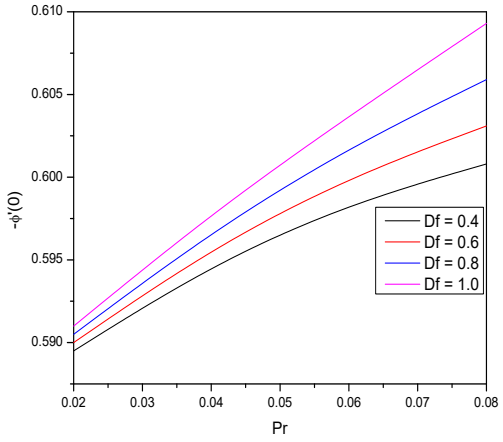

(c)

Figure 5.4: "Effect of Df on the skin friction coefficient, Nusselt number and Sherwood number for WTC boundary conditions".

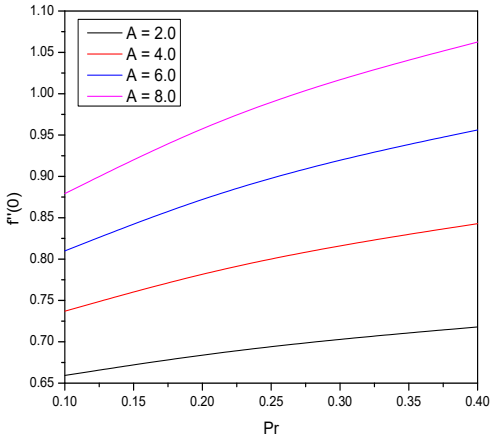

(a)

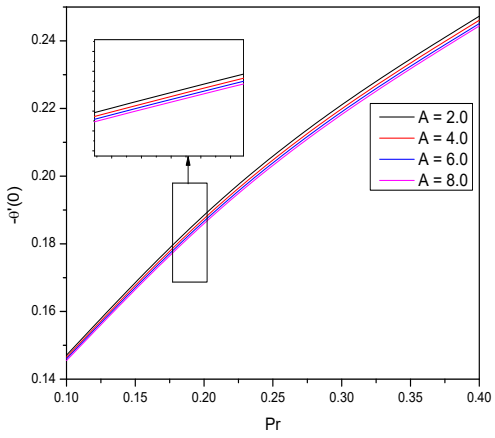

(b)

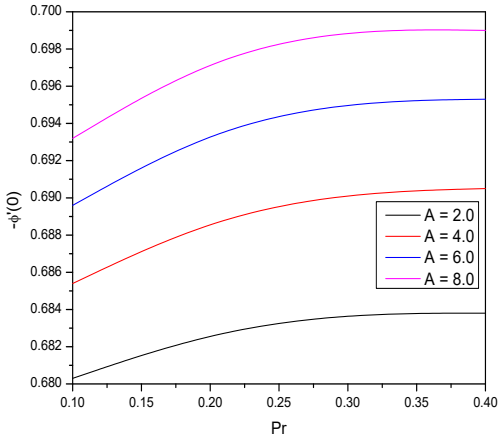

(c)

Figure 5.5: "Effect of A on the skin friction coefficient, Nusselt number and Sherwood number for HMF boundary conditions".

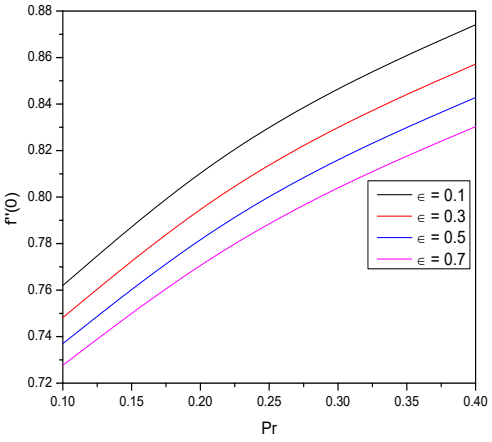

(a)

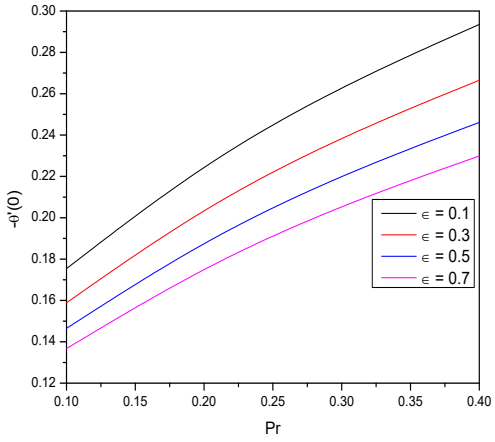

(b)

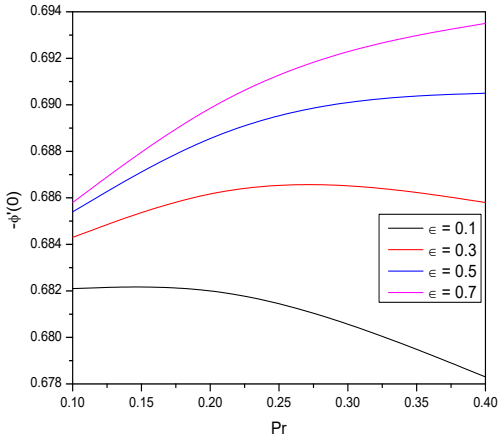

(c)

Figure 5.6: "Effect of $\in$ on the skin friction coefficient, Nusselt number and Sherwood number for HMF boundary conditions".

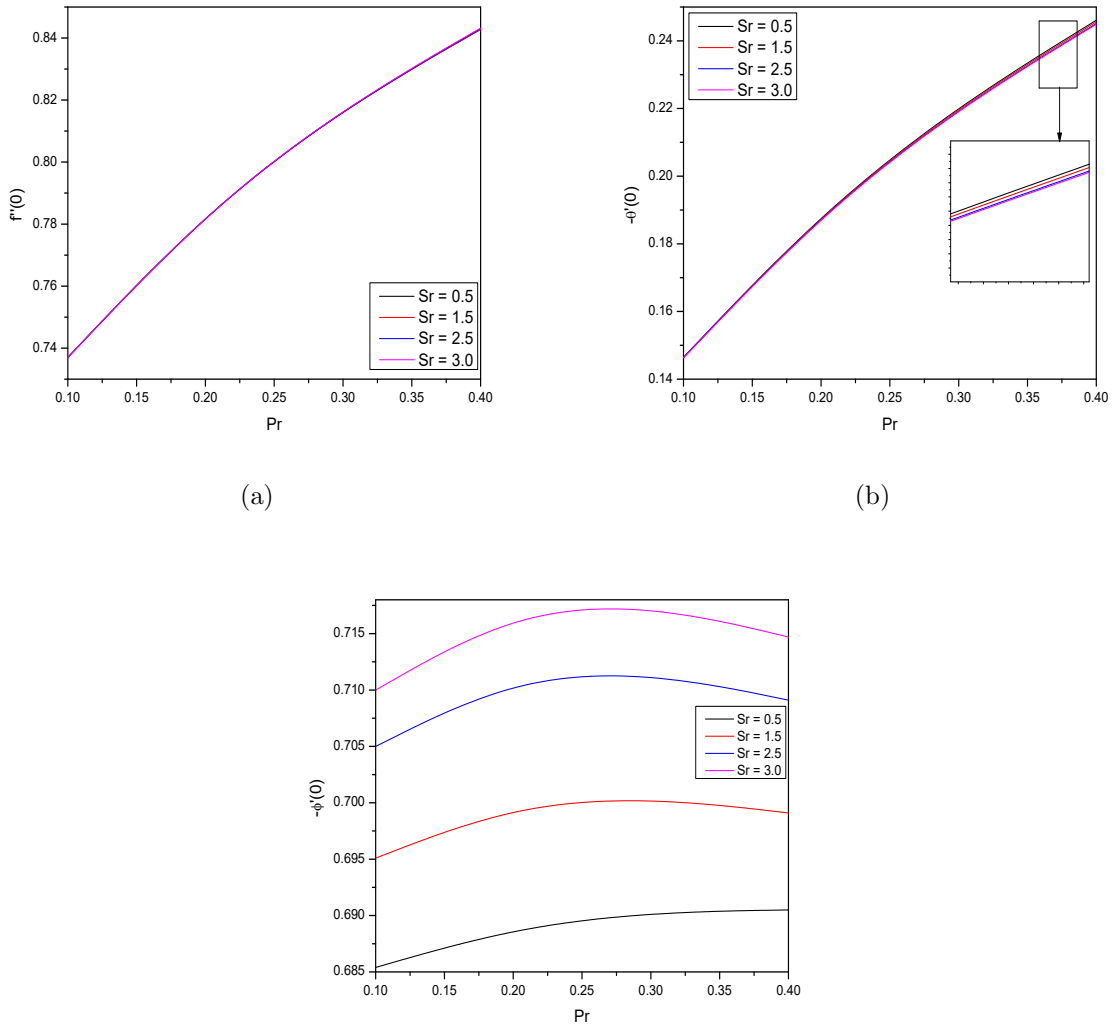

(a)

(b)

(c)

Figure 5.7: "Effect of Sr on the skin friction coefficient, Nusselt number and Sherwood number for HMF boundary conditions".

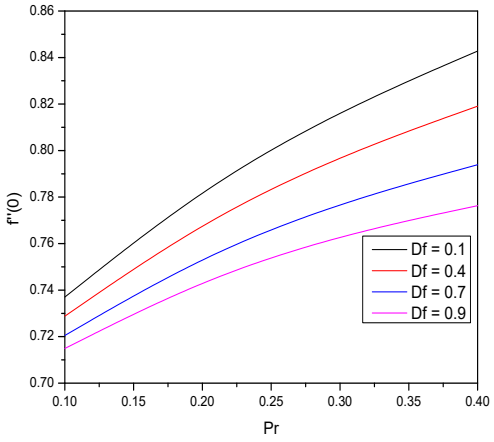

(a)

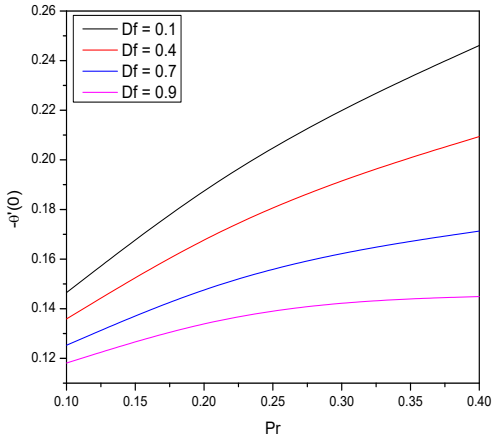

(b)

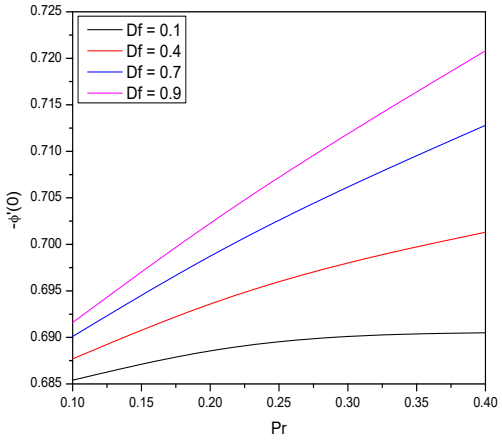

(c)

Figure 5.8: "Effect of Df on the skin friction coefficient, Nusselt number and Sherwood number for HMF boundary conditions".

Chapter 6

The Effect of Variable Viscosity and Thermal Conductivity on the Free Convection Flow Past a Rotating Cone [1]

6.1 Introduction

The convective boundary layer flow over a rotating cone is important for the model of innumerable engineering apparatus like heat swaps, discarding and geothermal basins, containers for fissionable trash, rotating heat exchangers, rotating cone reactors for bio-fuels production, gas or marine turbine, are extensively utilized by the energy, automobile and chemical industries. Earlier research of flow and heat transfer in rotating systems are given by Dorffman [16] and Kreith [31]. Since then, several researchers have been examining the convective heat and mass transfer over a rotating cone under various physical conditions. Fildes *et al.* [19] focused on analysing the effects of traveling modes on the boundary layer flow over a rotating cone in a still fluid system. Hayat *et al.* [24] investigated the importance of magnetic field and chemical reaction in the mixed convective unsteady flow of viscous liquid over a rotating cone. Ullah *et al.* [88] presented instability analyses for cones rotating within magnetic field.

This chapter deals with the study of an incompressible viscous fluid flow and along over

[1] Communicated to "**International Journal of Applied and Computational Mathematics**"

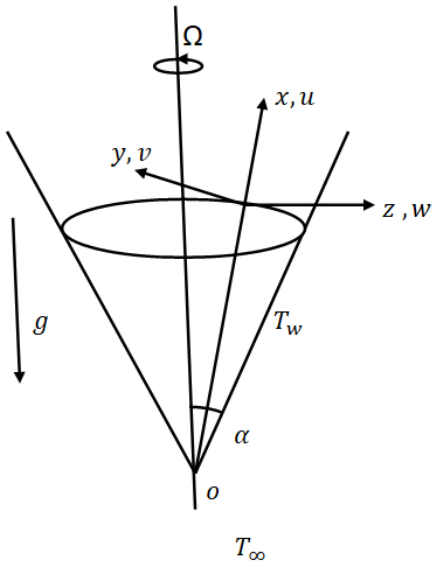

Figure 6.1: ““Geometry of the flow field.

a rotating cone with changeable viscosity and thermal conductivity. The pseudo-spectral approach is used to solve the governing equations after they have been linearized using the successive linearization method. This technique was efficaciously applied to solve the convection heat and mass transfer problems. The impacts of various flow and geometry factors on the velocity component, temperature, and heat transfer rate are thoroughly examined.

6.2 Mathematical Formulation

Consider the laminar viscous incompressible fluid flow over a cone rotating about its axis with angular velocity Ω. We consider the cartesian rectangular coordinate system in which x-axis is along a meridional section, y-axis is along a circular section and the z-axis is normal to the cone surface. The coordinate system and the geometry of the problem is depicted in Fig. (6.1). The local radius of the cone is r and semi-vertical angle of the cone is α. The local radius at a point located and the radius of a cone can be guesstimated by $r = (xsin\phi)$. Let $(u,\ v,\ w)$ be the velocity vector. The free stream temperature is T_∞. The variations in the temperature are responsible for the buoyancy forces in the fluid flow and the flow is assumed to be axisymmetric.

Applying Boussinesq approximation and utilizing the boundary layer assumptions, the

equations describing the flow are.

$$\frac{\partial u}{\partial x} + \frac{\partial w}{\partial z} + \frac{u}{x} = 0 \tag{6.1}$$

$$\rho\left(u\frac{\partial u}{\partial x} + w\frac{\partial u}{\partial z} - \frac{v^2}{x}\right) = \frac{\partial}{\partial z}\left(\mu\frac{\partial u}{\partial z}\right) + \rho g\beta\cos\alpha(T - T_\infty) \tag{6.2}$$

$$\rho\left(u\frac{\partial v}{\partial x} + w\frac{\partial v}{\partial z} + \frac{uv}{x}\right) = \frac{\partial}{\partial z}\left(\mu\frac{\partial v}{\partial z}\right) \tag{6.3}$$

$$\left(u\frac{\partial T}{\partial x} + w\frac{\partial T}{\partial z}\right) = \frac{\partial}{\partial z}\left(\alpha\frac{\partial T}{\partial z}\right) \tag{6.4}$$

where T represents the temperature of the fluid, g represents the gravitational acceleration, μ represents the variable viscosity, ρ represents the fluid density, β represents the coefficient of thermal expansion, C_p represents the specific heat and k represents the variable thermal conductivity of the fluid.

The viscosity and thermal conductivity are considered to be a linear function of the temperature [5] and are given by

$$\mu = \mu_\infty[1 + \lambda(T_\infty - T) \quad \text{and} \quad k = k_0[1 + \gamma(T - T_\infty)], \tag{6.5}$$

where μ_∞ and,k_0 represent the absolute viscosity and the thermal conductivity of the fluid, respectively, λ and γ are constants.

The bounday conditions for the velocity are given as

$$u = 0 \quad , v = r\Omega \quad w = 0 \quad \text{at} \quad z = 0 \quad \text{and} \quad u \to 0 \quad v \to 0 \quad \text{as} \quad z \to \infty \tag{6.6}$$

In addition, for the temperature on the surface of the cone, one can either have constant temperature T_w (CWT) or a constant heat flux q_w (CHF).Thus, the conditions for the temperature on the boundary conditions are written as

$$\textbf{Type - I} : T = T_w \quad \text{at} \quad z = 0 \tag{6.7}$$

$$\textbf{Type - II} : k\frac{\partial T}{\partial z} = q_w \quad \text{at} \quad z = 0 \tag{6.8}$$

and far away from the cone, the temperature of the free stream is constant i.e. $T \to T_\infty$, as $z \to \infty$

In order to obtain non-dimensional equations,we introduce the following non-dimensional

Transformations

$$\left.\begin{aligned}
&\eta = \left(\frac{\Omega \sin\alpha}{\nu}\right)^{\frac{1}{2}} z, \quad u = \frac{1}{2} x\Omega \sin\alpha f'(\eta), \\
&v = x\Omega \sin\alpha g(\eta), \quad w = (\nu\Omega \sin\alpha)^{\frac{1}{2}} f(\eta), \\
&T = T_\infty + (T_w - T_\infty)\theta(\eta), \text{ where } T_w - T_\infty = (T_L - T_\infty)\frac{x}{L} \text{for CWT case} \\
&T = T_\infty + \left(\frac{\Omega \sin\alpha}{\nu}\right)^{\frac{1}{2}} \frac{q_w}{k}\theta(\eta), \text{ where } q_w = q_0 \frac{x}{L} \text{for CHF case}
\end{aligned}\right\} \tag{6.9}$$

Applying the similarity transformations (6.9) in the Eqs. (6.1) to (6.4), we get the following non-dimensional equations

$$(1+A)f''' - A\theta f''' - ff'' + \frac{1}{2}f'^2 - A\theta' f'' - 2g^2 - 2\lambda\theta = 0 \tag{6.10}$$

$$(1+A)g'' - A\theta g'' - Ag'\theta' + f'g - fg' = 0 \tag{6.11}$$

$$\frac{1}{\Pr}\theta'' + \frac{1}{\Pr} \in \theta\theta'' + \frac{\in}{\Pr}\theta'^2 + \frac{1}{2}f'\theta - f\theta' = 0 \tag{6.12}$$

where $Re_L = \dfrac{L^2\Omega \sin\alpha}{\nu}$ is the Reynolds number, L is the typical length, $Pr = \dfrac{\nu}{\alpha_0}$ is the Prandtl number, $Gr_1 = \dfrac{L^2 g\beta \cos\phi(T_w - T_\infty)}{\nu^2}$ is the Grashof number and $\lambda = \dfrac{Gr_1}{Re_L^2}$ for CWT case, $Gr_2 = \dfrac{L^2 g\beta \cos\phi q_w}{\nu^2}$ is the Grashof number and $\lambda = \dfrac{Gr_2}{Re_L^2}$ for CHF case. Here λ is the dimensionless buoyancy parameter, A is the viscosity parameter and $\in$ is the thermal conductivity parameter.

The dimensionless form of conditions on the boundary are

$$f(0) = f'(0) = 0, \quad g(0) = 1, \quad \theta(0) = 1, \quad f'(\infty) = g(\infty) = \theta(\infty) = 0 \quad \text{for CWT case.} \tag{6.13}$$

$$f(0) = f'(0) = 0, \quad g(0) = 1, \quad \theta'(0) = -1, \quad f'(\infty) = g(\infty) = \theta(\infty) = 0 \quad \text{for CHF case.} \tag{6.14}$$

The quantities of practical interests are the surface skin-friction coefficient in x- and y-directions and local rate of heat-transfer in terms of Nusselt number. The non-dimensional form of skin-friction coefficient C_{fx} and C_{fy} Nusselt number (Nu) for CWT boundary con-

ditions are

$$C_{fx} = -Re_x{}^{-\frac{1}{2}} f''(0), \quad \text{and} \quad C_{fy} = -Re_x{}^{-\frac{1}{2}} g'(0) \tag{6.15}$$

The non-dimensional form of Nusselt number (Nu) is

$$Nu^I = \theta'(0) \text{ for CWT case} \quad \text{and} \quad Nu^{II} = \frac{1}{\theta(0)} \text{ for CHF case} \tag{6.16}$$

6.3 Methodology

The set of differential equations (6.10) - (6.12) are linearized by means of a successive linearization method (SLM) [55]. The solutions of the ensuing linearized equations are attained by employing the Chebyshev spectral method [7].

On applying the procedure explained in Chapter 2 to the Eqs. (6.10) - (6.12), we get the following linearized equations.

$$a_1 f_i^{''} + a_2 f_i^{''} + a_3 f_i^{'} + a_4 f_i + a_5 g_i + a_6 \theta_i^{'} + a_7 \theta_i = a_8 \tag{6.17}$$

$$b_1 f_i^{'} + b_2 f_i + b_3 g_i^{''} + b_4 g_i^{'} + b_5 g_i + b_6 \theta_i^{'} + b_7 \theta_i = b_8 \tag{6.18}$$

$$c_1 f_i^{'} + c_2 f_i + c_3 \theta_i^{''} + c_4 \theta_i^{'} + c_5 \theta_i = c_6 \tag{6.19}$$

where

$$a_1 = \left((1+A) - A\sum \theta_m\right), a_2 = \left(-\sum f_m - A\sum \theta_m^{'}\right),$$
$$a_3 = -\sum f_m^{'}, a_4 = -\sum f_m^{''}, a_5 = -4\sum g_m, a_6 = -A\sum f_m^{''},$$

$$a_7 = -A\sum f_m^{'''} - 2\lambda$$

$$a_8 = \left(A\sum \theta_m - (1+A)\right)\sum f_m^{'''} + \left(\sum f_m + A\sum \theta_m^{'}\right)\sum f_m^{''} - \frac{1}{2}\sum f_m^{'^2} + 2\sum g_m{}^2 + 2\lambda\sum \theta_m$$

$$b_1 = \sum g_m, b_2 = -\sum g_m^{'}, b_3 = \left((1+A) - A\sum \theta_m\right)$$

$$b_4 = -A\sum \theta_m^{'} - \sum f_m, b_5 = \sum f_m^{'}, b_6 = -A\sum g_m^{'}, b_7 = -A\sum g_m^{''}$$

$$b_8 = \left(A\sum \theta_m - (1+A)\right)\sum g_m^{''} + A\sum g_m^{'}\sum \theta_m^{'} - \sum f_m^{'}\sum g_m + \sum f_m\sum g_m^{'}$$

$$c_1 = \frac{1}{2}\sum \theta_m, c_2 = -\sum \theta'_m, c_3 = \frac{1}{Pr} + \frac{\in}{\Pr}\sum \theta_m$$

$$c_4 = \frac{2\in}{Pr}\sum \theta'_m - \sum f_m, c_5 = \frac{\in}{Pr}\sum \theta''_m + \frac{1}{2}\sum f'_m$$

$$c_6 = \left(-\frac{1}{Pr} - \frac{\in}{Pr}\sum \theta_m\right)\sum \theta''_m - \frac{\in}{\Pr}\sum \theta'^2_m + \sum f_m \sum \theta'_m - \frac{1}{2}\sum f'_m \sum \theta_m$$

The conditions (6.13) and (6.14) changes to

$$f_i(0) = f'_i(0) = 0, \quad g_i(0) = 1, \quad \theta_i(0) = 1, \quad f'_i(\infty) = g_i(\infty) = \theta_i(\infty) = 0 \quad \text{for CWT case.} \tag{6.20}$$

$$f_(0) = f'_i(0) = 0, \quad g_i(0) = 1, \quad \theta'_i(0) = -1, \quad f'_i(\infty) = g_i(\infty) = \theta_i(\infty) = 0 \quad \text{for CHF case.} \tag{6.21}$$

As explained in Chapter 2, applying Chebyshev pseudo spectral method on the system of linearized equations (6.17),(6.18) and (6.19), we get the following equation in the matrix form

$$A_{i-1}X_i = R_{i-1} \tag{6.22}$$

whereA_{i-1} is a square matrix of order $3N+3$ and X_i and R_{i-1} are column matrices of order $3N+3$ given by

$$A_{i-1} = \begin{pmatrix} A_{11}^{(i)} & A_{12}^{(i)} & A_{13}^{(i)} \\ A_{21}^{(i)} & A_{22}^{(i)} & A_{23}^{(i)} \\ A_{31}^{(i)} & A_{32}^{(i)} & A_{33}^{(i)} \end{pmatrix}, X_i = \begin{pmatrix} F_i \\ G_i \\ \Theta_i \end{pmatrix}, R_i = \begin{pmatrix} r_1^{(i)} \\ r_2^{(i)} \\ r_3^{(i)} \end{pmatrix} \tag{6.23}$$

where

$$F_i = [f_i(\zeta_0), f_i(\zeta_1), ..., f_i(\zeta_{N-1}), f_i(\zeta_N)]^T,$$

$$G_i = [g_i(\xi_0), g_i(\xi_1), .., g_i(\xi_{N-1}), g_i(\xi_N)]^T,$$

$$\Theta_i = [\theta_i(\xi_0), \theta_i(\xi_1), ...\theta_i(\xi_{N-1}), \theta_i(\xi_N)]^T,$$

$$A_{11}^{(1)} = a_1D^3 + a_2D^2 + a_3D + a_4I, A_{12}^{(1)} = a_5I, A_{13}^{(1)} = a_6D + a_7I$$

$$A_{21}^{(1)} = b_1D + b_2I, A_{22}^{(1)} = b_3D^2 + b_4I, A_{23}^{(1)} = b_6D + b_7I$$

$$A_{31}^{(1)} = c_1D + c_2I, A_{32}^{(1)} = 0, A_{33}^{(1)} = c_3D^2 + c_4D + c_5I$$

$$r_1^{(1)} = [a_8(\xi_0), a_8(\xi_1), ..., a_8(\xi_{N-1}), a_8(\xi_N)]^T$$

$$r_2^{(1)} = [b_8(\xi_0), b_8(\xi_1), ..., b_8(\xi_{N-1}), b_8(\xi_N)]^T$$

$$r_3^{(1)} = [c_6(\xi_0), c_6(\xi_1), ..., c_6(\xi_{N-1}), c_6(\xi_N)]^T$$

where the superscript T stands for transpose, I is the identity O is the zero matrix. Finally, the solution is given by

$$X_i = A_{i-1}^{-1} R_{i-1}$$

6.4 Results and Discussion

The variation of the velocity component f', the circumferential velocity g and the temperature θ, local Nusselt Number N_u, and the local skin friction coefficients in the tangential and azimuthal directions C_{fx}, C_{fx} for diverse values of viscosity parameter, buoyancy parameter and thermal conductivity parameter for constant wall temperature and heat flux cases depicted graphically.

The impact of viscosity parameter A on the velocity components, temperature, coefficient of skin friction and heat transfer rate is depicted in Fig.6.2 for type - I boundary conditions. It is detected that from Fig. 6.2(a) that the tangential velocity f is seen to be decreasing towards the cone surface and subsequently increasing for an increase in A. Figure 6.2(b) shows that with rising values of A, the circumferential velocity g increases away from the cone surface. It is observed from 6.2(c) that there is a marginal rise in temperature with higher values of A. The dimensionless tangential skin-friction $(-f''(0))$ and azimuthal skin-friction$(-g'(0))$ grow as A increases as depicted in Figs. 6.2(d) and 6.2(e). The Nusselt number $(-\theta'(0))$, which is shown in Fig. 6.2(f), is rising together with the value of A .

The effect of thermal conductivity parameter $\in$ on the velocity, temperature, coefficient of skin frictions and heat transfer rate is depicted in Fig. 6.3 for type – I boundary conditions. From Fig. 6.3(a), it is observed that the tangential velocity f rises as the values of in rise. The circumferential velocity g is not significantly affected by in. As the value of $\in$ is increasing, it is observed from Fig.6.3(c) that the temperature also increasing. Figures 6.3(d) and 6.3(e) show that both the skin frictions rise as the value of $\in$ rises. According to Fig. 6.3(f), the Nusselt number is dropping as the parameter in increases.

Figure 6.4 presents the variation of the velocity, temperature, coefficient of skin frictions and heat transfer rate for type – I boundary conditions. From Fig. 6.4(a) it is observed that the tangential velocity f increases near the cone surface and then decreases as the parameter *lambda* increases. As *lambda* increases, the circumferential velocity$g$ decreases slightly, as shown in Fig. 6.4(b). Figure 6.4(c) shows that the temperature *theta* decreases as the

value of *lambda* increases. Figures 6.4(d) and 6.4(e) show that the tangential skin-friction $(-f"(0))$ and azimuthal skin-friction $(-g'(0))$ both increase as *lambda* increases. As shown in Fig. 6.4(f), the rate of heat transfer decreases as the value of *lambda* increases.

The impact of viscosity parameter A on the velocity component, temperature, coefficient of skin friction and heat transfer rate is depicted in Fig.6.5for type – II boundary conditions. Figure 6.5(a) reveals that the tangential velocity f increases near the cone surface and then decreases as A increases. From figures 6.5(b), it is observed that circumferential velocity$g$ decreases near the cone surface and shows very little variation away from the cone. As shown in Fig. 6.5(b), the effect of A on temperature *theta* is insignificant. The tangential skin friction $(-f"(0))$ and azimuthal skin-friction $(-g'(0))$ both increase with an increase in A, as shown in Figs. 6.5(d) and 6.5(e). As depicted in Fig. 6.5(f), the Nusselt number decreases as A increases.

The influence of $\in$ on the velocity, temperature, coefficient of skin frictions and heat transfer rate is depicted in Fig. 6.6 for type – II boundary conditions. From Fig. 6.6(a), it is observed that the tangential velocity$f$ increases as the value of *in* increases. As presented in Fig. 6.6(a), the effect of *in* on circumferential velocity g is insignificant. The temperature rises as the value of *in* rises, as shown by Fig.6.6(c). It is observed from Figures 6.6(d) and 6.6(e) that as the value of the *in* increases, so do the tangential and azimuthal skin-frictions. The Nusselt number increases as the parameter *in* increases, as shown in 6.6(f).

The Effect of λ on velocity, temperature, coefficient of skin frictions and heat transfer rate are depicted in Figure 6.7 From Fig. 6.7(a) it is observed that the tangential velocity f increases near the cone surface and then decreases as the parameter *lambda* increases. As *lambda* increases, the circumferential velocity g decreases slightly, as shown in in Fig. 6.7(b). Figure 6.7(c) reveals that the temperature *theta* decreases as the value of *lambda* increases.. Figures 6.7(d) and 6.7(e) show that the tangential skin-friction $(-f"(0))$ and azimuthal skin-friction $(-G'(0))$ both increase as *lambda* increases. The rate of heat transfer increases as the value of *lambda* increases as depicted in Fig. 6.4(f).

6.5 Conclusion

By assuming temperature dependent viscosity and thermal conductivity, the laminar free convection flow across a rotating vertical cone is investigated. The similarity transformed equations are used to reduce the flow equations to ordinary differential equations. The non-

dimensional equations are linearized successively, and the solution of the resulting system is found using the Chebyshev spectral method.

- When the viscosity parameter is increased, the tangential velocity near the cone surface decreases, then increases away from the cone. As one moves away from the cone, the circumferential velocity increases.
- For enhancing values of the viscosity parameter, the dimensionless tangential skin-friction, azimuthal skin-friction, and rate of heat transfer all rise.
- As the values of in are increased, the tangential velocity and temperature rise..
- The Nusselt number is decreasing with an increase in $\in$ while the skin friction coefficients are rising.
- The tangential and azimuthal skin friction increase while heat transfer rate decreases as $lambda$ increases.

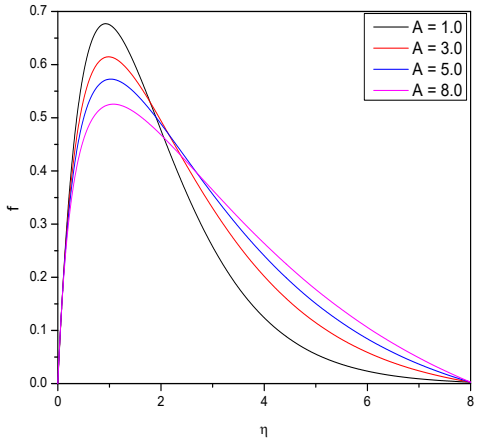

(a)

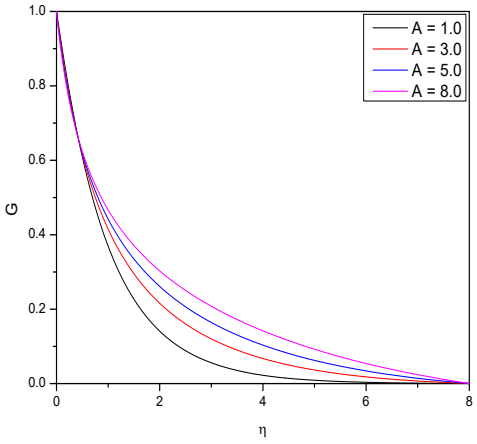

(b)

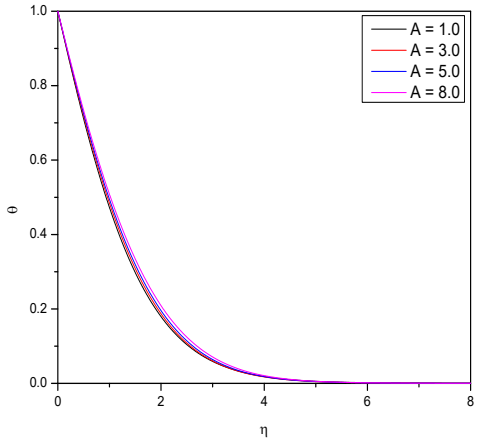

(c)

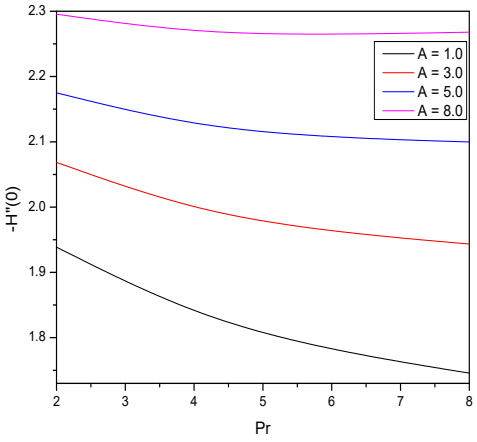

(d)

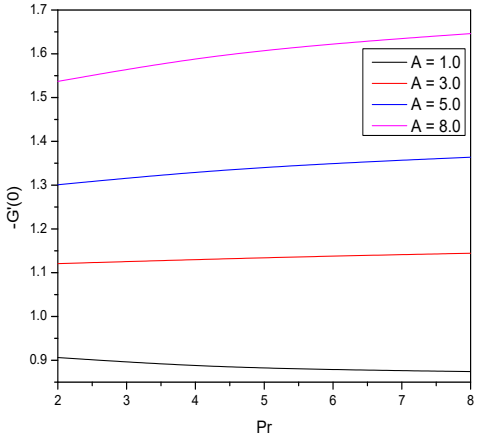

(e)

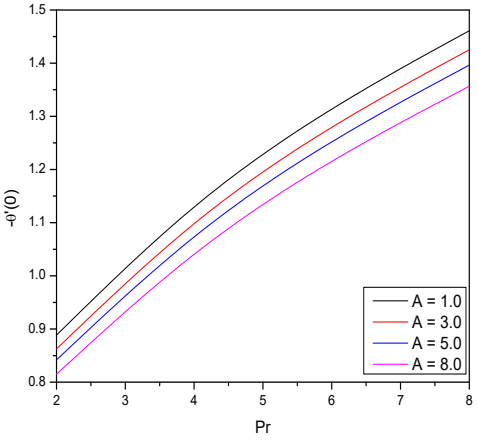

(f)

Figure 6.2: "Effect of A on the Velocity, Temperature, tangential and azimuthal skin friction coefficient and Nusselt number for CWT boundary conditions".

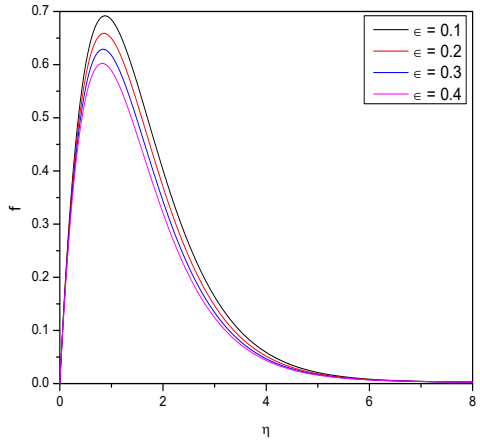

(a)

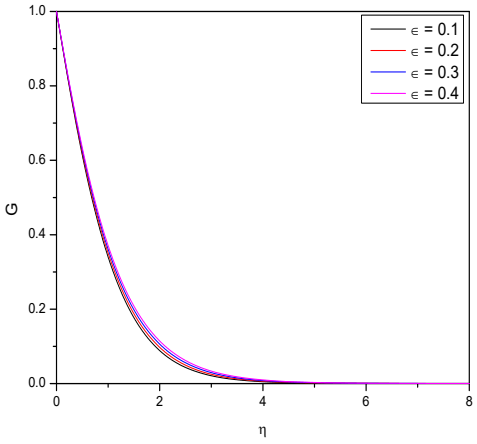

(b)

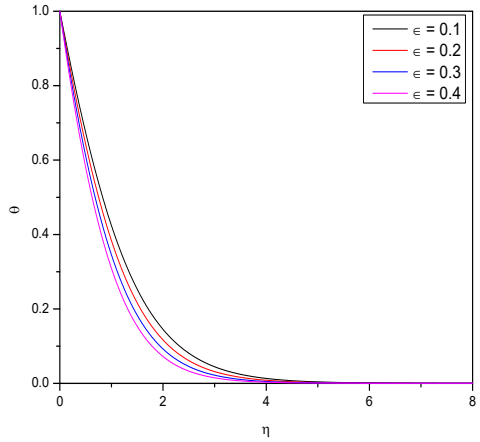

(c)

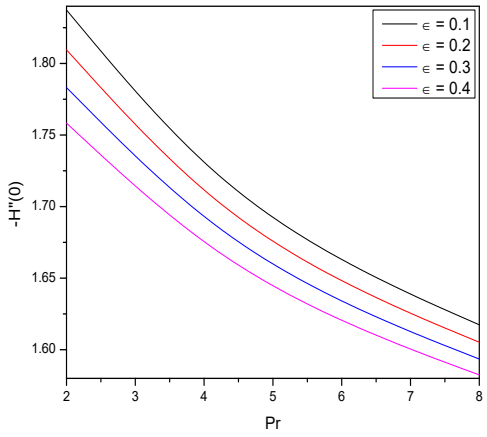

(d)

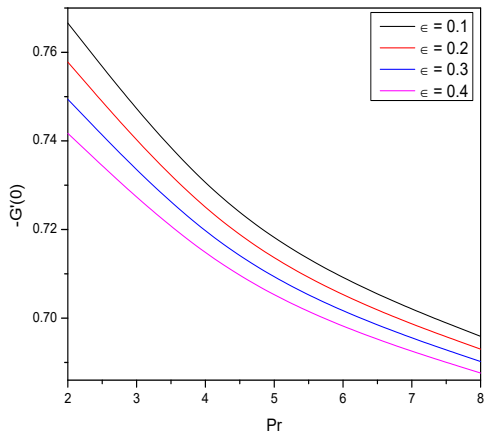

(e)

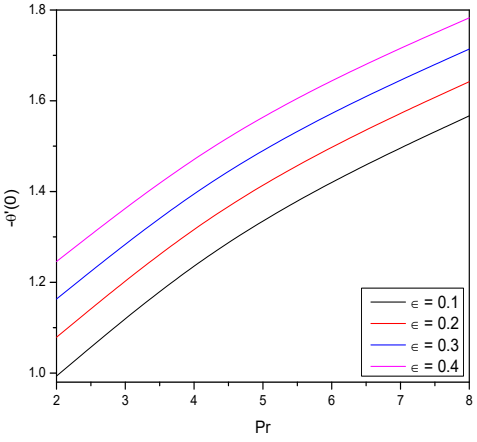

(f)

Figure 6.3: "Effect of $\in$ on the Velocity, Temperature, tangential and azimuthal skin friction coefficient and Nusselt number for CWT boundary conditions".

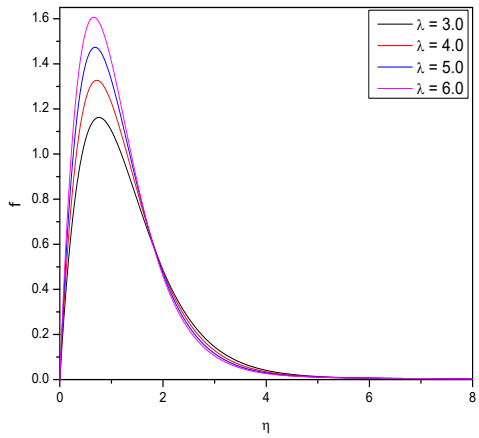

(a)

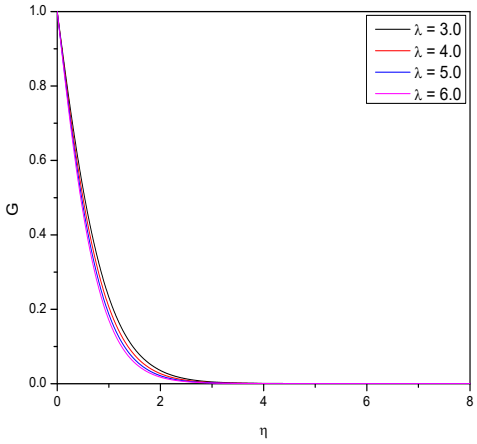

(b)

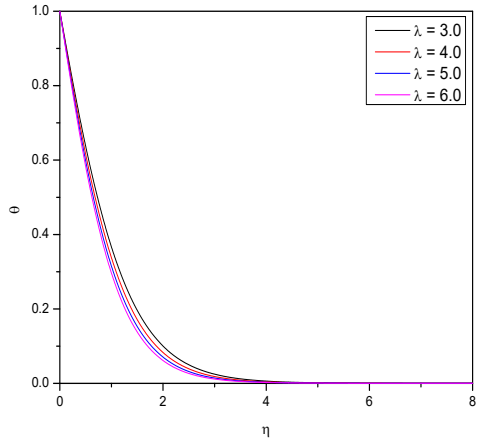

(c)

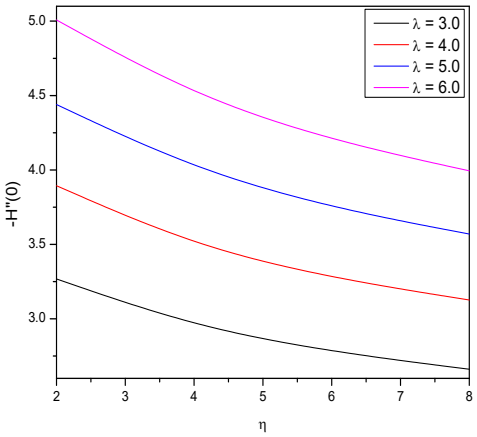

(d)

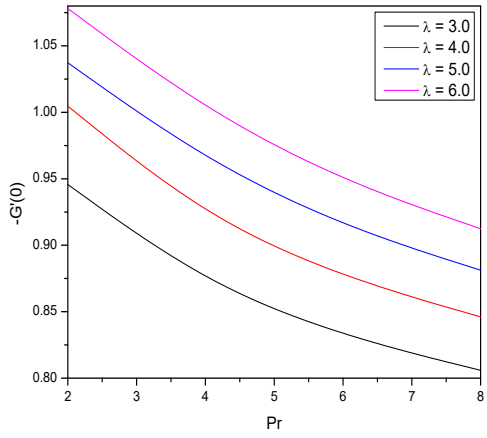

(e)

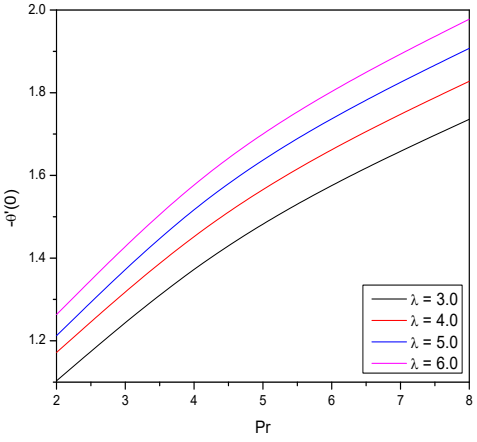

(f)

Figure 6.4: "Effect of λ on the Velocity, Temperature, tangential and azimuthal skin friction coefficient and Nusselt number for CWT boundary conditions".

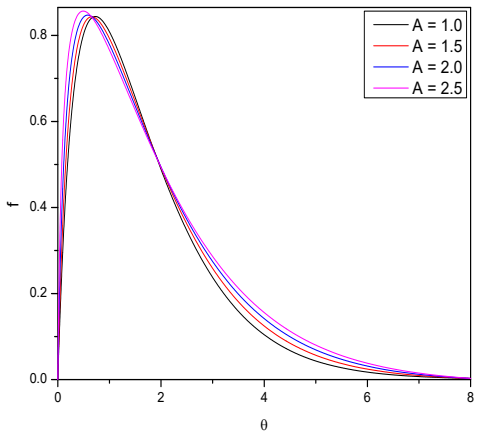

(a)

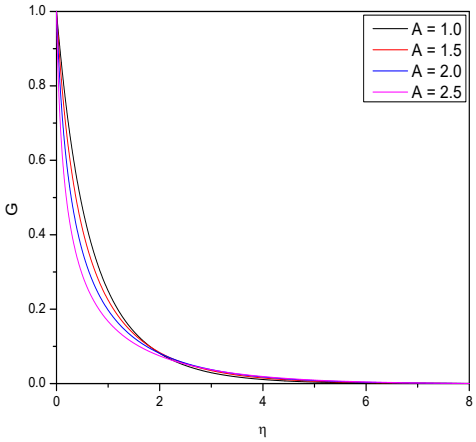

(b)

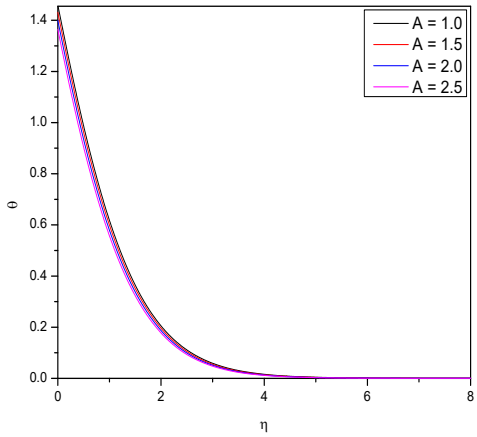

(c)

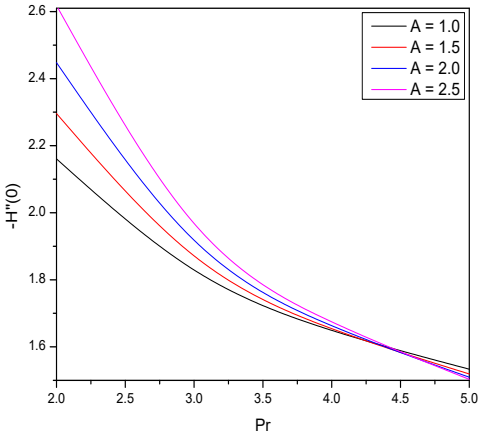

(d)

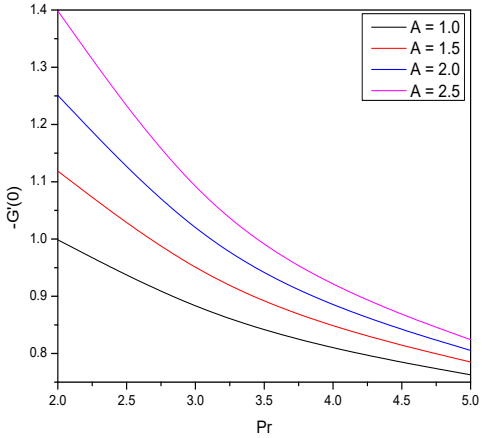

(e)

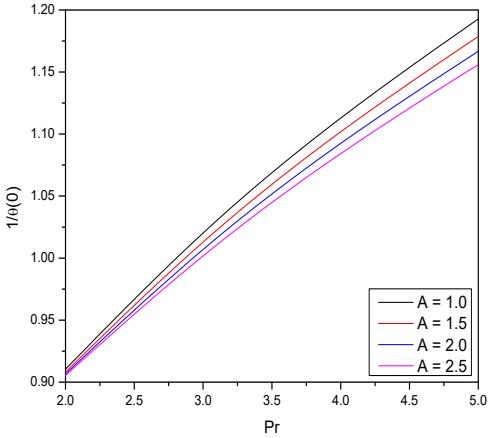

(f)

Figure 6.5: "Effect of A on the Velocity, Temperature, tangential and azimuthal skin friction coefficient and Nusselt number for CHF boundary conditions".

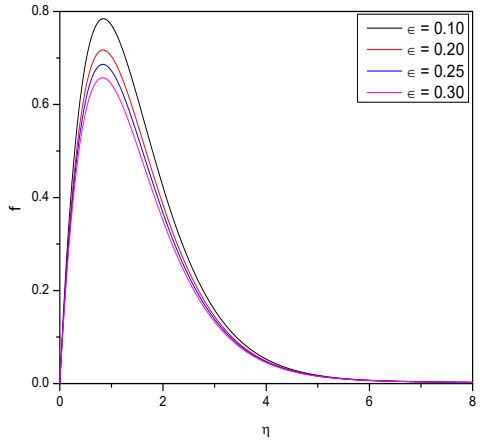

(a)

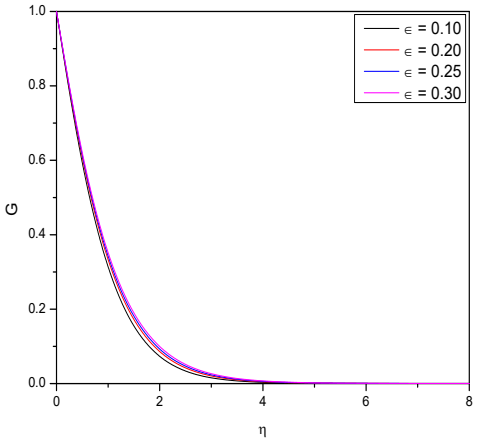

(b)

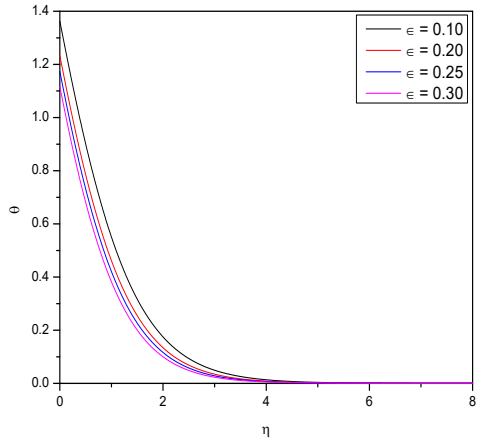

(c)

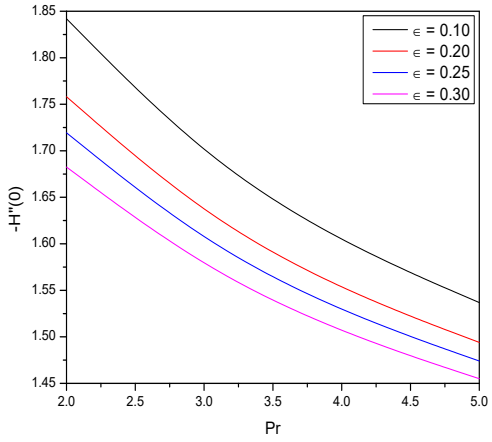

(d)

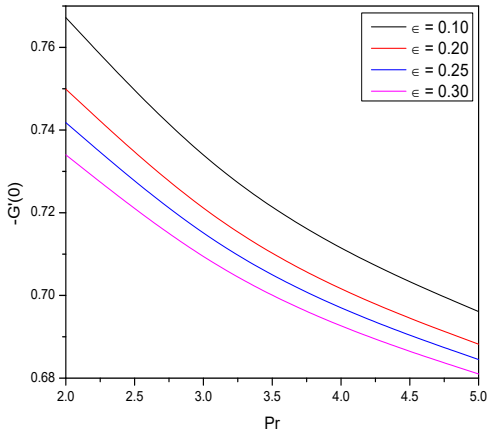

(e)

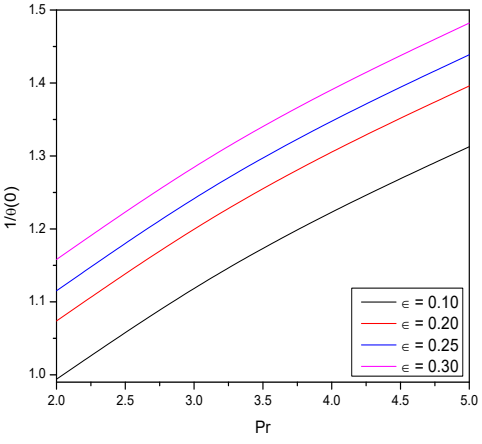

(f)

Figure 6.6: "Effect of $\in$ on the Velocity, Temperature, tangential and azimuthal skin friction coefficient and Nusselt number for CHF boundary conditions".

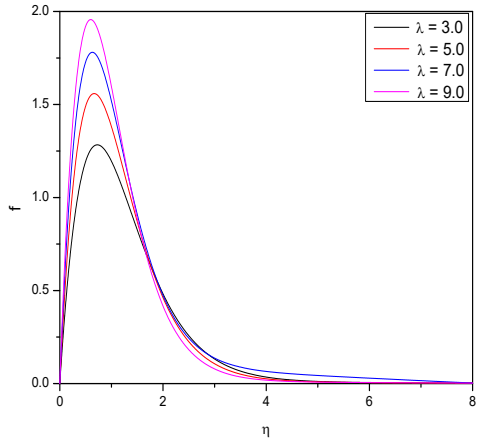

(a)

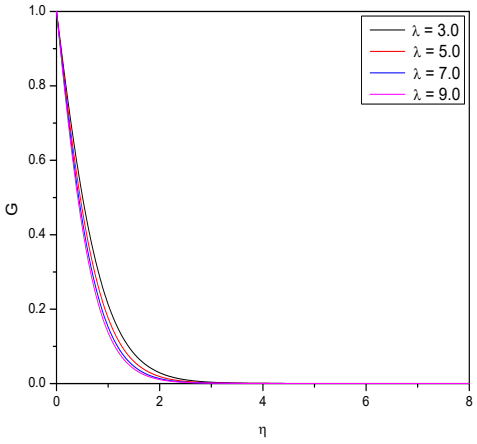

(b)

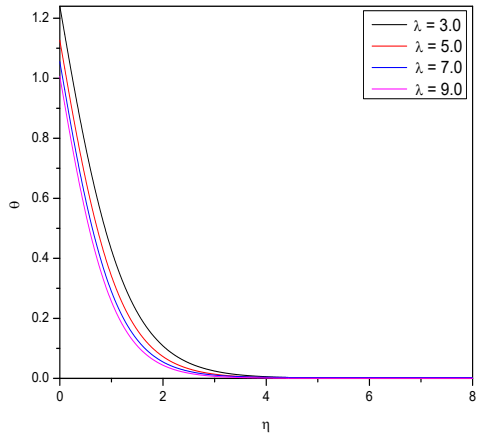

(c)

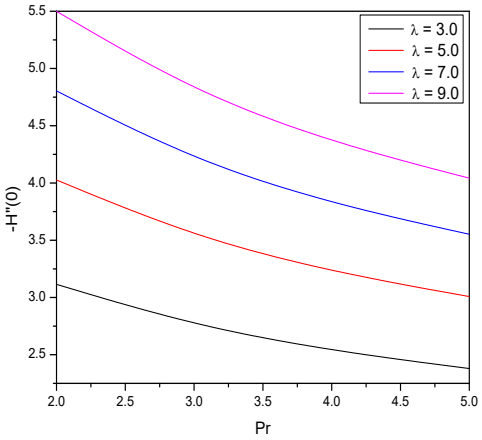

(d)

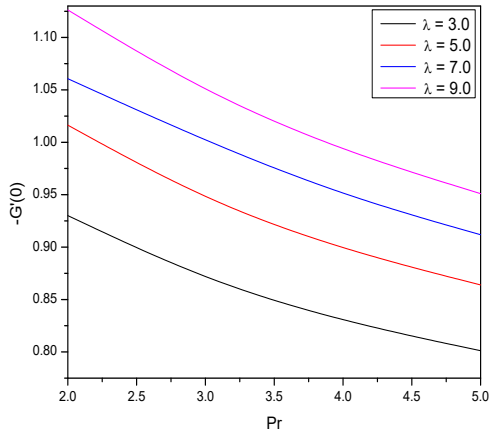

(e)

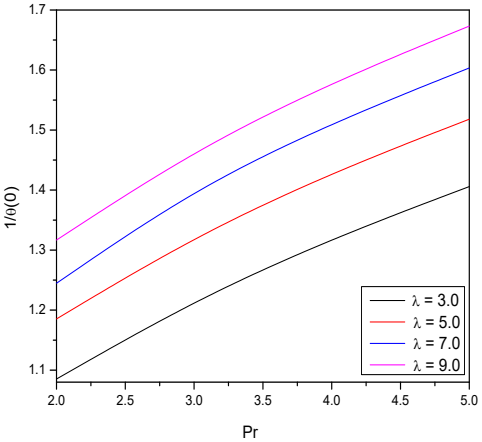

(f)

Figure 6.7: "Effect of λ on the Velocity, Temperature, tangential and azimuthal skin friction coefficient and Nusselt number for CHF boundary conditions".

Chapter 7

The Heat and Mass Transfer Across a Rotating Cone With Variable Fluid Properties [1]

7.1 Introduction

The investigation of flow and (or) heat and mass transfer over rotating bodies is of significant importance due to its prevalence in many industrial, geophysical, geothermal, technological, and engineering applications. Such a study is important in the design of turbines and turbo-machines, automotive engineering, estimating the flight path of rotating wheels and spin-stabilized missiles, energy systems, medical equipment, processing engineering and in the modeling of many geophysical vortices. Turkyilmazoglu [87] inspected the heat transfer pattern in viscous fluid confined by a rotating cone Saleem [73] studied the impact of heat and mass transfer on time-dependent flow of a third-grade convective fluid due to an infinitely rotating upright cone.

The convective heat and mass transfer over a rotating cone with changeable viscosity and thermal conductivity is presented in this chapter. The pseudo-spectral approach is used to solve the governing equations after they have been linearized using the successive linearization method. This technique was efficaciously applied to solve the convection heat and mass transfer problems. The impacts of various flow and geometry factors on the velocity component, temperature, and heat transfer rate are thoroughly examined.

[1] Communicated to "**Computational Thermal Science**"

7.2 Mathematical Formulation

Consider the laminar viscous incompressible fluid flow over a cone rotating about its axis with angular velocity Ω. The coordinate system and the geometry of the problem is depicted in Fig. (6.1). The local radius of the cone is r and semi-vertical angle of the cone is α. The local radius at a point located and the radius of a cone can be guesstimated by $r = (xsin\phi)$. The variations in the temperature are responsible for the buoyancy forces in the fluid flow and the flow is assumed to be axisymmetric. Applying Boussinesq approximation and utilizing the boundary layer assumptions, the equations describing the flow are.

$$\frac{\partial u}{\partial x} + \frac{\partial w}{\partial z} + \frac{u}{x} = 0 \tag{7.1}$$

$$\rho\left(u\frac{\partial u}{\partial x} + w\frac{\partial u}{\partial z} - \frac{v^2}{x}\right) = \frac{\partial}{\partial z}\left(\mu\frac{\partial u}{\partial z}\right) + \rho g\left[\beta_T(T - T_\infty) + \beta_C(C - C_\infty)\right]\cos\alpha \tag{7.2}$$

$$\rho\left(u\frac{\partial v}{\partial x} + w\frac{\partial v}{\partial z} + \frac{uv}{x}\right) = \frac{\partial}{\partial z}\left(\mu\frac{\partial v}{\partial z}\right) \tag{7.3}$$

$$\left(u\frac{\partial T}{\partial x} + w\frac{\partial T}{\partial z}\right) = \frac{\partial}{\partial z}\left(\alpha\frac{\partial T}{\partial z}\right) \tag{7.4}$$

$$u\frac{\partial C}{\partial x} + w\frac{\partial C}{\partial z} = \frac{\partial}{\partial z}\left(D_s\frac{\partial C}{\partial z}\right) \tag{7.5}$$

The quantities used in the above equations ar already defined in the previous chapters.

The viscosity and thermal conductivity are considered to be a linear function of the temperature [5] and are given by

$$\mu(T) = \mu_\infty[1 + \lambda(T_\infty - T)] \quad and \quad k(T) = k_0[1 + \gamma(T_\infty - T)] \tag{7.6}$$

where μ_∞ and,k_0 represent the absolute viscosity and the thermal conductivity of the fluid, respectively, λ and γ are constants. The boundary conditions for the velocity are given as

$$u = 0 \quad , v = r\Omega \quad w = 0 \quad \text{at} \quad z = 0 \quad \text{and} \quad u \to 0 \quad v \to 0 \quad \text{as} \quad z \to \infty \tag{7.7}$$

In addition, for the temperature and concentration on the surface of the cone, one can either have constant temperature T_w and concentration and C_w (CWT) or a constant heat flux q_w and mass flux and q_w (CHF).Thus, the conditions for the temperature on the boundary conditions are written as

$$\textbf{Type - I (CWT)} : T = T_w \quad C = C_w \quad \text{at} \quad z = 0 \tag{7.8}$$

$$\textbf{Type - II (CHF)} : k\frac{\partial T}{\partial z} = q_w \quad k\frac{\partial C}{\partial z} = q_m \quad \text{at} \quad z = 0 \tag{7.9}$$

and far away from the cone, the temperature and concentration of the free stream are constant i.e. $T \to T_\infty$, $C \to C_\infty$ as $z \to \infty$ The following non-dimensional transformations are utilised to get the non-dimensional equations

$$\left.\begin{aligned}
&\eta = \left(\frac{\Omega \sin\alpha}{\nu}\right)^{\frac{1}{2}} z,\ u = \frac{1}{2}x\Omega \sin\alpha f'(\eta),\ v = x\Omega \sin\alpha g(\eta),\ w = (\nu\Omega \sin\alpha)^{\frac{1}{2}} f(\eta),\\
&T = T_\infty + (T_w - T_\infty)\theta(\eta),\ \text{where } T_w - T_\infty = (T_L - T_\infty)\frac{x}{L}\text{for CWT case}\\
&T = T_\infty + \left(\frac{\Omega \sin\alpha}{\nu}\right)^{\frac{1}{2}} \frac{q_w}{k}\theta(\eta),\ \text{where } q_w = q_0\frac{x}{L}\text{for CHF case,}\\
&C = C_\infty + (C_w - C_\infty)\theta(\eta),\ \text{where } C_w - C_\infty = (C_L - C_\infty)\frac{x}{L}\text{for CWT case}\\
&C = C_\infty + \left(\frac{\Omega \sin\alpha}{\nu}\right)^{\frac{1}{2}} \frac{q_w}{k}\theta(\eta),\ \text{where } q_w = q_0\frac{x}{L}\text{for CHF case}
\end{aligned}\right\} \tag{7.10}$$

Applying the similarity transformations (7.10) in the Eqs. (7.1) to (7.4), we get the following non-dimensional equations

$$(1+A)f''' - A\theta f''' - ff'' + \frac{1}{2}f'^2 - A\theta' f'' - 2g^2 - 2\lambda\left[\theta - 2B\phi\right] = 0 \tag{7.11}$$

$$(1+A)g'' - A\theta g'' - Ag'\theta' + f'g - fg' = 0 \tag{7.12}$$

$$\frac{1}{Pr}\theta'' + \frac{1}{Pr} \in \theta\theta'' + \frac{\in}{Pr}\theta'^2 + \frac{1}{2}f'\theta - f\theta' = 0 \tag{7.13}$$

$$\frac{1}{Sc}\phi'' + \frac{\in}{Sc}\theta\phi'' + \frac{1}{Sc} \in \theta'\phi' + \frac{1}{2}f'\phi - f\phi' = 0 \tag{7.14}$$

where $B = \dfrac{\beta_c(C_w - C_\infty)}{\beta_T(T_w - T_\infty)}$ denotes the Buoyancy ratio. The remaining quantities are already defined in the previous chapters.

The dimensionless form of conditions on the boundary are

$$\left.\begin{array}{l} f(0) = f'(0) = 0, \quad g(0) = 1, \quad \theta(0) = 1, \quad \phi(0) = 1, \\ f'(\infty) = g(\infty) = \theta(\infty) = \phi(\infty) = 0 \end{array}\right\} \quad \text{for CWT case.} \tag{7.15}$$

$$\left.\begin{array}{l} f(0) = f'(0) = 0, \quad g(0) = 1, \quad \theta'(0) = -1, \quad \phi'(0) = -1 \\ f'(\infty) = g(\infty) = \theta(\infty) = \phi(\infty) = 0 \end{array}\right\} \text{for CHF case.} \tag{7.16}$$

The quantities of practical interests are the surface skin-friction coefficient in x- and y-directions and local rate of heat-transfer in terms of Nusselt number. The non-dimensional form of skin-friction coefficients C_{fx} and C_{fy} are

$$C_{fx} = -{Re_x}^{-\frac{1}{2}} f''(0), \quad C_{fy} = -{Re_x}^{-\frac{1}{2}} g'(0) \tag{7.17}$$

The non-dimensional form of Nusselt numbers (Nu) and Sherwood number (Sh) for CWT case are

$$Nu^I = -{Re_x}^{-\frac{1}{2}} \theta'(0), \quad Sh^I = -{Re_x}^{-\frac{1}{2}} \phi'(0), \tag{7.18}$$

The non-dimensional form of Nusselt numbers (Nu) and Sherwood number (Sh) for CHF case are

$$Nu^{II} = \frac{1}{\theta(0)}, \quad Sh^{II} = \frac{1}{\phi(0)} \tag{7.19}$$

7.3 Methodology

The set of differential equations (7.11) - (7.14) are linearized by means of a successive linearization method (SLM) [55]. The solutions of the ensuing linearized equations are attained by employing the Chebyshev spectral method [7]. On applying the procedure explained in Chapter 2 to the Eqs. (7.11) - (7.14), we get the following linearized equations.

$$a_1 f_i''' + a_2 f_i'' + a_3 f_i' + a_4 f_i + a_5 g_i + a_6 \theta_i' + a_7 \theta_i + a_8 \phi_i = a_9 \tag{7.20}$$

$$b_1 f_i' + b_2 f_i + b_3 g_i'' + b_4 g_i' + b_5 g_i + b_6 \theta_i' + b_7 \theta_i = b_8 \tag{7.21}$$

$$c_1 f_i' + c_2 f_i + c_3 \theta_i'' + c_4 \theta_i' + c_5 \theta_i = c_6 \tag{7.22}$$

$$d_1 f_i' + d_2 f_i + d_3 \theta_i' + d_4 \theta_i + d_5 \phi_i'' + d_6 \phi_i' + d_7 \phi_i = d_8 \tag{7.23}$$

Where

$$a_1 = \left((1+A) - A\sum \theta_m\right), \quad a_2 = \left(-\sum f_m - A\sum \theta_m^{'}\right),$$
$$a_3 = -\sum f_m^{'}, \quad a_4 = -\sum f_m^{''}, \quad a_5 = -4\sum g_m, \quad a_6 = -A\sum f_m^{''},$$

$$a_7 = -A\sum f_m^{'''} - 2\lambda, \quad a_8 = -2B$$

$$a_9 = \left(A\sum \theta_m - (1+A)\right)\sum f_m^{'''} + \left(\sum f_m + A\sum \theta_m^{'}\right)\sum f_m^{''} - \frac{1}{2}\sum f_m^{'2} + 2\sum g_m^{\ 2} + 2\lambda\sum \theta_m + 2B\sum \phi_m$$

$$b_1 = \sum g_m, \quad b_2 = -\sum g_m^{'}, \quad b_3 = \left((1+A) - A\sum \theta_m\right)$$

$$b_4 = -A\sum \theta_m^{'} - \sum f_m, \quad b_5 = \sum f_m^{'}, \quad b_6 = -A\sum g_m^{'}, \quad b_7 = -A\sum g_m^{''}$$

$$b_8 = \left(A\sum \theta_m - (1+A)\right)\sum g_m^{''} + A\sum g_m^{'}\sum \theta_m^{'} - \sum f_m^{'}\sum g_m + \sum f_m\sum g_m^{'}$$

$$c_1 = \frac{1}{2}\sum \theta_m, \quad c_2 = -\sum \theta_m^{'}, \quad c_3 = \frac{1}{\mathrm{Pr}} + \frac{\in}{\mathrm{Pr}}\sum \theta_m$$

$$c_4 = \frac{2\in}{\mathrm{Pr}}\sum \theta_m^{'} - \sum f_m, \quad c_5 = \frac{\in}{\mathrm{Pr}}\sum \theta_m^{''} + \frac{1}{2}\sum H_m^{'}$$

$$c_6 = \left(-\frac{1}{\mathrm{Pr}} - \frac{\in}{\mathrm{Pr}}\sum \theta_m\right)\sum \theta_m^{''} - \frac{\in}{\mathrm{Pr}}\sum \theta_m^{'2} + \sum f_m\sum \theta_m^{'} - \frac{1}{2}\sum f_m^{'}\sum \theta_m$$

$$d_1 = \frac{1}{2}\sum \phi_m, \quad d_2 = -\frac{1}{2}\sum \phi_m^{'}, \quad d_3 = \frac{\in}{Sc}\sum \phi_m^{'}, \quad d_4 = \frac{\in}{Sc}\sum \phi_m^{''}$$

$$d_5 = \frac{1}{Sc} + \frac{\in}{Sc}\sum \theta_m, \quad d_6 = \frac{\in}{Sc}\sum \theta_m^{'} - \frac{1}{2}\sum f_m, \quad d_7 = \frac{1}{2}\sum f_m^{'}$$

$$d_8 = \left(-\frac{1}{Sc} - \frac{\in}{Sc}\sum \theta_m\right)\sum \phi_m^{''} + \left(-\frac{\in}{Sc}\sum \theta_m^{'} + \frac{1}{2}\sum f_m\right)\sum \phi_m^{'} - \frac{1}{2}\sum f_m^{'}\sum \phi_m$$

The equivalent conditions to Equations (7.24) and (7.25) are

$$\left.\begin{array}{l} f_i(0) = f_i'(0) = 0, \quad g_i(0) = 1, \quad \theta_i(0) = 1, \quad \phi_i(0) = 1, \\ f_i'(\infty) = g_i(\infty) = \theta_i(\infty) = \phi_i(\infty) = 0 \end{array}\right\} \quad \text{for CWT case.} \qquad (7.24)$$

$$\left.\begin{array}{l} f_i(0) = f_i'(0) = 0, \quad g_i(0) = 1, \quad \theta_i'(0) = -1, \quad \phi_i'(0) = -1 \\ f_i'(\infty) = g_i(\infty) = \theta_i(\infty) = \phi_i(\infty) = 0 \end{array}\right\} \text{for CHF case.} \qquad (7.25)$$

As explained in Chapter 2, applying Chebyshev pseudo spectral method on the system

of linearized equations (7.20),(7.21),(7.22) and (7.23), we get the following equation in the matrix form

$$A_{i-1}X_i = R_{i-1} \tag{7.26}$$

whereA_{i-1} is a square matrix of order $4N+4$ and X_i and R_{i-1} are column matrices of order $4N+4$ given by

$$A_{i-1} = \begin{pmatrix} A_{11}^{(i)} & A_{12}^{(i)} & A_{13}^{(i)} & A_{14}^{(i)} \\ A_{21}^{(i)} & A_{22}^{(i)} & A_{23}^{(i)} & A_{24}^{(i)} \\ A_{31}^{(i)} & A_{32}^{(i)} & A_{33}^{(i)} & A_{34}^{(i)} \\ A_{41}^{(i)} & A_{42}^{(i)} & A_{43}^{(i)} & A_{44}^{(i)} \end{pmatrix}, X_i = \begin{pmatrix} F_i \\ G_i \\ \Theta_i \\ \Phi_i \end{pmatrix}, R_i = \begin{pmatrix} r_1^{(i)} \\ r_2^{(i)} \\ r_3^{(i)} \\ r_4^{(i)} \end{pmatrix} \tag{7.27}$$

where

$$f_i = [f_i(\xi_0), f_i(\xi_1), ..., f_i(\xi_{N-1}), f_i(\xi_N)]^T,$$

$$G_i = [g_i(\xi_0), g_i(\xi_1), .., g_i(\xi_{N-1}), g_i(\xi_N)]^T,$$

$$\Theta_i = [\theta_i(\xi_0), \theta_i(\xi_1), ...\theta_i(\xi_{N-1}), \theta_i(\xi_N)]^T,$$

$$\Phi_i = [\phi_i(\xi_0), \phi_i(\xi_1), ...\phi_i(\xi_{N-1}), \phi_i(\xi_N)]^T,$$

$$A_{11}^{(1)} = a_1D^3 + a_2D^2 + a_3D + a_4I, A_{12}^{(1)} = a_5I, A_{13}^{(1)} = a_6D + a_7I, A_{14}^{(1)} = a_8I$$

$$A_{21}^{(1)} = b_1D + b_2I, A_{22}^{(1)} = b_3D^2 + b_4D + b_5I, A_{23}^{(1)} = b_6D + b_7I, A_{24}^{(1)} = 0$$

$$A_{31}^{(1)} = c_1D + c_2I, A_{32}^{(1)} = 0, A_{33}^{(1)} = c_3D^2 + c_4D + c_5I, A_{34}^{(1)} = 0$$

$$A_{41}^{(1)} = d_1D + d_2I, A_{42}^{(1)} = 0, A_{43}^{(1)} = d_3D + d_4I, A_{44}^{(1)} = d_5D^2 + d_6D + d_7I$$

$$r_1^{(1)} = [a_9(\xi_0), a_9(\xi_1), ..., a_9(\xi_{N-1}), a_9(\xi_N)]^T$$

$$r_2^{(1)} = [b_8(\xi_0), b_8(\xi_1), ..., b_8(\xi_{N-1}), b_8(\xi_N)]^T$$

$$r_3^{(1)} = [c_6(\xi_0), c_6(\xi_1), ..., c_6(\xi_{N-1}), c_6(\xi_N)]^T$$

$$r_4^{(1)} = [d_8(\xi_0), d_8(\xi_1), ..., d_8(\xi_{N-1}), d_8(\xi_N)]^T$$

Where the superscript T stands for transpose, I is the identity O is the zero matrix. Finally, the solution is given by

$$X_i = A_{i-1}^{-1}R_{i-1}$$

7.4 Results and Discussion

The influences of viscosity parameter A, the dimensionless buoyancy parameter λ, buoyancy number B, and thermal conductivity parameter $\in$ on the the tangential skin friction coefficient C_{fx}, azimuthal skin friction coefficient C_{fy}, Nusselt NumberNu and Sherwood number Sh for constant wall temperature and heat flux cases are depicted graphically. ‘ The effect of the viscosity parameter A on the coefficients of skin friction, Nusselt number, and Sherwood number is depicted in Fig. 7.1 for type - I boundary conditions. Figures 7.1(a) and 7.1(b) show that the tangential and azimuthal skin friction coefficients increase as A increases. As shown in Fig. 7.1(c), the local Nusselt number $(-\theta'(0))$ decreases as A increases. As presented in Fig. 7.1(d), increasing the parameter A reduces the local Sherwood number $(-\phi'(0))$.

Figure 7.2 displays the variation of tangential and azimuthal skin-friction coefficients $(-f''(0)$ and $-g'(0))$, Nusselt number $(-\theta'(0))$ and Sherwood number $(-\phi'(0))$ for various values of $\in$. According to Figs. 7.2(a), 7.2(a) and 7.2(d), both the Skin friction coefficient and Sherwood number decrease as $\in$ increases. The and the Nusselt number increase as the value of $\in$ increases, as shown in Fig. 7.2(d).

The impact of the parameter λ on $-f''(0)$, $-g'(0)$, $-\theta'(0)$ and $-\phi'(0)$ is presented in Fig.7.3 for type - I boundary conditions. It is noticed from Figs. 7.3(a) and 7.3(b) that both the tangential and azimuthal skin friction coefficients increase as λ increases. Figures 7.3(c) and 7.3(d) reveal that Nusselt number and Sherwood number both increase as the value of λ increases.

The consequence of buoyancy parameter B on the ttangential and azimuthal skin-friction coefficients $(-f''(0)$ and $-g'(0))$, Nusselt number $(-\theta'(0))$ and Sherwood number $(-\phi'(0))$ is displayed in Fig.7.4 for type - I boundary conditions. It is clear from Figs. 7.4(a),7.4(b) 7.4(c), and 7.4(d) that increasing B increases the skin friction coefficients, Nusselt number, and Sherwood number.

The impact of viscosity parameter A on the coefficients of skin frictions, Nusselt number and Sherwood number are depicted in Fig.7.5 for type - II boundary conditions. Fig. 7.5(a) and 7.5(b) show that the tangential velocity increases initially and then decreases as A increases. The azimuthal skin friction coefficient (C_{fy}), local Nusselt number $(-\theta'(0))$ and the local Sherwood number $(-\phi'(0))$ decrease as A increases presented in Fig. 7.5(c) and 7.5(d) .

The variation of $-f''(0)$, $-g'(0)$, $-\theta'(0)$ and $-\phi'(0)$ for various values of $\in$ is presented in Fig. 7.6. It is observed from Fig. 7.6(a) that the influence of $\in$ on the tangential skin friction coefficient is negligible. Further, Fig. 7fig9b shows that the azimuthal skin friction coefficient decrease slightly as $\in$ increases. The Nusselt number increases while the Sherewood number decreases as the value of $\in$ increases, as displayed in Fig. 7.6(c) and Fig. 7.6(d).

The effect of the parameter λ on the coefficients of skin frictions, Nusselt number and Sherwood number is portrayed in Fig.7.7 for type - II boundary conditions. It is noticed from Figs. 7.7(a) and 7.7(b) that both the tangential and azimuthal skin friction coefficients increase as λ increases. Figs. 7.7(c) and 7.7(d) reveal that the Nusselt number and Sherewood number both increase as the value of λ increases.

The effect of buoyancy parameter B on $-f''(0)$, $-g'(0)$, $-\theta'(0)$ and $-\phi'(0)$ is depicted in Fig.7.8 for type - II boundary conditions. It is evident from Figs. 7.8(a),7.8(b) 7.8(c), and 8.10(d) that increasing B raises both the skin friction coefficients, Nusselt number, and Sherewood number.

7.5 Conclusion

The hear and mass transfer across a rotating vertical cone is investigated with temperature dependent viscosity and thermal conductivity. The flow equations are reduced to ordinary differential equations using similarity transformed equations. The non-dimensional equations are linearized successively, and the resulting system is solved using the Chebyshev spectral method.

- As the viscosity parameter increases, the tangential and azimuthal skin friction coefficients increasewhere as the Nusselt number ans Sherwood number decrease.
- The tangential and azimuthal skin friction coefficient and Sherwood number decrease where as the Nusselt number increase as the thermal conductivity parameter increases.
- The tangential and azimuthal skin friction coefficients, Nusselt number and Sherewood number increase as the value of λ increases
- An increase in the buoyancy ratio raises the tangential and azimuthal skin friction coefficients, Nusselt number, and Sherewood number.

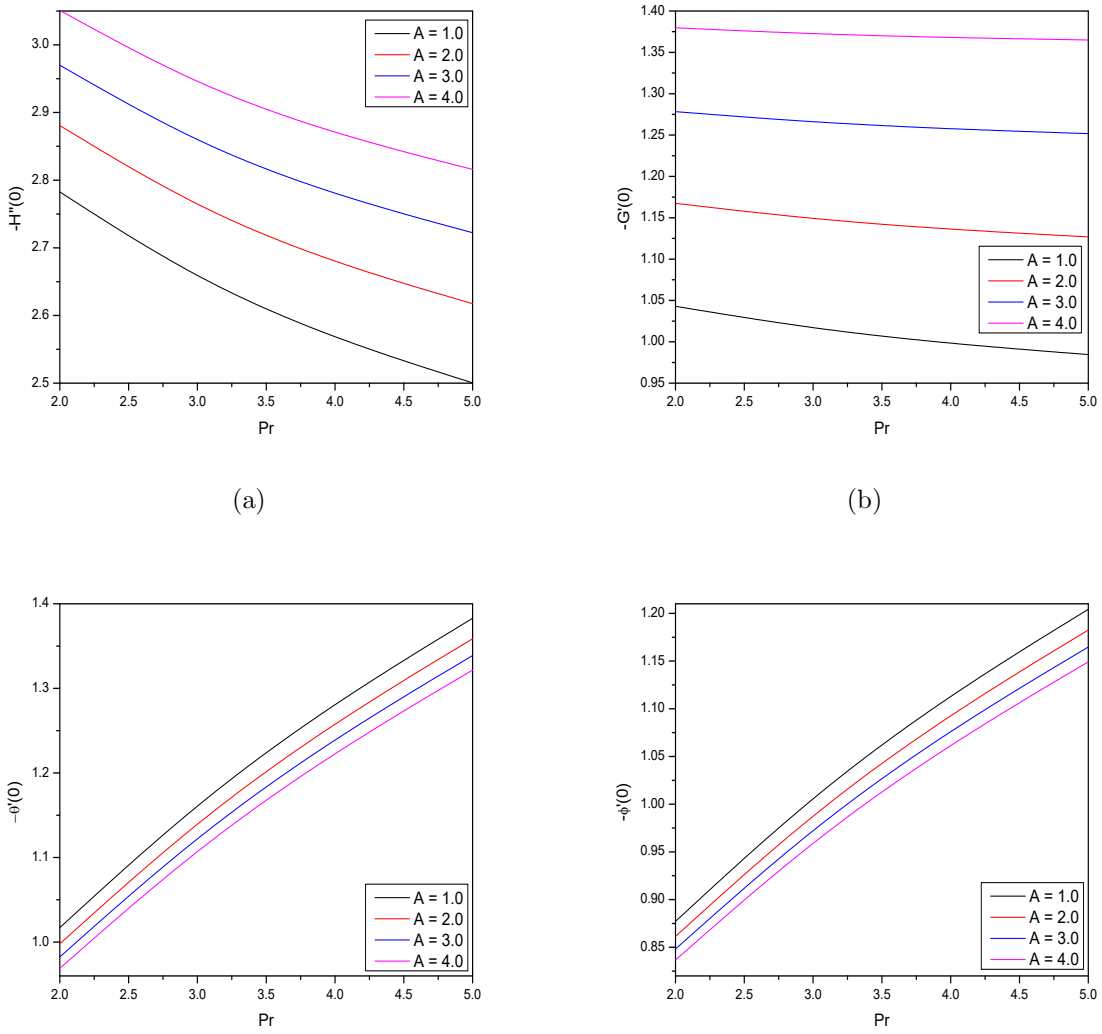

Figure 7.1: "Effect of A on the tangential skin friction coefficient, azimuthal skin friction coefficient, Nusselt number and Sherwod number for CWT boundary conditions".

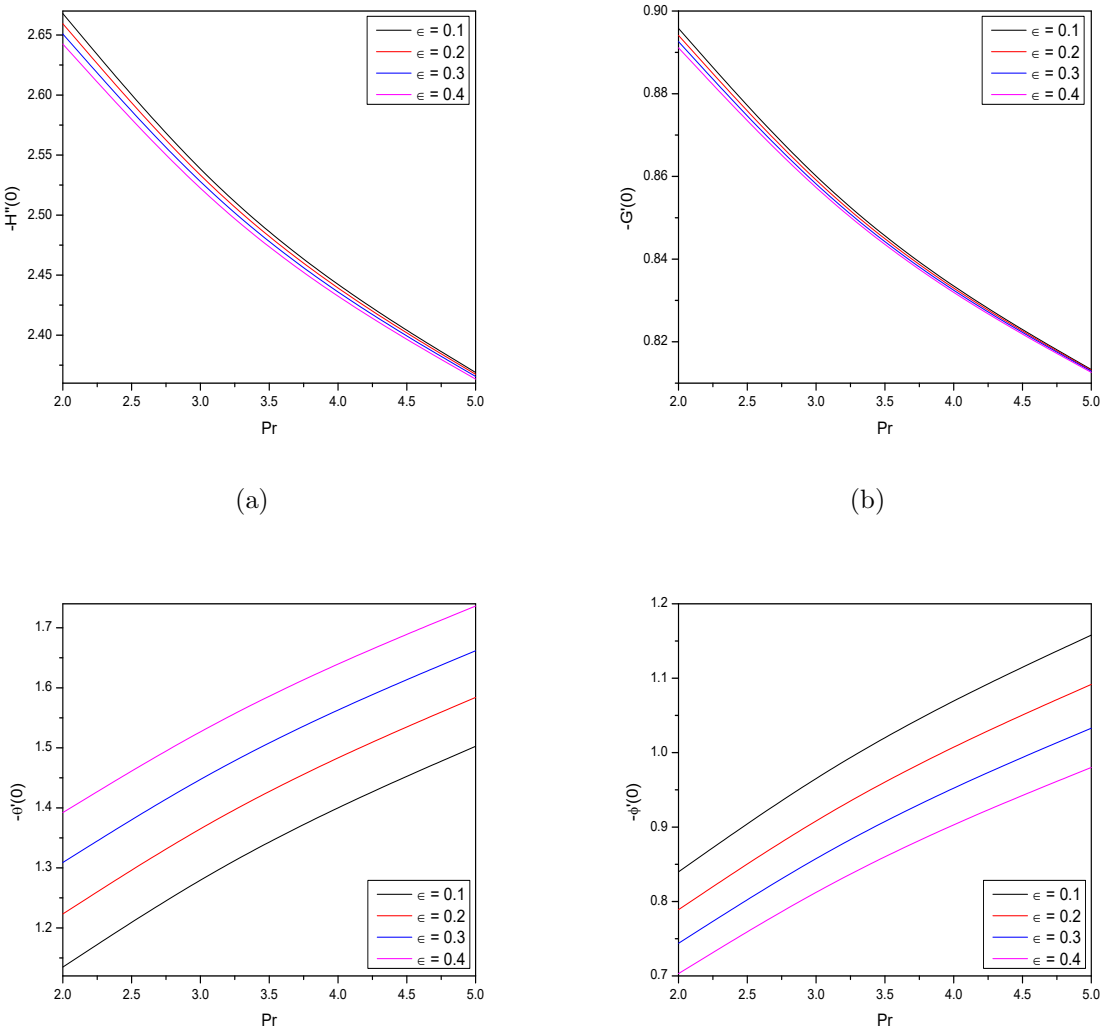

Figure 7.2: "Effect of $\in$ on the tangential skin friction coefficient, azimuthal skin friction coefficient, Nusselt number and Sherwod number for CWT boundary conditions".

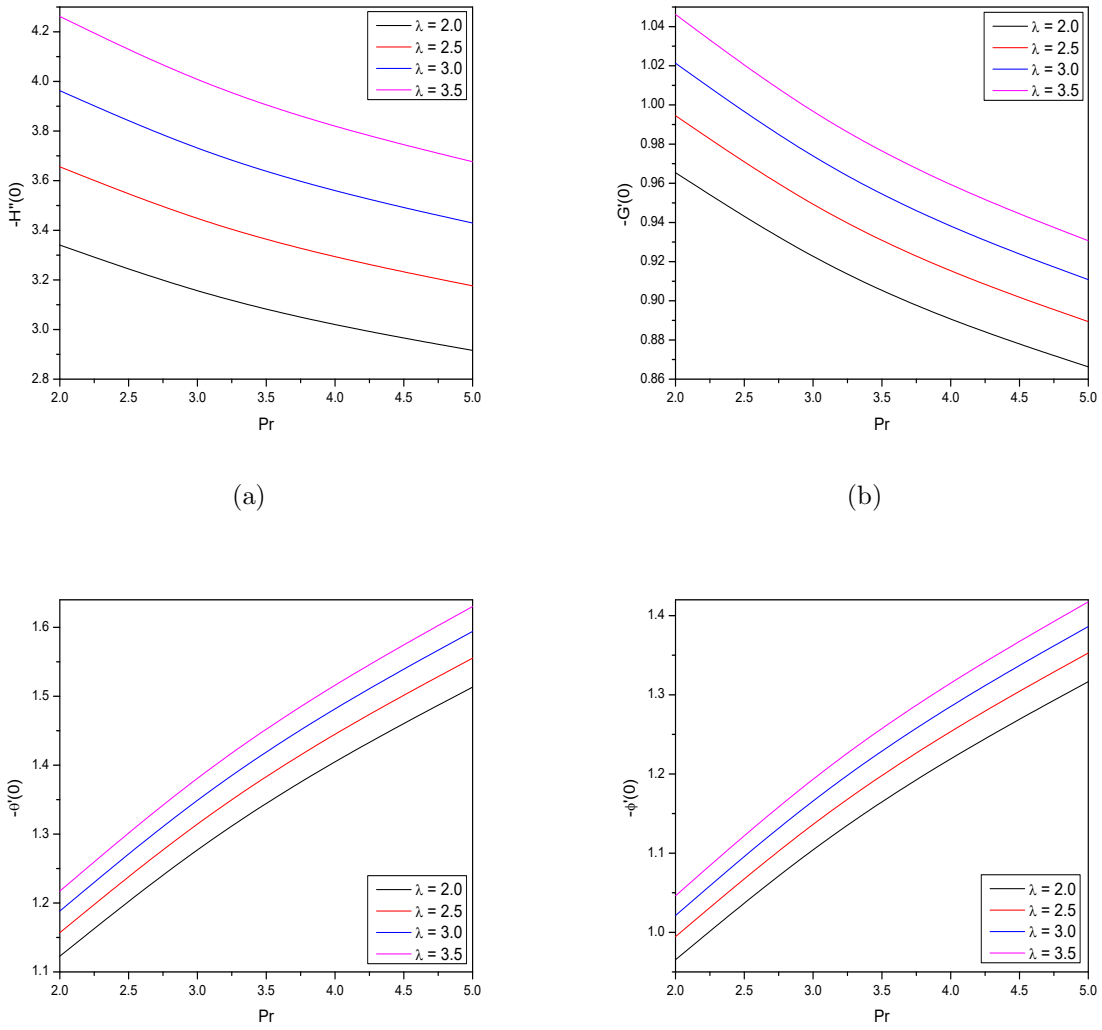

Figure 7.3: "Effect of λ on the tangential skin friction coefficient, azimuthal skin friction coefficient, Nusselt number and Sherwod number for CWT boundary conditions".

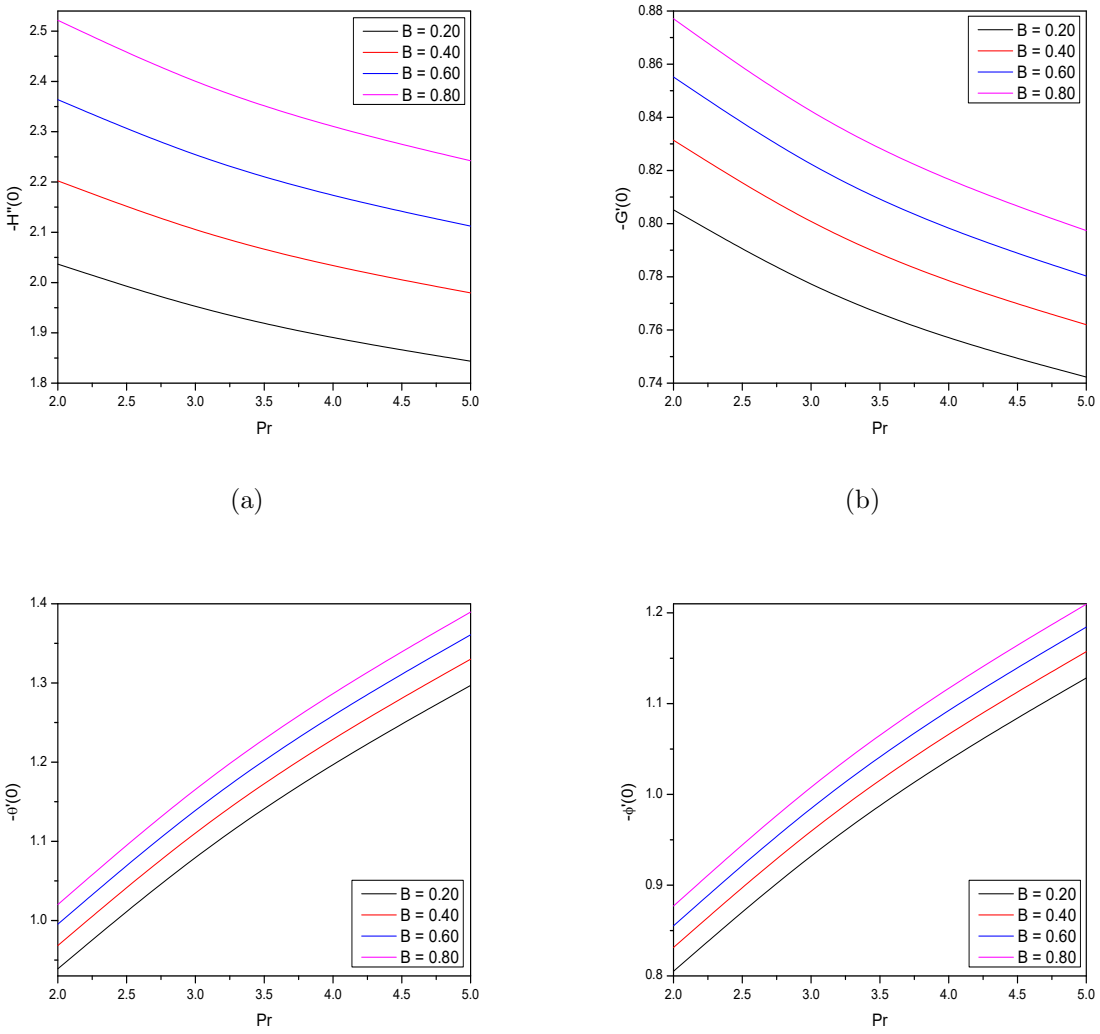

Figure 7.4: "Effect of B on the tangential skin friction coefficient, azimuthal skin friction coefficient, Nusselt number and Sherwod number for CWT boundary conditions".

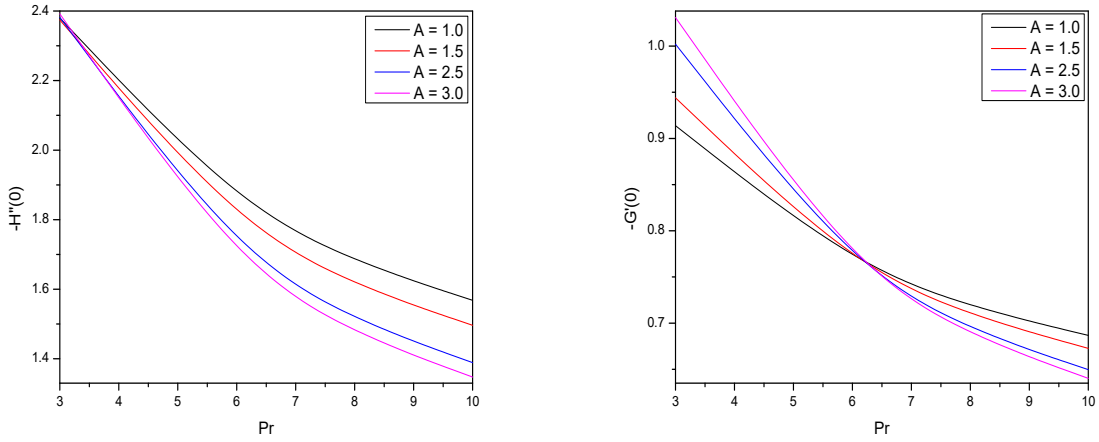

(a)

(b)

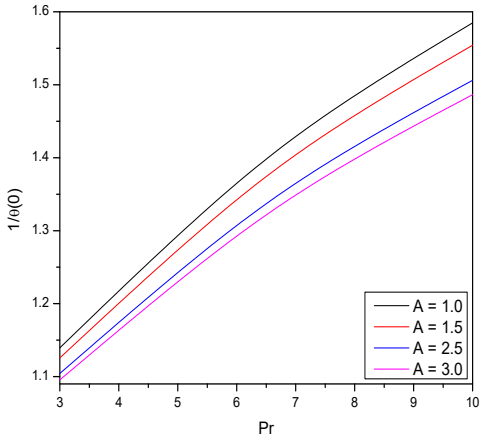

(c)

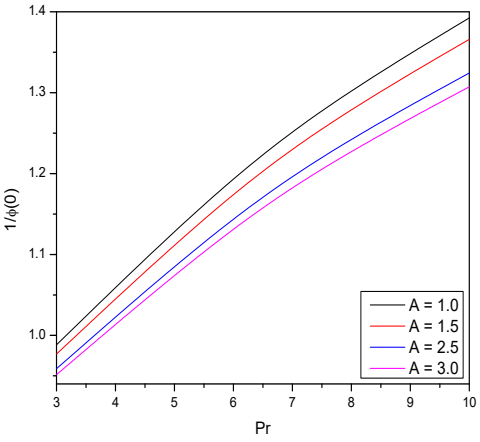

(d)

Figure 7.5: "Effect of A on the tangential skin friction coefficient, azimuthal skin friction coefficient, Nusselt number and Sherwod number for HMF boundary conditions".

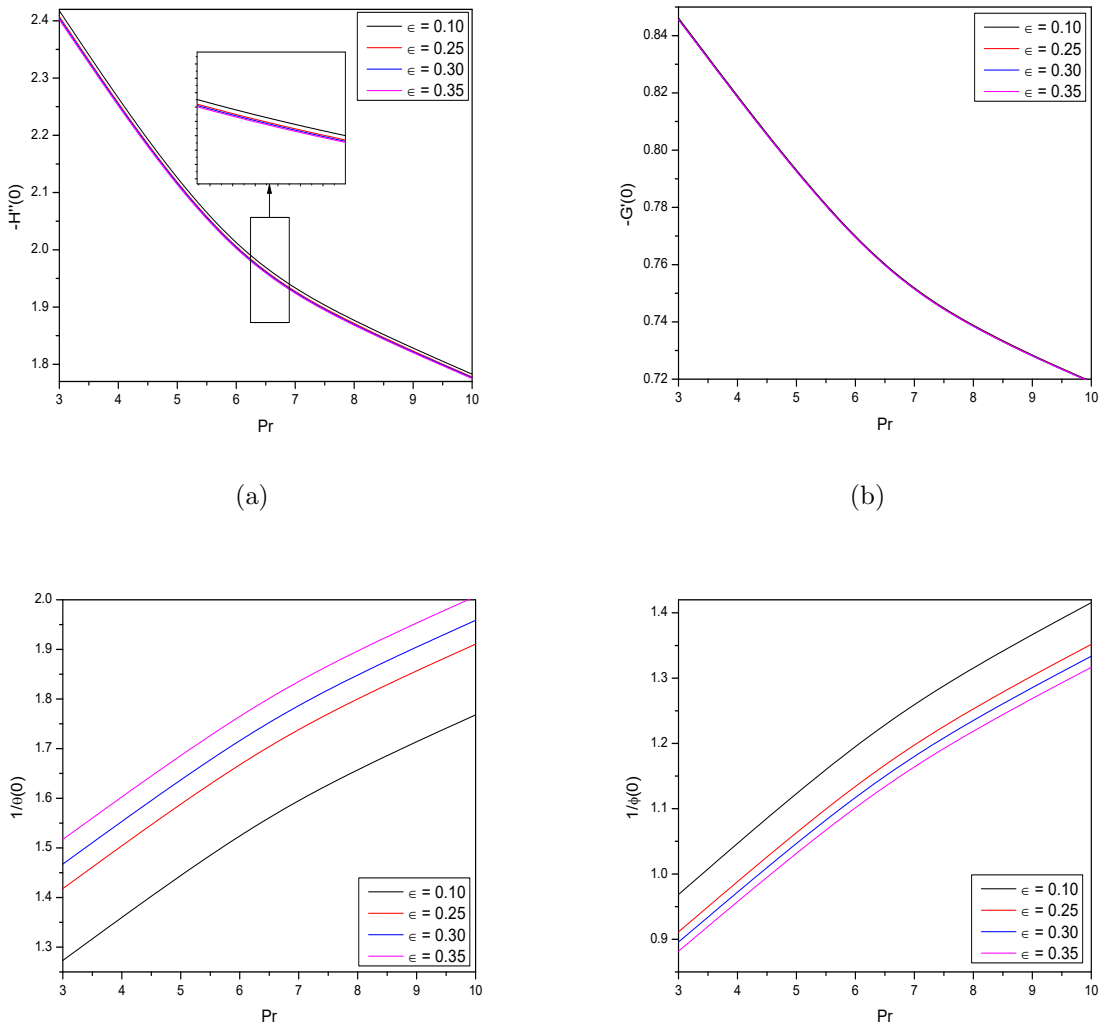

Figure 7.6: "Effect of $\in$ on the tangential skin friction coefficient, azimuthal skin friction coefficient, Nusselt number and Sherwod number for HMF boundary conditions".

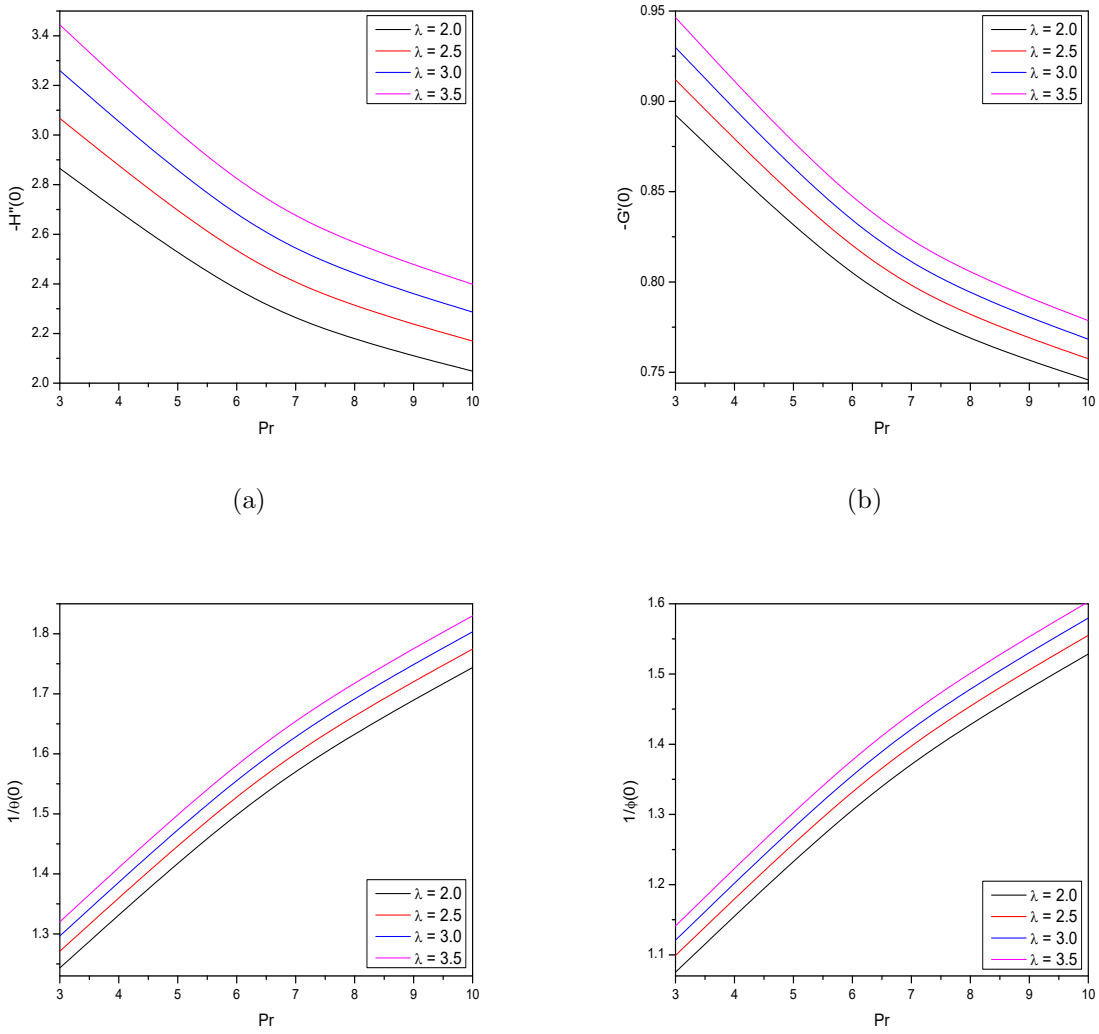

Figure 7.7: "Effect of λ on the tangential skin friction coefficient, azimuthal skin friction coefficient, Nusselt number and Sherwod number for HMF boundary conditions".

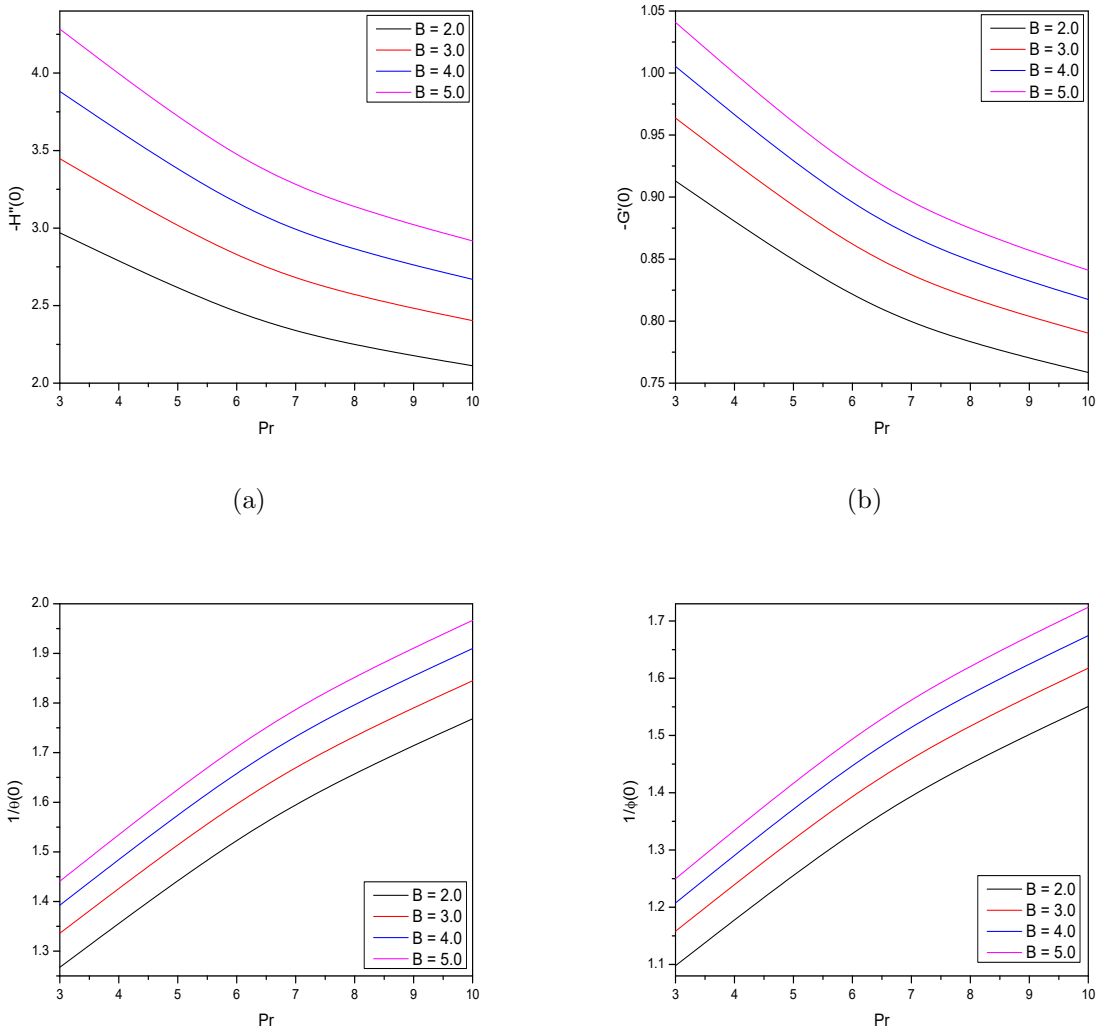

Figure 7.8: "Effect of B on the tangential skin friction coefficient, azimuthal skin friction coefficient, Nusselt number and Sherwod number for HMF boundary conditions".

Chapter 8

Effect of Soret and Dufour on the Flow Across a Rotating Cone With Variable Fluid Properties [1]

8.1 Introduction

If one property's diffusivity is significantly higher than the other, the study of double diffusive convection becomes difficult. Furthermore, when two transport processes operate concurrently, they interact and cause cross-diffusion effects. Soret and Dufour coefficients are used to describe the flux of mass caused by a temperature gradient and the flux of heat caused by a concentration gradient, respectively. There are only few studies, for example, [82], [39], [90] and references therin, available on the effect of cross diffusion on double diffusive convection on rotating cone because of the complexity in determining these coefficients.

In this chapter, the study of Soret and Dufour effects on the viscous fluid flow along over a rotating cone with changeable viscosity and thermal conductivity is considered. This chapter is an extension of the chapter - 7 by including the cross diffusion effects. The pseudo-spectral approach is used to solve the governing equations after they have been linearized using the successive linearization method. This technique was efficaciously applied to solve the convection heat and mass transfer problems. The impacts of various flow and geometry factors on the velocity component, temperature, and heat transfer rate are thoroughly examined.

[1] Communicated to "**Journal of Applied Nonlinear Dynamics**"

8.2 Mathematical Formulation

Consider the laminar viscous incompressible fluid flow over a cone rotating about its axis with angular velocity Ω. The coordinate system and the geometry of the problem is depicted in Fig. (6.1). The local radius of the cone is r and semi-vertical angle of the cone is α. In addition to the assumptions made in the previous chapter, cross diffusion effects are incorporated in the flow.

Applying Boussinesq approximation and utilizing the boundary layer assumptions, the equations describing the flow are.

$$\frac{\partial u}{\partial x} + \frac{\partial w}{\partial z} + \frac{u}{x} = 0 \tag{8.1}$$

$$\rho\left(u\frac{\partial u}{\partial x} + w\frac{\partial u}{\partial z} - \frac{v^2}{x}\right) = \frac{\partial}{\partial z}\left(\mu\frac{\partial u}{\partial z}\right) + \rho g\left[\beta_T(T - T_\infty) + \beta_C(C - C_\infty)\right]\cos\alpha \tag{8.2}$$

$$\rho\left(u\frac{\partial v}{\partial x} + w\frac{\partial v}{\partial z} + \frac{uv}{x}\right) = \frac{\partial}{\partial z}\left(\mu\frac{\partial v}{\partial z}\right) \tag{8.3}$$

$$u\frac{\partial T}{\partial x} + v\frac{\partial T}{\partial y} = \frac{\partial}{\partial y}\left(\alpha\frac{\partial T}{\partial y}\right) + \frac{D_s K_T}{C_S C_P}\frac{\partial^2 c}{\partial y^2} \tag{8.4}$$

$$u\frac{\partial C}{\partial x} + v\frac{\partial C}{\partial y} = \frac{\partial}{\partial y}(D_s\frac{\partial C}{\partial y}) + \frac{D_s K_T}{T_m}\frac{\partial^2 T}{\partial y^2} \tag{8.5}$$

The quantities used in the above equations ar already defined in the previous chapters.

The viscosity and thermal conductivity are considered to be a linear function of the temperature [5] and are given by

$$\mu(T) = \mu_\infty[1 + \lambda(T_\infty - T)] \quad and \quad k(T) = k_0[1 + \gamma(T_\infty - T)] \tag{8.6}$$

where μ_∞ and,k_0 represent the absolute viscosity and the thermal conductivity of the fluid, respectively, λ and γ are constants.

The boundary conditions for the velocity are given as

$$u = 0 \quad , v = r\Omega \quad w = 0 \quad \text{at} \quad z = 0 \quad \text{and} \quad u \to 0 \quad v \to 0 \quad \text{as} \quad z \to \infty \tag{8.7}$$

In addition, for the temperature and concentration on the surface of the cone, one can either have constant temperature T_w and concentration and C_w (CWT) or a constant heat

flux q_w and mass flux and q_w (CHF).Thus, the conditions for the temperature on the boundary conditions are written as

$$\textbf{Type - I (CWT)} : T = T_w \quad C = C_w \quad \text{at} \quad z = 0 \tag{8.8}$$

$$\textbf{Type - II (CHF)} : k\frac{\partial T}{\partial z} = q_w \quad k\frac{\partial C}{\partial z} = q_m \quad \text{at} \quad z = 0 \tag{8.9}$$

and far away from the cone, the temperature and concentration of the free stream are constant i.e. $T \to T_\infty$, $C \to C_\infty$ as $z \to \infty$

The following non-dimensional transformations are utilised to get the non-dimensional equations

$$\left.\begin{aligned}
&\eta = \left(\frac{\Omega \sin\alpha}{\nu}\right)^{\frac{1}{2}} z,\ u = \frac{1}{2}x\Omega \sin\alpha f'(\eta),\ v = x\Omega \sin\alpha g(\eta),\ w = (\nu\Omega \sin\alpha)^{\frac{1}{2}} f(\eta),\\
&T = T_\infty + (T_w - T_\infty)\theta(\eta),\ \text{where } T_w - T_\infty = (T_L - T_\infty)\frac{x}{L} \text{for CWT case}\\
&T = T_\infty + \left(\frac{\Omega \sin\alpha}{\nu}\right)^{\frac{1}{2}} \frac{q_w}{k}\theta(\eta),\ \text{where } q_w = q_0\frac{x}{L} \text{for CHF case,}\\
&C = C_\infty + (C_w - C_\infty)\theta(\eta),\ \text{where } C_w - C_\infty = (C_L - C_\infty)\frac{x}{L} \text{for CWT case}\\
&C = C_\infty + \left(\frac{\Omega \sin\alpha}{\nu}\right)^{\frac{1}{2}} \frac{q_w}{k}\theta(\eta),\ \text{where } q_w = q_0\frac{x}{L} \text{for CHF case}
\end{aligned}\right\} \tag{8.10}$$

Applying the similarity transformations (8.10) in the Eqs. (8.1) to (8.4), we get the following non-dimensional equations.

$$(1+A)f''' - A\theta f''' - ff'' + \frac{1}{2}f'^2 - A\theta' f'' - 2g^2 - 2\lambda\left[\theta - 2B\phi\right] = 0 \tag{8.11}$$

$$(1+A)g'' - A\theta g'' - Ag'\theta' + f'g - fg' = 0 \tag{8.12}$$

$$\frac{1}{\Pr}\theta'' + \frac{1}{\Pr} \in \theta\theta'' + \frac{\in}{\Pr}\theta'^2 + \frac{1}{2}f'\theta - f\theta' + D_f\phi'' = 0 \tag{8.13}$$

$$\frac{1}{Sc}\phi'' + \frac{\in}{Sc}\theta\phi'' + \frac{1}{Sc} \in \theta'\phi' + \frac{1}{2}f'\phi - f\phi' + Sr\theta'' = 0 \tag{8.14}$$

The parameters are already defined in the previous chapters.

The dimensionless form of conditions on the boundary are

$$\left.\begin{array}{l} f(0) = f'(0) = 0, \quad g(0) = 1, \quad \theta(0) = 1, \quad \phi(0) = 1, \\ f'(\infty) = g(\infty) = \theta(\infty) = \phi(\infty) = 0 \end{array}\right\} \quad \text{for CWT case.} \tag{8.15}$$

$$\left.\begin{array}{l} f(0) = f'(0) = 0, \quad g(0) = 1, \quad \theta'(0) = -1, \quad \phi'(0) = -1 \\ f'(\infty) = g(\infty) = \theta(\infty) = \phi(\infty) = 0 \end{array}\right\} \text{for CHF case.} \tag{8.16}$$

The quantities of practical interests are the surface skin-friction coefficient in x- and y-directions and local rate of heat-transfer in terms of Nusselt number. The non-dimensional form of skin-friction coefficient C_{fx} and C_{fy} are

$$C_{fx} = -{Re_x}^{-\frac{1}{2}} f''(0), \quad C_{fy} = -{Re_x}^{-\frac{1}{2}} g'(0) \tag{8.17}$$

The non-dimensional form of Nusselt numbers (Nu) and Sherwood number (Sh) for CWT case are

$$Nu^I = -{Re_x}^{-\frac{1}{2}} \theta'(0), \quad Sh^I = -{Re_x}^{-\frac{1}{2}} \phi'(0), \tag{8.18}$$

The non-dimensional form of Nusselt numbers (Nu) and Sherwood number (Sh) for CHF case are

$$Nu^{II} = \frac{1}{\theta(0)}, \quad Sh^{II} = \frac{1}{\phi(0)} \tag{8.19}$$

8.3 Methodology

The set of differential equations (8.11) - (8.14) are linearized by means of a successive linearization method (SLM) [55]. The solutions of the ensuing linearized equations are attained by employing the Chebyshev spectral method [7]. On applying the procedure explained in Chapter 2 to the Eqs. (8.11) - (8.14), we get the following linearized equations.

$$a_1 f_i'' + a_2 f_i'' + a_3 f_i' + a_4 f_i + a_5 g_i + a_6 \theta_i' + a_7 \theta_i + a_8 \phi_i = a_9 \tag{8.20}$$

$$b_1 f_i' + b_2 f_i + b_3 g_i'' + b_4 g_i' + b_5 g_i + b_6 \theta_i' + b_7 \theta_i = b_8 \tag{8.21}$$

$$c_1 f_i' + c_2 f_i + c_3 \theta_i'' + c_4 \theta_i' + c_5 \theta_i + c_6 \phi_i'' = c_7 \tag{8.22}$$

$$d_1 f_i' + d_2 f_i + d_3 \theta_i'' + d_4 \theta_i' + d_5 \theta_i + d_6 \phi_i'' + d_7 \phi_i' + d_8 \phi_i = d_9 \tag{8.23}$$

where

$$a_1 = \left((1+A) - A\sum \theta_m\right), \quad a_2 = \left(-\sum f_m - A\sum \theta_m^{'}\right),$$
$$a_3 = -\sum f_m^{'}, \quad a_4 = -\sum f_m^{''}, \quad a_5 = -4\sum g_m, \quad a_6 = -A\sum f_m^{''},$$

$$a_7 = -A\sum {}_f m^{'''} - 2\lambda, \quad a_8 = -2B$$

$$a_9 = \left(A\sum \theta_m - (1+A)\right)\sum f_m^{'''} + \left(\sum f_m + A\sum \theta_m^{'}\right)\sum f_m^{''} - \frac{1}{2}\sum f_m^{'2}$$
$$+2\sum g_m{}^2 + 2\lambda\sum \theta_m + 2B\sum \phi_m$$

$$b_1 = \sum g_m, \quad b_2 = -\sum g_m^{'}, \quad b_3 = \left((1+A) - A\sum \theta_m\right)$$

$$b_4 = -A\sum \theta_m^{'} - \sum f_m, \quad b_5 = \sum f_m^{'}, \quad b_6 = -A\sum g_m^{'}, \quad b_7 = -A\sum g_m^{''}$$

$$b_8 = \left(A\sum \theta_m - (1+A)\right)\sum g_m^{''} + A\sum g_m^{'}\sum \theta_m^{'} - \sum f_m^{'}\sum f_m + \sum f_m\sum g_m^{'}$$

$$c_1 = \frac{1}{2}\sum \theta_m, \quad c_2 = -\sum \theta_m^{'}, \quad c_3 = \frac{1}{\mathrm{Pr}} + \frac{\in}{\mathrm{Pr}}\sum \theta_m$$

$$c_4 = \frac{2\in}{\mathrm{Pr}}\sum \theta_m^{'} - \sum f_m, \quad c_5 = \frac{\in}{\mathrm{Pr}}\sum \theta_m^{''} + \frac{1}{2}\sum f_m^{'}, \quad C_6 = D_f$$

$$c_7 = \left(-\frac{1}{\mathrm{Pr}} - \frac{\in}{\mathrm{Pr}}\sum \theta_m\right)\sum \theta_m^{''} - \frac{\in}{\mathrm{Pr}}\sum \theta_m^{'2} + \sum f_m\sum \theta_m^{'} - \frac{1}{2}\sum f_m^{'}\sum \theta_m$$

$$d_1 = \frac{1}{2}\sum \phi_m, \quad d_2 = -\frac{1}{2}\sum \phi_m^{'}, \quad d_3 = Sr, \quad d_4 = \frac{\in}{Sc}\sum \phi_m^{'}, \quad d_5 = \frac{\in}{Sc}\sum \phi_m^{''}$$

$$d_6 = \frac{1}{Sc} + \frac{\in}{Sc}\sum \theta_m, \quad d_7 = \frac{\in}{\mathrm{Pr}}\sum \theta_m^{'} - \frac{1}{2}\sum f_m, \quad d_8 = \frac{1}{2}\sum f_m^{'}$$

$$d_9 = \left(-\frac{1}{Sc} - \frac{\in}{Sc}\sum \theta_m\right)\sum \phi_m^{''} + \left(-\frac{\in}{Sc}\sum \theta_m^{'} + \frac{1}{2}\sum f_m\right)\sum \phi_m^{'} - \frac{1}{2}\sum f_m^{'}\sum \phi_m$$

The equivalent conditions to Equations (8.15) and (8.16) are

$$\left.\begin{array}{l} f_i(0) = f_i'(0) = 0, \quad g_i(0) = 1, \quad \theta_i(0) = 1, \quad \phi_i(0) = 1, \\ f_i'(\infty) = g_i(\infty) = \theta_i(\infty) = \phi_i(\infty) = 0 \end{array}\right\} \quad \text{for CWT case.} \qquad (8.24)$$

$$\left.\begin{array}{l} f_i(0) = f_i'(0) = 0, \quad g_i(0) = 1, \quad \theta_i'(0) = -1, \quad \phi_i'(0) = -1 \\ f_i'(\infty) = g_i(\infty) = \theta_i(\infty) = \phi_i(\infty) = 0 \end{array}\right\} \text{for CHF case.} \qquad (8.25)$$

As explained in Chapter 2, applying Chebyshev pseudo spectral method on the system of linearized equations (8.20),(8.21),(8.22) and (8.23), we get the following equation in the

matrix form

$$A_{i-1}X_i = R_{i-1} \tag{8.26}$$

whereA_{i-1} is a square matrix of order $4N+4$ and X_i and R_{i-1} are column matrices of order $4N+4$ given by

$$A_{i-1} = \begin{pmatrix} A_{11}^{(i)} & A_{12}^{(i)} & A_{13}^{(i)} & A_{14}^{(i)} \\ A_{21}^{(i)} & A_{22}^{(i)} & A_{23}^{(i)} & A_{24}^{(i)} \\ A_{31}^{(i)} & A_{32}^{(i)} & A_{33}^{(i)} & A_{34}^{(i)} \\ A_{41}^{(i)} & A_{42}^{(i)} & A_{43}^{(i)} & A_{44}^{(i)} \end{pmatrix}, X_i = \begin{pmatrix} F_i \\ G_i \\ \Theta_i \\ \Phi_i \end{pmatrix}, R_i = \begin{pmatrix} r_1^{(i)} \\ r_2^{(i)} \\ r_3^{(i)} \\ r_4^{(i)} \end{pmatrix} \tag{8.27}$$

where

$$F_i = [f_i(\xi_0), f_i(\xi_1), ..., f_i(\xi_{N-1}), f_i(\xi_N)]^T,$$

$$G_i = [g_i(\xi_0), g_i(\xi_1), .., g_i(\xi_{N-1}), g_i(\xi_N)]^T,$$

$$\Theta_i = [\theta_i(\xi_0), \theta_i(\xi_1), ...\theta_i(\xi_{N-1}), \theta_i(\xi_N)]^T,$$

$$\Phi_i = [\phi_i(\xi_0), \phi_i(\xi_1), ...\phi_i(\xi_{N-1}), \phi_i(\xi_N)]^T,$$

$$A_{11}^{(1)} = a_1D^3 + a_2D^2 + a_3D + a_4I, A_{12}^{(1)} = a_5I, A_{13}^{(1)} = a_6D + a_7I, A_{14}^{(1)} = a_8I$$

$$A_{21}^{(1)} = b_1D + b_2I, A_{22}^{(1)} = b_3D^2 + b_4D + b_5I, A_{23}^{(1)} = b_6D + b_7I, A_{24}^{(1)} = 0$$

$$A_{31}^{(1)} = c_1D + c_2I, A_{32}^{(1)} = 0, A_{33}^{(1)} = c_3D^2 + c_4D + c_5I, A_{34}^{(1)} = 0$$

$$A_{41}^{(1)} = d_1D + d_2I, A_{42}^{(1)} = 0, A_{43}^{(1)} = d_3D^2 + d_4D + d_5I, A_{44}^{(1)} = d_6D^2 + d_7D + d_8I$$

$$r_1^{(1)} = [a_9(\xi_0), a_9(\xi_1), ..., a_9(\xi_{N-1}), a_9(\xi_N)]^T$$

$$r_2^{(1)} = [b_8(\xi_0), b_8(\xi_1), ..., b_8(\xi_{N-1}), b_8(\xi_N)]^T$$

$$r_3^{(1)} = [c_6(\xi_0), c_6(\xi_1), ..., c_6(\xi_{N-1}), c_6(\xi_N)]^T$$

$$r_4^{(1)} = [d_8(\xi_0), d_8(\xi_1), ..., d_8(\xi_{N-1}), d_8(\xi_N)]^T$$

Where the superscript T stands for transpose, I is the identity O is the zero matrix. Finally, the solution is given by

$$X_i = A_{i-1}^{-1}R_{i-1}$$

8.4 Results and Discussion

The variation of tangential skin friction coefficient, azimuthal skin friction coefficient, local Nusselt Number, and Sherwood number for diverse values of A,$\in$, λ, B, Df and Sr is depicted graphically.

Figure 8.1 depicts the effect of the viscosity parameter A on the coefficients of skin friction, Nusselt number, and Sherwood number for type - I boundary conditions. Figures 8.1(a) and 8.1(b) show that the tangential and azimuthal skin friction coefficients increase as A increases. As presented in Fig. 8.1(c), the Nusselt number $(-\theta'(0))$ decreases as A increases. As presented in Fig. 8.1(d), increasing the parameter A reduces the local Sherwood number $(-\phi'(0))$.

The variation of tangential skin-friction coefficient $(-f''(0))$, azimuthal skin-friction coefficient $(-g'(0))$, Nusselt number $(-\theta'(0))$ and Sherwood number $(-\phi'(0))$ for various values of $\in$ and Pr is portrayed in Fig. 8.2. According to Figs. 8.2(a), 8.2(a) and 8.2(c), both the Skin friction coefficient and Nusselt number decrease as $\in$ increases. The and the Sherewood number increase as the value of $\in$ increases, as shown in Fig. 8.7(d).

The impact of the parameter λ on $-f''(0)$, $-g'(0)$, $-\theta'(0)$ and $-\phi'(0)$ is presented in Fig.8.3 for type - I boundary conditions. It is noticed from Figs. 8.3(a) and 8.3(b) that both the tangential and azimuthal skin friction coefficients increase as λ increases. Figures 8.3(c) and 8.3(d) reveal that Nusselt number and Sherwood number both increase as the value of λ increases.

The consequence of buoyancy parameter B on the tangential skin-friction coefficient $(-f''(0))$, azimuthal skin-friction coefficient $(-g'(0))$, Nusselt number $(-\theta'(0))$ and Sherwood number $(-\phi'(0))$ is displayed in Fig.8.4 for type - I boundary conditions. It is clear from Figs. 8.4(a),8.4(b) 8.4(c), and 8.4(d) that increasing B increases the skin friction coefficients, Nusselt number, and Sherwood number.

The effect of Dufour number Df on $-f''(0)$, $-g'(0)$, $-\theta'(0)$ and $-\phi'(0)$ is depicted in Fig.8.5 for type - I boundary conditions It is observed from Figs. 8.5(a) and 8.5(b) that both the skin friction coefficients increase with an increase in the Dufour number. Figure 8.5(c) shows that the rate of heat transfer increases as the Dufour number increases. The Sherwood number decreases as Df increases, as shown in Fig. 8.5(d).

The variation of $-f''(0)$, $-g'(0)$, $-\theta'(0)$ and $-\phi'(0)$ with Soret number Sr is displayed in Fig.8.6 for type - I boundary conditions It is noticed from Figs. 8.6(a),8.6(b) and 8.6(d)

that both the skin friction coefficients and the rate of heat transfer increase as the Soret number increases. According to Fig. 8.6(d), the rate of mass transfer decreases as the value of Sr increases.

The influence of viscosity parameter A on the coefficients of skin frictions, Nusselt number and Sherwood number are depicted in Fig.8.7 for type - II boundary conditions. Fig. 9.7(a) and 8.7(b) show that the tangential and azimuthal skin friction coefficients increase as A increases. the local Nusselt number $(-\theta'(0))$ and the local Sherwood number $(-\phi'(0))$ increase as A increases presented in Fig. 8.7(c) and 8.7(d) .

The variation of $-f''(0)$, $-g'(0)$, $-\theta'(0)$ and $-\phi'(0)$ for various values of $\in$ is presented in Fig. 8.8. It is observed from Figs. 8.8(a) and 8.8(b) that the tangential and azimuthal skin friction coefficient decrease as $\in$ increases. The Nusselt number increases while the Sherewood number decreases as the value of $\in$ increases, as displayed in Fig. 8.8(c) and Fig. 8.8(d).

The impact of the parameter λ on the coefficients of skin frictions, Nusselt number and Sherwood number is portrayed in Fig.8.9 for type - II boundary conditions. It is noticed from Figs. 8.9(a) and 8.9(b) that both the tangential and azimuthal skin friction coefficients increase as λ increases. Figs. 8.9(c) and 8.9(d) reveal that the Nusselt number and Sherewood number both increase as the value of λ increases.

The consequence of buoyancy parameter B on $-f''(0)$, $-g'(0)$, $-\theta'(0)$ and $-\phi'(0)$ is depicted in Fig.8.10 for type - II boundary conditions. It is evident from Figs. 8.10(a),8.10(b) 8.10(c), and 8.10(d) that increasing B raises both the skin friction coefficients, Nusselt number, and Sherewood number.

The effect of Dufour number Df on the coefficients of skin frictions, Nusselt number and Sherwood number is depicted in Fig.8.11 for type - II boundary conditions It is observed from Figs. 8.11(a) and 8.11(b) that both the skin friction coefficients increase with an increase in the Dufour number. Figure 8.11(c) shows that the rate of heat transfer decreases as the Dufour number increases. The Sherewood number is increases as Df increases, as depicted in Fig. 8.11(d).

The variation of $-f''(0)$, $-g'(0)$, $-\theta'(0)$ and $-\phi'(0)$ with Soret number Sr is displayed in Fig.8.12 for type - II boundary conditions It is noticed from Figs. 8.12(a),8.12(b) and 8.12(c) that increasing the Soret number increases both the skin friction coefficients and the rate of heat transfer. According to Fig. 8.12(d), the rate of mass transfer decreases as the value of Soret number increases.

8.5 Conclusion

The cross diffusion effect on convection flow across a rotating vertical cone is investigated with temperature dependent viscosity and thermal conductivity. The flow equations are reduced to ordinary differential equations using similarity transformed equations. The non-dimensional equations are linearized successively, and the resulting system is solved using the Chebyshev spectral method.

- The Dufour number increases both the skin friction coefficients and the Sherwood number while decreasing the Nusselt number.
- The tangential and azimuthal skin friction coefficients, as well as the rate of heat transfer, increase as the Soret number increases, whereas the rate of mass transfer decreases.

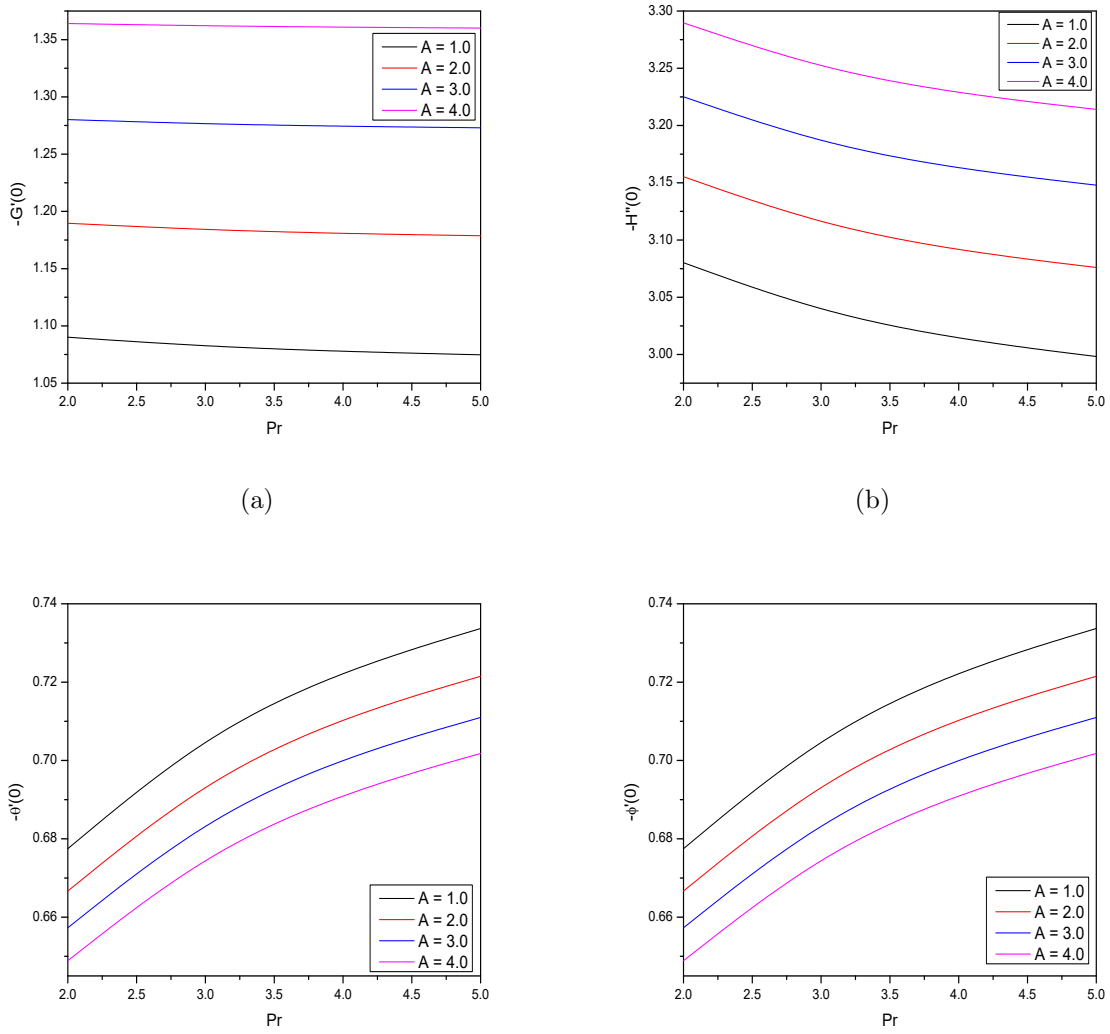

Figure 8.1: Effect of A on the "tangential skin friction coefficient", "azimuthal skin friction coefficient", "Nusselt number" and "Sherwod number" for CWT boundary conditions.

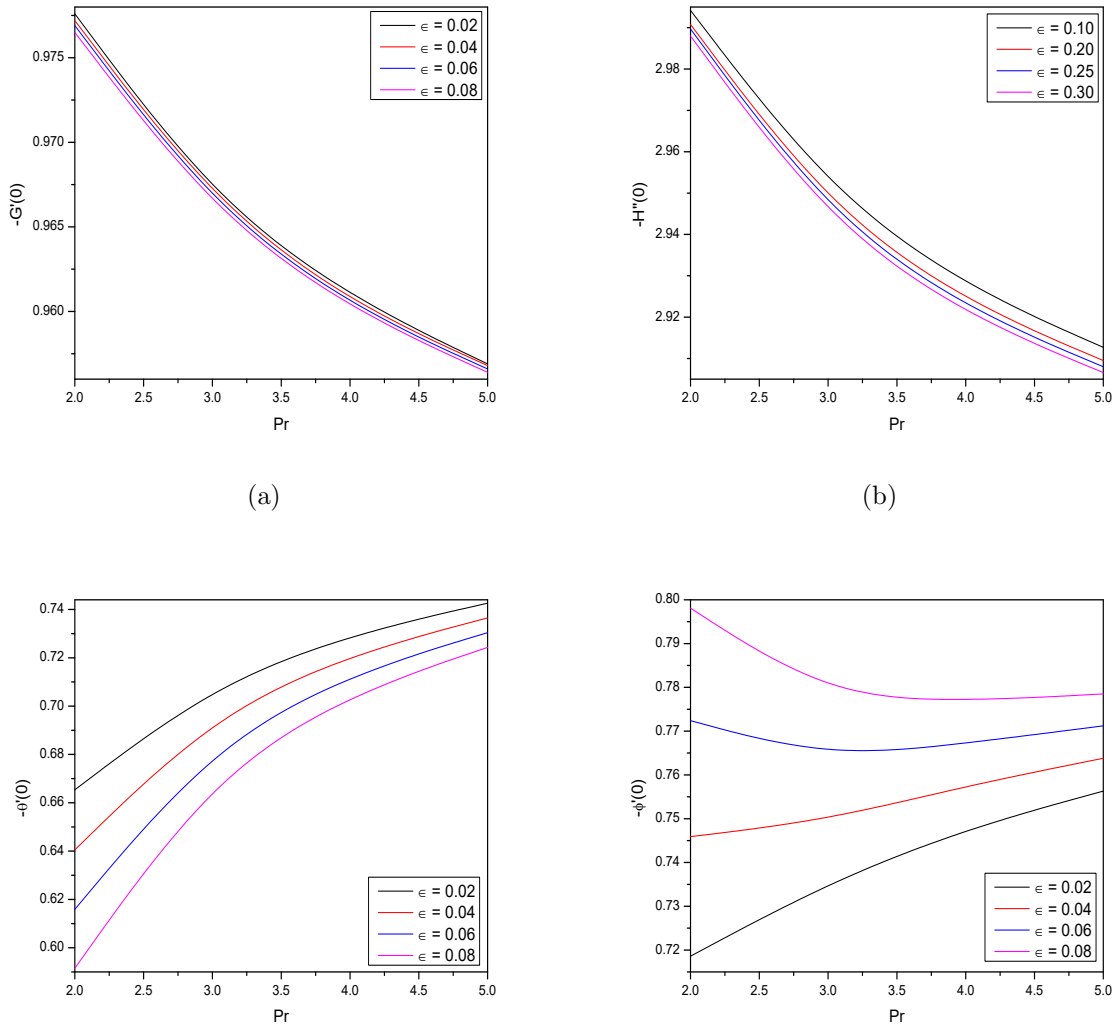

Figure 8.2: Effect of $\in$ on the "tangential skin friction coefficient", "azimuthal skin friction coefficient", "Nusselt number" and "Sherwod number" for CWT boundary conditions.

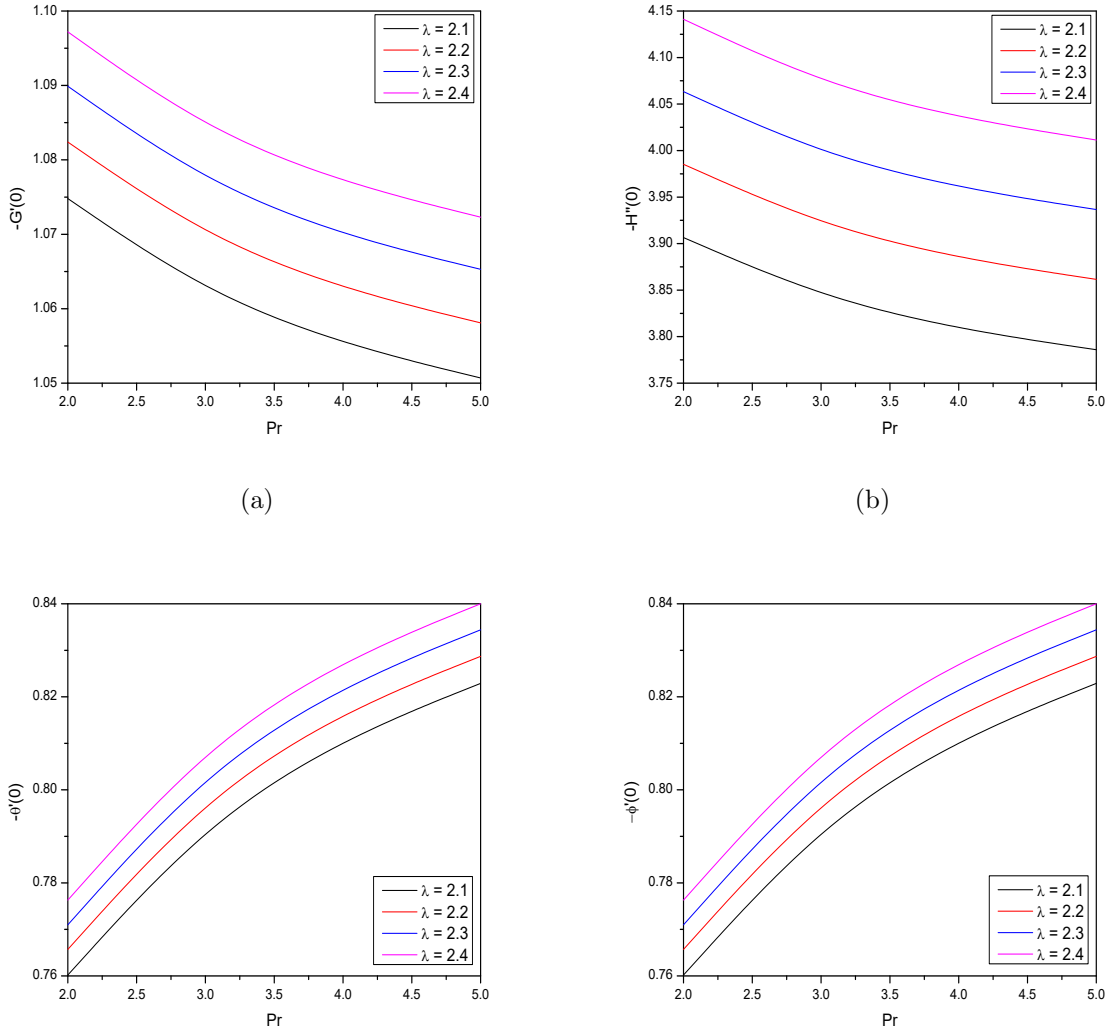

Figure 8.3: Effect of λ on the "tangential skin friction coefficient", "azimuthal skin friction coefficient", "Nusselt number" and "Sherwod number" for CWT boundary conditions.

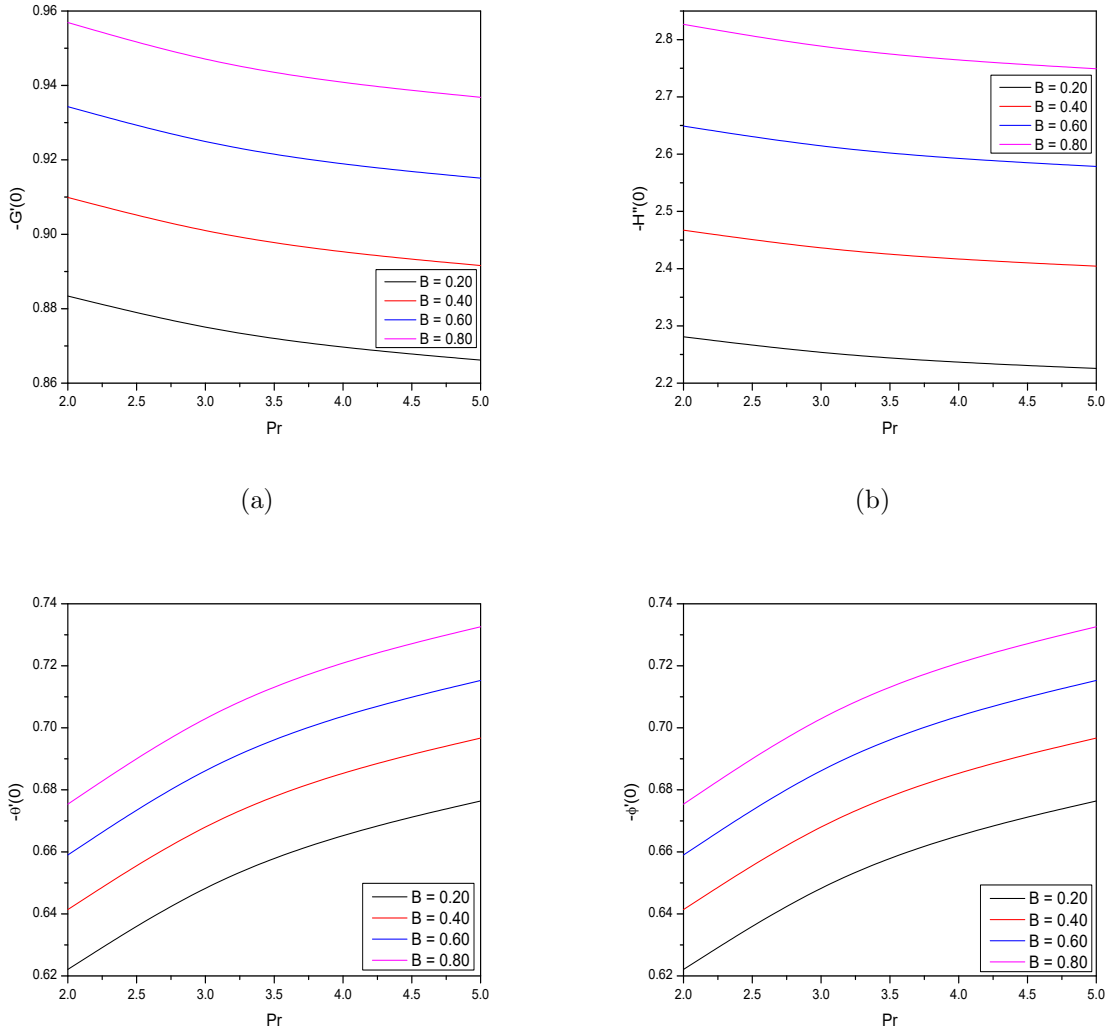

Figure 8.4: Effect of B on the "tangential skin friction coefficient", "azimuthal skin friction coefficient", "Nusselt number" and "Sherwod number" for CWT boundary conditions.

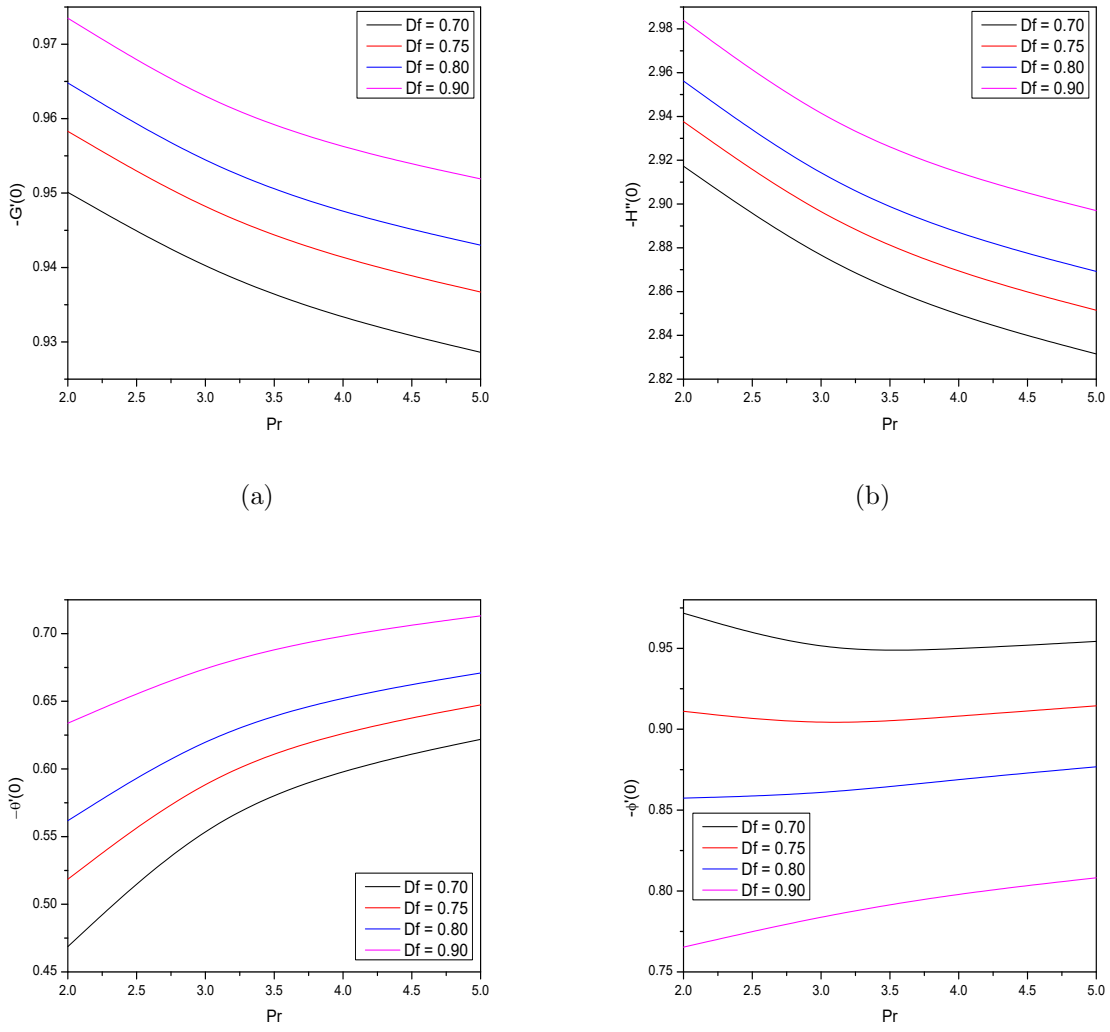

Figure 8.5: Effect of Df on the "tangential skin friction coefficient", "azimuthal skin friction coefficient", "Nusselt number" and "Sherwod number" for CWT boundary conditions.

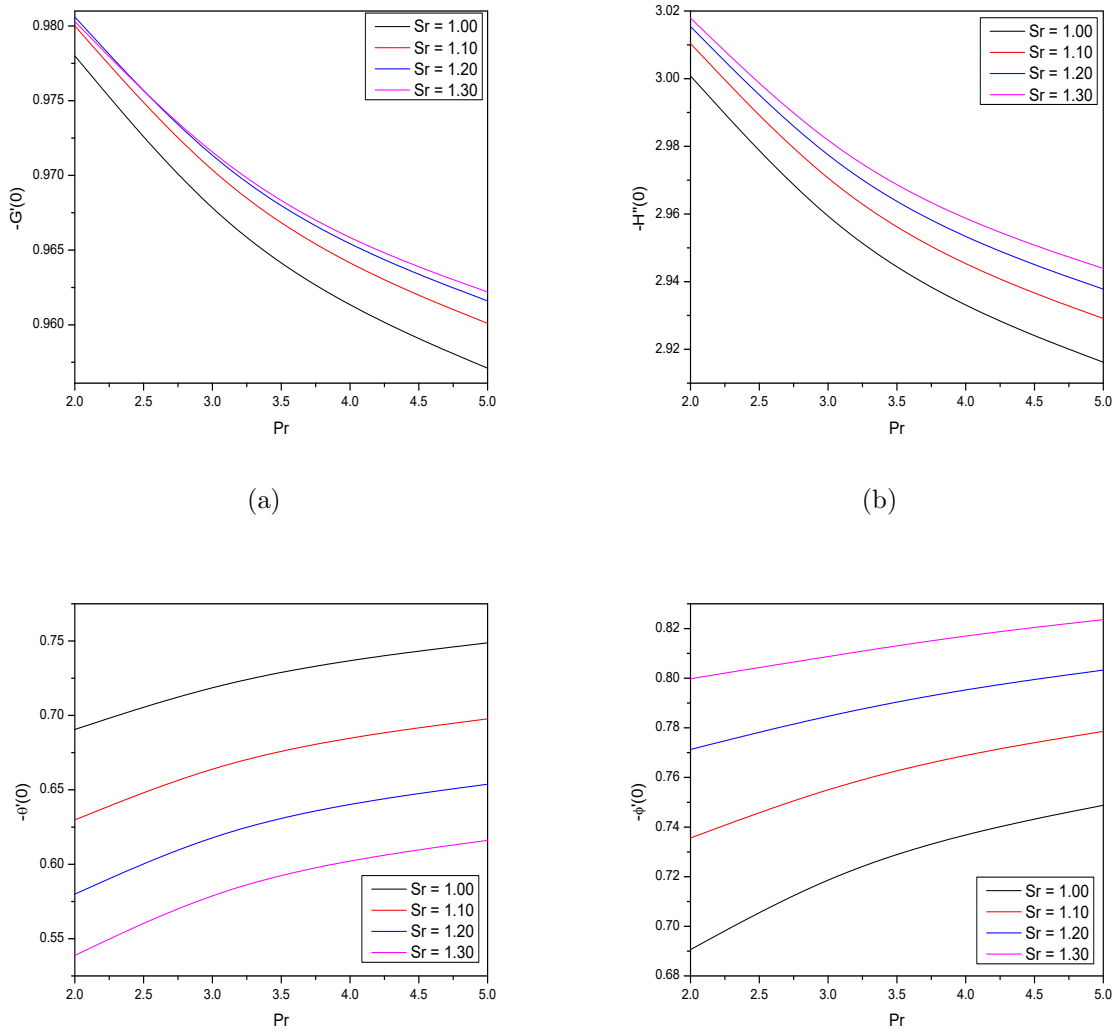

Figure 8.6: Effect of Sr on the "tangential skin friction coefficient", "azimuthal skin friction coefficient", "Nusselt number" and "Sherwod number" for CWT boundary conditions.

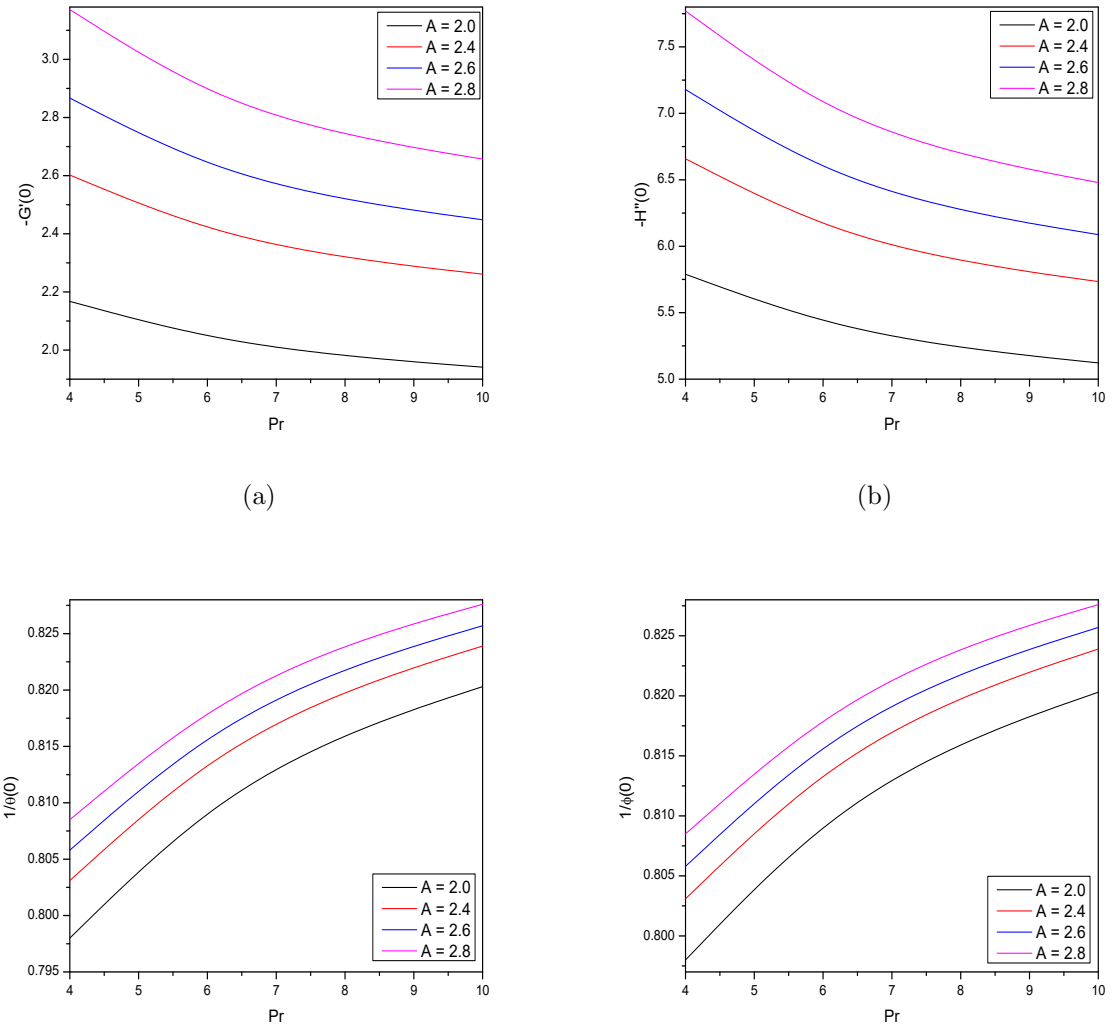

Figure 8.7: Effect of A on the "tangential skin friction coefficient", "azimuthal skin friction coefficient", "Nusselt number" and "Sherwod number" for HMF boundary conditions.

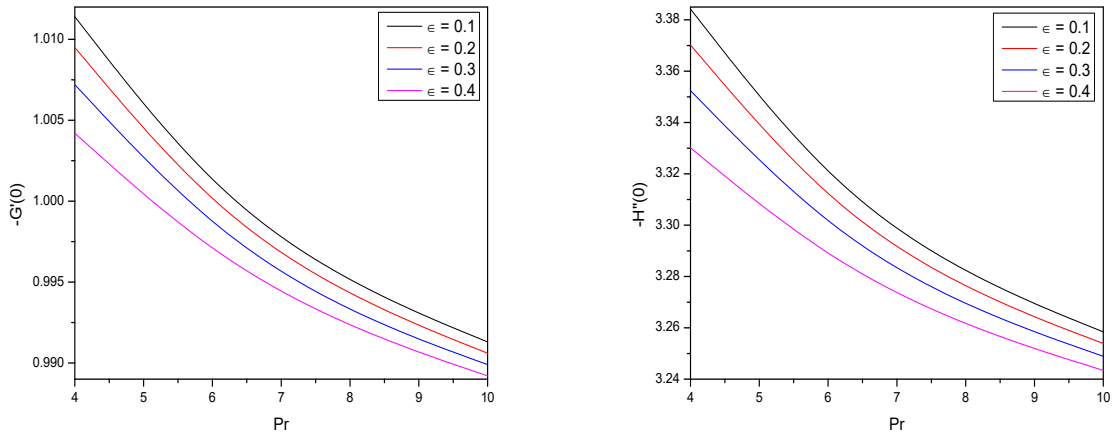

(a)

(b)

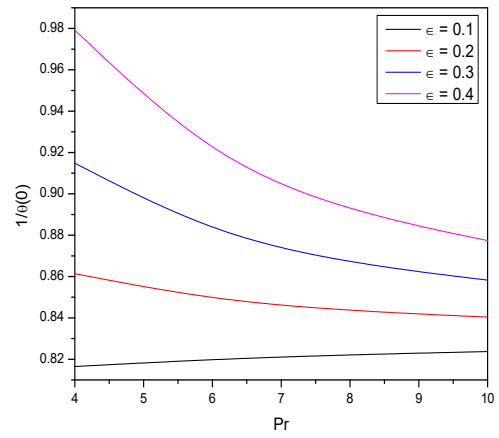

(c)

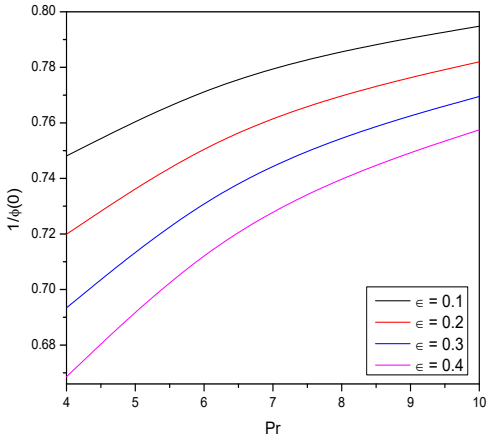

(d)

Figure 8.8: Effect of $\in$ on the "tangential skin friction coefficient", "azimuthal skin friction coefficient", "Nusselt number" and "Sherwod number" for HMF boundary conditions.

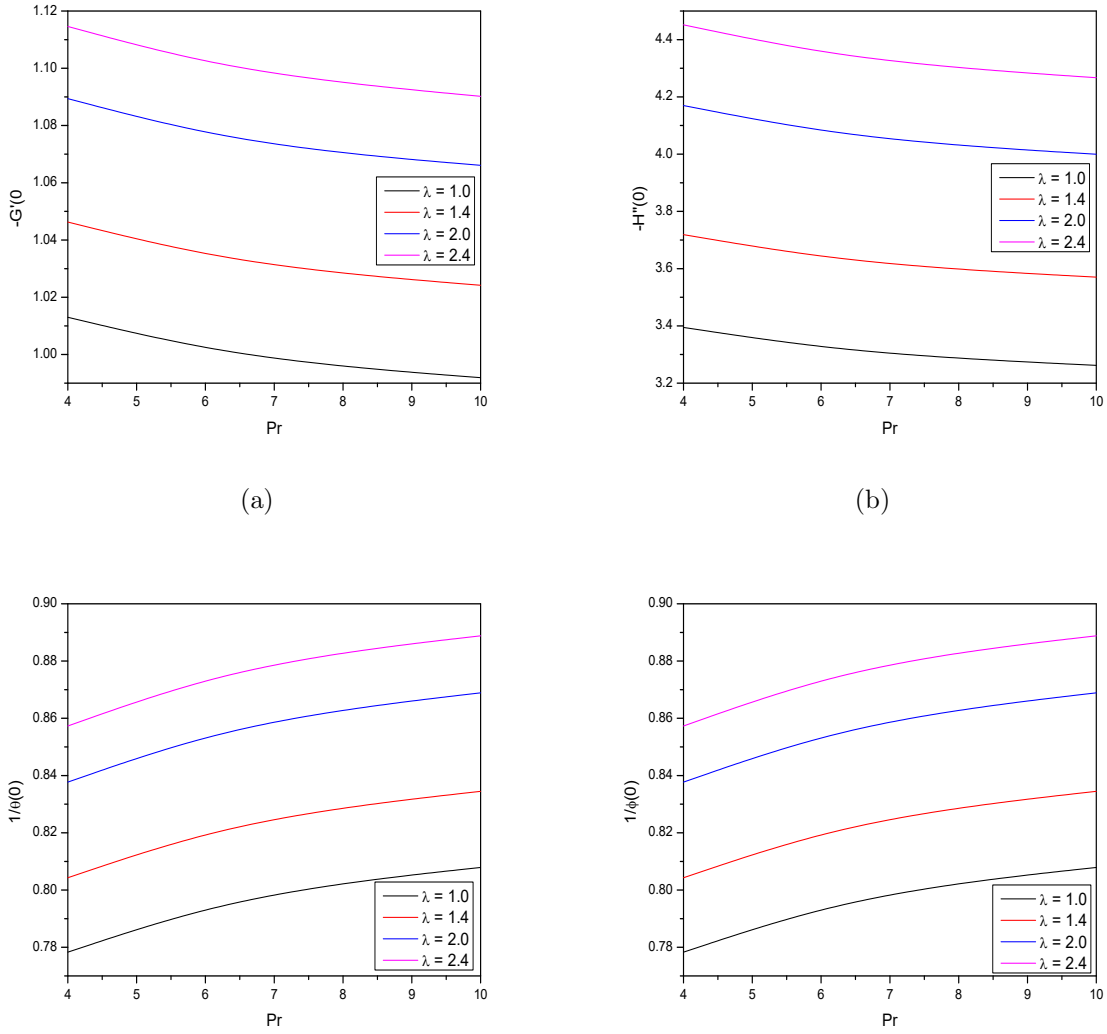

Figure 8.9: Effect of λ on the "tangential skin friction coefficient", "azimuthal skin friction coefficient", "Nusselt number" and "Sherwod number" for HMF boundary conditions.

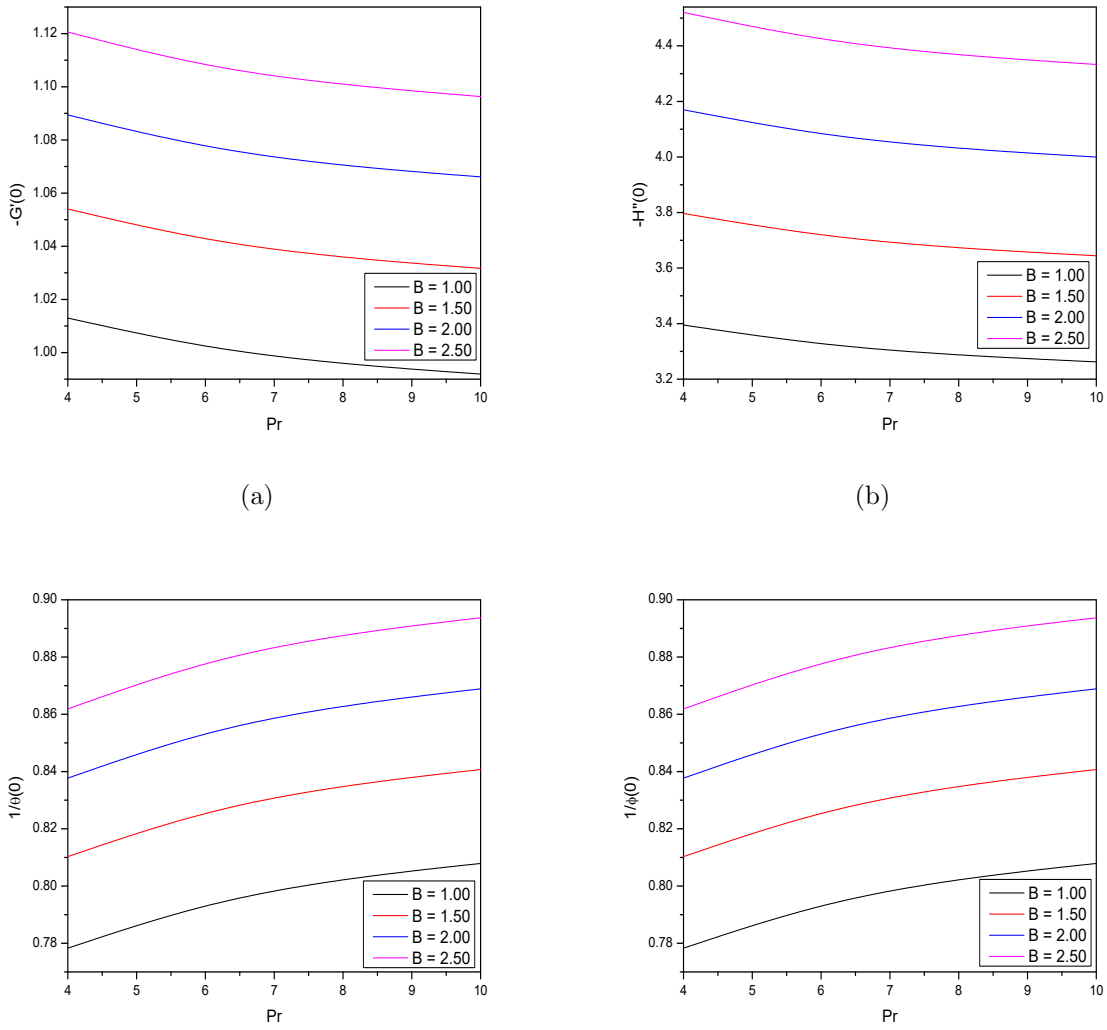

Figure 8.10: Effect of B on the "tangential skin friction coefficient", "azimuthal skin friction coefficient", "Nusselt number" and "Sherwod number" for HMF boundary conditions.

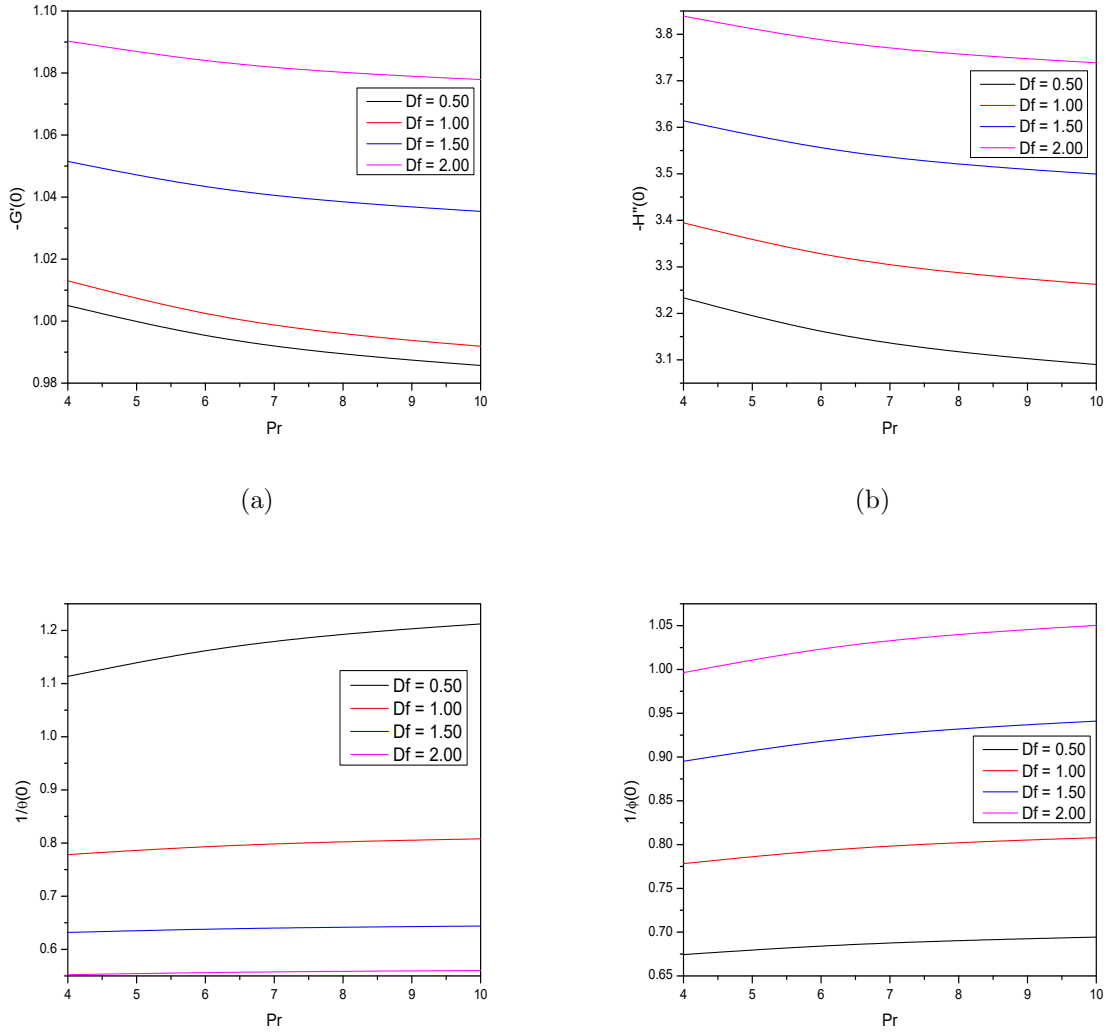

Figure 8.11: Effect of Df on "tangential skin friction coefficient", "azimuthal skin friction coefficient", "Nusselt number" and "Sherwod number" for HMF boundary conditions.

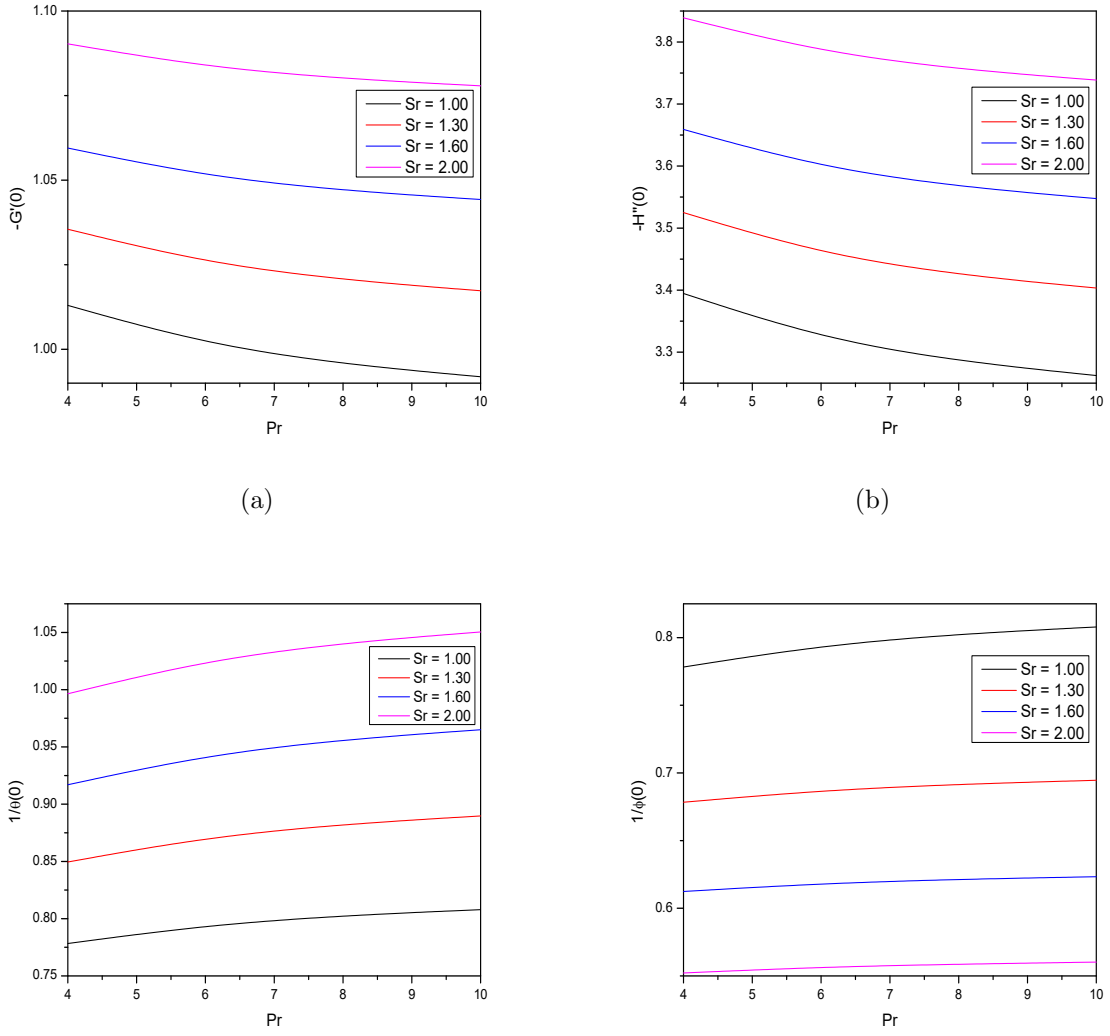

Figure 8.12: Effect of Sr on "tangential skin friction coefficient", "azimuthal skin friction coefficient", "Nusselt number" and "Sherwod number" for HMF boundary conditions.

Chapter 9

Influence of Chemical Reaction and Thermal Radiation on the Flow Across a Rotating Cone with Variable Fluid Properties [1]

9.1 Introduction

The study of thermal radiation effects on heat and mass transfer with chemical reaction are of considerable importance in chemical technology and hydrometallurgical industries. For example, "formation of smog" is a first order homogeneous chemical reaction. In the case of $NO2$ emissions from automobiles and other smokestacks, $NO2$ reacts chemically in the atmosphere with unburned hydrocarbons (aided by sunlight) to form peroxyacetyl nitrate, which forms an envelope known as photochemical smog. Furthermore, the effect of radiation on convective heat transfer problems is becoming increasingly important in astrophysical flows, electrical power generation, space vehicle re-entry, solar power technology, and other industrial areas.s.

The effects of chemical reaction and thermal radiation on the incompressible viscous fluid flow over a rotating cone in the presence of changeable viscosity and thermal conductivity are studied in this chapter. The pseudo-spectral approach is used to solve the governing equations after they have been linearized using the successive linearization method. This

[1] Communicated to "**Heat Transfer**"

technique was efficaciously applied to solve the convection heat and mass transfer problems. The impacts of various flow and geometry factors on the velocity component, temperature, and heat transfer rate are thoroughly examined.

9.2 Mathematical Formulation

Consider the laminar viscous incompressible fluid flow over a cone rotating about its axis with angular velocity Ω. The coordinate system and the geometry of the problem is depicted in Fig. (6.1). In addition to the assumptions made in the chapter - 7, the chemical reaction and radiation effects are incorporated in the flow.

Applying Boussinesq approximation and utilizing the boundary layer assumptions, the equations describing the flow are.

$$\frac{\partial u}{\partial x} + \frac{\partial w}{\partial z} + \frac{u}{x} = 0 \tag{9.1}$$

$$\rho\left(u\frac{\partial u}{\partial x} + w\frac{\partial u}{\partial z} - \frac{v^2}{x}\right) = \frac{\partial}{\partial z}\left(\mu\frac{\partial u}{\partial z}\right) + \rho g\left[\beta_T(T - T_\infty) + \beta_C(C - C_\infty)\right]\cos\alpha \tag{9.2}$$

$$\rho\left(u\frac{\partial v}{\partial x} + w\frac{\partial v}{\partial z} + \frac{uv}{x}\right) = \frac{\partial}{\partial z}\left(\mu\frac{\partial v}{\partial z}\right) \tag{9.3}$$

$$\left(u\frac{\partial T}{\partial x} + w\frac{\partial T}{\partial z}\right) = \frac{\partial}{\partial z}\left(\alpha\frac{\partial T}{\partial z}\right) - \frac{1}{\rho c_p}\frac{\partial q_r}{\partial Z} \tag{9.4}$$

$$u\frac{\partial C}{\partial x} + w\frac{\partial C}{\partial z} = \frac{\partial}{\partial z}\left(\alpha\frac{\partial C}{\partial z}\right) - k_r(C - C_\infty) \tag{9.5}$$

where k_r denotes the rate of chemical reaction and q^r denotes the radiative heat flux term.

The radiative heat flux q^r is described by the Rosseland approximation such that

$$q_r = \frac{4\sigma^*}{3k^*}\frac{\partial T^4}{\partial z} \tag{9.6}$$

where σ^* represents the Stefan-Boltzmann constant and k^* represents the mean absorption coefficient. We assume that the temperature differences within the flow are small enough so that T^4 can be expressed as a linear function of temperature. This is achieved by expanding T^4 in a Taylor series about T_infty while ignoring higher-order terms. Thus

$$T^4 \approx 4T_\infty^3 T - 3T_\infty^4 \tag{9.7}$$

Using (9.6) and (9.7) in the last term of the Eq. (9.4), we get

$$\left(u\frac{\partial T}{\partial x}+w\frac{\partial T}{\partial z}\right)=\frac{\partial}{\partial z}\left(\alpha\frac{\partial T}{\partial z}\right)-\frac{16\sigma^{*}T_{\infty}^{3}}{3\rho c_{p}k^{*}}\frac{\partial^{2}T}{\partial z^{2}} \tag{9.8}$$

The viscosity and thermal conductivity are considered to be a linear function of the temperature [5] and are given by

$$\mu(T)=\mu_{\infty}[1+\lambda(T_{\infty}-T)]\quad and\quad k(T)=k_{0}[1+\gamma(T_{\infty}-T)] \tag{9.9}$$

where μ_{∞} and,k_0 represent the absolute viscosity and the thermal conductivity of the fluid, respectively, λ and γ are constants.

The boundary conditions for the velocity are given as

$$u=0\quad ,v=r\Omega\quad w=0\quad \text{at}\quad z=0\quad \text{and}\quad u\to 0\quad v\to 0\quad \text{as}\quad z\to\infty \tag{9.10}$$

In addition, for the temperature and concentration on the surface of the cone, one can either have constant temperature T_w and concentration and C_w (CWT) or a constant heat flux q_w and mass flux and q_w (CHF).Thus, the conditions for the temperature on the boundary conditions are written as

$$\textbf{Type - I (CWT)}: T=T_{w}\quad C=C_{w}\quad \text{at}\quad z=0 \tag{9.11}$$

$$\textbf{Type - II (CHF)}: k\frac{\partial T}{\partial z}=q_{w}\quad k\frac{\partial C}{\partial z}=q_{m}\quad \text{at}\quad z=0 \tag{9.12}$$

and far away from the cone, the temperature and concentration of the free stream are constant i.e. $T\to T_{\infty}$, $C\to C_{\infty}$ as $z\to\infty$

The following non-dimensional Transformations are introduced to get the dimensionless

equations

$$\left.\begin{aligned}
&\eta = \left(\frac{\Omega \sin\alpha}{\nu}\right)^{\frac{1}{2}} z,\ u = \frac{1}{2} x\Omega \sin\alpha f'(\eta),\ v = x\Omega \sin\alpha g(\eta),\ w = (\nu\Omega \sin\alpha)^{\frac{1}{2}} f(\eta),\\
&T = T_\infty + (T_w - T_\infty)\theta(\eta),\ \text{where } T_w - T_\infty = (T_L - T_\infty)\frac{x}{L} \text{for CWT case}\\
&T = T_\infty + \left(\frac{\Omega \sin\alpha}{\nu}\right)^{\frac{1}{2}} \frac{q_w}{k}\theta(\eta),\ \text{where } q_w = q_0 \frac{x}{L} \text{for CHF case,}\\
&C = C_\infty + (C_w - C_\infty)\theta(\eta),\ \text{where } C_w - C_\infty = (C_L - C_\infty)\frac{x}{L} \text{for CWT case}\\
&C = C_\infty + \left(\frac{\Omega \sin\alpha}{\nu}\right)^{\frac{1}{2}} \frac{q_w}{k}\theta(\eta),\ \text{where } q_w = q_0 \frac{x}{L} \text{for CHF case}
\end{aligned}\right\} \tag{9.13}$$

Applying the similarity transformations (9.13) in the Eqs. (9.1) to (9.4), we get the following non-dimensional equations

$$(1+A)f''' - A\theta f''' - ff'' + \frac{1}{2}f'^2 - A\theta' f'' - 2G^2 - 2\lambda\theta - 2B\phi = 0 \tag{9.14}$$

$$(1+A)g'' - A\theta g'' - Ag'\theta' + f'g - fg' = 0 \tag{9.15}$$

$$\left(Rd + \frac{1}{\Pr}\right)\theta'' + \frac{\in}{\Pr}\theta\theta'' + \frac{\in}{\Pr}\theta'^2 + \frac{1}{2}f'\theta - f\theta' = 0 \tag{9.16}$$

$$\frac{1}{Sc}\phi'' + \frac{\in}{Sc}\theta\phi'' + \frac{1}{Sc} \in \theta'\phi' + \frac{1}{2}f'\phi - f\phi' - \gamma\phi = 0 \tag{9.17}$$

where $Rd = \frac{1}{\mu c_p}\frac{16\sigma^* T_\infty^3}{3k\sigma}$ is the radiation parameter, $\gamma = \frac{k_r}{\Omega Sin\alpha}$ is the chemical reaction parameter.

The dimensionless form of conditions on the boundary are

$$\left.\begin{aligned}
&f(0) = f'(0) = 0, \quad g(0) = 1, \quad \theta(0) = 1, \quad \phi(0) = 1,\\
&f'(\infty) = g(\infty) = \theta(\infty) = \phi(\infty) = 0
\end{aligned}\right\} \quad \text{for CWT case.} \tag{9.18}$$

$$\left.\begin{aligned}
&f(0) = f'(0) = 0, \quad g(0) = 1, \quad \theta'(0) = -1, \quad \phi'(0) = -1\\
&f'(\infty) = g(\infty) = \theta(\infty) = \phi(\infty) = 0
\end{aligned}\right\} \text{for CHF case.} \tag{9.19}$$

The quantities of practical interests are the surface skin-friction coefficient in x- and y-

directions and local rate of heat-transfer in terms of Nusselt number. The non-dimensional form of skin-friction coefficient C_{fx} and C_{fy} are

$$C_{fx} = -{Re_x}^{-\frac{1}{2}} f''(0), \quad C_{fy} = -{Re_x}^{-\frac{1}{2}} g'(0) \tag{9.20}$$

The non-dimensional form of Nusselt numbers (Nu) and Sherwood number (Sh) for CWT case are

$$Nu^I = -{Re_x}^{-\frac{1}{2}} \theta'(0), \quad Sh^I = -{Re_x}^{-\frac{1}{2}} \phi'(0), \tag{9.21}$$

The non-dimensional form of Nusselt numbers (Nu) and Sherwood number (Sh) for CHF case are

$$Nu^{II} = \frac{1}{\theta(0)}, \quad Sh^{II} = \frac{1}{\phi(0)} \tag{9.22}$$

9.3 Methodology

The set of differential equations (9.14) - (9.17) are linearized by means of a successive linearization method (SLM) [55]. The solutions of the ensuing linearized equations are attained by employing the Chebyshev spectral method [7]. On applying the procedure explained in Chapter 2 to the Eqs. (9.14) - (9.17), we get the following linearized equations.

$$a_1 f_i''' + a_2 f_i'' + a_3 f_i' + a_4 f_i + a_5 g_i + a_6 \theta_i' + a_7 \theta_i + a_8 \phi_i = a_9 \tag{9.23}$$

$$b_1 f_i' + b_2 f_i + b_3 f_i'' + b_4 f_i' + b_5 f_i + b_6 \theta_i' + b_7 \theta_i = b_8 \tag{9.24}$$

$$c_1 f_i' + c_2 f_i + c_3 \theta_i'' + c_4 \theta_i' + c_5 \theta_i = c_6 \tag{9.25}$$

$$d_1 f_i' + d_2 f_i + d_3 \theta_i' + d_4 \theta_i + d_5 \phi_i'' + d_6 \phi_i' + d_7 \phi_i = d_8 \tag{9.26}$$

where

$$a_1 = \left((1+A) - A\sum \theta_m\right), \quad a_2 = \left(-\sum f_m - A\sum \theta_m'\right),$$
$$a_3 = -\sum f_m', \quad a_4 = -\sum f_m'', \quad a_5 = -4\sum g_m, \quad a_6 = -A\sum f_m'',$$

$$a_7 = -A\sum f_m''' - 2\lambda, \quad a_8 = -2B$$

$$a_9 = \left(A\sum \theta_m - (1+A)\right)\sum f_m''' + \left(\sum f_m + A\sum \theta_m'\right)\sum f_m'' - \frac{1}{2}\sum f_m'^2$$
$$+2{\sum g_m}^2 + 2\lambda\sum \theta_m + 2B\sum \phi_m$$

$$b_1 = \sum g_m, \quad b_2 = -\sum g_m^{'}, \quad b_3 = \Big((1+A) - A\sum \theta_m\Big)$$

$$b_4 = -A\sum \theta_m^{'} - \sum f_m, \quad b_5 = \sum f_m^{'}, \quad b_6 = -A\sum g_m^{'}, \quad b_7 = -A\sum g_m^{''}$$

$$b_8 = \Big(A\sum \theta_m - (1+A)\Big)\sum g_m^{''} + A\sum g_m^{'}\sum \theta_m^{'} - \sum f_m^{'}\sum g_m + \sum f_m \sum g_m^{'}$$

$$c_1 = \frac{1}{2}\sum \theta_m, \quad c_2 = -\sum \theta_m^{'}, \quad c_3 = (Rd + \frac{1}{\Pr}) + \frac{\in}{\Pr}\sum \theta_m$$

$$c_4 = \frac{2\in}{\Pr}\sum \theta_m^{'} - \sum f_m, \quad c_5 = \frac{\in}{\Pr}\sum \theta_m^{''} + \frac{1}{2}\sum f_m^{'}$$

$$c_6 = \Big(-\frac{1}{\Pr} - \frac{\in}{\Pr}\sum \theta_m\Big)\sum \theta_m^{''} - \frac{\in}{\Pr}\sum \theta_m^{'^2} + \sum f_m \sum \theta_m^{'} - \frac{1}{2}\sum f_m^{'}\sum \theta_m$$

$$d_1 = \frac{1}{2}\sum \phi_m, \quad d_2 = -\sum \phi_m^{'}, \quad d_3 = \frac{\in}{Sc}\sum \phi_m^{'}, \quad d_4 = \frac{\in}{Sc}\sum \phi_m^{''}, \quad d_5 = \frac{1}{Sc} + \frac{\in}{Sc}\sum \theta_m$$

$$d_6 = \frac{\in}{Sc}\sum \theta_m^{'} - \sum f_m, \quad d_7 = \frac{1}{2}\sum f_m^{'} - \gamma,$$

$$d_8 = \Big(-\frac{1}{Sc} - \frac{\in}{Sc}\sum \theta_m\Big)\sum \phi_m^{''} + \Big(-\frac{\in}{Sc}\sum \theta_m^{'} + \sum f_m\Big)\sum \phi_m^{'} - \frac{1}{2}\sum f_m^{'}\sum \phi_m + \gamma\sum \phi_m$$

The equivalent conditions to Equations (9.18) and (9.19) are

$$\left.\begin{array}{l} f_i(0) = f_i'(0) = 0, \quad g_i(0) = 1, \quad \theta_i(0) = 1, \quad \phi_i(0) = 1, \\ f_i'(\infty) = g_i(\infty) = \theta_i(\infty) = \phi_i(\infty) = 0 \end{array}\right\} \quad \text{for CWT case.} \tag{9.27}$$

$$\left.\begin{array}{l} f_i(0) = f_i'(0) = 0, \quad g_i(0) = 1, \quad \theta_i'(0) = -1, \quad \phi_i'(0) = -1 \\ f_i'(\infty) = g_i(\infty) = \theta_i(\infty) = \phi_i(\infty) = 0 \end{array}\right\} \text{for CHF case.} \tag{9.28}$$

As explained in Chapter 2, applying Chebyshev pseudo spectral method on the system of linearized equations (9.23),(9.24),(9.25) and (9.26), we get the following equation in the matrix form

$$A_{i-1}X_i = R_{i-1} \tag{9.29}$$

whereA_{i-1} is a square matrix of order $4N+4$ and X_i and R_{i-1} are column matrices of order $4N+4$ given by

$$A_{i-1} = \begin{pmatrix} A_{11}^{(i)} & A_{12}^{(i)} & A_{13}^{(i)} & A_{14}^{(i)} \\ A_{21}^{(i)} & A_{22}^{(i)} & A_{23}^{(i)} & A_{24}^{(i)} \\ A_{31}^{(i)} & A_{32}^{(i)} & A_{33}^{(i)} & A_{34}^{(i)} \\ A_{41}^{(i)} & A_{42}^{(i)} & A_{43}^{(i)} & A_{44}^{(i)} \end{pmatrix}, X_i = \begin{pmatrix} F_i \\ G_i \\ \Theta_i \\ \Phi_i \end{pmatrix}, R_i = \begin{pmatrix} r_1^{(i)} \\ r_2^{(i)} \\ r_3^{(i)} \\ r_4^{(i)} \end{pmatrix} \tag{9.30}$$

where

$$A_{11}^{(1)} = a_1 D^3 + a_2 D^2 + a_3 D + a_4 I, A_{12}^{(1)} = a_5 I, A_{13}^{(1)} = a_6 D + a_7 I, A_{14}^{(1)} = a_8 I$$

$$A_{21}^{(1)} = b_1 D + b_2 I, A_{22}^{(1)} = b_3 D^2 + b_4 D + b_5 I, A_{23}^{(1)} = b_6 D + b_7 I, A_{24}^{(1)} = 0$$

$$A_{31}^{(1)} = c_1 D + c_2 I, A_{32}^{(1)} = 0, A_{33}^{(1)} = c_3 D^2 + c_4 D + c_5 I, A_{34}^{(1)} = 0$$

$$A_{41}^{(1)} = d_1 D + d_2 I, A_{42}^{(1)} = 0, A_{43}^{(1)} = d_3 D + d_4 I, A_{44}^{(1)} = d_5 D^2 + d_6 D + d_7 I$$

$$r_1^{(1)} = [a_9(\xi_0), a_9(\xi_1), ..., a_9(\xi_{N-1}), a_9(\xi_N)]^T$$

$$r_2^{(1)} = [b_8(\xi_0), b_8(\xi_1), ..., b_8(\xi_{N-1}), b_8(\xi_N)]^T$$

$$r_3^{(1)} = [c_6(\xi_0), c_6(\xi_1), ..., c_6(\xi_{N-1}), c_6(\xi_N)]^T$$

$$r_4^{(1)} = [d_8(\xi_0), d_8(\xi_1), ..., d_8(\xi_{N-1}), d_8(\xi_N)]^T$$

9.4 Results and Discussion

The effects of viscosity parameter, buoyancy parameter and thermal conductivity parameter on the local skin friction coefficients, local Nusselt Number and local Sherwood number are depicted graphically for constant wall temperature and heat flux cases.

Figure 9.1 depicts the effect of the viscosity parameter A on the coefficients of skin friction, Nusselt number, and Sherwood number for type - I boundary conditions. Figures 9.1(a) and 9.1(b) show that the tangential and azimuthal skin friction coefficients increase as A increases. As shown in Fig. 9.1(c), the local Nusselt number $(-\theta'(0))$ decreases as A increases. As presented in Fig. 9.1(d), increasing the parameter A slightly reduces the local Sherwood number $(-\phi'(0))$.

The variation of tangential and azimuthal skin-friction coefficients $(-f''(0))$ and $-g'(0))$, Nusselt number $(-\theta'(0))$ and Sherwood number $(-\phi'(0))$ for different values of $\in$ and Pr is portrayed in Fig. 9.2. According to Figs. 9.2(a) and 9.2(c), the tangential Skin friction coefficient and Nusselt number increase as $\in$ rises. The azimuthal skin friction coefficient and the Sherewood number reduce as the value of $\in$ rises, as shown in Figs. 9.2(b) and 9.2(d).

The impact of the parameter λ on $-f''(0)$, $-g'(0)$, $-\theta'(0)$ and $-\phi'(0)$ is presented in

Fig.9.3 for type - I boundary conditions. It is noticed from Figs. 9.3(a) and 9.3(b) that Both the tangential and azimuthal skin friction coefficients increase as λ increases. Figures 9.3(c) and 9.3(d) reveal that Nusselt number and Sherwood number both increase as the value of λ increases.

The consequence of buoyancy parameter B on the tangential skin-friction coefficient $(-f''(0))$, azimuthal skin-friction coefficient $(-g'(0))$, Nusselt number $(-\theta'(0))$ and Sherwood number $(-\phi'(0))$ is displayed in Fig.9.4 for type - I boundary conditions. It is clear from Figs. 9.4(a),9.4(b) 9.4(c), and 9.4(d) that increasing B increases the skin friction coefficients, Nusselt number, and Sherwood number.

The effect of radiation parameter Rd on $-f''(0)$, $-g'(0)$, $-\theta'(0)$ and $-\phi'(0)$ is depicted in Fig.9.5 for type - I boundary conditions It is observed from Figs. 9.5(a) and 9.5(b) that both the skin friction coefficients increase with an increase in the radiation parameter. Figure 9.5(c) shows that the rate of heat transfer decreases as the radiation parameter increases. The Sherwood number increases as Rd increases, as shown in Fig. 9.5(d).

The variation of $-f''(0)$, $-g'(0)$, $-\theta'(0)$ and $-\phi'(0)$ with chemical reaction parameter γ is displayed in Fig.9.6 for type - I boundary conditions It is noticed from Figs. 9.6(a),9.6(b) and 9.6(c) that both the skin friction coefficients and the rate of heat transfer decrease as the chemical reaction parameter increases. According to Fig. 9.6(d), the rate of mass transfer increases as the value of γ increases.

The influence of viscosity parameter A on the coefficients of skin frictions, Nusselt number and Sherwood number are depicted in Fig.9.7 for type - II boundary conditions. Fig. 9.7(a) and 9.7(b) show that the tangential and azimuthal skin friction coefficients increase as A increases. the local Nusselt number $(-\theta'(0))$ and the local Sherwood number $(-\phi'(0))$ increase as A increases as presented in Fig. 9.7(c) and 9.7(d) .

The variation of $-f''(0)$, $-g'(0)$, $-\theta'(0)$ and $-\phi'(0)$ for various values of $\in$ and Pr is presented in Fig. 9.8. It is observed from Figs. 9.8(a) and 9.8(b) that the tangential and azimuthal skin friction coefficient decrease as $\in$ increases. The Nusselt number increases while the Sherewood number decreases as the value of $\in$ increases, as displayed in Fig. 9.8(c) and Fig. 9.8(d).

The impact of the parameter λ on the coefficients of skin frictions, Nusselt number and Sherwood number is portrayed in Fig.9.9 for type - II boundary conditions. It is noticed from Figs. 9.9(a) and 9.9(b) that both the tangential and azimuthal skin friction coefficients increase as λ increases. Figs. 9.9(c) and 9.9(d) reveal that the Nusselt number and Sherewood

number both increase as the value of λ increases.

The consequence of buoyancy parameter B on $-f''(0)$, $-g'(0)$, $-\theta'(0)$ and $-\phi'(0)$ is depicted in Fig.9.10 for type - II boundary conditions. It is evident from Figs. 9.10(a),9.10(b) 9.10(c), and 9.4(d) that increasing B raises both the skin friction coefficients, Nusselt number, and Sherewood number.

The effect of radiation parameter Rd on the coefficients of skin frictions, Nusselt number and Sherwood number is depicted in Fig.9.11 for type - II boundary conditions It is observed from Figs. 9.11(a) and 9.11(b) that both the skin friction coefficients increase with an increase in the radiation parameter. Figure 9.11(c) shows that the rate of heat transfer decreases as the radiation parameter increases. The Sherewood number is increases as Rd increases, as depicted in Fig. 9.11(d).

The variation of $-f''(0)$, $-g'(0)$, $-\theta'(0)$ and $-\phi'(0)$ with chemical reaction parameter γ is displayed in Fig.9.12 for type - II boundary conditions It is noticed from Figs. 9.12(a),9.12(b) and 9.12(c) that increasing the chemical reaction parameter decreases both the skin friction coefficients and the rate of heat transfer. According to Fig. 9.12(d), the rate of mass transfer increases as the value of γ increases.

9.5 Conclusion

The effects of thermal radiation and chemical reaction on convection flow across a rotating vertical cone were investigated under the assumption of temperature dependent viscosity and thermal conductivity. The flow equations are reduced to ordinary differential equations using similarity transformed equations. The non-dimensional equations are linearized successively, and the resulting system is solved using the Chebyshev spectral method.

- The tangential and azimuthal skin friction coefficients increase as the viscosity parameter increases for both types of boundary conditions.
- The radiation parameter increases both the skin friction coefficients and the Sherwood number while decreasing the Nusselt number.
- The tangential and azimuthal skin friction coefficients, as well as the rate of heat transfer, decrease as the chemical reaction parameter increases, whereas the rate of mass transfer increases.

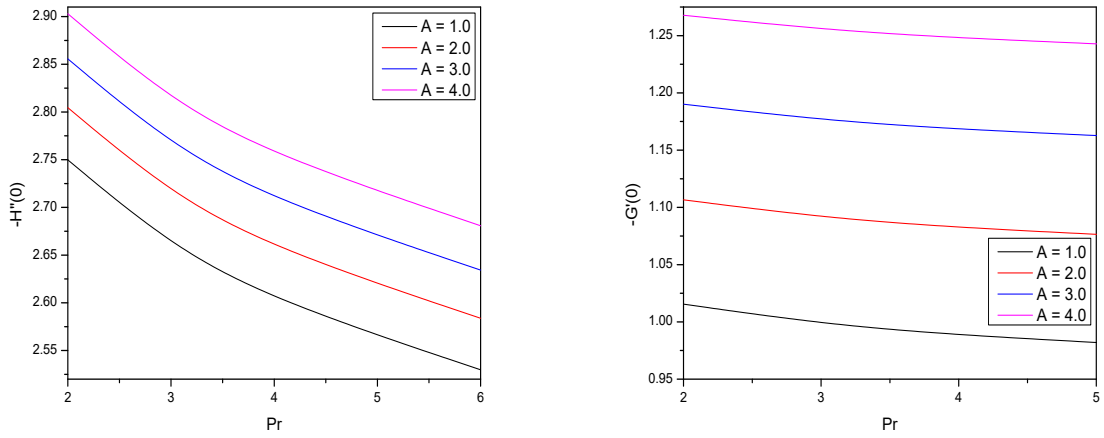

(a)

(b)

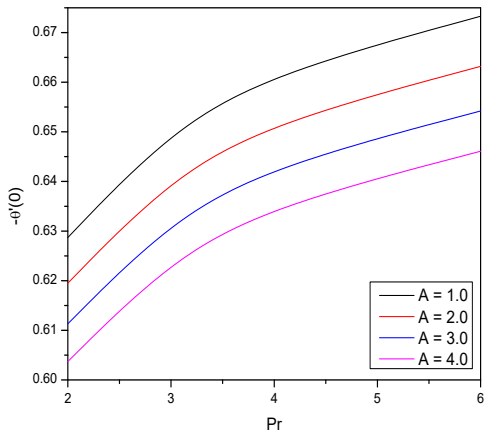

(c)

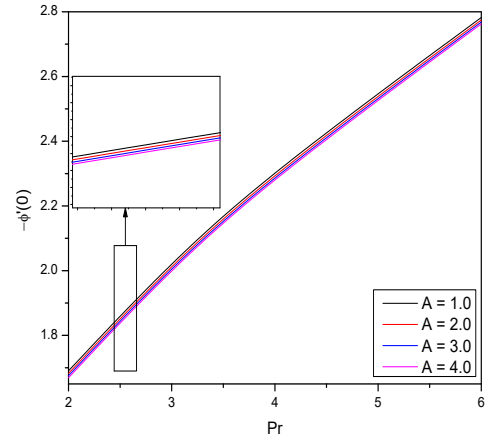

(d)

Figure 9.1: Effect of A on the "tangential skin friction coefficient", "azimuthal skin friction coefficient", "Nusselt number" and "Sherwod number" for CWT boundary conditions.

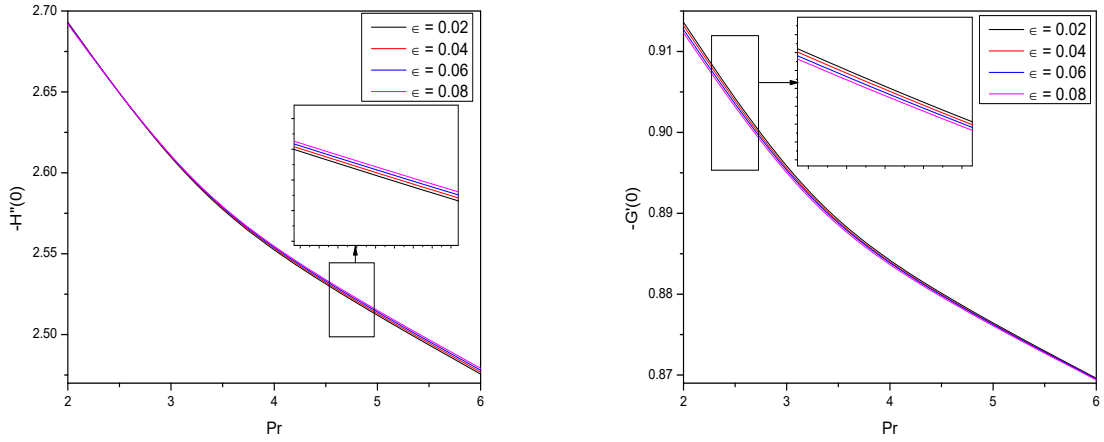

(a)

(b)

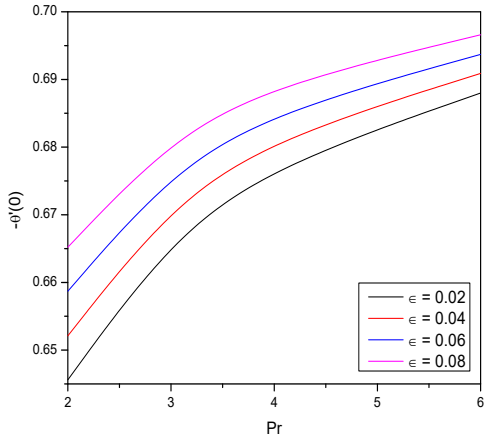

(c)

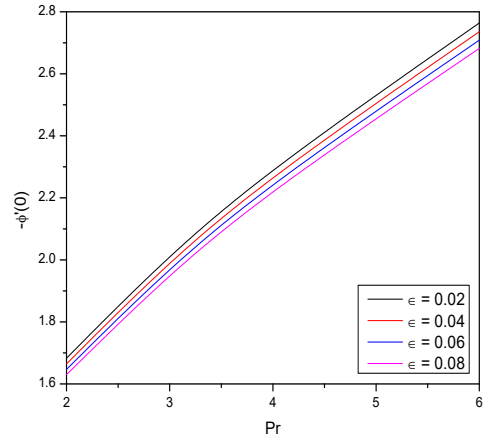

(d)

Figure 9.2: Effect of $\in$ on the "tangential skin friction coefficient", "azimuthal skin friction coefficient", "Nusselt number" and "Sherwod number" for CWT boundary conditions.

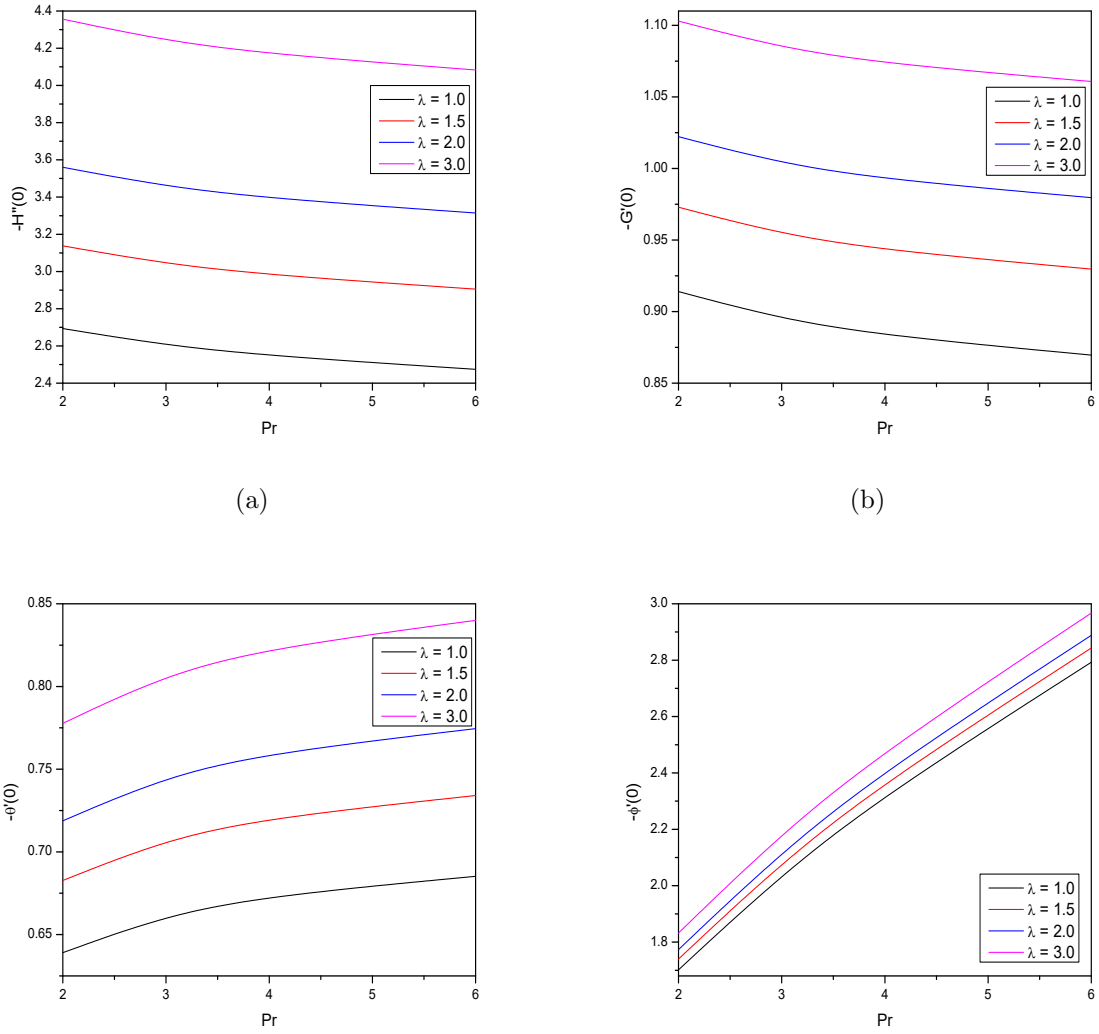

Figure 9.3: Effect of λ on the "tangential skin friction coefficient", "azimuthal skin friction coefficient", "Nusselt number" and "Sherwod number" for CWT boundary conditions.

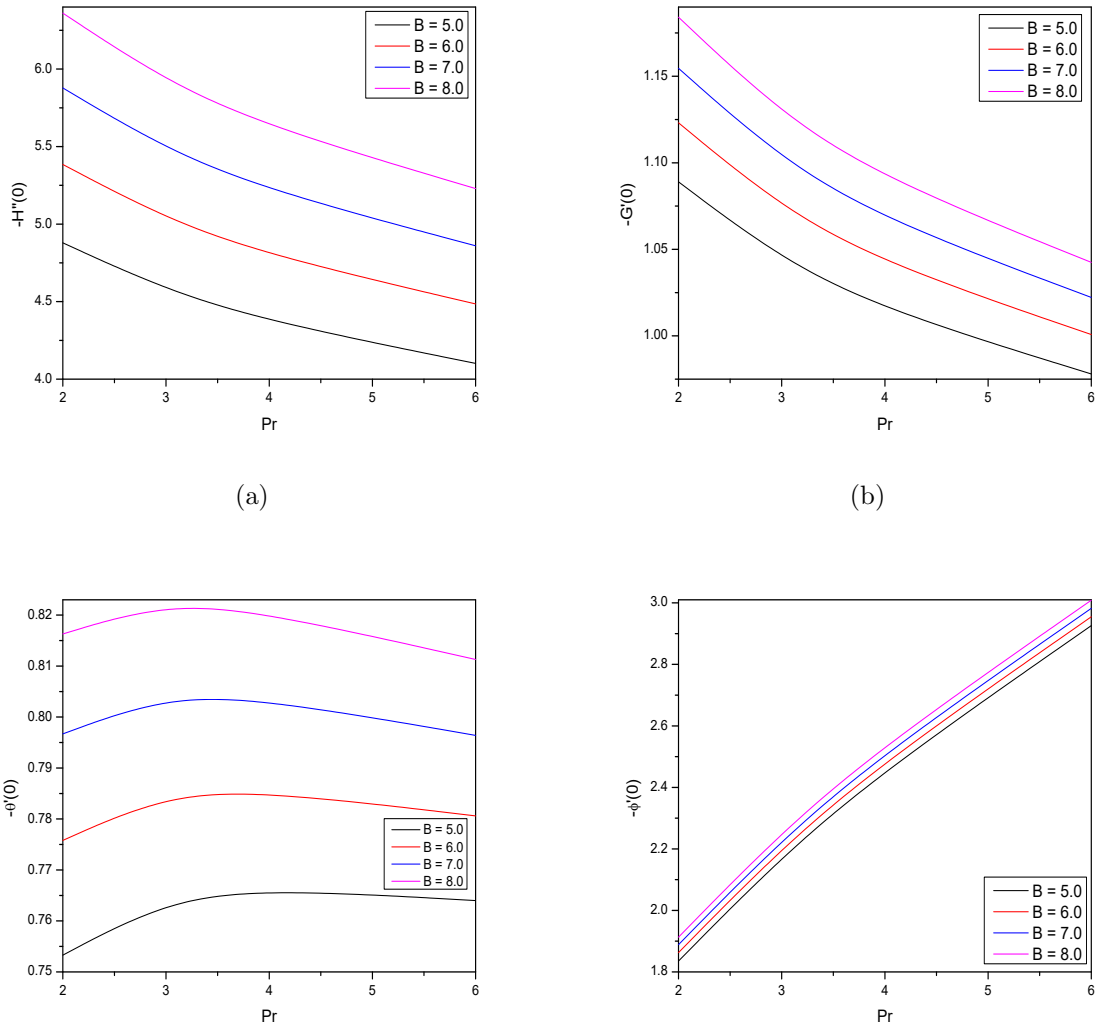

Figure 9.4: Effect of B on the "tangential skin friction coefficient", "azimuthal skin friction coefficient", "Nusselt number" and "Sherwod number" for CWT boundary conditions.

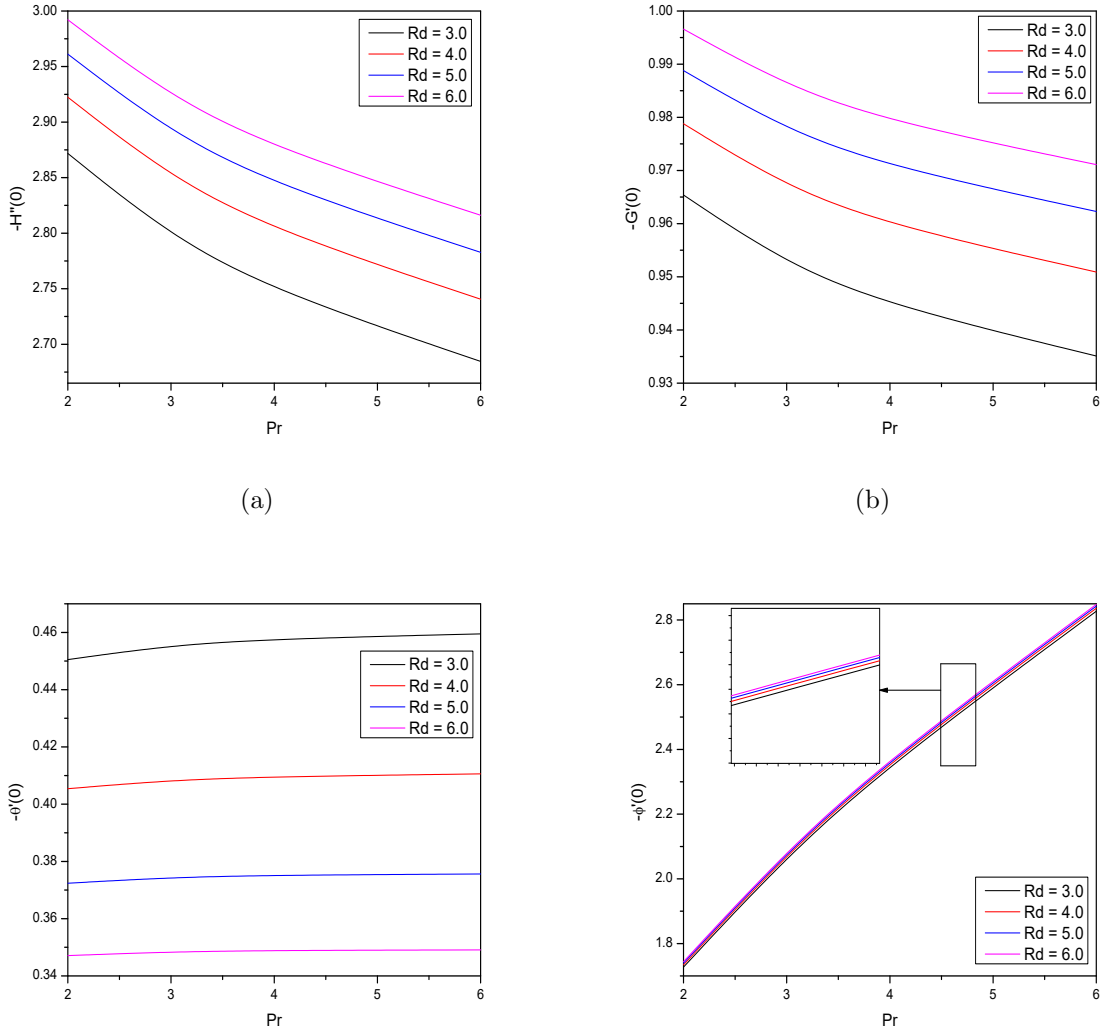

Figure 9.5: Effect of *Rd* on the "tangential skin friction coefficient", "azimuthal skin friction coefficient", "Nusselt number" and "Sherwod number" for CWT boundary conditions.

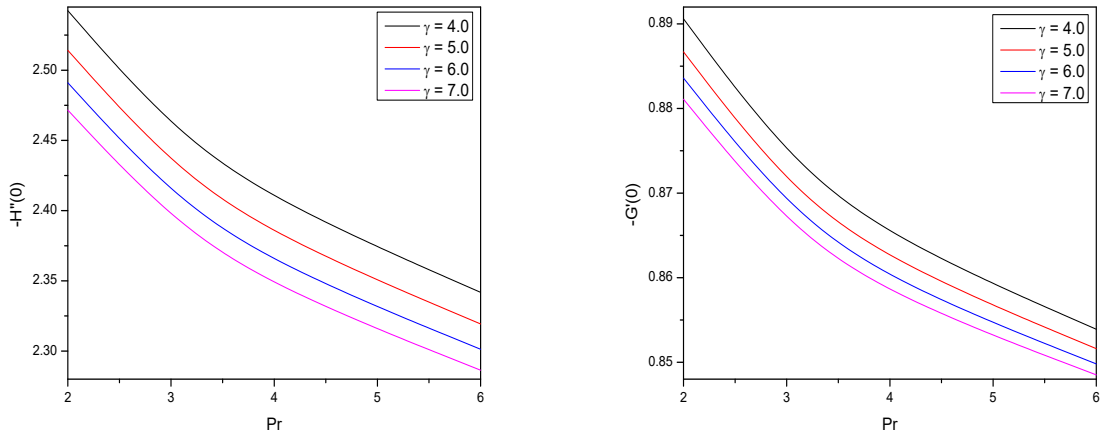

(a)

(b)

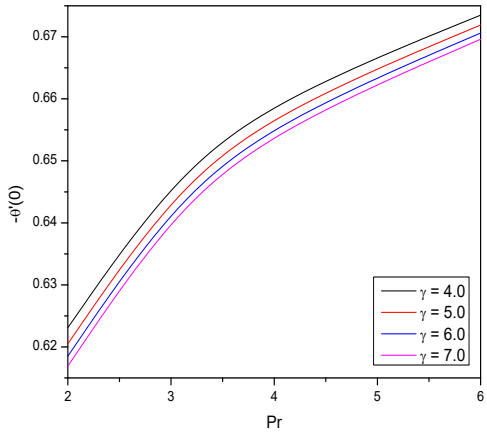

(c)

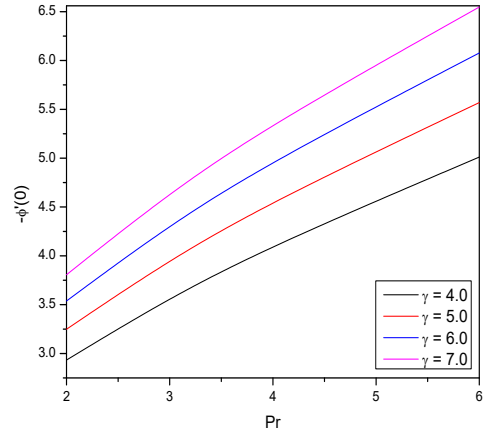

(d)

Figure 9.6: Effect of γ on the "tangential skin friction coefficient", "azimuthal skin friction coefficient", "Nusselt number" and "Sherwod number" for CWT boundary conditions.

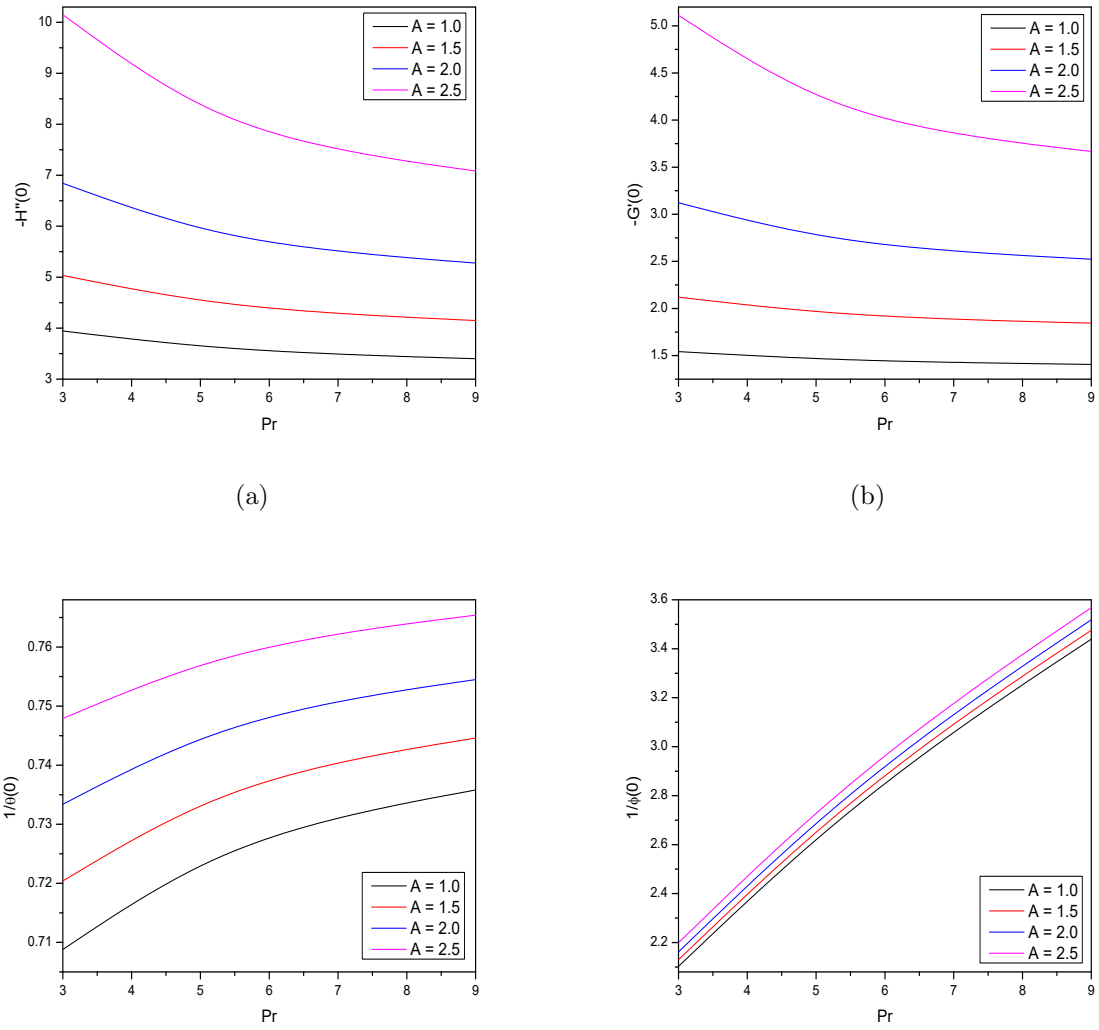

Figure 9.7: Effect of A on the "tangential skin friction coefficient", "azimuthal skin friction coefficient", "Nusselt number" and "Sherwod number" for HMF boundary conditions.

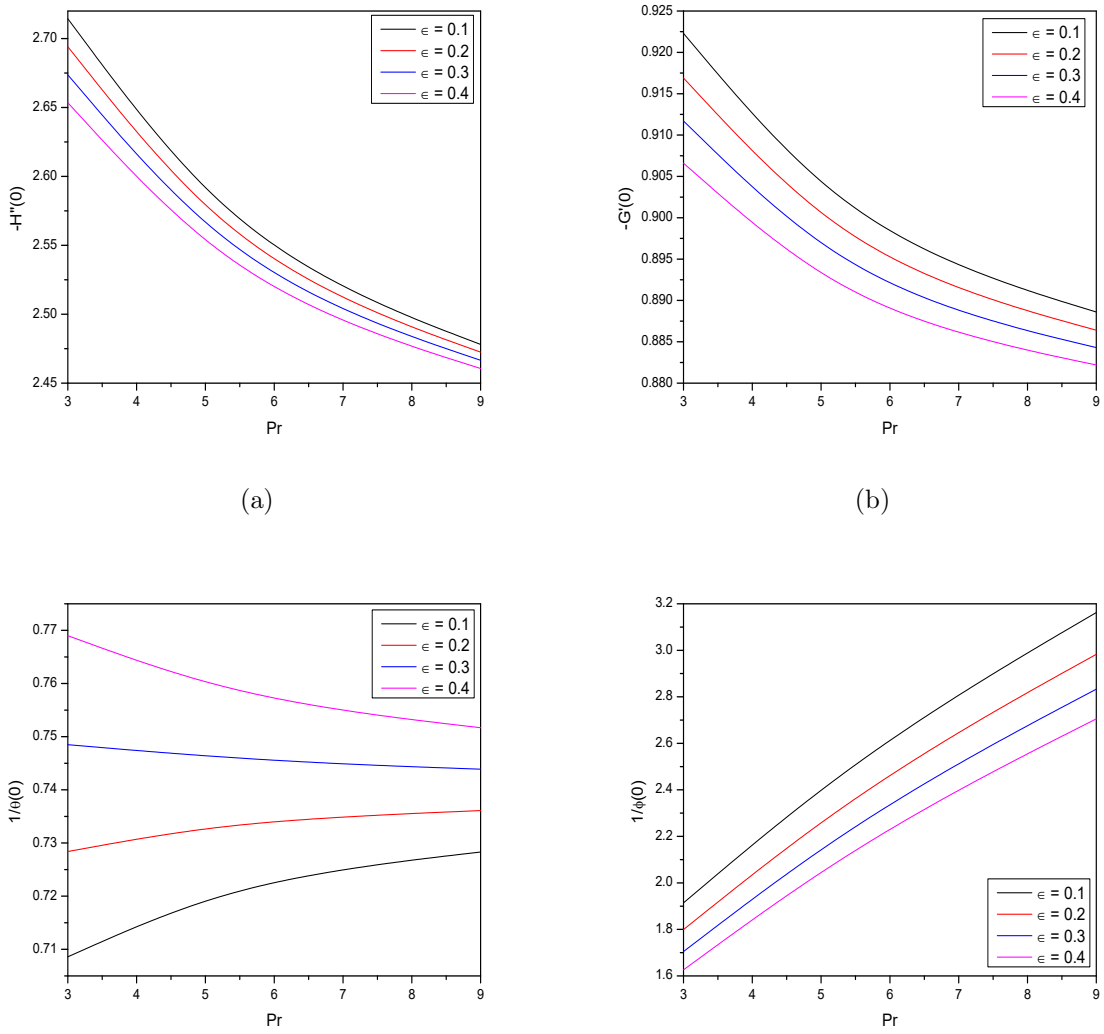

Figure 9.8: Effect of $\in$ on the "tangential skin friction coefficient", "azimuthal skin friction coefficient", "Nusselt number" and "Sherwod number" for HMF boundary conditions.

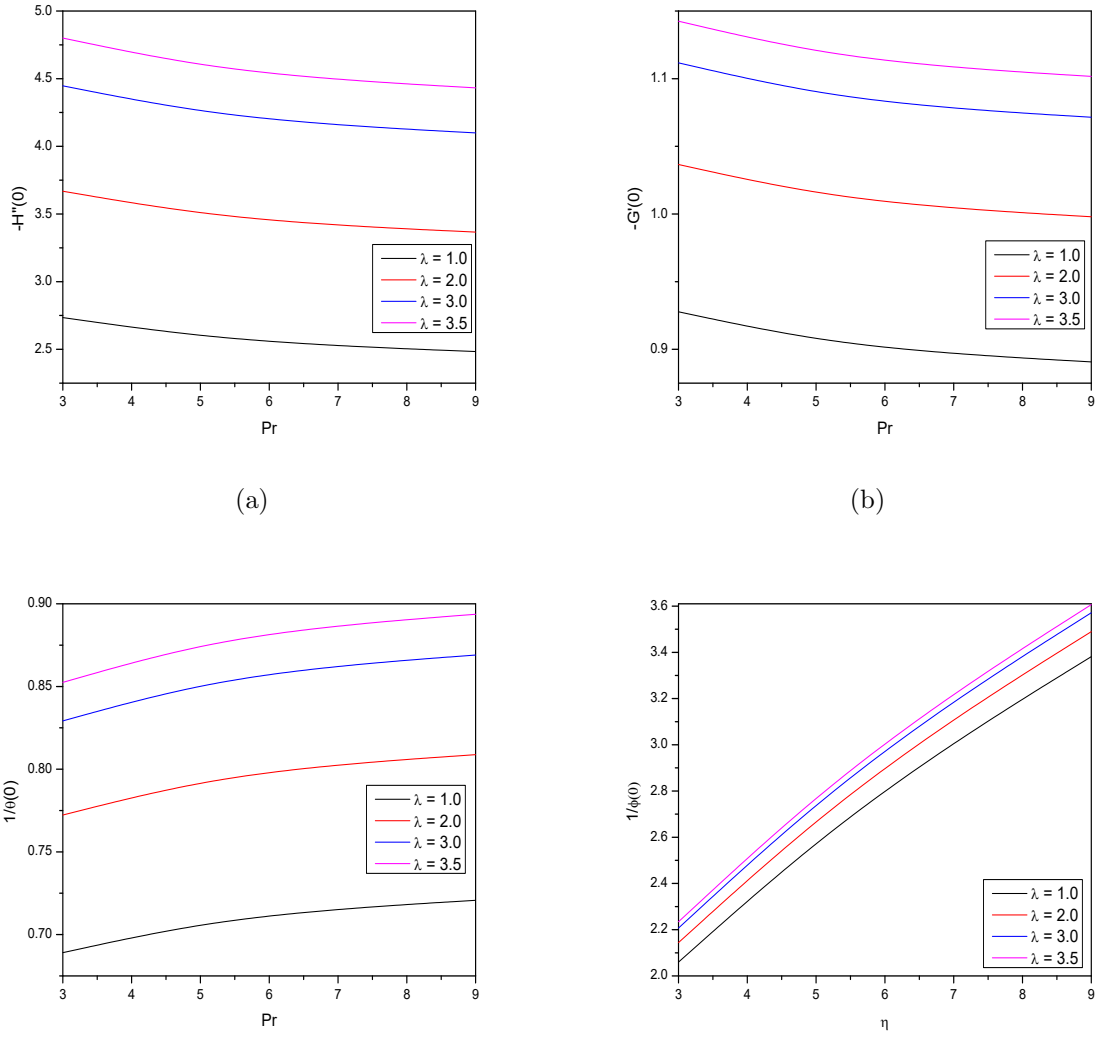

Figure 9.9: Effect of λ on the "tangential skin friction coefficient", "azimuthal skin friction coefficient", "Nusselt number" and "Sherwod number" for HMF boundary conditions.

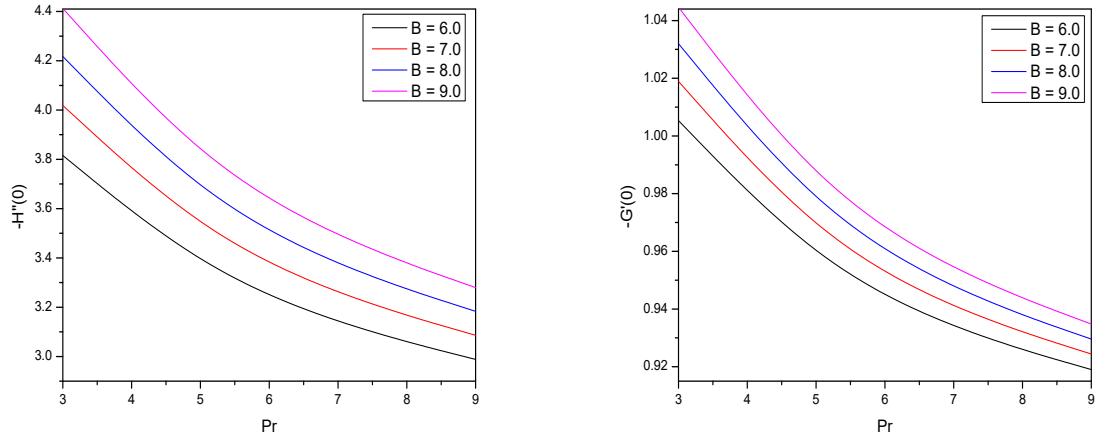

(a)

(b)

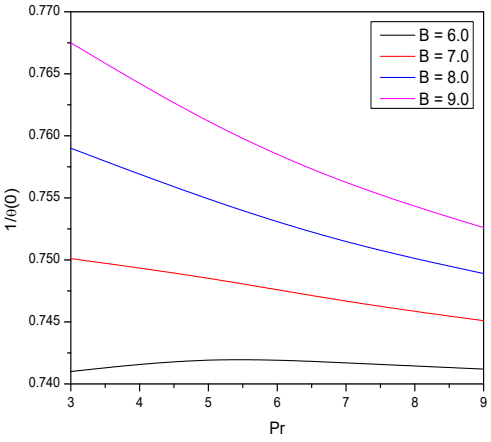

(c)

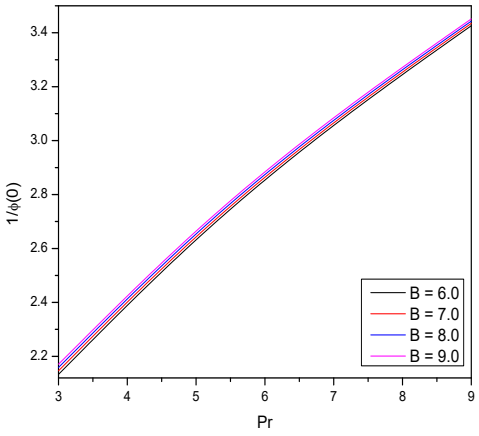

(d)

Figure 9.10: Effect of B on the "tangential skin friction coefficient", "azimuthal skin friction coefficient", "Nusselt number" and "Sherwod number" HMF boundary conditions.

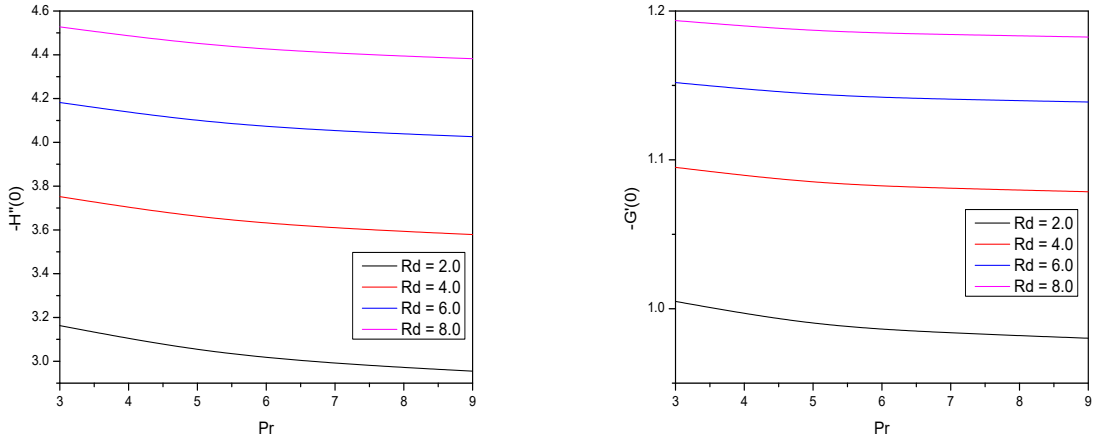

(a)

(b)

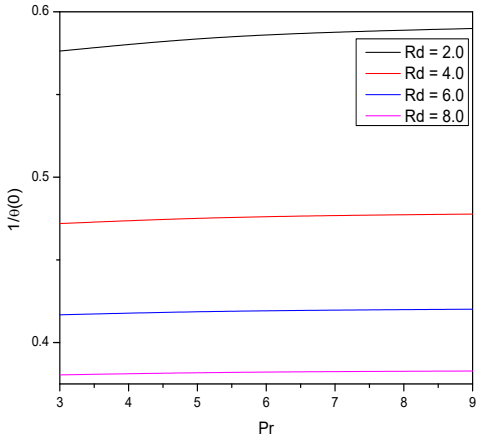

(c)

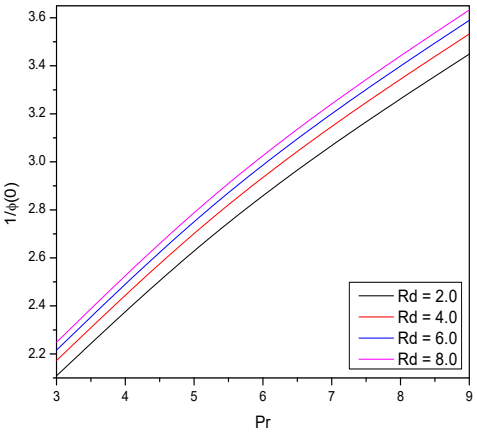

(d)

Figure 9.11: Effect of *Rd* on the "tangential skin friction coefficient", "azimuthal skin friction coefficient", "Nusselt number" and "Sherwod number" for HMF boundary conditions.

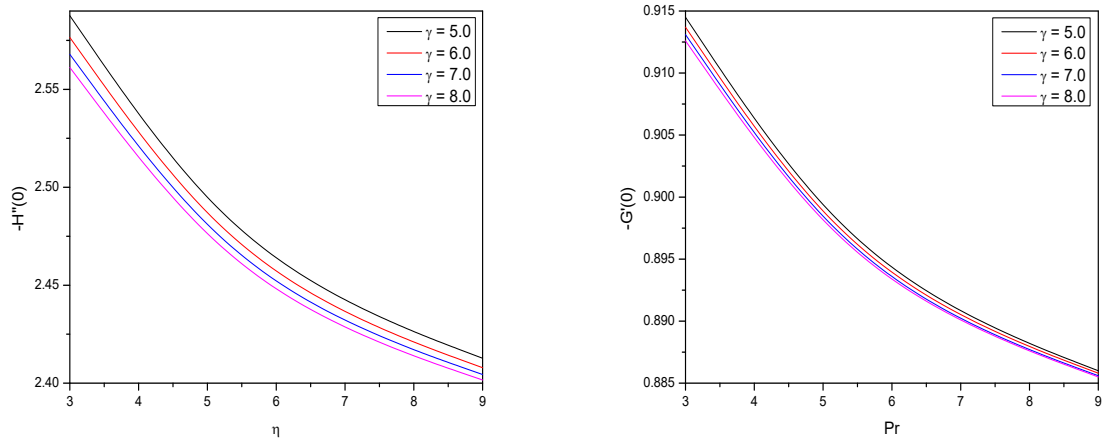

(a) (b)

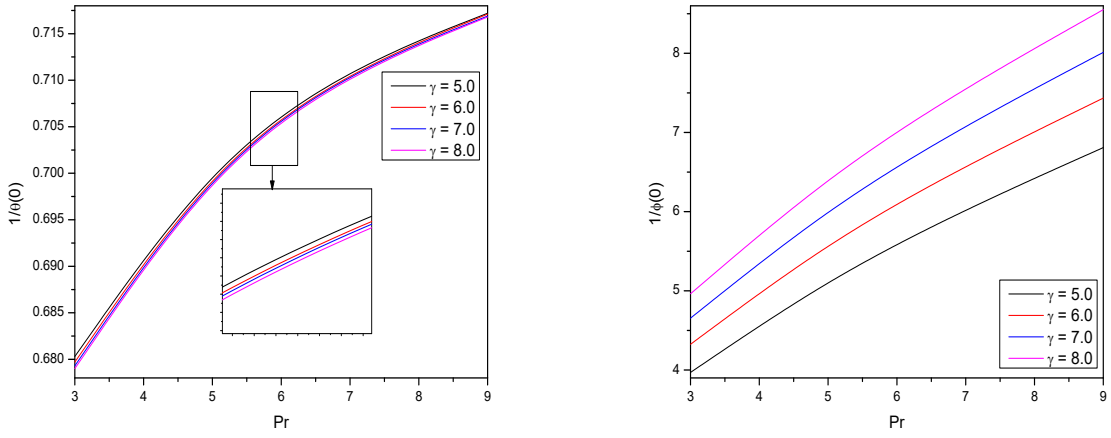

(c) (d)

Figure 9.12: Effect of γ on the "tangential skin friction coefficient", "azimuthal skin friction coefficient", "Nusselt number" and "Sherwod number" for HMF boundary conditions".

Chapter 10

Summary and Conclusions

In this thesis, imcompressible viscous fluid flow over a vertical and rotating cone is considered. The equations governing the flow in Chapters - 2 through Chapters - 9 are transformed into a system of nonlinear ordinary differential equations using suitable transformations. The nonlinear ordinary differential equations were linearized by utlizing the successive linearization method. The solution of the resulting equations are obtained by Chebyshev collocation method.

The effects of variable viscosity and thermal conductivity on the steady convective heat and mass transfer along a vertical cone in a viscous fluid is studied in part-II. The objective of this part is to study the effects of variable viscosity paramter, varaible thermal cinductivity paramter, Soret and Dufour on the velocity, temperature, concentration, skin friction coefficients, Nusselt number, Sherwood number. The important observations made from this study are listed below :

- If the viscosity parameter is enhanced, the velocity adjacent to the cone surface increases, while the reverse tendency is detected sufficiently away from the cone surface.
- The local heat transfer rate decreases with increasing the viscosity and thermal conductivity parameters for CWT conditions but the reverse tend is noticed for CHF conditions.
- For both the conditions, the coefficient of skin friction and mass transfer improves and rate of heat transfer reduce with the variable thermal conductivity parameter increases.
- An enhancement in Soret number enhances the coefficient of skin friction and rate of heat transfer but reduces the Sherwood number for both WTC and HMF cases.

- The coefficient of skin friction and Sherwood numbers rise whereas the heat transfer rate is reducing as the Dufour parameter increase.

Part-III deals with convective heat and mass transfer along a rotating cone embedded in a viscous fluid with variable viscosity and thermal conductivity. Examining effects of variable flid properties, Soret, Dufour, thermal radation and chemical reaction on the velocity, temperature and concentration profiles and skin friction coefficients, heat and mass transfer rates are the objectives of this section. The main observations of these studies are

- For increasing values of the viscosity parameter, the dimensionless tangential skin-friction, azimuthal skin-friction, and rate of heat transfer all rise.
- The Nusselt number is decreasing with an increase in $\in$ while the skin friction coefficients are rising.
- The tangential and azimuthal skin friction increase while heat transfer rate decreases as *lambda* increases.
- An increase in the buoyancy ratio raises the tangential and azimuthal skin friction coefficients, Nusselt number, and Sherewood number.
- The Dufour number increases both the skin friction coefficients and the Sherwood number while decreasing the Nusselt number.
- The tangential and azimuthal skin friction coefficients, as well as the rate of heat transfer, increase as the Soret number increases, whereas the rate of mass transfer decreases.
- The radiation parameter increases both the skin friction coefficients and the Sherwood number while decreasing the Nusselt number.
- The tangential and azimuthal skin friction coefficients, as well as the rate of heat transfer, decrease as the chemical reaction parameter increases, whereas the rate of mass transfer increases.

The work presented in the thesis can be extended to analyze the various effects like MHD, Hall effect, Hall and Ion slip, viscous dissipation, binary chemical reaction, etc. Further, this work can be extended by studying the analysis in various non-Newtonian fluids like Casson fluids, Jeffrey fluids, Power-law fluids. This work can also be extended to porous media.

In the recent past, the study of stability analysis has attracted the curiosity of many researchers. Thus, the work presented in the thesis can be extended to study the stability of the boundary layer flows in Newtonian and/or non-Newtonian fluids.

Bibliography

[1] T Adachi, Y Takahashi, T Akinaga, and J Okajima. Effect of viscosity on pumping-up of newtonian fluid driven by a rotating cone. *Journal of Flow Control Measurement and Visualization*, 6:57–65, 2018.

[2] U Ahmad, M Ashraf, A Al-Zubaidi, A Ali, and S Saleem. Effects of temperature dependent viscosity and thermal conductivity on natural convection flow along a curved surface in the presence of exothermic catalytic chemical reaction. *PloS one*, 16(7):e0252485, 2021.

[3] D. Anilkumar and S. Roy. Unsteady mixed convection flow on a rotating cone in a rotating fluid. *Appl. Math. Comput.*, 155(2):545–561, 2004.

[4] FG Awad, P Sibanda, SS Motsa, and OD Makinde. Convection from an inverted cone in a porous medium with cross-diffusion effects. *Computers and Mathematics with Applications.*, 61:1431–1441, 2011.

[5] GK Batchelor and GK Batchelor. *An introduction to fluid dynamics*. Cambridge university press, 2000.

[6] H Blasius. Grenzschichten in flüssigkeiten mit kleiner reibung. *Z. Für Angew. Math. Und Phys*, 56:1–37, 1908.

[7] JP Boyd. Spectral methods in fluid dynamics (c. canuto, my hussaini, a. quarteroni, and ta zang). *SIAM Review*, 30(4):666–668, 1988.

[8] WH Braun, S Ostrach, and JE Heighway. Free-convection similarity flows about two dimensional and axisymmetric bodies with closed lower ends. *Int Journal Heat Mass Transf*, 2:121–135, 1961.

[9] C. Canuto, MY Hussaini, A Quarteroni, and TA Zang. *Spectral methods fundamentals in single domains*. Springer, Berlin, 2006.

[10] C Canuto, MY Hussaini, A Quarteroni, and TA Zang. *Spectral methods: evolution to complex geometries and applications to fluid dynamics*. Springer Science & Business Media, 2007.

[11] AJ Chamkha and AM Rashad. Unsteady heat and mass transfer by mhd mixed convection flow from a rotating vertical cone with chemical reaction and soret and dufour effects. *Canadian Journal of Chemical Engineering*, 92:758–767, 2014.

[12] CY Cheng. Soret and dufour effects on natural convection heat and mass transfer from a vertical cone in a porous medium. *International Communications in Heat and Mass Transfer*, 36(10):1020–1024, 2009.

[13] CY Cheng. Soret and dufour effects on heat and mass transfer by natural convection from a vertical truncated cone in a fluid-saturated porous medium with variable wall temperature and concentration. *International Communications in Heat and Mass Transfer*, 37(8):1031–1035, 2010.

[14] M Das, S Nandi, B Kumbhakar, and GS Seth. Soret and dufour effects on mhd nonlinear convective flow of tangent hyperbolic nanofluid over a bidirectional stretching sheet with multiple slips. *Journal of Nanofluids*, 10(2):200–213, 2021.

[15] WS Don and A Solomonoff. Accuracy and speed in computing the chebyshev collocation derivative. *SIAM J. Sci. Comput.*, 16:1253–1268, 1995.

[16] LA Dorffmann. *Hydrodynamic resistance and the heat loss of rotating solids*. Oliver and Boyd, Edinburgh, 1963.

[17] MC Ece. Free convection flow about a cone under mixed thermal boundary conditions and a magnetic field. *Applied Mathematical Modelling*, 29(11):1121–1134, 2005.

[18] ERG Eckert and RM Drake. *Analysis of Heat and Mass Transfer*. McGraw-Hill, New York, NY, 1972.

[19] MR Fildes, ZM Hussain, J Unadkat, and SJ Garrett. Analysis of boundary layer flow over a broad rotating cone in still fluid with non-stationary modes. *Physics of Fluids*, 32:124118, 2020.

[20] M Ganapathirao, G Revathi, and R Ravindran. Unsteady mixed convection boundary layer flow over a vertical cone with non-uniform slot suction (injection). *Meccanica*, 49:673–686, 2014.

[21] I Ghoneim, MG Reddy, and AM Megahed. Numerical solution for natural convection fluid flow along a vertical cone with variable diffusivity and wall heat and mass fluxes embedded in a porous medium. *International Journal of Modern Physics C*, 32(06):2150074, 2021.

[22] JP Hartnett and EC Deland. The influence of prandtl number on the heat transfer from rotating nonisothermal disks and cones. *Journal of Heat Transfer*, 83(1):95–96, 1961.

[23] MF Hasan, MM Molla, M Kamrujjaman, and S Siddiqa. Natural convection flow over a vertical permeable circular cone with uniform surface heat flux in temperature-dependent viscosity with three-fold solutions within the boundary layer. *Computation*, 10:60, 2022.

[24] T Hayat, SA Khan, MI Khan, and A Alsaedi. Irreversibility characterization and investigation of mixed convective reactive flow over a rotating cone. *Computer methods and programs in biomedicine*, 185:105168, 2020.

[25] S Hazarika, S Ahmed, and SW Yao. Investigation of cu–water nano-fluid of natural convection hydro-magnetic heat transport in a darcian porous regime with diffusion-thermo. *Applied Nanoscience*, pages 1–11, 2021.

[26] RG Hering and RJ Grosh. Laminar free convection from a non-isothermal cone. *International Journal of Heat and Mass Transfer*, 5(11):1059–1068, 1962.

[27] H Herwig and G Wickern. The effect of variable properties on laminar boundary layer flow. *Wärme-und Stoffübertragung*, 20(1):47–57, 1986.

[28] K. Himasekhar, PKS Sarma, and K Janardhan. Laminar mixed convection from a vertical rotating cone. *International Communications in Heat and Mass Transfer*, 16:99–106, 1989.

[29] MA Hossain and MS Munir. Natural convection flow of a viscous fluid about a truncated cone with temperature-dependent viscosity and thermal conductivity. *International Journal of Numerical Methods for Heat & Fluid Flow*, 2001.

[30] MA Hossain and SC Paul. Free convection from a vertical permeable circular cone with non-uniform surface heat flux. *Heat and Mass Transfer*, 37(2):167–173, 2001.

[31] TF Irvine and JP Hartnett. Convection heat transfer in rotating systems. *Advances in Heat Transfer*, 5:129–251, 1969.

[32] NG Kafoussias. Effects of mass transfer on free convective flow past a vertical isothermal cone surface. *International journal of engineering science*, 30(3):273–281, 1992.

[33] NG Kafoussias and EW Williams. Thermal-diffusion and diffusion thermo effects on mixed free-forced convective and mass transfer boundary layer flow with temperature dependent viscosity. *International Journal of Engineering Science*, 33:1369–1384, 1995.

[34] RM Kannan, P Bapuji, and M Sajid. Free convective flow past a vertical cone with magnetohydrodynamics / heat generation / absorption with variable heat flux. *Mathematical Modelling of Engineering Problems,*, 9(1):11–18, 2022.

[35] RM Kannan, P Bapuji, and P Sambath. Group solution for free convection flow of dissipative fluid from non-isothermal vertical cone. *AIP Conference Proceedings*, 2112:020014, 2019.

[36] A Kaushik. Numerical solutions for free convection flow past a vertical cone using alternating direction implicit (adi) technique. *International Journal of Research and Innovation in Applied Science*.

[37] WM Kays and Crawford ME. *Convective heat and mass transfer*, volume 4. McGraw-Hill New York, 1980.

[38] M Khan, T Salahuddin, and MA Altanji. viscously dissipated blasisus boundary layer flow with variable thermo-physical properties: An entropy generation study. *Int. Comm. Heat Mass Transf*, 131:105873, 2022.

[39] SA Khan, T Hayat, A Alsaedi, and S Momani. Entropy generation and dufour and soret effects in radiative flow by a rotating cone. *Physica Scripta*, 96(2):025209, 2020.

[40] Y Khan, Q Wu, N Faraz, and A Yildirim. The effects of variable viscosity and thermal conductivity on a thin film flow over a shrinking/stretching sheet. *Computers & Mathematics with Applications*, 61(11):3391–3399, 2011.

[41] YM Li, Khan. MI, SA Khan, SU Khan, Z Shah, and P Kumam. An assessment of the mathematical model for estimating of entropy optimized viscous fluid flow towards a rotating cone surface. *Scientific Reports*, 11(1):10259, 2021.

[42] CR Lin and CO Chen. Free convection flow from a vertical isothermal cone with temperature-dependent viscosity. *Polymer-Plastics Technology and Engineering*, 32(4):277–287, 1993.

[43] A Mahdy. Heat transfer and flow of a casson fluid due to a stretching cylinder with the soret and dufour effects. *Journal of Engineering Physics and Thermophysics*, 88(4):928–936, 2015.

[44] ZG Makukula, SS Motsa, and P Sibanda. On a new solution for the viscoelastic squeezing flow between two parallel plates. *J. of Adv. Research in Appl. Math.*, 2:31–38, 2010.

[45] ZG Makukula, P Sibanda, and SS Motsa. A note on the solution of the von karman equations using series and chebyshev spectral methods. *Boundary Value Problems*, 471793, 2010.

[46] ZG Makukula, P Sibanda, and SS Motsa. A novel numerical technique for two dimensional laminar flow between two moving porous walls. *Mathematical Problems in Engineering.*, 2010:15, 2010.

[47] M.Y. Malik, H Jamil, T Salahuddin, S Bilal, KU Rehman, and Z Mustafa. Mixed convection dissipative viscous fluid flow over a rotating cone by way of variable viscosity and thermal conductivity. *Results in Physics*, 6:1126–1135, 2016.

[48] B Mallikarjuna, AM Rashad, AJ Chamkha, and SR S. Hariprasad. Chemical reaction effects on mhd convective heat and mass transfer flow past a rotating vertical cone embedded in a variable porosity regime. *Afrika Matematika*, 27:645–665, 2016.

[49] OP Meena, J Pranitha, and AJ Chamkha. Influence of soret and dufour effects on mixed convection flow over a vertical cone with injection/suction effects. *Journal of Porous Media*, 24:73–88, 2021.

[50] OP Meena, J Pranitha, and D Srinivasacharya. Mixed convection fluid flow over a vertical cone saturated porous media with double dispersion and injection/suction effects. *International Journal of Applied and Computational Mathematics*, 7:1–20, 2021.

[51] HJ Merk and JA Prins. Thermal convection in laminar boundary layers i. *Applied Scientific Research, Section A*, 4:11–24, 1954.

[52] HJ Merk and JA Prins. Thermal convection in laminar boundary layers ii. *Applied Scientific Research, Section A*, 4(3):195–206, 1954.

[53] MM Molla and RSR Gorla. Natural convection flow from an isothermal horizontal circular cylinder with temperature dependent viscosity. *Heat and Mass Transfer*, 41(7):594–598, 2005.

[54] MM Molla, A Rahman, and LT Rahman. Natural convection flow from an isothermal sphere with temperature dependent thermal conductivity. *Journal of Naval Architecture and Marine Engineering*, 2(2):53–64, 2005.

[55] S Motsa and S Shateyi. Successive linearisation solutionyof free convection non-darcy flow with heat and mass transfer. *Advanced topics in mass transfer*, 19:425–438, 2011.

[56] SS Motsa and P Sibanda. A new algorithm for solving singular ivps of lane-emden type. *Proceedings of the* 4^{th} *International Conference on Applied Mathematics, Simulation and Modelling*, pages 176–180, 2010.

[57] Z Mustafa, T Javed, T Hayat, and A Alsaedi. Unsteady mhd chemically reactive dissipative flow of nanofluid due to rotating cone. *Numerical Heat Transfer, Part A: Applications*, 82:441–454, 2022.

[58] TY Na and JP Chiou. Laminar natural convection over a frustum of a cone. *Applied Scientific Research*, 35.

[59] T Naseem, U Nazir, ER El-Zahar, AM Algelany, and M Sohail. Numerical computation of dufour and soret effects on radiated material on a porous stretching surface with temperature-dependent thermal conductivity. *Fluids*, 6(6):196, 2021.

[60] E Osalusi, JS Side Charles, RE Harris, and P Clark. The effect of combined viscous dissipation and joule heating on unsteady mixed convection mhd flow on a rotating cone in a rotating fluid with variable properties in the presence of hall and ion-slip currents. *International Communications in Heat and Mass Transfer*, 35:413–429, 2008.

[61] AO Oyem, WN Mutuku, and AS Oke. Variability effects on magnetohydrodynamic for blasius and sakiadis flows in the presence of dufour and soret about a flat plate. *Engineering Reports*, 2(10):e12249, 2020.

[62] G Palani and AR Ragavan. Free convection flow past a vertical cone with a chemical reaction in the presence of transverse magnetic field. *Journal of Engineering Physics and Thermophysics*, 88(5):1256–1263, 2015.

[63] PM Patil, N Kumbarwadi, and AJ Chamkha. Unsteady mixed convection over an exponentially stretching surface: Influence of darcy-forchheimer porous medium and cross diffusion. *Journal of Porous Media*, 24(2), 2021.

[64] PM Patil and I Pop. Effects of surface mass transfer on unsteady mixed convection flow over a vertical cone with chemical reaction. *Heat and Mass Transfer*, 47:1453–1464, 2011.

[65] F Patrulescu, T Grosan, and I Pop. Mixed convection boundary layer flow from a vertical truncated cone in a nanofluid. *International Journal of Numerical Methods for Heat & Fluid Flow*, 24:1175–1190, 2014.

[66] I Pop, T Grosan, and M Kumari. Mixed convection along a vertical cone for fluids of any prandtl number: case of constant wall temperature. *International Journal of Numerical Methods for Heat & Fluid Flow*, 13:815–829, 2003.

[67] B Pullepu, P Sambath, M Selva Rani, AJ Chamkha, and KK Viswanathan. Numerical solutions of free convective flow from a vertical cone with mass transfer under the influence of chemical reaction and heat generation/absorption in the presence of uwt/uwc. *Journal Of Applied Fluid Mechanics,*, 9(1):343–356, 2016.

[68] MM Rahman, AA Mamun, MA Azim, and MA Alim. Effects of temperature dependent thermal conductivity on magnetohydrodynamic (mhd) free convection flow along a vertical flat plate with heat conduction. *Nonlinear Analysis: Modelling and Control*, 13(4):513–524, 2008.

[69] R Ravindran, S Roy, and E Momoniat. Effects of injection (suction) on a steady mixed convection boundary layer flow over a vertical cone. *International Journal of Numerical Methods for Heat & Fluid Flow*, 19:432–444, 2009.

[70] MG Reddy and N Sandeep. Free convective heat and mass transfer of magnetic bioconvective flow caused by a rotating cone and plate in the presence of nonlinear thermal radiation and cross diffusion. *Journal of Computational & Applied Research in Mechanical Engineering*, 7(1):1–21, 2017.

[71] H Rosali, A Ishak, R Nazar, and I Ioan Pop. Mixed convection boundary layer flow past a vertical cone embedded in a porous medium subjected to a convective boundary condition. *Propulsion and Power Research*, 5(2):118–122, 2016.

[72] S Roy and D Anilkumar. Unsteady mixed convection from a rotating cone in a rotating fluid due to the combined effects of thermal and mass diffusion. *International Journal of Heat and Mass Transfer*, 47:1673–1684, 2004.

[73] S Saleem. Heat and mass transfer of rotational flow of unsteady third-grade fluid over a rotating cone with buoyancy effects. *Mathematical Problems in Engineering*, 2021:5544540, 2021.

[74] S Saleem and S Nadeem. Theoretical analysis of slip flow on a rotating cone with viscous dissipation effects. *Journal of Hydrodynamics*, 27:616–623, 2015.

[75] BR Sharma and B Buragohain. Effect of soret dufour, variable viscosity and variable thermal conductivity on unsteady free convective flow past a vertical cone. *American Journal of Heat and Mass Transfer*, 4(1):53–63, 2017.

[76] BR Sharma and K Hemanta. Mhd flow, heat and mass transfer about a permeable rotating vertical cone in presence of radiation, chemical reaction and heat generation or absorption effects. *Latin American Applied Research - An international journal*, 46(3):109–114, 2016.

[77] S Shateyi and SS Motsa. Variable viscosity on magnetohydrodynamic fluid flow and heat transfer over an unsteady stretching surface with hall effect. *Boundary Value Problems*, 2010:1–20, 2010.

[78] PJ Singh and S Roy. Unsteady mixed convection flow over a vertical cone due to impulsive motion. *International Journal of Heat and Mass Transfer*, 50:949–959, 2007.

[79] R Sivaraj, A Benazir, S Srinivas, and AJ Chamkha. Investigation of cross-diffusion effects on casson fluid flow in existence of variable fluid properties. *The European Physical Journal Special Topics*, 228(1):35–53, 2019.

[80] C Soret. *Influence de la température sur la distribution des sels dans leurs solutions.* 1880.

[81] D Srinivasacharya and P Jagadeeshwar. Effect of variable properties on the flow over an exponentially stretching sheet with convective thermal conditions. model. *Meas. Control B*, 87(1):7–14, 2018.

[82] C Sulochana, SP Samrat, and N Sandeep. Numerical investigation of magnetohydrodynamic (mhd) radiative flow over a rotating cone in the presence of soret and chemical reaction. *Propulsion and Power Research*, 7:91–101, 2018.

[83] HS Takhar, AJ Chamkha, and G Nath. Unsteady mixed convection flow from a rotating vertical cone with a magnetic field. *Heat and Mass Transfer*, 39:297–304, 2003.

[84] CL Tien and IJ Tsuji. A theoretical analysis of laminar forced flow and heat transfer about a rotating cone. *Journal of Heat Transfer*, 87(2):184–190, 1965.

[85] LN Trefethen. *Spectral methods in MATLAB.* SIAM.

[86] M Turkyilmazoglu. On the purely analytic computation of laminar boundary layer flow over a rotating cone. *International Journal of Engineering Science*, 47:875–882, 2009.

[87] M Turkyilmazoglu. A note on the induced flow and heat transfer due to a deforming cone rotating in a quiescent fluid. *Journal of Heat Transfer*, 140(12):124502, 2018.

[88] LR Ullah, A Samad, and A Nawaz. The convective instability of the boundary-layer flow over a rotating cone in and out of a uniform magnetic field. *European Journal of Mechanics B-fluids*, 87:12–23, 2021.

[89] JC Umavathi and S Mohiuddin. Mixed convection flow of permeable fluid in a vertical channel in the presence of first-order chemical reaction: Variable properties. *Special Topics & Reviews in Porous Media: An International Journal*, 9(2), 2018.

[90] K Verma, D Borgohain, and BR Sharma. Soret and dufour effects on mhd flow about a rotating vertical cone in presence of radiation. *Journal of Mathematical and Computational Science*, 11(3):3188–3204, 2021.

[91] KA Yih. Radiation effect on mixed convection over an isothermal cone in porous media. *Heat and Mass Transfer*, 37:53–57, 2001.

[92] WS Yu, HT Lin, and TY Hwang. Conjugate heat transfer of conduction and forced convection along wedges and a rotating cone. *International Journal of Heat and Mass Transfer*, 34:2497–2507, 1991.

[93] J Zueco, S Ahmed, and L M López-González. 2-d unsteady free convective heat and mass transfer newtonian hartmann flow with thermal diffusion and soret effects: Network model and finite differences. *International Journal of Heat and Mass Transfer*, 110:467–475, 2017.